INSTITUTO SUPERIOR TÉCNICO
Universidade Técnica de Lisboa

Analysis of Technologies for Long Term Evolution in UMTS

Sara Mendes Duarte

Dissertation submitted for obtaining the degree of
Master in Electrical and Computer Engineering

Jury

Supervisor: Prof. Luis M. Correia

Co-Supervisor: Mr. Luis Santo

President: Prof. António L. C. Topa

Members: Prof. António Rodrigues

September 2008

To my parents, brother, sister and niece

"The significant problems we face cannot be solved at the same level of thinking we were at when we created them."

Albert Einstein (1879-1955)

Acknowledgements

First I would like to thank to Professor Luís M. Correia for giving me the opportunity to write this thesis and for the knowledge and experience sharing that were of extreme importance throughout this work. I am thankful for the valuable time during our weekly meetings, as well as for his advice, which will also be useful in my professional life, help and guidance that were a key factor to finish this work with the demanded and desired quality.

To Optimus, especially to Luís Santo and David Antunes for all the constructive critics, technical support, suggestions, advice, and to their precious time to answer all my doubts. Their knowledge and experience were very helpful throughout this journey.

To all GROW members for the clarifications, all the support and the contact with several other areas of wireless mobile communications through the participation in the GROW meetings.

I also want to thank all the RF2 lab partners, Armando Marques, Filipe Leonardo, Ricardo Preguiça, Telmo Batista and Vikash Mukesh, for their constructive critics, useful suggestions, different points of view and availability. In a more personal level, I would like to thank to Telmo Batista, for all of the above, as well as for their friendship, good company and support, which was essential for the completion of this thesis, and to Ricardo Preguiça for all the knowledge exchange and support.

I want to thank, also, to João Lopes and Luís Salvado for their availability, patience and knowledge sharing, which was of great importance in the development of this thesis.

A enormous thanks to Miguel Amorim for his unconditional patience, understanding and help, to my friends Margarida Lourenço and Patrícia Rodrigues, and to all my IST friends crew, specially to Guilherme Pereira, for all the help, support, encouragement and company, and for giving me the strength and motivation, without which, the completion of this work would have been a more difficult task.

Last but not of least importance, I would like to thank all my family, especially to my father, for all the good writing suggestions and revisions, mother, brother, sister, who gave me the greatest joy during this time, and grandparents to whom I am very grateful for their unconditional love, care, understanding, and support, which kept me going in the hardest times.

Abstract

The main purpose of this thesis was to study LTE technologies in terms of capacity and coverage. For this purpose, a single user model was developed, where the maximum cell radius is calculated considering that there is only one user in the network. To have a more realist approach, a multiple users and multiple services scenario model was developed as well, enabling a network performance analysis. The results from the single user model show that QPSK is the modulation for which it is possible to achieve a higher radius in DL 0.49 km, while the radius for 16QAM and 64QAM are 0.34 and 0.19 km. In the 900 MHz frequency band there is an increase of 150% on the radius compared with the 2100 MHz one, while in 2600 MHz there is a decrease of 35%. The UL radii are on average 45% lower from the DL ones. The results from the multiple users' simulator show an average cell radius of 0.21 km and 0.11 km for DL and UL, respectively. For DL, one obtains 6.78 Mbps for the overall BS throughput, and a coverage area of 79.3% of the total area, while for UL, the BS has a throughput of 3.3 Mbps, and 27.7% of coverage area of the total one.

Keywords

LTE, OFDMA, MIMO, Capacity, Coverage

Resumo

O principal objectivo desta tese foi estudar as tecnologias do LTE, em termos de capacidade e cobertura. Para esse efeito, foi desenvolvido um modelo mono-utilizador onde o raio máximo de uma célula é calculado tendo em conta que só há um utilizador na rede. Para uma análise mais realista, um simulador para um cenário de múltiplos utilizadores e múltiplos serviços foi desenvolvido permitindo a análise do desempenho da rede. Os resultados do modelo mono-utilizador mostram que, QPSK é a modulação com a qual é possível obter maiores raios, 0.49 km no DL enquanto para 16QAM e 64 QAM são 0.34 e 0.19 km. Na banda de frequência dos 900 MHz há um aumento de 150% no raio comparando com o raio da banda dos 2100 MHz. Na banda dos 2600 MHz há uma redução no raio de 35%. Os raios do UL são em media 45% menores que os do DL. Os resultados do simulador de múltiplos utilizadores mostram que uma célula tem um raio médio de 0,21 km e 0,11 km para o DL e UL, respectivamente. Para o DL, obtém-se um débito de 6,78 Mbps para uma BS e uma área coberta de 79,3% da total, enquanto para o UL, a BS tem um débito de 3,3 Mbps, e 27,7% de área coberta da total.

Palavras-chave

LTE, OFDMA, MIMO, Capacidade, Cobertura

Table of Contents

List of Figures

List of Tables

List of Acronyms

2G	2nd Generation
3G	3rd Generation
3GPP	3rd Generation Partnership Project
4G	4th Generation
A1	Alternative 1
A2	Alternative 2
ACK	ACKnowledgement
A/D	Analogue-to-Digital
AMC	Adaptative Modulation and Coding
AMR	Adaptative MultiRate
AMR-WB	AMR WideBand
AoA	Angle of Arrival
ARQ	Automatic Repeat reQuest
ASN	Access Service Network
ASN-GW	ASN GateWay
BER	Bit Error Ratio
BLEP	BLock Error Probability
BLER	BLock Error Ratio
BPSK	Binary Phase Shift Keying
BS	Base Station
CDMA	Code Division Multiple Access
CIR	Channel Impulse Response
CN	Core Network
CP	Cyclic Prefix
CPICH	Common Pilot CHannel
CQI	Channel Quality Information
CS	Circuit Switch
CSN	Connectivity Service Network
CTC	Convolutional Turbo Code
D/A	Digital-to-Analogue
DCH	Dedicated transport CHanel
DFT	Discrete Fourier Transform

DL	DownLink
DPCCH	Dedicated Physical Control CHannel
DS-CDMA	Direct-Sequence CDMA
DTX	Discontinuous Transmission
ECR	Effective Code Rate
E-DCH	Enhanced DCH
E-DPCCH	E-DCH Dedicated Physical Control CHannel
E-DPDCH	E-DCH Dedicated Physical Data CHannel
EIRP	Equivalent Isotropic Radiated Power
eNB	evolved-Node B
EPA	Extended Pedestrian A
EPC	Evolved Packet Core
ETU	Extended Typical Urban
EVA	Extended Vehicular A
E-UTRAN	Evolved-UTRAN
FDD	Frequency Division Duplex
FDMA	Frequency Division Multiple Access
FFT	Fourier Fast Transform
FRC	Fixed Reference CHannel
GBR	Guaranteed Bit Rate
GBSB	Geometrically Based Single Bounce
GGSN	Gateway GPRS Support Node
GMSC	Gateway MSC
GPRS	General Packet Radio Service
GSM	Global System for Mobile communications
HARQ	Hybrid ARQ
HLR	Home Location Register
HS-DPCCH	High-Speed Dedicated Physical Control CHannel
HS-PDSCH	High-Speed Physical Downlink Shared CHannel
HS-SCCH	High-Speed Shared Control CHannel
HSDPA	High Speed Downlink Packet Access
HS-DSCH	High-Speed Downlink Shared CHannel
HSPA	High-Speed Packet Access
HSUPA	High Speed Uplink Packet Access
ICI	Inter Channel Interference
IEEE	Institute of Electrical and Electronics Engineers
IFFT	Inverse Fourier Fast Transform

IMT	International Mobile Telecommunications
ISI	Inter Symbol Interference
ITU	International Telecommunication Union
ITU-R	ITU Radiocommunication Sector
LTE	Long Term Evolution
MAC-hs	MAC high speed
ME	Mobile Equipment
MIMO	Multiple Input Multiple Output
MME	Mobility Management Entity
MMS	Multimedia Message Service
MPC	MultiPath Component
MSC	Mobile Switching Centre
MT	Mobile Terminal
OFDM	Orthogonal Frequency-Division Multiplexing
OFDMA	Orthogonal Frequency-Division Multiple Access
OVSF	Orthogonal Variable Spreading Factor
PAR	Peak to Average power Ratio
PBCH	Physical Broadcast CHannel
P-CPICH	Primary-Common PIlot CHannel
PDCP	Packet Data Convergence Protocol
PDN	Packet Data Network
PF	Proportional Fair
P-GW	PDN Gateway
PLMN	Public Land Mobile Network
PS	Packet Switch
P-SCH	Primary–Synchronisation CHannel
PUSCH	Physical Uplink Shared CHannel
QAM	Quadrature Amplitude Modulation
QoS	Quality of Service
QPSK	Quaternary Phase Shift Keying
RB	Radio Bearer
RLC	Radio Link Control
RMG	Relative MIMO Gain
RNC	Radio Network Controller
RR	Round Robin
RRC	Radio Resource Control
RRM	Radio Resource Management

RT	Real Time
RTT	Round Trip Time
RTWP	Received Total Wideband Power
Rx	Receiver
SAE	System Architecture Evolution
SC	Single Carrier
SF	Spreading Factor
SGSN	Serving GPRS Support Node
S-GW	Serving GateWay
SINR	Signal to Interference plus Noise Ratio
SISO	Single Input Single Output
SMS	Short Message Service
SNR	Signal to Noise Ratio
SPI	Scheduling Priority Indicator
SRB	Signalling Radio Bearer
SS	Subscriber Station
S-SCH	Secondary–Synchronisation CHannel
TDD	Time Division Duplex
ToA	Time of Arrival
TTI	Time Transmission Interval
Tx	Transmitter
UE	User Equipment
UL	UpLink
UMTS	Universal Mobile Telecommunications System
UPH	UE Power Headroom
USIM	UMTS Subscriber Identity Module
UTRAN	UMTS Terrestrial Radio Access Network
VLR	Visitor Location Register
VoIP	Voice over Internet Protocol
WCDMA	Wide Code Division Multiple Access
WiMAX	Worldwide Interoperability for Microwave Access

List of Symbols

α	DL orthogonality factor
β	Maximum interference value considered
δ	Frequency Offset
Δf	Subcarriers Bandwidth
$\overline{\varepsilon_r}$	Mean relative error
η	Load Factor
μ	Mean value of the distribution
μ_{RMG}	Average RMG
$\bar{\xi}$	Mean correlation between links in a MIMO system
ρ	Signal to Noise Ratio
ρ_I	Signal-to-Interference-plus-Noise Ratio
ρ_{pilot}	P-CPICH E_c/N_0 when HSDPA is active
σ	Standard Deviation
σ^2	Variance
σ^2_{RMG}	RMG distribution variance depending on the cell-type, N_T and N_R
Σ	Singular values of matrix $\boldsymbol{H}$
a_{pd}	Average power decay
B	Passband Bandwidth
B_C	Coherence Band
B_N	Subchannel Bandwidth
BS_{active}	Number of BS actives
C_0	Constant
C_{MIMO}	Capacity gain of a MIMO system
C_{SISO}	Capacity gain of a SISO system
d	Distance between the user and the BS
$d_{max\ user\ i}$	Distance to the BS of the further away user for sector i
e	Relative Error
E_b	Energy per user bit
f	Frequency
F	Receiver's noise figure
F_a	Activity factor
g	Inverse of the RMG distribution
G_{div}	Diversity gain

$G_{M/S}$	Relative MIMO Gain
G_{MHA}	Masthead amplifier gain
G_r	Receiving antenna gain
G_t	Transmitting antenna gain
$\boldsymbol{H}$	Matrix containing the CIRs
h_{ij}	CIR between signal from the j^{th} Tx antenna to the i^{th} Rx antenna
$\boldsymbol{H_n}$	Normalised channel transfer matrix related to $\boldsymbol{T}$
$I_{inter\ n}$	Normalised inter-cell interference
$\boldsymbol{I_{NR}}$	N_R dimensional identity matrix
k_d	Dependence of the multiscreen diffraction loss versus distance
L_0	Free space loss
L_c	Cable losses between transmitter and antenna
L_{int}	Indoor penetration
L_p	Path loss
L_{ref}	Propagation model losses
L_{tm}	Approximation for the multi-screen diffraction loss
L_{tt}	Rooftop-to-street diffraction loss
L_u	Body losses
M	Total Margin
M_{FF}	Fast fading margin
M_I	Interference margin
M_{SF}	Slow fading margin
N	Total noise power
$\boldsymbol{n}$	Vector containing power of noise received by each antenna
N_0	Noise spectral density
N_R	Number of Rx antennas
N_S	Number of subcarriers
N_{SF}	Number of symbols per sub-frame
N_T	Number of Tx antennas
N_u	Number of users
$N_{u\ BS}$	Total number of users in the BS
N_{uhj}	Number of users per hour performing the service j in the BS
N_{uhBS}	Number of users served in an hour in the BS
$N_{U\ h\ NT}$	Total number of users in the network per hour
N_{u_j}	Number of users in the BS *j*
$N_{U_{max}}^{BS}$	Number of users of the most populated BS
$N_{u\ NT}$	Total number of users in the network
N_z	Number of samples
P_{HSDPA}	HSDPA transmit power

$P_{HS\text{-}DSCH}$	Received power of the HS-DSCH summing over all active HS-PDSCH codes
P_{inter}	Received inter-cell interference
P_{intra}	Received intra-cell interference
P_{noise}	Received noise power
P_{pilot}	P-CPICH transmit power
P_r	Power available at the receiving antenna
P_t	Power fed to the transmitting antenna
P_{total}	Total Node B transmit power
P_{tx}	Transmission power
RB_{user}	Number of RB attributed to the user
R_b	Throughput
$R_{b\ BS}$	BS instantaneous served throughput
RB_{BS}	Total BS number of RBs
$R_{b\ max}$	Maximum throughput
$R_{b\ N\ BS}$	BS normalised throughput
$R_{b\ NT}$	Network Throughput
RB_{NT}	Network RBs
$R_{b\ RB}$	RB instantaneous throughput
r_{BS}	BS radius
$R_{b(QPSK/16QAM/64QAM)}$	Total BS throughput for one modulation
$R_{b(QPSK/16QAM/64QAM)\ NT}$	Total Network throughput for one modulation
$R_{b\ user}$	Users instantaneous throughput
R_c	Chip rate
r_{NT}	Network radius
s	Slope of the Sigmoid function
SF_{16}	HS-PDSCH SF of 16
SG_{BS}	BS Satisfaction Grade
SG_{NT}	Network Satisfaction Grade
$S_{U\ NT}$	Network average ratio of served users
T	Total BS traffic transferred in one hour
$\boldsymbol{T}$	Non-normalised channel transfer matrix, containing the channel transfer gains for each pair of antennas
T_d	Duration of one OFDM symbol
T_G	Guard Time
T_N	Separation between carriers
T_{NT}	Total Network Traffic per hour
T_S	Period of one subcarrier
T_{SF}	Sub-frame period
u	Random value with a Uniform distribution

$\boldsymbol{U}$	Unitary matrices containing the singular vectors of matrix $\boldsymbol{H}$ after SVD
$U_{(QPSK/16QAM/64QAM)}$	Number of users for one modulation in the BS
$U_{(QPSK/16QAM/64QAM)\ NT}$	Number of users for one modulation in the Network
$\boldsymbol{V}$	Unitary matrices containing the singular vectors of matrix $\boldsymbol{H}$ after SVD
V_{uj}	Volume per user associated to service j in the BS
$\boldsymbol{X}$	Fourier transform of the $\boldsymbol{x}$
$\boldsymbol{X}$	Vector of transmitted symbols from the input antennas
$\boldsymbol{Y}$	Fourier transform of the $\boldsymbol{y}$
$\boldsymbol{y}$	Vector of symbols on the receiving site
z	Set of samples
z_i	Sample i
z_r	Reference Value

List of Software

Borland C++ Builder	ANSI C++ Integrated Development Environment
MapBasic	Programming software and language to create additional tool and functionalities for the MapInfo
MapInfo	Geographic Information Systems (GIS) software
Matlab	Computational math tool
Microsoft Excel	Calculation tool
Microsoft Visio	Design tool (e.g. flowcharts, diagrams, etc)
Microsoft Word	Text editor tool

Chapter 1

Introduction

This chapter gives a brief overview of the work. Before establishing work targets and original contributions, the scope and motivations are brought up. The current State-of-the-Art on the scope of the work is also presented. At the end of the chapter, the work structure is provided.

1.1 Overview

Wireless communications is, by any measure, the fastest growing segment of the communications industry. As such, it has captured the attention of the media and the imagination of the public. Cellular systems have experienced an exponential growth over the last years. Indeed, cellular phones have become a critical business tool and part of everyday life in most developed countries, as they are rapidly supplanting the old wire line systems. The explosive growth of wireless systems coupled with the proliferation of laptop and palmtop computers indicate a bright future for wireless networks, both as stand-alone systems and as part of the larger networking infrastructure. However, many technical challenges remain in designing robust wireless networks that deliver the performance necessary to support emerging applications [Gold05].

In 1999, the 3rd Generation Partnership Project (3GPP) launched Universal Mobile Telecommunication System (UMTS), one of the 3rd Generation (3G) systems, also called Release '99, as a response to the needs of higher data rates, being deployed on top of the 2nd Generation (2G) network, Global System for Mobile communications (GSM). The UMTS air interface is Wideband Code Division Multiple Access (WCDMA), featuring a data up to 384 kbps for the Downlink (DL) and Uplink (UL), despite having a theoretical maximum for DL of 2Mbps. Although packet-data communications were already supported in the first release of the UMTS standard, as an evolution, emerges in 2002 Release 5, introducing the High Speed Downlink Packet Access (HSDPA) and bringing further enhancements to the provisioning of packet-data services, both in terms of system and end-user performance. This release enables a more realistic 2 Mbps and even beyond, with data rates up to 14 Mbps. The DL packet-data enhancements of HSDPA are complemented by Enhanced UL, introduced in Release 6, also known as High Speed UL Packet Access (HSUPA). HSDPA and HSUPA are often jointly referred to as High-Speed Packet Access (HSPA), being build upon the basic structure, and with a requirement on backwards compatibility, since it is implemented on already deployed networks.

Release 7 brings a number of further substantial enhancements to end-user performance, network capacity and network architecture. This is referred to as 'HSPA Evolution', and consists of both the introduction of new major features, such as Multiple Input Multiple Output (MIMO) technology, and many smaller improvements to existing structures, which, when taken together as a package, represent a major increase in performance and capabilities.

In the end of 2004, 3GPP under the need for 4th Generation (4G) requirements took the initiative to define a radio interface that was based on the latest developments. This was labelled "Long Term Evolution" (LTE), also referred to as Super 3G, and is being specified as part of Release 8, further pushing the radio capabilities higher, allowing an upgrade of UMTS to 4G mobile communication technology [BoTa07]. Releases 7 and 8 solutions for HSPA evolution are worked in parallel with LTE development, and some aspects of LTE work are also expected to reflect on HSPA evolution. The

fundamental aims of this evolution will be met through improved coverage and capacity, improving data rates and reducing latency, to further improve service provisioning and reduce user and operator costs. LTE targets have more complex spectrum situations and also fewer restrictions on backwards compatibility. To support the new packet-data capabilities provided by the LTE radio interface, an evolved core network has been developed. The work on specifying the core network is commonly known as System Architecture Evolution (SAE). Release 8 is planned to be ratified as a standard in December 2008 [DPSB07].

An overview of the different wireless technologies and their peak network performance capabilities is shown in Figure 1.1, where it is possible to confirm that LTE will bring higher peak data rates, making use of new multi-antenna techniques and higher spectrum.

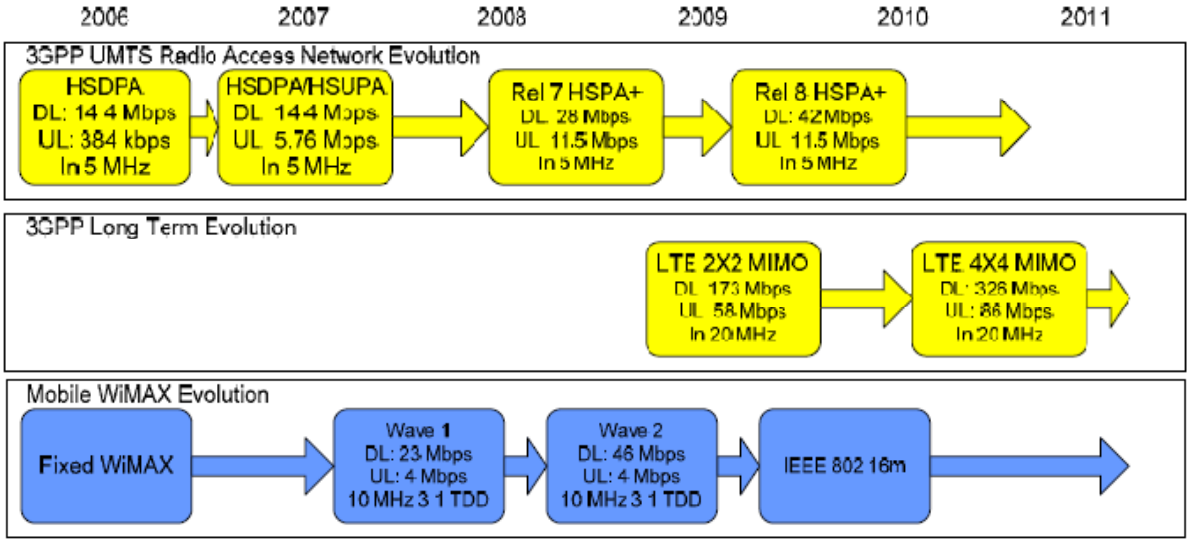

Figure 1.1.Evolution of TDMA and OFDM Systems (adapted from [RYSA07]).

From Figure 1.1, one notices that another standard is emerging as a potential LTE alternative, developed by Institute of Electrical and Electronics Engineering (IEEE), i.e., 802.16, also known as Worldwide Interoperability for Microwave Access (WiMAX), having the primary objective of making (fixed) broadband wireless access wider and cheaply available. Later, the original standard was enhanced so that improved radio features and support for mobility were addressed as well, known by Mobile WiMAX. The proposed work plan, for IEE 802.16m, allows completion of the standard by December 2009 for approval by March 2010. This standard achieves 100 Mbps for a high mobility scenario (250 km/h) and 1Gbps for a low mobility scenario [EMQG08].

In order to establish a new global platform to build the next generation (4G) of mobile service, the International Telecommunication Union (ITU) Radiocommunications Sector (ITU-R), has established a group named International Mobile Telecommunications-Advanced (IMT-Advanced). These systems include the new capabilities of IMT that go beyond those of IMT-2000 (3G systems). This new generation of mobile services will bring fast data access, unified messaging and broadband multimedia, in the form of new interactive services. Such systems provide access to a wide range of telecommunication services including advanced services supported by mobile and fixed networks, which are increasingly packet-based [BoTa07].

The main purpose of this thesis is to study LTE technologies and their impacts on a network, addressing coverage and capacity aspects. The objectives of this thesis were accomplished through the development and implementation of a single user model, in order to evaluate the radius for this scenario and performing a first network coverage analysis. Afterwards a multiple users' model in a multiple services scenario was developed ("scenario to closer" from real network behaviour), allowing several analyses regarding network settings variation being tested. For the development of these models a great amount of information, which provides solutions for LTE implementation, was collected and analysed. The different standardised bandwidths and also MIMO configurations were compared. The frequency band has an enormous influence on network behaviour; therefore an analysis for the possible LTE frequency bands was performed. The impact of the penetration services percentages and the number of users in this network were also evaluated.

This thesis was made in collaboration with the portuguese mobile operator Optimus.

The main contribution of this thesis is the analysis of the LTE network, in both DL and UL, focusing on capacity and coverage issues. A model to calculate the user's throughput as a function of the distance was implemented, which allows analysing several network parameter variations, as system bandwidth, frequency band, transmission power, MIMO configuration, among others. The simulator allows one to evaluate the influence of the different parameters on system performance, giving more emphasis to coverage and capacity.

1.2 Structure of the Dissertation

This work is composed by 5 chapters, including the present one, and followed by a set of annexes.

In Chapter 2, MIMO and multicarrier systems are introduced, regarding the fact that they are one of the main features of LTE. The main advantages and considerations about MIMO systems capacity can be found in MIMO section. Multicarrier systems, like Orthogonal Frequency-Division Multiplexing (OFDM) and Orthogonal Frequency-Division Multiple Access (OFDMA) are described, and their key challenges are exploited. Afterwards, LTE lower releases are presented, UMTS basic aspects being explained, and the new features of HSDPA and HSUPA being pointed out. The last section of the chapter provides an overview of LTE networks, and a comparison with WiMAX is done at the end.

Chapter 3 starts by presenting the developed theoretical single service radius model. Afterwards, the simulator developed for multiple users and services, based on previous simulators, is presented, being the main modifications pointed out. The LTE DL and UL modules developed are detailed afterwards. The input and output files are highlighted, and the simulator assessment is presented jointly with the analysis concerning the number of users in the default scenario.

Chapter 4 begins with the description of the default scenario. In the following parts of the chapter, results for DL and UL simulations are presented, for both single and multiple users' models. First, the study of DL is examined, starting by presenting the default scenario over which several parameters

are varied. Afterwards, the same analyses are presented for UL, a comparison between UL and DL being also performed.

This thesis concludes with Chapter 5, where the main conclusions of the work are drawn, and suggestions for future works are pointed out.

A set of annexes with auxiliary information and results is also included. In Annex A, one presents the detailed link budget used throughout this thesis. Annex B contains information on the Signal to Noise Ratio (SNR) and throughput interpolations for the different modulations as well as MIMO configuration. In Annex C, a description of Relative MIMO Gain (RMG) model takes place and the model information is shown. In Annex D, one presents information regarding the multiple services users' generation, as well as the default and alternative profiles characterisation. The flowcharts regarding the 3 used reduction strategies for LTE DL and UL multiple users' simulator are shown in Annex E. In Annex F and G, one shows the user's interface to the single user model and to the multiple services simulator, respectively. The main reasons for choosing two reference services, instead of one, are indicated in Annex H. Finally, in Annex I, one presents auxiliary results regarding the single user model, and in Annex J and K additional results regarding the multiple users' simulator are presented for DL and UL, respectively.

Chapter 2

Basic Concepts

This chapter provides an introduction to the main technologies that are related to the scope of this thesis. First MIMO and multicarrier systems are presented, followed by the description of UMTS Terrestrial Radio Access Network (UTRAN) system architecture jointly with the radio interface and an analysis of the interference and capacity. Later, HSPA main features and characteristic are introduced. An overview of LTE is done, approaching the system architecture, radio interface, a capacity and coverage analysis, and to finalise a comparison with WiMAX system. At the end of the chapter, current services and application in UMTS are approached.

2.1 MIMO

A brief overview of the general aspects of MIMO system is presented, followed by the capacity aspects of this system.

2.1.1 General Aspects

MIMO is recognised as a good solution in the development of the forthcoming generation of broadband wireless networks [ECGF05]. This system takes advantage of the multipath propagation, where the Receiver (Rx) antenna is reached by many copies of the transmitted signal. The difference in each component propagation path results in diversity of Time of Arrival (ToA), Angle of Arrival (AoA), signal amplitude and phase. In order to achieve a better performance, MIMO systems take advantage of all arriving arrays [Maćk07]. It exploits independently the transmission channels between the Transmitter (Tx) and Rx antennas.

The diversity reception, well known in various radio applications, improves only the Bit Error Ratio (BER) statistics and reduces the probability of total outage [Koko05]. However the MIMO scheme, which is the result of parallel deployment of several space-separated antennas at input and output, does not only improve BER performance but also causes an increase of channel capacity [Maćk07]. Nevertheless, the capacity in such system strongly depends on the propagation conditions in the radio channel and can vary significantly [Dziu04].

A MIMO system is composed by N_T Tx antennas and N_R Rx antennas, Figure 2.1. The relation between input and output is given by,

$$\boldsymbol{y}_{[N_R]} = \boldsymbol{H}_{[N_R \times N_T]} * \boldsymbol{x}_{[N_T]} + \boldsymbol{n}_{[N_T]} \quad (2.1)$$

where:

- $\boldsymbol{y}_{[Nr]}$ is the vector of symbols on the receiving site;
- $\boldsymbol{x}_{[Nt]}$ is the vector of transmitted symbols from the input antennas;
- $\boldsymbol{n}$ the vector containing power of noise received by each antenna;
- h_{ij} is a Channel Impulse Response (CIR) between signal from the j^{th} Tx antenna to the i^{th} Rx antenna;
- $\boldsymbol{H}_{[NrxNt]}$ is a matrix containing the CIRs;
- (*) an operator of a convolution of digital signals.

$\bar{\xi}$ is the mean correlation between links in a MIMO system, and is defined by:

$$\bar{\xi} = \frac{1}{(N_T N_R)^2} \sum_{k=1}^{N_T} \sum_{l=1}^{N_R} \sum_{m=1}^{N_T} \sum_{n=1}^{N_R} \xi(h_{kl}, h_{mn}). \quad (2.2)$$

The rank of matrix $\boldsymbol{H}$, leads to the number of parallel subchannels. In an environment rich in scatters generating many Multipath Components (MPCs), the number of uncorrelated sub-channels is possibly

high, in which case a maximum system performance is observed [Maćk07].

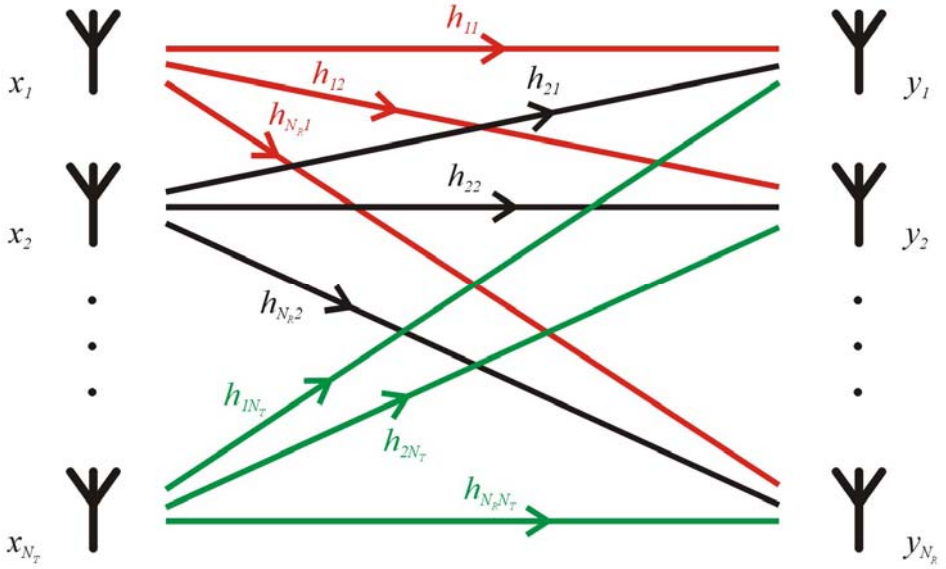

Figure 2.1 MIMO scheme (extracted from [Maćk07]).

2.1.2 Capacity

According to the general principles of information theory, the capacity of the radio channel is bounded by Shannon's rule [Proa01], which represents the capacity of a Single Input Single Output (SISO) system, normally taken as reference:

$$C_{SISO_{[bps/Hz]}} = log_2(1+\rho) \tag{2.3}$$

where:

- C_{SISO} is the capacity of a radio channel;
- ρ is the SNR.

In an ideal case, it can be shown that the channel capacity grows linearly with the number of Tx and Rx antennas [ECGF05]. This means that, in MIMO systems, it is possible to establish multiple parallel subchannels, which operate simultaneously on the same frequency band and at the same time. With some assumptions, the theoretical capacity of such a system has been presented in [FoGa98]:

$$C_{MIMO_{[bps/Hz]}} = log_2\left\{det\left[\boldsymbol{I}_{N_R} + \frac{\rho}{N_T}\boldsymbol{H}_n\boldsymbol{H}_n^H\right]\right\} \tag{2.4}$$

where:

- $\boldsymbol{I}_{NR}$ is the N_R dimensional identity matrix;
- ρ is defined at each Rx antenna as:

  $$\rho = \frac{P_{total}}{P_{noise}} b \tag{2.5}$$

  where:

  - P_{noise} is the noise power at the Rx antenna.
- $\boldsymbol{H}_n$ is the normalised channel transfer matrix related to $\boldsymbol{T}$ as:

  $$\boldsymbol{H}_n = \boldsymbol{T}/_b \tag{2.6}$$

- ***T*** is the non-normalised channel transfer matrix, containing the channel transfer gains for each pair of antennas;
- *b* is defined as:

$$b^2=R[|\boldsymbol{T}|]^2=\frac{1}{N_T N_R}\sum_{m=1}^{N_R}\sum_{n=1}^{N_T}|T_{mn}|^2 \quad (2.7)$$

Since the correlation varied between zero and one, it is possible to derive the upper and lower bounds for capacity from (2.4). If there is no correlation between parallel paths (ξ=0), matrix ***H*** will be the identity one and the maximum capacity is achieved:

$$C_{MIMO_{\xi=0}}=min(N_T;N_R)log_2\left(1+\frac{\rho}{N_T}\right) \quad (2.8)$$

On the contrary, when all subchannels are totally correlated (ξ=1), the minimum capacity of a MIMO channel occurs:

$$C_{MIMO_{\xi=1}}=log_2\left(1+min(N_T;N_R)\frac{\rho}{N_T}\right) \quad (2.9)$$

When the channel is known at the Tx, meaning the correlation between subchannels (CIR matrix ***H***) is known at the Tx, the waterfilling power distribution can be performed. In specified conditions this allows to operate with the maximum achievable capacity.

The Relative MIMO Gain (RMG) can be defined as the relation between the capacities of a MIMO system relative to the SISO one:

$$G_{M/S}=\frac{C_{MIMO}}{C_{SISO}} \quad (2.10)$$

2.2 Multicarrier Systems

OFDM and OFDMA are multicarrier systems, a brief description of both is presented in this section, as well as the challenges in multicarrier systems. This section is based on [Gold05].

2.2.1 OFDM and OFDMA

The basic idea of a multicarrier modulation is to divide the transmitted bitstream into many different substreams and send these over many different channels. It is based on the principle of transmitting simultaneously many narrow-band orthogonal frequencies, subcarriers. The number of subcarriers is noted as N_s. These frequencies are orthogonal to each other, which eliminates the interference between channels. If a data symbol is N_s times longer, compared to Single Carrier (SC), it provides to OFDM a much better multipath resistance, which together with orthogonal carriers allows a high spectral efficiency.

The basic premise of a multicarrier modulation is to split this wideband system into N_s linearly-modulated subsystem in parallel, each with Subchannel Bandwidth is:

$B_N = B / N_s$ (2.11)

where:

- B is the passband bandwidth.

The bandwidth subchannel is lower than the Coherence Band (B_C) for N_s sufficiently large and ensures relatively flat fading on each subchannel. Also, with N_s sufficiently large, the symbol time is much longer than the delay spread, so each subchannel experiences low Inter Symbol Interference (ISI) degradation.

The input data stream is linearly-modulated, resulting in a complex symbol stream. This symbol stream is divided into *N* substreams via a serial-to-parallel converter, as shown in Figure 2.2.

OFDM theory shows that the Inverse Fourier Fast Transform (IFFT) of magnitude N_s, applied on N_s symbols, realises one OFDM signal, where each symbol is transmitted on one of the N_s orthogonal frequencies. The IFFT operator realises the reverse operation of the Fast Fourier Transform (FFT). The FFT is a matrix computation that allows the Discrete Fourier Transform (DFT) to be computed. When N_s is power of 2 the complexity of the FFT is reduced [Nuay07].

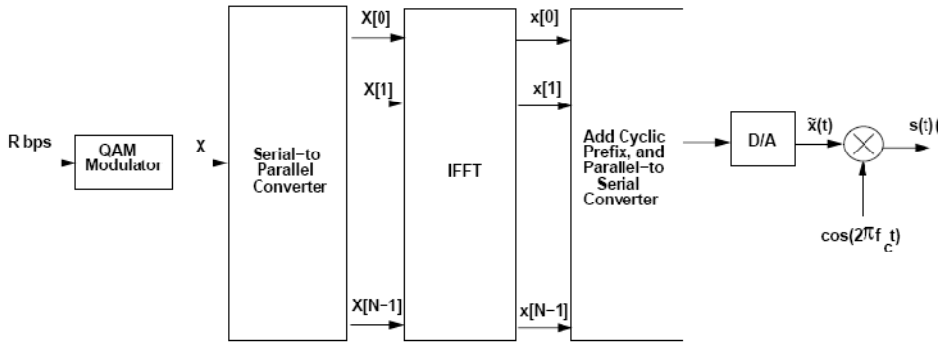

Figure 2.2. OFDM with IFFT implementation (Tx) (extracted from [Gold05]).

Since the channel output is a linear convolution instead a circular one (needed for IFFT/FFT), a special prefix is added to the input called a Cyclic Prefix (CP), so the linear convolution between the input and impulse response can be turned into a circular convolution. The addition of the CP with μ symbols on a data block with N_s symbols is shown at Figure 2.3.

The CP can also serve to eliminate ISI between the data blocks, since CP samples are also the first samples (as guard interval) of the channel output which are affected by ISI. These samples can be discarded without any loss relative to the original sequence, since there is no new information.

At the receiver the “tail” of the ISI associated with the end of a given OFDM symbol is added back to the beginning of the symbol, which recreates the effect of a cyclic prefix, Figure 2.4. This zero prefix reduces the transmit power relative to cyclic prefix by $N_s/(N_s+\mu)$, since the prefix does not require any transmit power. However, the noise from the received tail is added back into the beginning of the symbol, which increases the noise power by $(N_s+\mu)/N_s$.

CP allows the receiver to absorb much more efficiently the delay spread due to the multipath and to maintain frequency orthogonality. This CP is a temporal redundancy that must be taken into account in

data rates computations. The ratio μ/N_s is chosen taking some considerations into account. If the multipath effect is important, a high value of this ratio is needed, which increases the redundancy and then decreases the useful data rate. On the other hand if the multipath effect is lighter, a relatively smaller value of this ratio can be used [Nuay07].

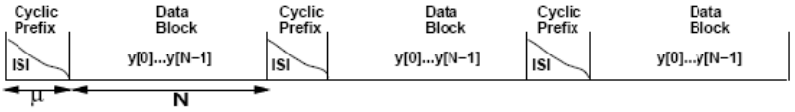

Figure 2.3. ISI between Data Blocks in Channel Output (extracted from [Gold05]).

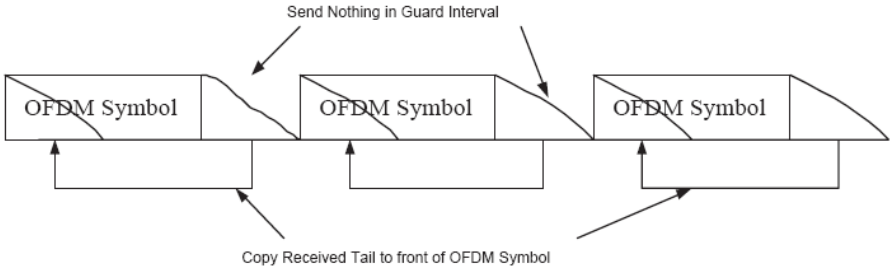

Figure 2.4. Creating a circular channel with an All-Zero Prefix (extracted from [Gold05]).

OFDM transmission was originally conceived for a single user; therefore, it had to be associated to a multiple user access scheme so that several users could be served. OFDMA is the scheme to be used. OFDMA allows the access of multiple users on the available bandwidth. Each user is assigned a specific time-frequency resource.

OFDMA subcarriers are divided into subsets of subcarriers, each subset representing a subchannel, as shown in Figure 2.5). In the DL, a subchannel may be intended for different receivers or groups of receivers; in the UL a transmitter may be assigned one or more subchannels. The subcarriers forming one subchannel may be adjacent or not [Nuay07].

The multiple access has a new dimension with OFDMA. A DL or an UL user will have a time and a subchannel allocation for each of its communications, as illustrated in Figure 2.6.

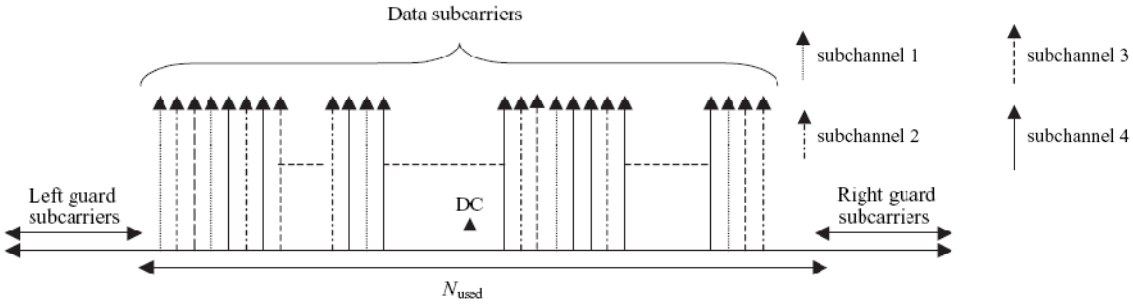

Figure 2.5. Illustration of the OFDMA principle (extracted from [Nuay07]).

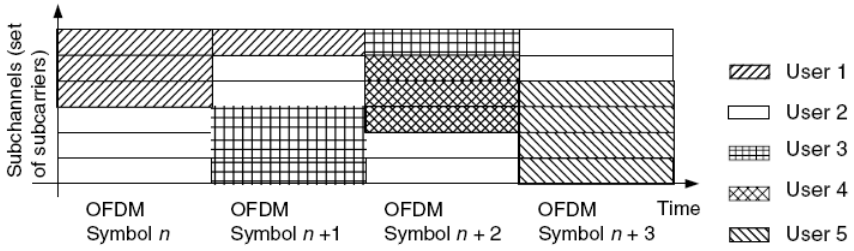

Figure 2.6. Illustration of the OFDMA multiple access (extracted from [Nuay07]).

2.2.2 Key Challenges

The Peak to Average power Ratio (PAR) is a very important attribute of a communication system. A low PAR allows the transmit power amplifier to operate efficiently, whereas a high PAR forces the transmit power amplifier to have a large *backoff* in order to ensure linear amplification of the signal. Operation in the linear region of this response is generally required to avoid signal distortion, so the peak value is constrained to be in this region. Having the average and peak values as close together as possible, is desirable, in order to have the power amplifier operating at the maximum efficiency.

For N subcarriers, as is proved in [Gold05], the maximum PAR is N. In practice, full coherent addition of all N symbols is highly improbable, so the observed PAR is typically less than N, usually many dB. Nevertheless, PAR increases approximately linearly with the number of subcarriers. So, although it is desirable to have N as large as possible in order to keep the overhead associated with the cyclic prefix down, a large PAR is an important penalty that must be paid for a large N. A high PAR requires high resolution for the receiver Analogue/Digital (A/D) convertor, since the dynamic range of the signal is much larger for high PAR signals. High resolution A/D conversion places a complexity and power burden on the receiver front end.

The orthogonality of the subchannels in OFDM modulation is assured by the subcarrier separation $\Delta f = 1/T_N$, Figure 2.7. In practice the separation of the subcarriers is imperfect, so the Δf is not exactly equal to $1/T_N$. This is generally caused by mismatched oscillators, Doppler frequency shifts or timing synchronisations errors, so the orthogonality of the subchannels will be degraded since the received samples of the FFT will contain interference from adjacent channels. Thus, it is important to analyse the Inter Channel Interference (ICI).

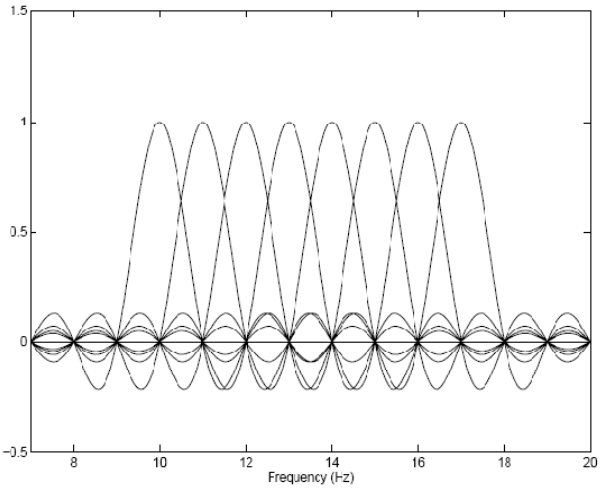

Figure 2.7. OFDM Overlapping Subcarriers with $\Delta f = 1$Hz (extracted from [Gold05]).

The total ICI power on subcarrier i, where the subcarrier signal is $x_i(t) = e^{j2\pi it/T_N}$, is given by

$$ICI_i = \sum_{m \neq i} |I_m|^2 \approx C_0 (T_N \delta)^2 \quad (2.12)$$

where:

- C_0 is a constant;

- δ/T_N is the frequency offset when the signal is demodulated.

By (2.11) it can be observed that as T_N increases, the subcarriers grow narrower and hence more closely spaced, which results in more ICI. Another conclusion is that ICI grows quadratically with the frequency offset δ, but ICI not appears to be directly affected by N. However, if N is large, forces T_N to be also large, which will make the subcarriers to be closer together. Along with the larger PAR that comes with larger N, the increased ICI is another reason to pick N as low as possible, given that the overhead budget can be met. There are a number of ways to reduce ICI for a given choice of N, or reduce PAR, presented in [Gold05].

2.3 UMTS

This section gives an overview of UMTS, Release '99, based on [HoTo04]. First the architecture is presented together with its elements. A brief description of the radio interface, WCDMA, follows the system architecture and finally coverage and capacity are evaluated.

2.3.1 Network architecture

The UMTS architecture is the same of GSM. The network is grouped into three high-level modules, which are specified by the 3GPP. They are:

- User Equipment (UE);
- UTRAN;
- Core Network (CN).

This architecture is represented in Figure 2.8. For UE and UTRAN completely new protocols were made because they are based on the needs of WCDMA. On the contrary CN is updated from GSM/ General Packet Radio Service (GPRS).

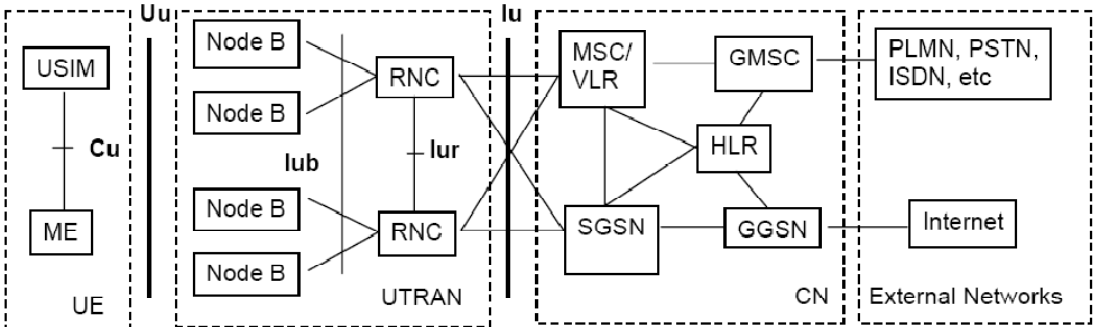

Figure 2.8. UMTS network architecture (extracted from [HoTo04]).

The UE interfaces with the user and the radio interface. It is composed by the Mobile Equipment (ME) and the UMTS Subscriber Identity Module (USIM). The ME is the Mobile Terminal (MT) used for radio communication over the Uu interface and USIM is a smartcard that holds the subscriber identity, performs authentication algorithms, and stores authentication and encryption keys and some

information that is needed at the terminal. USIM and ME communicate over the Cu interface.

UTRAN is responsible for the entire radio interface. It consists of two distinct elements:

- Node B, the Base Station (BS) which switch the data flow between the Iub and the Uu interfaces and also have a small participation in the Radio Resource Management (RRM);
- Radio Network Controller (RNC), is responsible for controlling the Node B's that are connected to it by the Iub interface. The RNC carries out the RRM, e.g. outer loop power control, packet scheduling and handover control.

In UTRAN all RNCs are connected by the Iur interface with each other.

The CN upgraded from GSM, is responsible for switching and routing calls and data to external networks, like the internet (Packet Switch (PS) network) and public Switched telephone network (Circuit Switch (CS) network).

CN main elements are:

- Home Location Register (HLR) is a database where the operator subscriber's information is stored, such as allowed services, user location for routing calls and preferences;
- Mobile Switching Centre/Visitor Location Register (MSC/VLR) that is the switch (MSC) and database (VLR) which serves the UE in its location CS services;
- Gateway MSC (GMSC) it is where all incoming and outgoing CS connections carry by. It is the switch at the point where UMTS Public Land Mobile Network (PLMN) is connected to external CS network;
- Serving GPRS Support Node (SGSN) that have similar functionalities to MSC/VLR but is normally used for PS services.
- Gateway GPRS Support Node (GGSN) functionality is analogous to that of GMSC but is in relation to PS services.

The innovations made on UE and UTRAN make possible to Release '99 support soft handover, opposite to GSM, where only was possible hard handover. At hard handover the connection between the old BS and the UE is first interrupted before the UE establishes a new connection with the new BS. In UMTS hard handover can be inter-frequency or inter-system. In the former, the Node Bs have different carriers and in the later it is a handover to other system, e.g. GSM [Molis04]. Soft and softer handovers are very similar, at soft handover the UE is connected to more than one BS at the same time and at the softer handover the UE is transferred from one sector of a cell to another sector of the same cell.

2.3.2 Radio Interface

The UMTS air interface is based on WCDMA, which is a wideband Direct-Sequence Code Division Multiple Access (DS-CDMA) system. In this the user information bits are spread over a wide bandwidth by multiplying the user data with quasi-random bits (called chips) derived from CDMA spreading codes. WCDMA main parameters are summarised in Table 2.1.

Table 2.1. Main WCDMA parameters (adapted from [HoTo04]).

Multiple access method	DS-CDMA
Duplexing method	FDD
Base station synchronisation	Asynchronous operation
Chip rate [Mcps]	3.84
Frame length [ms]	10
Service multiplexing	Multiple services with different quality of service requirements multiplexed on one connection
Multirate concept	Variable spreading factor and multicode
Detection	Coherent using pilot symbols or common pilot
Multiuser detection, smart antennas	Supported by the standard, optional in the implementation
Modulation	UL: Binary Phase Shift Keying (BPSK) DL: Quaternary Phase Shift Keying (QPSK)

The chip rate of 3.84 Mcps leads to a carrier bandwidth of approximately 4.4MHz. Between each other carriers have a bandwidth of 5 MHz which gives the possibility for the operators to change the central frequency for 200 kHz to minimise, e.g., the interference between carriers. The data capacity among users can change from frame to frame. This allows WCDMA to support a highly variable user data rates, special in PS data services.

UMTS can operate in two modes, Frequency Division Duplex (FDD) and Time Division Duplex (TDD). In this thesis only UMTS-FDD is analysed. UMTS-FDD uses the 2100 frequency band, [1920, 1980] MHz for the UL and [2110, 2170] MHz for DL.

WCDMA has two operations in the multiple access, spreading and scrambling, applied to physical channels. Channelisation codes, on spreading, are responsible for separating transmissions from the same source, in DL at the same sector and in UL are used to separate physical data and control information from the same UE. In WCDMA, this code use Orthogonal Variable Spreading Factor (OVSF), which allows different Spreading Factors (SF) and the orthogonality between different spreading codes of different length it is maintained. So the number of channelisation codes is given by the SF. Scrambling codes are mainly used to distinguish signals from UEs and/or BSs. Scrambling is used on top of spreading so that the signal bandwidth is not changed and the symbol rate just makes signals from different sources separable from each other. This allows the use of identical spreading codes for several transmitters.

In relation to channels, UMTS have two different types of channels, transport and physical channels. In what concern to the transport channels it is distinguished common transport channels and dedicated transport channels. A description of these channels can be found in [HoTo04]. Dedicated channels, contrary to common ones, are present in both UL and DL. They are used to transmit both higher layer signalling and actual user data. There is only one dedicated channel, the Dedicated transport Channel (DCH), supporting some features like, fast power control, fast data rate and soft handover.

Power control is an essential part of any CDMA system, as it is necessary to control mutual

interference. If there was no power control a single UE could block a whole cell. There are two different types of power control, open and closed-loop. The former is used to supply the initial power to the UE that is initiating a connection and the latter is crucial in a WCDMA system.

2.3.3 Capacity and Coverage

Capacity and interference, contrary to GSM, are user dependent. With the use of WCDMA the frequency reuse is one, so the system is usually interference limited.

There are three main limited factors:

1. Number of available codes in DL;
2. DL transmission power;
3. System load.

The first limits the number of simultaneous active users within a cell and on the bit rate required by the type of services each user is accessing. To allow higher data rates in the network, SF must decreases and consequently the number of users in the network also decreases. Since that Node B have a maximum transmitting power, it is also a limit because power is shared among all UE in the cell. The last one, but of paramount importance, affects the cell coverage.

The load factor depends on the services, and since there is asymmetry between UL and DL, the load factor is different between the two, and should not be higher than 50% in UL or 70% in DL. These two factors are given by:

$$\eta_{UL}=(1+I_{inter\,n})\sum_{j=1}^{N_u}\frac{1}{1+\frac{R_c/R_{b_j}}{\left(E_b/N_0\right)_j F_{a_j}}} \tag{2.13}$$

$$\eta_{DL}=(1+I_{inter_n})\sum_{j=1}^{N_u}F_{a_j}\cdot\frac{\left(E_b/N_0\right)_j}{R_c/R_{b_j}}\left[(1-\alpha_j)+I_{inter_{n_j}}\right] \tag{2.14}$$

where:

- η_{DL}, is DL load factor;
- η_{UL}, is UL load factor;
- N_U, is the number of active users;
- $I_{inter\,n}$, is the normalised inter-cell interference (between [40, 60]% in UL and 0% in DL);
- $R_{b\,j}$, is the bit rate associated to service of user j;
- $F_{a\,j}$, is the activity factor of user j (50 % for voice and 100 % for data);
- α_j, is the code orthogonality factor of user j (typically in [50, 90]%);
- R_c, is the chip rate of WCDMA;
- $(E_b/N_0)_j$, is the signal-to-noise ratio, energy per user bit divided by the noise spectral density of user j.

The interference margin used in the link budget is defined as:

$$M_{I\ [\mathrm{dB}]}=-10\log(1-\eta) \tag{2.15}$$

When η is near one, the system reaches its top capacity and the margin interference goes to infinity,

consequently a raise of the load factor leads to a reduction in coverage, via the increase of M_l.

DL transmission power is also a limiting factor in cell capacity and is expressed by:

$$P_{Tx}^{BS} = \frac{N_0 R_c}{1-\overline{\eta_{DL}}} \sum_{j=1}^{N_u} F_{a_j} \cdot \overline{L_{p_j}} \frac{\left(E_b/N_0\right)_j}{R_c/R_{b_j}} \quad (2.16)$$

where:

- $\overline{L_{p_j}}$ is the average path loss between the user *j* and the BS.

Given the limitation of DL transmission power, raising it is not an efficient technique for increasing cell capacity. There are other techniques to increase cell capacity in a more efficient way.

The radius of a given cell can be estimated taking into account the definition of the path loss and the model of the average power decay with distance [Corr08]. The radius of a cell is given by,

$$d_{[km]} = 10^{\frac{P_t\,[dBm] + G_t\,[dBi] - P_r\,[dBm] + G_r\,[dBi] - L_{ref}}{10 \cdot a_{pd}}} \quad (2.17)$$

where:

- L_{ref} are propagation model losses;
- a_{pd} is the average power decay;
- P_t, is the power fed to the transmitting antenna;
- G_t, is the gain of the transmitting antenna;
- P_r, is the power available at the receiving antenna;
- G_r, is the gain of the receiving antenna.

In a mobile communications system, beside coverage and capacity, is important to take the effect of mobility in the system into account. With mobility, parameters, like fading margin, change, among others, which are going to affect system performance.

2.4 HSDPA

HSDPA key technologies and channels are presented in this section, based on [HoTo06]. A brief characterisation of performance, capacity and coverage of HSDPA follow an overview on RRM.

2.4.1 Key Updates

With the demand of higher data rates, 3GPP launched Release 5 with expected peak data rates of 10Mbps. Designed to be deployed together with Release '99, HSDPA improves capacity and spectral efficiency by means of fast physical layer (L1) retransmission and transmission combining, as well as fast link adaptation controlled by the Node B. To achieve higher data rates, a new higher order modulation is used, 16 Quadrature Amplitude Modulation (QAM) with 4bits per symbol, but it can only be used under good radio signal quality due to additional decision boundaries. QPSK is also used,

mainly to maximise coverage and robustness.

While in Release '99 the scheduling is based on the RNC, and Node B has power control functionalities, in HSDPA scheduling and fast link adaptation based on physical layer retransmission were moved to Node B, as presented in Table 2.2. These new functionalities of scheduling and retransmission at the Node B are just possible with the use of buffering in the Node B.

Table 2.2. New functionalities on different elements due to HSDPA (adapted from [HoTo06]).

RNC	HSDPA radio resource and mobility management HSDPA Iub traffic management Larger data volume
Node B	Data buffering Automatic Repeat Request (ARQ) handling Feedback decoding Flow control Downlink scheduling 16QAM modulation
UE	ARQ handling with soft value buffer Feedback generation and transmission 16QAM demodulation

With these new functionalities the need to introduce new channels emerged. A new user data channel was created and two other channels were added for signalling purposes. HSDPA is always operated with Release '99 in parallel, which can be used to carry CS services and the Signalling Radio Bearer (SRB), but does not support features like power control and soft handover. More detailed information about these channels is given in [HoTo06].

2.4.2 Radio Resource Management

RRM algorithms, using HSDPA physical enhancements, increase the capacity and end user performance, being also responsible for assuming network stability. Figure 2.9 shows schematics overview of the most essential HSDPA RRM algorithms at the RNC and the Node B.

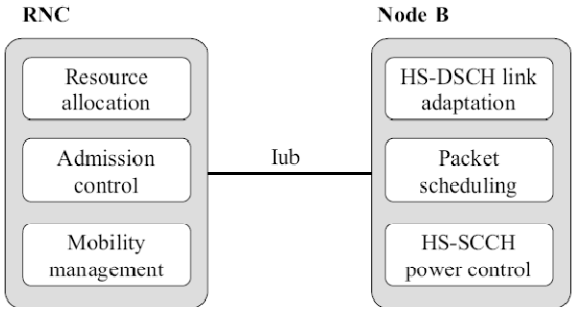

Figure 2.9. Overview of the most relevant HSDPA RRM algorithms (extracted from [HoTo06]).

High-Speed DL Shared Channel (HS-DSCH) link adaptation, responsibility of Node B, is to adapt the bit rate every Time Transmission Interval (TTI) when a user is scheduled for transmission. This is

based on Channel Quality Information (CQI) reports, which are periodically sent by the UE informing about the maximum transport block size that can be correctly received. Also in the Node B, packet scheduling controls how each HSDPA user is served. It is based on quality feedback, UE capability, resource availability, buffer status, QoS and priority. There are many algorithms to perform packet scheduling, such as Round Robin (RR) and Proportional Fair (PF). On the former, all HSDPA users have equal probability for scheduling, and it does not consider their QoS requirements, while the latter is based on feedback information and it provides a fairer split of the available resources among users, also enabling the enhancement of HSDPA cell throughput and coverage.

High-Speed Shared Control Channel (HS-SCCH) power control algorithms, performed by Node B, adjust the transmission power every TTI. This power regulation is based on CQI reports or Dedicated Physical Control Channel (DPCCH) power control commands.

At RNC, resource allocation algorithms manage the power and channelisation codes assigned to the Node B. As channelisation codes for High-Speed Physical DL Shared Channel (HS-PDSCH) can only be used for HSDPA, it leads to a voice or data call blocking of Release '99 users if the codes reserved to HS-PDSCH are too many. In this case the resource allocation is responsible for deciding and releasing some of the HS-PDSCH codes to avoid voice call blocking. It is also responsible for allocation of multiple HS-SCCH codes in code multiplexing and for power management of Real Time (RT) DCH connections. Admission control, also performed by RNC, is used to decide if a new user is accepted in the cell and to decide if it is going to be served using HSDPA or DCH (Release '99). Considering QoS requirements and the measurements given by the Node B, this algorithm can decide if the Node B has enough capacity to serve new users with the required service, maintaining all others users with their specific QoS. Finally, the mobility management, also at RNC, decides the HS-DSCH serving cell and manages Node B's buffer to minimise the loss of data packets, since there is no soft handover in HSDPA. HS-DSCH handovers are synchronised, allowing full coverage, mobility and avoiding packet losses [PeTM04]. The RNC establishes the active set and makes handover decision typically based on UE Common Pilot Channel (CPICH) measurements.

In HSDPA, it is possible to consider three types of handover:

- inter Node B HS-DSCH to HS-DSCH handovers, between different Nodes B,
- intra Node B HS-DSCH to HS-DSCH handovers, between 2 sectors in the same Node B and HS-DSCH to DCH handover,
- HS-DSCH to DCH, it happens when the UE moves to a non-HSDPA area or UE entering HSDPA zones.

In inter Node B handover, packet losses due to changes in the HS-DSCH serving cell can be minimised with the RNC acknowledged (ACK) mode or when duplicate packets are sent on RLC unacknowledged mode. In intra Node B handover, with MAC-high speed (MAC-hs) preservation, packet losses are avoided. Since High-Speed Dedicated Physical Control Channel (HS-DPCCH) is received simultaneous by both sectors, in intra Node B handover, UL coverage is improved.

2.4.3 Capacity and Coverage

HSDPA performance depends on network algorithms, deployment scenarios, traffic generated, QoS and UE receiver performance and capability.

HSDPA uses a SF of 16, but only 15 codes can be allocated for data transmission, as one is needed for HS-SCCH and common channels. On UE until 5, 10 or 15 codes can be allocated, but in the Node B the 15 codes can be allocated. There are 12 HSDPA UE categories as shown in Table 2.3.

Table 2.3. HSDPA terminal capacity categories (extracted from [HoTo06]).

UE Category	Maximum number of parallels codes per HS-DSCH	Modulation	Minimum inter-TTI interval	ARQ type at maximum data rate	Achievable Maximum data rate [Mbps]
1	5	QPSK & 16QAM	3	Soft	1.2
2	5	QPSK & 16QAM	3	IR	1.2
3	5	QPSK & 16QAM	2	Soft	1.8
4	5	QPSK & 16QAM	2	IR	1.8
5	5	QPSK & 16QAM	1	Soft	3.6
6	5	QPSK & 16QAM	1	IR	3.6
7	10	QPSK & 16QAM	1	Soft	7.2
8	10	QPSK & 16QAM	1	IR	7.2
9	15	QPSK & 16QAM	1	Soft	10.2
10	15	QPSK & 16QAM	1	IR	14.4
11	5	QPSK only	2	Soft	0.9
12	5	QPSK only	1	Soft	1.8

The metrics used to assess network performance in HSDPA are different from those used in Release '99. For HSDPA, the signal to noise ratio (E_b/N_0) is not used, since the HS-DSCH bit rate varies every TTI with the use if different modulations and coding schemes, Effective Code Rate (ECR) and number of HS-PDSCH channels. So the performance of HSDPA can be evaluated by the HS-DSCH Signal to Interference plus Noise Ratio (SINR) for link budget planning and network dimensioning, after de-spreading the HS-PDSCH. The HS-DSCH SINR for a single antenna Rake receiver can be defined as:

$$\rho_i = SF_{16} \cdot \frac{P_{HS\text{-}DSCH}}{(1-\alpha)\cdot P_{intra} + P_{inter} + P_{noise}} \quad (2.18)$$

where:

- ρ_I is the SINR
- SF_{16} is the HS-PDSCH SF of 16;
- $P_{\text{HS-DSCH}}$ is the received power of the HS-DSCH summing over all active HS-PDSCH codes;
- P_{intra} is the received intra-cell interference;
- P_{inter} is the received inter-cell interference.

There are other measurements used for performance analysis, like instantaneous HS-DSCH SINR and the average HS-DSCH SINR, the former measure the SINR per TTI on the HS-DSCH in order to accomplish a certain Block Error Ratio (BLER) for a given HS-PDSCH number of codes, type of modulation and coding scheme, while the latter indicates the HS-DSCH SINR average experienced by

a user over fast fading. For network dimensioning the pilot E_c/N_0 is used as a measurement. This is based on the wideband average Primary-Common Pilot Channel (P-CPICH) E_c/N_0 and with it is possible to achieve HSDPA single user throughput. Expression (2.18) shows how the average HS-DSCH SINR can be expressed as a function of P-CPICH E_c/N_0.

$$SINR = SF_{16} \cdot \frac{P_{HSDPA}}{\frac{P_{pilot}}{\rho_{pilot}} \alpha P_{total}} \quad (2.19)$$

where:

- PHSDPA is the HSDPA transmit power;
- Pilot is the P-CPICH transmit power;
- ρpilot is the P-CPICH Ec/N0 when HSDPA is active.

The average cell throughput increases with the number of HS-PDSCH codes having a growth of 50% when the number of codes is modified from 5 to 10. Fast link adaptation and Hybrid ARQ (HARQ) contributes to have a capacity gain of almost 70 % when compared to Release 99 [HoTo06].

2.5 HSUPA

In this section, the HSUPA key technologies and channels are presented, based on [HoTo06]. Characterisation of performance, capacity and coverage of HSUPA follow an overview on its RRM.

2.5.1 Key Updates

In order to match UL and DL capabilities, 3GPP specified the Release 6, the Enhanced DCH (E-DCH), often referred as HSUPA. HSUPA is not a standalone feature, since it uses most of the basic features of Release '99 in order to work, the improvement being on the radio interface, maintaining all other network elements unchanged. Table 2.4 presents the new elements functions.

Similarly to HSDPA, HSUPA introduces a faster physical layer HARQ, Node B scheduling and, optionally, a shorter TTI of 2ms. The HARQ in HSUPA is fully synchronous with incremental redundancy and operates in soft handover. Scheduling moved to Node B and as HSUPA is a many-to-one structure, contrary to HSDPA, a dedicated channel approach was chosen. The modulation used in Release '99 for the UL, BPSK, was adopted for HSUPA since it has also transmission with multiple channels, avoiding complex implementations at the UE side.

For HSUPA new channels were, also, added, like in HSDPA. For the DL three channels were added, two for scheduling control and one retransmission support. For the UL the DCH channels from Release '99 were left unchanged and two new channels were introduced, one for new control information and another for carrying data the E-DCH Dedicated Physical Data Channel (E-DPDCH). For HSUPA, the E-DCH is a dedicated channel, like DCH in Release '99, but with fast retransmission and scheduling. More detailed information about these channels is given in [HoTo06].

The E-DPDCH is a channel parallel to all UL dedicated channels of Release 5, and it is used to transmit from the UE to the Node B due to transport channel processing. The most notable differences from DPDCH of Release '99 are the new TTI length of 2ms and minimum SF of 2. The former allows delivering twice as many channel bits per code than the minimum SF of 4 that the DPDCH supports and the last is used due to its potential delay benefit. The E-DCH Dedicated Physical Control Channel (E-DPCCH) is used to transmit out-of bound information about E-DPDCH transmission from the UE to the Node B.

Table 2.4. New functionalities on different elements due to HSDPA (adapted from [HoTo06]).

RNC	HSUPA radio resource and mobility management HSUPA Iub capacity allocation Larger uplink data volume Packet re-ordering
Node B	Data buffering ARQ handling with soft value buffer Feedback encoding Uplink scheduling against interference/baseband/Iub capacity
UE	ARQ handling Transmitted power and buffer status feedback generation and transmission Multicode transmission Uplink scheduling

A comparison of the key features for Release '99, HSDPA and HSUPA is show at Table 2.5.

Table 2.5. Release 99, HSDPA and HSUPA comparison table (extracted from [HoTo06]).

Feature	Release '99 (DCH)	HSDPA (HS-DSCH)	HSUPA (E-DCH)
Variable SF	Yes	No	Yes
Fast power control	Yes	No	Yes
Adaptive modulation	No	Yes	No
BTS based scheduling	No	Yes	Yes
Fast L1 HARQ	No	Yes	Yes
Soft handover	Yes	No	Yes
TTI length [ms]	80, 40, 20, 10	2	10, 2

2.5.2 Radio Resource Management

As in HSDPA RRM algorithms, using HSUPA physical layer enhancements increase the capacity and end user performance, being also responsible for ensuring network stability. RRM consists of functions located in the RNC, Node B and UE, as shown in Figure 2.10.

For the RNC, one considers resource allocation, admission control, QoS parameters and mobility management. For the Node B, the new functions, compared to Release '99, are fast packet

scheduling and the HARQ. Resource allocation is an algorithm responsible for establishing the maximum received wideband power level at the Node B. HSUPA scheduler can allocate the power for E-DCH users since that is not used by DCH connections and is still below the maximum wideband power level. The RNC can also send a congestion indication to Node B. A number of QoS parameters are given by RNC to the Node B and it can be used to packet scheduling. The decisions are made by the Node B taking those parameters into account. Admission control is responsible for authorising new users, based on information like the number of active HSUPA users, UL interference levels (based on Received Total Wideband Power (RTWP) measurements), Scheduling Priority Indicator (SPI) of new calls, Guaranteed Bit Rate (GBR) for all other existing call, bit rates on both DCH and E-DCH, and also DL limitations. With the algorithm mobility management, the RNC decides which cells belong to the active set, with the maximum of 4 Node Bs and which one is serving the HSUPA. The serving cells for HSUPA and HSDPA can be different, although typically they are the same and the serving cell change would take place at the same time.

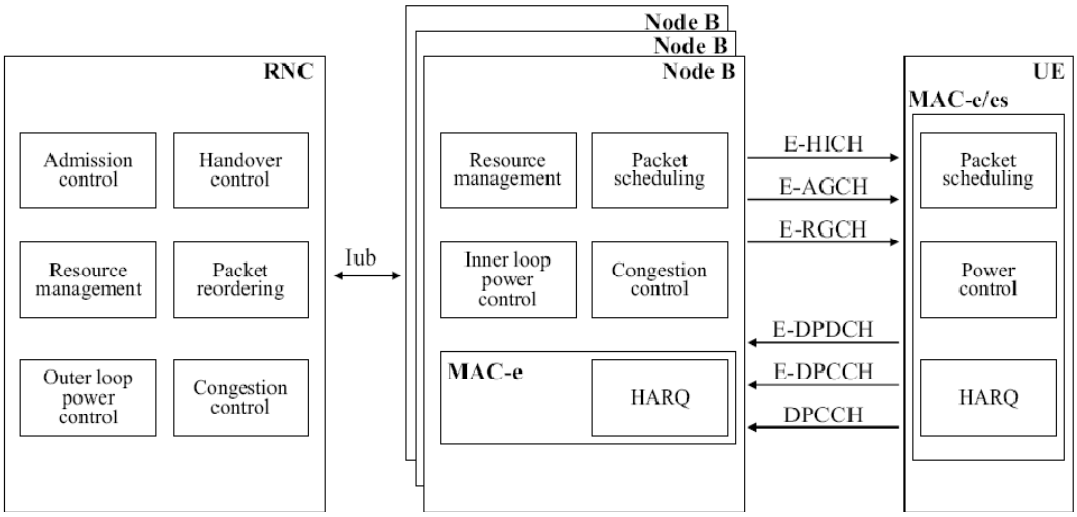

Figure 2.10. Overview of the different functional RRM blocks for HSUPA (extracted from [HoTo06]).

For the Node B the main innovation at Release 6 is the fast packet scheduling with HARQ retransmission. There are two scheduling different modes defined for HSUPA, scheduling with HARQ control signalling and non scheduled mode controlled by RNC, very similar to DCH scheduling for Release '99, but with physical layer retransmission.

2.5.3 Capacity and Coverage

As in HSDPA, performance in HSUPA depends highly on network algorithms, deployment scenarios, UE transmitter capability, Node B performance and capability and type of traffic. In HSUPA there are six UE classes defined, Table 2.6. For performance testing purposes, 3GPP defined a set of E-DCH channel configurations, Fixed Reference Channels (FRCs).

E_c/N_0 is the performance metric used by HSUPA, the as used in Release '99, since there is no Adaptative Modulation and Coding (AMC). In order to achieve higher data rates, a high E_c/N_0 is required at the Node B, which leads to an increase of the UL noise and consequently the cell

coverage area decreases. Taking this into account, a maximum level for UL noise may be defined for macro-cells, though it limits high data throughputs. FRC5 represents a first-phase HSUPA UE, FRC2 and FRC6 represents future release UEs, with advanced capabilities, like supporting 2ms for TTI and higher coding rate. As expected, for FRC2 higher throughputs are achieved, although the maximum shown can only be accomplished for high E_c/N_0 values, which in real networks may be difficult to achieve.

Table 2.6. HSUPA terminal capability categories (adapted from [HoTo06]).

UE Category	FRC	TTI length [ms]	Codes	Coding rate	Maximum theoretical bit rate [Mbps]	Physical Layer Data Rates [Mbps]
1	7	10	SF16	0.29	0.069	0.72
1	4	10	SF4	0.53	0.508	0.72
2	1	2	2 × SF4	0.71	1.353	1.45
2 and 3	5	10	2 × SF4	0.51	0.980	1.45
4	2	2	2 × SF2	0.71	2.706	2.91
4 and 5	6	10	2 × SF2	0.51	1.960	2
6	3	2	2×SF4 + 2×SF2	0.71	4.059	5.76

For HSUPA, a new measurement was introduced, the UE Power Headroom (UPH), that informs Node B of the available power resources. This measurement is similar to CQI, in the HSDPA case, but due to the inaccuracy in measurements, it cannot be used with the same functionality as the CQI.

Faster Retransmissions at L1 than in L2 RLC-based and the use of soft combining of retransmissions are the two main advantages of the use of L1 HARQ. The decrease of E_b/N_0, lead by faster retransmission, increase spectral efficiency, while the combining techniques can improve the performance of Node B. Increasing the Block Error Probability (BLEP) at first transmission leads to a lower E_b/N_0 requirement, which increases UL's spectral efficiency. Assuming realistic traffic, the cell throughput gain due to the use of L1 HARQ is approximately 15% to 20%.

Considering Node B based scheduling, it can provide the system with two main advantages, tighter control of total received UL power and faster reallocation of radio resources among users. The former, allows faster adaptation to interference variations, and, the later, dynamically take resources from users with low utilisation of allocated radio resources and redistributes them between users with high utilisation. Node B based scheduling provides a cell throughput increase of approximately 15% to 20% on top of the gain from L1 HARQ.

2.6 LTE

The LTE system architecture is presented, followed with a brief description of its radio interface. At the end a performance analysis is done. This section is based on [3GPP08].

2.6.1 Network Architecture

The LTE architecture is a flat architecture, as shown in Figure 2.11. Similar HSDPA and HSUPA, more intelligence is being added to the BS. The radio-related functionalities are all located in the BS, compared to HSDPA/HSUPA the new functionalities are Radio Link Control (RLC) Layer, Radio Resource Control (RRC) and Packet Data Convergence Protocol (PDCP) functionalities.

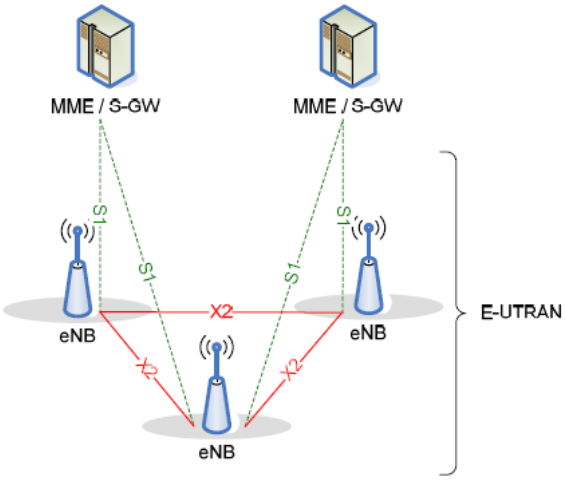

Figure 2.11. Overall E-UTRAN architecture (extracted from [3GPP08]).

The Evolved-UTRAN (E-UTRAN) consists of one single element, the evolved Node B (eNB) that has all functions for RRM, such as radio bearer control, radio admission control, connection mobility control and dynamic resource allocation (scheduling). eNBs are interconnected with each other by means of the *X2* interface. It is assumed that there is always an *X2* interface between the eNBs that need to communicate with each other, e.g., for purposes of handover. Connected to the eNBs, by means of *S1* interfaces, is the Evolved Packet Core (EPC). The EPC is composed by the Mobility Management Entity (MME) and the Serving Gateway (S-GW) and the Packet Data Network (PDN) Gateway (P-GW). The interface between core and radio access network is defined in such a way that implementation in the core network side would be possible with control (*S1_MME*) and user-plane (*S1_UE*) traffic processing in separate physical elements. The S1 interface supports a many-to-many relation between MMEs / S-GWs and eNBs.

The S-GW and P-GW were defined for processing the user-plane data, handling tasks related to the mobility management inside the LTE, as well as between other 3GPP radio technologies, IP header compression and encryption of user data streams and termination of user-plane packets for paging reason. MME handles the control plane signalling, and especially for mobility management and idle-mode handling by the distribution of paging messages to the eNBs.

The functional split between E-UTRAN and EPC is described in Figure 2.12. The functionalities of UMTS RNC were split between BS and S-GW, which has also the functionalities of SGSN. The P-GW is similar to GGSN and the MME to the HLR and VLR in UMTS.

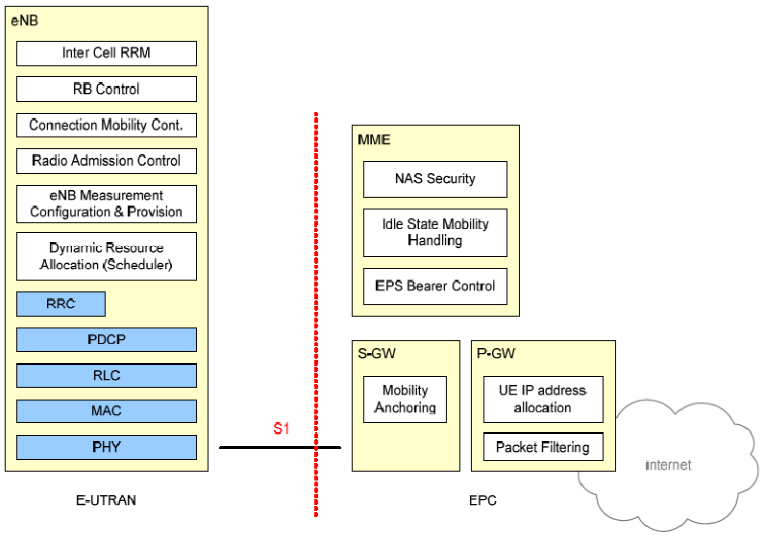

Figure 2.12. Functional split between E-UTRAN and EPC (extracted from [3GPP08]).

2.6.2 Radio Interface

The multiple access is based on the use of SC – Frequency Division Multiple Access (SC-FDMA) with cyclic prefix in the UL and OFDMA in the DL.

SC-FDMA with cyclic prefix has a QAM modulator coupled with the addition of the cyclic prefix. This technology brings some benefits. With cyclic prefix the ISI is eliminated, which enables the low complexity equaliser receiver. PAR is dominated by the modulation in use and SC-FDMA has the capability to reach a performance similar to OFDMA, assuming an equaliser is being used.

In the design, the physical layer parameter details have been picked in such a way that implementing multimode GSM/WCDMA/LTE devices would be simpler, as well as facilitating the measurements to/from GSM/WCDMA for radio-based handovers to enable seamless mobility.

The fundamental difference to WCDMA is now the use of different bandwidths, from 1.4 up to 20 MHz. Parameters have been chosen such that FFT lengths and sampling rates are easily obtained for all operation modes and at the same time ensuring the easy implementation of dual mode devices with a common clock reference. Table 2.7 shows the parameters for the different bandwidths

In what concerns transport channels there are similarities with Release ‘99 common channels. A brief description of the LTE transport channels can be found in [HoTo07]. The LTE physical layer is designed for maximum efficiency of packet-based transmission. For this reason there are only shared channels in the physical layer to enable dynamic resource utilisation. Additionally, there are two types of signal defined, which are, synchronisation signal, to facilitate cell search (similar to WCDMA Synchronisation Channel), and reference signal, for facilitating channel estimation and channel quality estimation.

LTE has two radio frame structures, frame structure type 1 that uses both FDD and TDD duplexing, and frame structure type 2 that uses TDD duplexing. Frame structure type 1 is optimised to co-exist with 3.84 Mcps UMTS. Frame structure type 2 is optimised to co-exist with 1.28 Mcps UMTS TDD,

also known as Time Division-Synchronous Code Division Multiple Access (TD-SCDMA). This thesis focus on frame structure type 1, since it is optimised to co-exist with the lower releases of UMTS and is has FDD. Frame structure type 1 is shown in Figure 2.13.

Table 2.7. Key Parameters for different bandwidths (extracted from [HoTo07]).

	1.4 MHz	3.0 MHz	5 MHz	10 MHz	15 MHz	20 MHz
Sub-frame (TTI) [ms]	1					
Sub-carrier spacing [kHz]	15					
Sampling [MHz]	1.92	3.84	7.68	15.36	23.04	30.72
FFT	128	256	512	1024	1536	2048
Sub-carriers	72+1	180+1	300+1	600+1	900+1	1200+1
Symbols per frame	4 with short CP and 6 with long CP					
Cyclic prefix	5.21 µs with short CP and 16.67 µs with long CP					

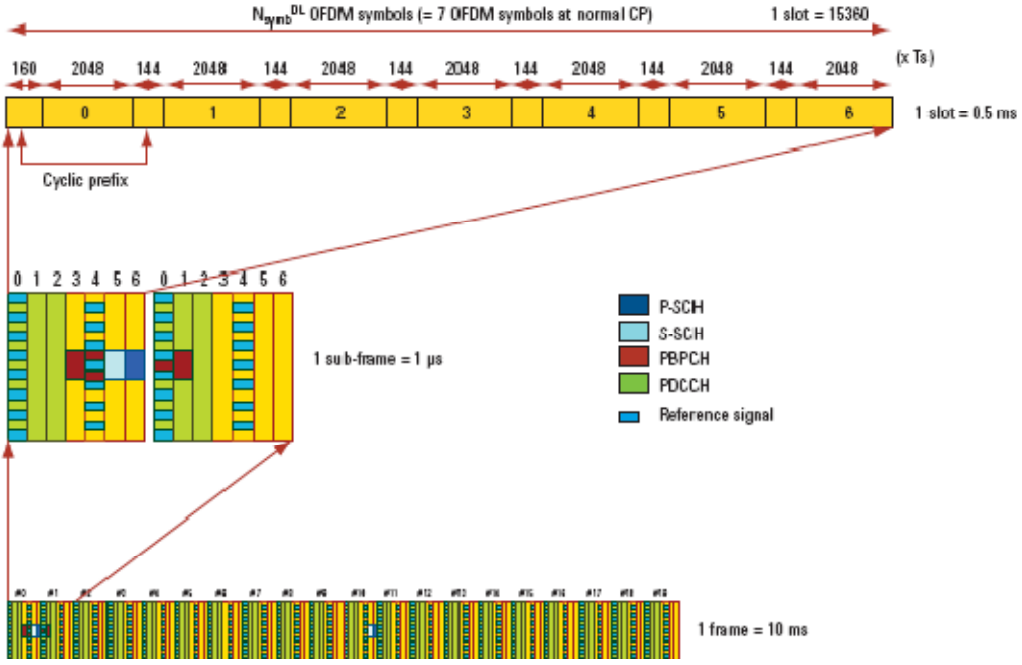

Figure 2.13. DL frame structure type 1 (Extracted from [Agil07]).

As it is shown at Figure 2.13, the DL radio frame has a duration of 10 ms and consists of 20 slots with a slot duration of 0.5 ms. Two slots comprise a sub-frame. A sub-frame, or TTI, has a duration of 1 ms compared to 2 ms TTI for HSPA systems. Shorter TTIs reduce the latency in the system, but add further demands on the MT processor. The physical mapping of DL physical signals for frame structure type 1 is:

- Reference signal, which is transmitted at OFDM symbol 0 and 4 of each slot. This depends on antenna port number;
- Primary–Synchronisation Channel (P-SCH), which is transmitted on symbol 6 of slots 0 and 10 of each radio frame;
- Secondary–Synchronisation channel (S-SCH), which is transmitted on symbol 5 of slots 0 and 10 of each radio frame;

- PBCH physical channel, which is transmitted on 72 sub-carriers centred around the DC sub-carrier.

The smallest time-frequency unit for DL transmission is called a resource element, which is one symbol on one sub-carrier. A group of 12 contiguous sub-carriers in frequency and one slot in time form a Resource Block (RB) as shown in Figure 2.14. Data is allocated to each UE in units of RB.

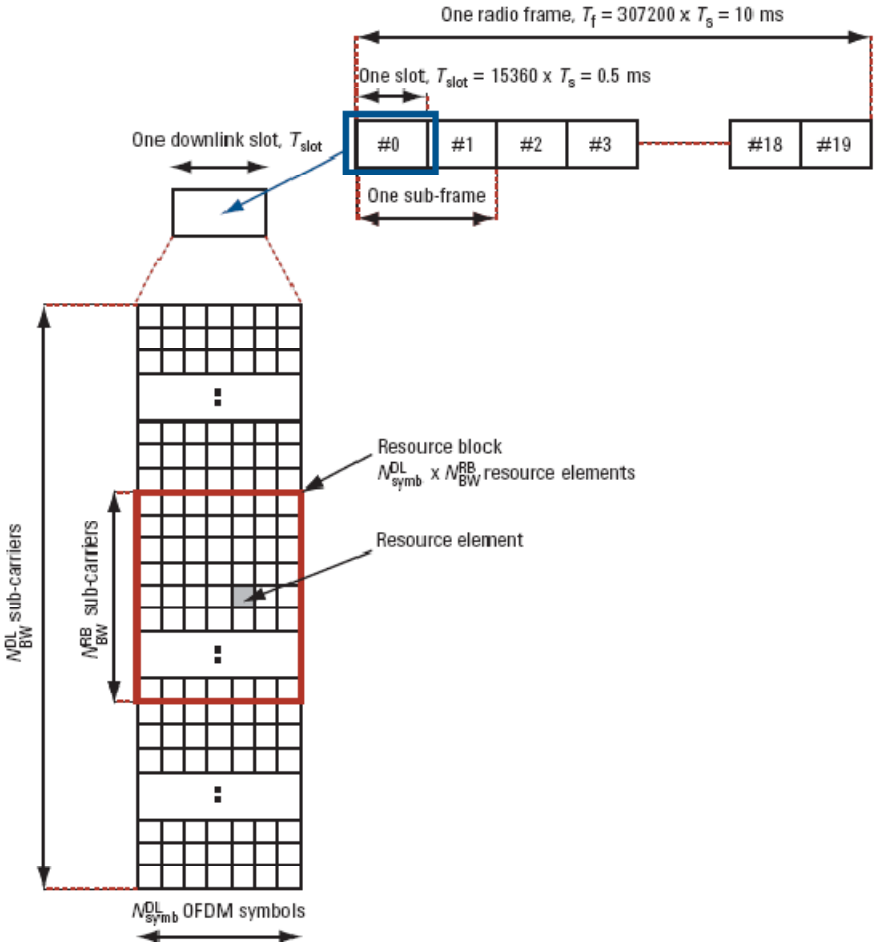

Figure 2.14. DL Resource Grid (extracted from [Agil07]).

For a frame structure type 1, using normal CP, a RB spans 12 consecutive sub-carriers and 7 consecutive OFDMA symbols over a slot duration. For extended CP there are 6 OFDMA symbols per slot. A CP is appended to each symbol as a guard interval. Thus, an RB has 84 resource elements (12 sub-carriers x 7 symbols) corresponding to one slot in the time domain and 180 kHz (12 sub-carriers x 15 kHz spacing) in the frequency domain. The size of a RB is the same for all bandwidths; therefore, the number of available physical RBs depends on the transmission bandwidth. In the frequency domain, the number of available RBs can range from 6, when transmission bandwidth is 1.4 MHz, to 100, when transmission bandwidth is 20 MHz.

The UL frame structure type 1 is the same as DL's one in terms of frame, slot, and sub-frame length. An UL slot structure is shown in Figure 2.15. The number of symbols in a slot depends on the CP length. For a normal CP, there are 7 SC-FDMA symbols per slot. For extended CP there are 6 SC-FDMA symbols per slot. UL demodulation reference signals, which are used for channel estimation for coherent demodulation, are transmitted in the fourth symbol (i.e., symbol number 3) of the slot.

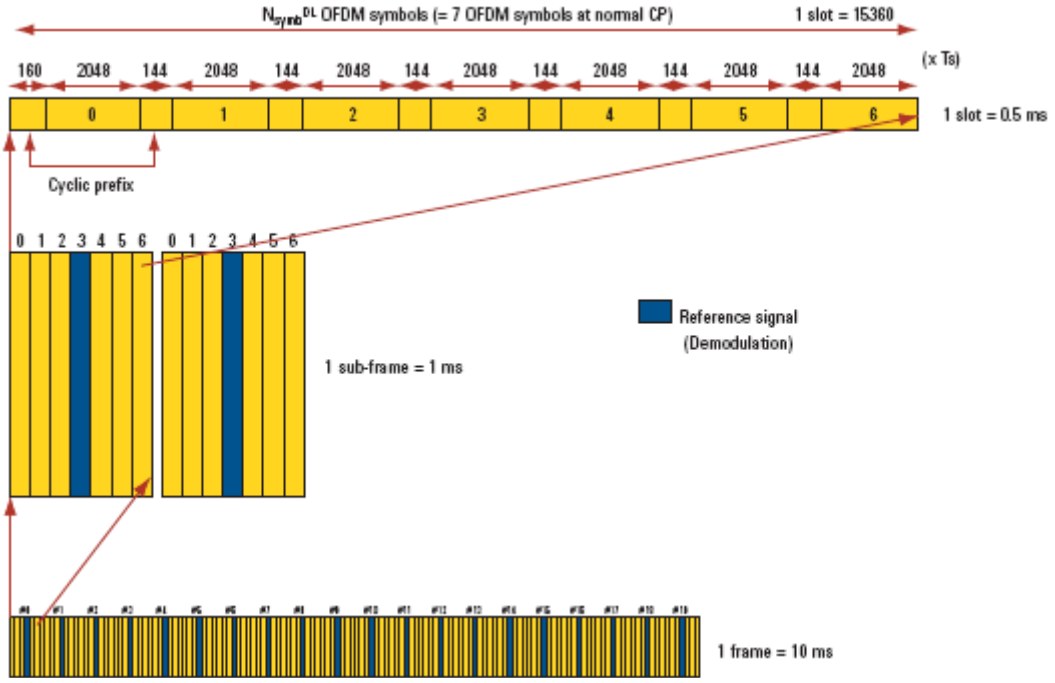

Figure 2.15. UL frame structure type 1 (extracted from [Agil07]).

For LTE there are three potential frequency bands, in the 3GPP specified UMTS spectrum, to operate, the 900 MHz band, [890;915] MHz for UL and [935;960] MHz for DL, the 2100 MHz frequency band and the 2600 MHz band, [2500;2570] MHz for UL and [2620;2690] MHz for the DL [Huaw07].

2.6.3 Capacity and Coverage

The resulting data rate for a particular user will depend on the number of resource blocks allocated, modulation applied, rate of the channel coding, whether MIMO is used or not and the configuration, amount of overhead, including whether long or short cyclic prefix is used.

The DL peak bit data rates can be calculated by,

$$R_{b\ [\text{Mbps}]} = \frac{\text{bits}}{\text{Hz}} \times N_s \times \frac{N_{SF}}{T_{SF}} \tag{2.20}$$

where:

- N_{SF} is the number of symbols per sub-frame;
- T_{SF} is the sub-frame period.

The achieve DL peak bit rates are shown in Table 2.8. QPSK modulation carries 2 bits per symbol, 16QAM 4bits per symbol and 64QAM 6 bits. And 2x2 MIMO further doubles the peak bit rate. Therefore, QPSK ½ rate coding carries 1bps/Hz, and 64QAM without any coding and with 2x2 MIMO carries 12 bps/Hz. The bandwidth is included in the calculation by taking the corresponding number of sub-carriers for each option, 72 per 1.4 MHz and 180 per 3.0 MHz bandwidth. For the bandwidths of 5, 10, and 20 MHz there are assumed 300, 600 and 1200 subcarriers respectively. It is assumed 13 data symbols per 1 ms sub-frame. The highest theoretical data rate is approximately 170 Mbps.

For the UL the achieve peak data rates are shown in Table 2.9. The peak data rates are lower in UL than in DL since single user MIMO is not specified in UL. MIMO can be used in UL as well to increase

cell data rates, not single-user peak data rates.

Figure 2.16 shows how the maximum system throughput values depend on the cell radius. It can be seen that with LTE for the same radii higher throughputs than in HSDPA, can be achieved. For the lowest radius an increase of 125% in the throughput is noticed and as the radius increases LTE overcomes the HSDPA throughput until 300%.

Table 2.8. DL peak bit rates (extracted from [HoTo07]).

		Peak bit rate per sub-carrier/bandwidth combination [Mbps]				
Modulation Coding		72/1.4 MHz	180/3.0 MHz	300/5.0 MHz	600/10 MHz	1200/20 MHz
QPSK ½	Single Stream	0.9	2.2	3.6	7.2	14.4
16QAM ½	Single Stream	1.7	4.3	7.2	14.4	28.8
16QAM ¾	Single Stream	2.6	6.5	10.8	21.6	43.2
64QAM ¾	Single Stream	3.9	9.7	16.2	32.4	64.8
64QAM 4/4	Single Stream	5.2	13.0	21.6	43.2	86.4
64QAM ¾	2x2 MIMO	7.8	19.4	32.4	64.8	129.6
64QAM 4/4	2x2 MIMO	10.4	25.9	43.2	86.4	172.8

Table 2.9. UL peak bit rates (extracted from [HoTo07]).

		Peak bit rate per sub-carrier/bandwidth combination [Mbps]				
Modulation Coding		72/1.4 MHz	180/3.0 MHz	300/5.0 MHz	600/10 MHz	1200/20 MHz
QPSK ½	Single Stream	0.9	2.2	3.6	7.2	14.4
16QAM ½	Single Stream	1.7	4.3	7.2	14.4	28.8
16QAM ¾	Single Stream	2.6	6.5	10.8	21.6	43.2
16QAM 4/4	Single Stream	3.5	8.6	14.4	28.8	57.6
64QAM ¾	Single Stream	3.9	9.0	16.2	32.4	64.8
64QAM 4/4	Single Stream	5.2	13.0	21.6	43.2	86.4

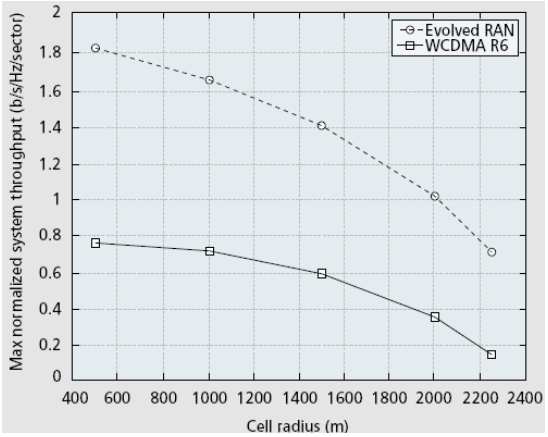

Figure 2.16. Normalised cell throughput vs. cell radius in fully loaded systems (extracted from [EFKM06]).

2.6.4 Comparison between LTE and Mobile WiMAX

One of the technologies that emerged as a potential alternative to cellular technology for wide-area networks, and therefore as an LTE alternative, is Mobile WiMAX, also known as WiMAX IEE/802.16e. This technology was initially developed for fixed broadband wireless access and is optimised for broadband data services, unlike LTE that was created with the purpose of provide data services over a network originally conceived for mobile voice services. The description of Mobile WiMAX is presented on [WIMA08] and [Nuay07].

As LTE in DL, Mobile WiMAX is based on OFDM/OFDMA, but in both UL and DL, and like LTE, it provides high data rates with MIMO antenna techniques in flexible sub-channelisation schemes. Despite these two systems have the same radio interface they have different OFDM/OFDMA parameters. The Table 2.10 summarises the principal attributes of the two systems that are being compared. The higher value for DL is obtained considering MIMO (2x2) mode.

Table 2.10. Summary of Comparative Features (adapted from [WiMF06b]).

Attributes	LTE	Mobile WiMAX
Duplex Mode	FDD	TDD
DL Multiple Access	OFDMA	OFDMA
UL Multiple Access	SC-FDMA	OFDMA
Channel Bandwidth	1.4,3,5,10,15,20 MHz	Scalable: 5,7,8.75,10 MHz
Frame Size	1 ms FDD	5 ms TDD
Modulation	QPSK, 16QAM, 64QAM	QPSK, 16 QAM, 64QAM
Coding	CTC	CTC
DL Peak Data Rate	172.8 Mbps (20 MHz BW)	46 Mbps – DL/UL= 3:1 32 Mbps – DL/UL= 1:1 (10 MHz BW)
UL Peak Data Rate	86.4 Mbps (20 MHz, Single Antenna)	4 Mbps – DL/UL = 3:1 7 Mbps – DL/UL = 1:1 (10 MHz BW)
Scheduling	Fast Scheduling in the DL and UL	Fast Scheduling in DL and UL
Spectral Efficiency - DL [bps/Hz]	2.73	1.91
Spectral Efficiency - UL [bps/Hz]	0.7	0.84
Mobility	High	Low/Mid

In what concerns to the system architecture, WiMAX has an architecture identical to the lower releases of 3GPP. LTE has a flat architecture, while WiMAX architecture can be divided in three general areas where which one performs a specific function in the connection as UMTS architecture.

UTRAN in UMTS/HSPA and Access Service Network (ASN) in Mobile WiMAX are the entities responsible for all functionalities concerned with the radio connectivity. The handover control is located in RNC in HSPA. In Mobile WiMAX, it can be inside the ASN Gateways (ASN-GW), in case of

profile A, or inside the BS if the profile chosen is the profile C. Scheduling is an important feature of RRC and is handled in Node B in HSPA and in ASN-GW or WiMAX BS, depending on the profile, in Mobile WiMAX. CN is the functional area that connects external PS or CS and UMTS PLMN. In Mobile WiMAX, the functions and equipment that enables IP connectivity to subscribers are part of Connectivity Service Network (CSN). Finally, the end-user is known as Subscriber Station (SS) in Mobile WiMAX and is denominated UE in UMTS/HSPA [Preg08].

2.7 Service and Applications

UMTS was designed to offer flexible services, on contrary of GSM that was designed to have an efficient delivery of voice services. UMTS represent as evolution in terms of capacity and data speeds, guaranteeing the appearance of whole new services in addition to existing ones. This section is based on [HoTo06] and [Molis04].

In order to allow efficient ways to accessing services and optimise system capacity, 3GPP defined four classes of services based on their Quality of Service (QoS) requirements. There are some important factors that distinguish them, such as traffic delay, the guaranteed bit rate and the different priorities. The four classes are conversational, Streaming, interactive and background.

The conversational class is mainly intended for speech services (e.g., CS or Voice over Internet Protocol (VoIP)). Since to this type of services is a real time one the delay should be on the order of 400ms or less, larger values being experienced as unpleasant interruptions by users, traffic is nearly symmetric between UL and DL. Video telephony has even tighter BER requirements than voice due to video compression, and it can be transmitted in CS or PS. It is supposed to work on the PS domain, and in order to guarantee an efficient VoIP service QoS differentiation and IP header compression are needed. This class has priority over others.

The speech codec used in UMTS employees Adaptative Multirate (AMR) with eight source rates, namely 12.2 kbps for GSM. Discontinuous Transmission (DTX) is used in the AMR codec in order to reduce the average required bit rate, leading to a lower interference level, hence increased capacity. In 3GPP Release 5 another codec was introduced, the AMR wideband (AMR-WB), which brought substantial voice quality enhancements compared to AMR narrowband or even the standard fixed telephone line; it operates on nine speech coding bit rates between 6.6 and 23.85 kbps.

The Streaming class represents the audio and video Streaming services. Multimedia Streaming enables the end user to access the data before the transfer is complete, which is achieved through a continuous stream transmission and the use of buffers in the final applications. In this case, the traffic is not symmetric; hence the DL traffic is the most significant. Larger delays than in conversational class can be tolerated, as the receiver typically buffers several seconds of Streaming material.

The interactive class encompasses user data request from a remote appliance (e.g., Web browsing), it means a communications scheme that is characterised by the request response pattern of the end

user. This class has a very asymmetric traffic and is tolerant to delay. For this class there are upper limits to tolerable delay, such as the time between choosing a certain Website and its actual appearance on the screen should not exceed a few seconds. For multiplayer games the Round Trip Time (RTT) is a very important parameter, especially in real time action games, which besides having transmitting and receiving packets at bit rates typically of 10-20 kbps, must be delivered with very low delay, setting high requirements for the network performance. In order to satisfy the most demanding players the end-to-end, delays must be as low as 70 to 80 ms.

Background class encompasses the services where transmission delays are not critical (e.g., Short Message Service (SMS), e-mail), on contrary to interactive class the end user is not waiting for a response within a short time. This type of services only spends the network resources when they are not needed for application from the former classes. This class, like the interactive class, is intolerant to transmission errors. Some of the applications in this class are the SMS, Multimedia Message Service (MMS) and e-mail delivery.

In the following table, Table 2.11, the main differences between the 3GPP classes are presented.

Table 2.11. Services and applications according to 3GPP (extracted from [3GPP01] and [3GPP02])

Service Class	Conversational	Streaming	Interactive	Background
Real time	Yes	Yes	No	No
Symmetric	Yes	No	No	No
Switching	CS	CS	PS	PS
Guaranteed rate	Yes	Yes	No	No
Delay	Minimum Fixed	Minimum Variable	Moderate Variable	High Variable
Buffer	No	Yes	Yes	Yes
Bursty	No	No	Yes	Yes
Example	Voice	Video on Demand	Web Browsing	E-mail

Chapter 3

Models and Simulator Description

The present chapter provides an overview of the single user radius model and the LTE DL/UL simulator. The former provides an overview of the network planning regarding cell radius for LTE DL and UL, when a single user is at the cell edge requiring a service. This model is a good tool for a first phase of network planning to estimate cell radii. The latter, based on an existing simulator, has the goal of enabling a more realist analysis case, with users randomly spread over the cell coverage areas when they are performing multiple services. The main outputs of this simulator are the average network radius, average network throughput, among others. At the end of this chapter the simulator assessment is presented with the study of the number of users to be considered in the simulations.

3.1 Single User Radius Model

The purpose of this section is to make an evaluation of the performance of LTE in a single user model. This evaluation is done by means of the maximum cell radius, which is the maximum distance that allows the user to be served with the requested throughput, calculated considering that there is only one user in the cell. Several parameters can be modified, such as:

- Total BS transmission power;
- Frequency;
- Bandwidths;
- Modulation scheme;
- MIMO configuration;
- BS and MT antenna gains;
- Environment, i.e., pedestrian, vehicular, indoor with low and high losses and fading margins.

Other parameters, like additional losses, noise factor, cable losses, user losses and diversity gain, in DL, can also be modified.

At the maximum throughputs obtained at the physical layer, Table B.5 and Table B.6, it is necessary to consider the reduction throughput due to coding rate, bandwidth efficiency, CP, pilot overhead (just in the DL) and dedicated and common control channel.

The limiting factors are the available bandwidth, modulation scheme and also MIMO configuration. These three factors restrain the maximum throughput. The LTE receiver sensitivity, as well as the path loss, are calculated by using Annex A expressions.

The goal of this model is to calculate the maximum cell radius for a given throughput, introduced in the user interface, Annex F. Using the expressions of the interpolations and extrapolations in Annex B, the requested throughput is mapped onto SNR for the receiver sensitivity, i.e., minimum received power that allows the user to be served with the requested throughput, (A.7).

In Annex B expressions, two channels are considered, the EPA 5Hz and the ETU 70Hz, described in Annex A. The EPA 5Hz is a pedestrian channel, therefore, it is attributed for pedestrian and indoor users and the ETU 70Hz is vehicular channel, therefore is attributed to the vehicular users.

Since that this expression were only available for 2×2 and 4×4 MIMO antenna configurations, in UL, only this two MIMO configurations were considered for this model. It is important to notice that, due to being a single user model, there is only one user in the cell, so the interference margin is not considered and all RBs are given to the user therefore, a low SNR is need rather than if a limited number of RBs was given. The maximum BS antenna gain is used in order to have the maximum radius, as well as the lowest frequency in the bands. Assumptions were taken like perfect radio channel conditions, interference due to both internal and external factors, and hence, noise raise is not

considered and uncorrelated sub-channels in MIMO are taken. This model is based on a snapshot of the cell, under the best radio condition, but both slow and fast margins are considered. Since the penetration margin varies with frequency, for 2100 and 2600 MHz frequency bands the same penetration margin is considered, since these two bands have very close frequencies. For 900 MHz band, margins are calculated by [XaVe02]:

$$M_{ind_{900\ MHZ}} = M_{ind_{2100\ MHZ}} - 20log\left(\frac{f_{2100}}{f_{900}}\right) \quad (3.1)$$

where:

- $M_{ind_{900\ MHZ}}$ is the indoor penetration at 900MHz;
- $M_{ind_{2100\ MHZ}}$ is the indoor penetration at 2100MHz;
- f_{2100} is the frequency at the 2100 MHz band;
- f_{900} is the frequency at the 900 MHz band.

The path loss is calculated using the link budget detailed in Annex A. From the COST-231 Walfish-Ikegami propagation model, one has [DaCo99]:

$$L_{p_{[dB]}} = L_{0_{[dB]}} + L_{tt_{[dB]}} + L_{tm_{[dB]}} = EIRP_{[dBm]} - P_{r_{[dBm]}} + G_{r_{[dBm]}} - M_{[dB]} \quad (3.2)$$

where:

- L_0 is the free space loss;
- L_{tt} is the rooftop-to-street diffraction loss;
- L_{tm} is the approximation for the multi-screen diffraction loss;
- $EIRP$ is the equivalent isotropic radiated power, given by (A.3) or (A.4);
- M is the total margin, given by (A.9).

Through the manipulation of (3.1) together with the L_{tt} and L_0 expressions from the COST-231 Walfisch-Ikegami model, the cell radius can be calculated by:

$$R_{[km]} = 10^{\frac{EIRP_{[dBm]} - Pr_{[dBm]} + Gr_{[dBi]} - M_{[dB]} - Ltt_{[dB]} - Ltm_{[dB]} - L0_{[dB]}}{20 + k_d}} \quad (3.3)$$

where:

- $L_{tt}^{'} = L_{tt} - k_d \cdot log_{10}(d_{[km]})$;
- k_d is the dependence of the multiscreen diffraction loss versus distance;
- $L_0^{'} = L_0 - 20 \cdot log_{10}(d_{[km]})$.

3.2 LTE DL/UL Simulator

The developed LTE simulator is introduced in this section. First, in Subsection 3.2.1, an overview of the simulator is presented, with the simulator's implementation being described in Subsection 3.2.2. In Subsection 3.2.3, input and output files are pointed out.

3.2.1 Simulator Overview

The main structure of the simulator developed in this thesis is presented in Figure 3.1, being adapted from the one developed in [Card06], [CoLa06], [Lope08], [Salv08] and [SeCa04]. Highlighted in red are the new modules added to the simulator, LTE DL and UL, while the main structure was left partially unchanged.

This simulator has the primary objective of analysing the performance of LTE in both DL and UL and consisting of 4 major modules:

- Users' generation;
- Network deployment without load;
- LTE DL analysis;
- LTE UL analysis.

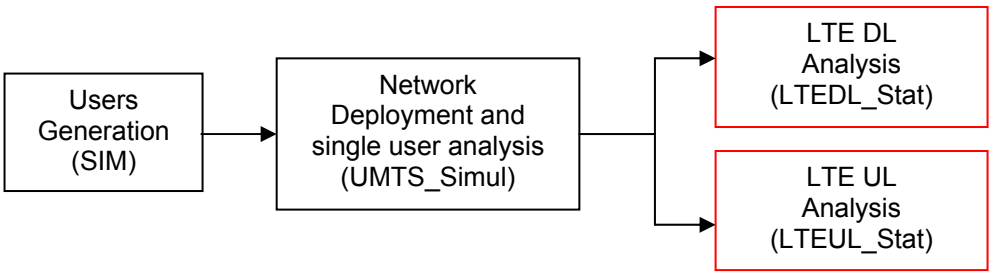

Figure 3.1. Simulator overview.

The user generation module is described in detail in [Lope08] and [Salv08], a file is created with the same information about the user and its location. Users are distributed randomly and services are also randomly distributed among user, according to a given service penetration percentage. The input files for the traffic distribution and the services penetration percentage, needed for users' generation, as well as QoS priority lists, are described in Annex D.

The network deployment module is described with detail in [CoLa06], being responsible for placing the users from the output file of the SIM program in the network, distributing them throughout the most populated areas. After the user's placement, the network is deployed. A first analysis of the network, is also performed, where the cell radius of each service for a single user is calculated, as well as the radius for two reference services, one for the centre of the city and another for the rest of the city. These two reference services define the BS cell coverage. The link budget used in this analysis is the one presented in Annex A. All users within the coverage area are the ones to be considered in the LTE DL and UL modules. In Annex G the user's manual is presented.

3.2.2 LTE DL and UL Analysis Implementation

The modules on LTE were implemented to enable the analysis of the impact caused by LTE DL and UL on the network. Through a snapshot approach, these two modules analysis the network capacity and coverage, calculating instantaneous network results as average radius, and number of users per BS. Also, an extrapolation is made to estimate the traffic and number of users per hour. First an analysis in the BS level is performed, being executed in all BSs. After obtaining some of the

parameters recorded for each BS, these modules compute averages, and extrapolates some results for the busy hour analysis. LTE DL and UL implementations are presented together, since they are analogous, with the differences being pointed out.

To perform the network analysis, some parameters are considered, which can be modified. For LTE DL/UL, one has:

- DL and UL transmission power;
- Frequency;
- MT antenna gain;
- User and cable losses;
- Noise figure;
- Signalling and control power percentage;
- Bandwidth;
- Reduction strategies;
- MIMO configuration;
- Interference margin;
- Environment;
- Masthead Amplifier Gain (UL);
- Diversity Gain (DL);
- Rayleigh Percentage;
- Power feeding antennas;
- Reference services.

Radio parameters, such as DL transmission power, MT antenna gain, user and cable losses, and noise figure are the same as the ones considered in Section 3.1. More parameters like QoS priority list, data volume and throughput for each service, can be changed, as it can be seen in Annex G.

The bandwidth, modulation and MIMO configuration are the key parameters for the performance evaluation of the LTE network. The bandwidth is responsible for the increase of the RBs available in the network, and the capacity of each RB depends on the MIMO configuration and the modulation. Therefore, the maximum instantaneous throughput at the BS is highly associated with these three parameters; still, in the simulator, it was considered that all the BSs have equal parameters, bandwidth and MIMO configuration. Since AMC was implemented the BSs capacity can only be evaluated through the maximum number of RBs that the bandwidth allows. The shared transmission power is not considered in the simulator, as this would require a per-TTI analysis, which is out of the scope of this work. The multiple users influence is simulated by the introduction of the interference margin, specific for each BS.

For signalling and control purposes, in DL, for each RB, one OFDM symbol is discounted related to the reference signals, and in UL one SC-FDMA symbol relate to the reference signals, as it is shown at Figure 2.13 and Figure 2.15, respectively. Concerning to the DL signalling the symbols occupied by the P-SCH and S-SCH are neglected, since they represent 12 OFDM symbol in a frame, which

corresponds to percentages lower than 0.2% in the best case, so the error for not be considered is so low that is assumed to be negligible.

As in DL the expressions available were for SIMO configuration it becomes necessary to calculate the SISO ones to afterwards obtain the RMG, (2.10), in order to obtain the RB throughput for the MIMO configurations considered. Since the difference in the path loss between a SISO and a SIMO configuration is the diversity gain that the SIMO has, in DL is possible to choose de diversity gain to be considered in the model to obtain an approximation for the SISO configuration, to, afterward, be possible to calculate the RMG. For RMG calculus is applied the RMG model, developed by [KuCo07], in order to obtain the RMG for each user, according to the MIMO configuration chosen and the distance of each user to the BS. This RMG model is not developed for the conditions that will be simulated, although it can be considered a good approximation to obtain the RMG, and is detailed in Annex C. For this model was used the implementation developed by [Bati08]. Since in UL, were just available expressions for 2×2 and 4×4 MIMO configurations, only these options of MIMO configurations are considered in DL and UL, like in single user scenario.

Regarding antennas power fed issues, two approaches can be foreseen. The first one assumes the same feeding power for all the antennas as for SISO, i.e., assuming, e.g., 40 dBm, all antennas would be fed with this power. The second approach, contrary to the first one, considers that the overall power available for the SISO system is split among the antennas, i.e., the additionally introduced antennas for the use of MIMO are fed with a portion of the power used for SISO, proportional to the number of antennas. These two approaches are available in the simulator.

The fading margins, slow and fast, are both probabilistic distributions, Log-normal and Rayleigh, respectively, as shown at Table 4.1, different from the one considered in the single user model. These probabilistic margins give a more realistic approach to the model. The ones developed by [Bati08] and [Marq08] are considered. These fading margins calculations are made for both UL and DL.

The considered reduction strategies are based on [Lope08] and [Salv08], but were adapted to LTE:

- “Throughput Reduction”, the throughput of all users is reduced by a number of RBs defined in the LTE-DL/ LTE-UL settings window, according to the bandwidth;
- “QoS Class Reduction”, all the users’ throughput of the same service is reduced by one RB, according to a list containing the services’ priorities;
- “QoS One by One Reduction”, for a specific service, each users’ throughput is reduced one by one, one RB, according to a priority list.

The same reduction strategies are used for both DL and UL. It is important to point out that the users making voice are only reduced when there are no users making data services. The 3 algorithms are detailed in Annex E.

The reference services are used to define the BS coverage radius, since in a single user model, one throughput corresponds to a maximum distance, being calculated for two reference services, the first for the city centre and the second for all the remaining parts of the city. This approach was taken in order to obtain better coverage in areas with lower number of BSs, as explained in Annex H.

To emulate the load in the cell, was calculated an interference margin for each BS, and besides the orthogonal modulation is need to account for the interference of the other users. The interference margin calculation is for both DL and UL and is explained in detailed in Annex A.

To consider the users that are in BS coverage area, a single user analysis is taken to calculate the cell radius, as mentioned before, and only these coverage users are considered in the DL and UL modules. The main difference in the path loss calculation between the single and multiple users scenarios is the interference margin considered in the multiple users scenario and the statistical fading margins contrary to single user scenario where the fading margins are statics. Due to the interference margin, path loss decreases, leading to a lower cell radius or throughput, depending on the analysis, when one compares the single user with the multiple users' scenarios. Another parameter that has influence on the cell radius is the reference environment, since each one has a specific attenuation and fading margins, presented in Section 4.1.

After all parameters are set, the radii for all considered services as well as the reference services radius are calculated. The minimum and maximum service throughputs can also be modified in the User Profile window for DL and UL, Figure G.6. The maximum throughput values are given by the system limitation due to bandwidths and MIMO configuration, and the minimum throughputs are limited by the minimum throughputs needed for each service.

With the coverage area of each BS calculated and the user introduced in the simulator, Figure G.9, the simulator calculates the number of users inside the BS coverage area, covered users, performing also the calculation of the uncovered area. The information is saved in files that are going to be used in LTEDL_Stat and LTEUL_Stat modules:

- "data.dat", which contains information of which BS serves each user, the user distance, service requested, type of environment, and others;
- "definitions.dat", with the radio parameters considered in the simulation, minimum and maximum throughput for each service, QoS priority, and other simulations' settings.

According to the distance between each user and the BS, if a user is in the coverage area of more than one BS, which is usual in urban scenarios, it will be connected to the closest BS. Despite this approach not being the best one regarding capacity, taking that the user into account should be connected to the BS with more resources available, in this point of the simulator the network is not yet created so that information is not available. Next, the throughput associated to the user distance is calculated and also the number of RBs that the user needs, i.e., considering the path loss as calculated in Annex A and mapping the SNR onto the throughput regarding the expressions in Annex B, the RB throughput is calculated and, afterwards, also the number of RBs to satisfied the requested throughput of the user. For AMC, the RB throughput for the 3 modulations, QPSK, 16QAM and 64 QAM, is calculated, according to the user SNR, being allocated to the user the modulation that gives a higher throughput. Since there is only available the expressions for one coding rate for each modulation, only an adaptive modulation is done in AMC. The same channels considered in single user model were considered in this multiple users one.

There can be three different situations concerning the throughput offered to the user:

- the user is served with the requested throughput – the throughput associated to the distance is higher than the service's throughput;
- the user is served with the throughput associated to distance – this throughput is higher than the minimum service, but lower than the maximum one;
- otherwise, the user is delayed.

The procedure to calculate the user throughput is shown in Figure 3.2, being important to point out that the throughput calculation is done as a function of the RB throughput. The user requested throughput is obtained by multiplying services' throughput by a random function with values between 0 and 1. This randomness is a more realistic approach, since in several cases the throughput limitation is not imposed by the radio access network, but by server's congestion. This approach was taken for both DL and UL.

The analysis of the system's capacity is carried out at the BS's level, by summing the number of RB of all served users. Two possible cases can occur:

- the sum is lower than the maximum allowed RB for the BS – all users are served without reduction;
- if not, it is first applied a optimisation algorithm for the RB, where all RB that have a use lower than 50% are not considered and, consequentially, user throughput is reduced, Figure 3.3. After that, if the sum is still higher than the maximum allowed RB for the BS one of the reduction strategies, shown in Annex E, is applied.

The maximum allowed RB values considered for the BS are shown in Table B.2. The optimisation is detailed in Figure 3.4 for DL and UL.

The cell radius calculation in the multiple user simulator is done differently from the single user simulator. The latter calculates the maximum cell radius using the method described in Section 3.1 while in the former the cell radius is defined by the farther served user from the BS. It is important to notice that capacity also limits the cell radius, since when the reduction strategies are executed, the users farther away from the BS have a higher probability of be delayed, with the exceptions of Voice users that just are reduced after all data users have been delayed. Therefore, if the users farther away are delayed, the BS cell radius BS decreases.

After the capacity analysis, several network parameters for each BS are calculated:

- instantaneous served throughput, $R_{b\,BS}$:

  $$R_{b\,BS\,[\text{Mbps}]} = \sum_{i=0}^{N_{u\,BS}} R_{b\,user_i\,[\text{Mbps}]} \tag{3.4}$$

  where:

  - $N_{u\,BS}$ is the total number of users in the BS;
  - $R_{b\,user}$ is the user instantaneous throughput.

    $$R_{b\,user\,[\text{Mbps}]} = RB_{user} \times R_{b\,RB\,[\text{Mbps}]} \tag{3.5}$$

    where:

    - RB_{user} is the number of RB attributed to the user;
    - $R_{b\,RB}$ is the RB instantaneous throughput.

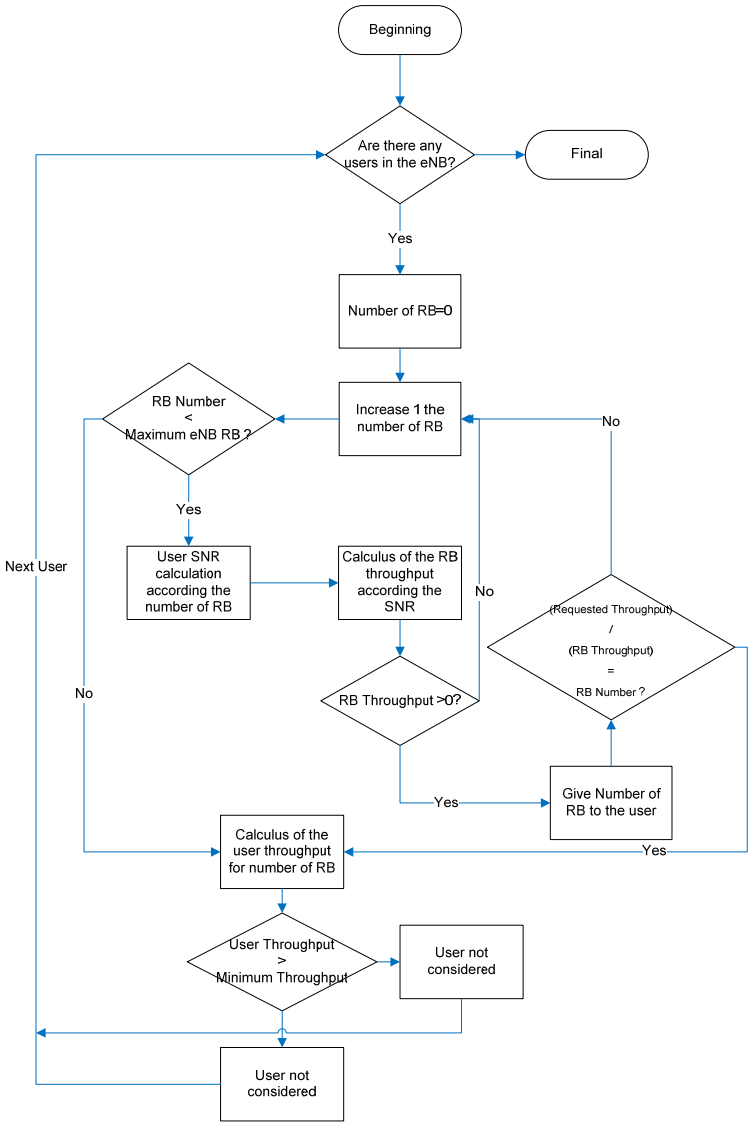

Figure 3.2. LTE user's throughput calculation algorithm.

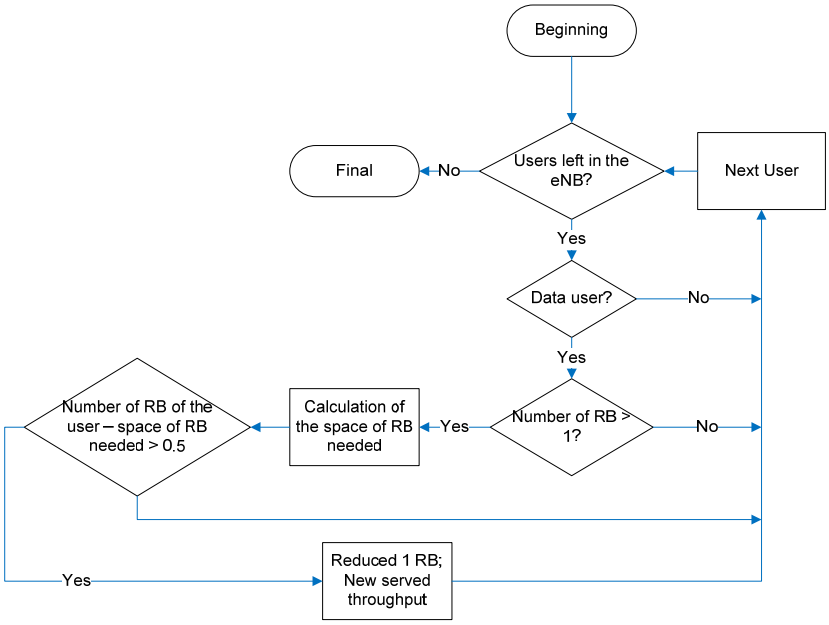

Figure 3.3. LTE optimisation of the RB of each user algorithm.

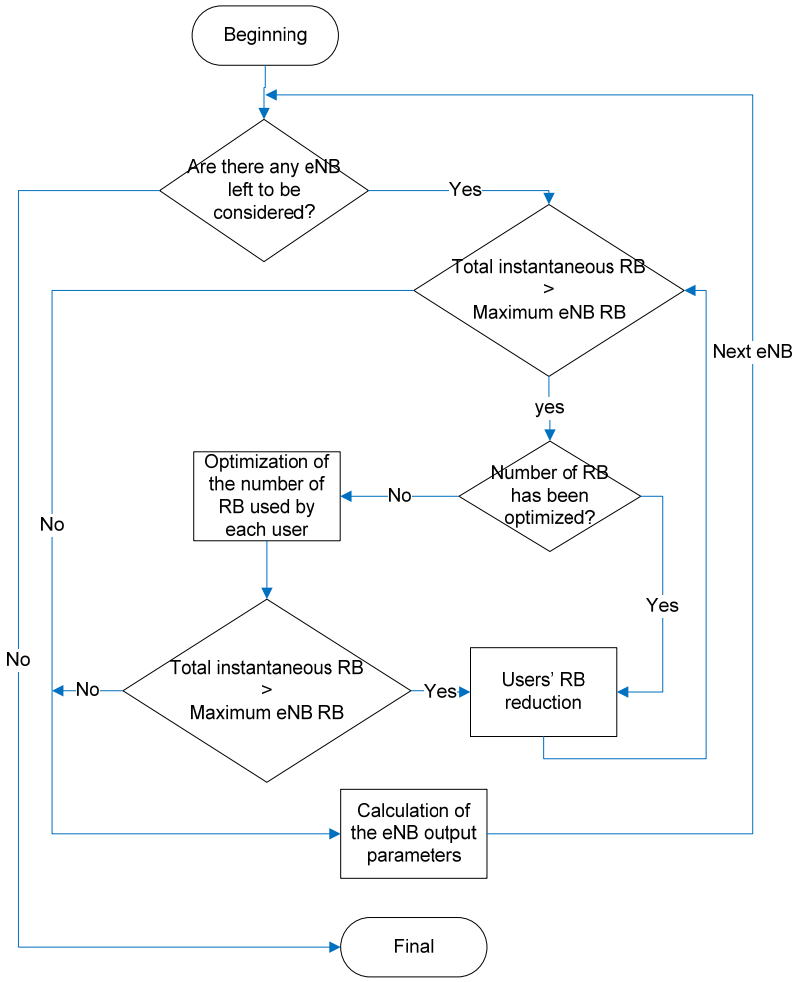

Figure 3.4. LTE algorithm to analyse the BS limitation.

- normalised throughput, $R_{b\,N\,BS}$:

$$R_{b_N\,BS}=\frac{R_{b\,BS\,[\mathrm{Mbps}]}}{R_{b_{max}\,BS\,[\mathrm{Mbps}]}} \tag{3.6}$$

where:

  - $R_{b\,max\,BS}$ is the maximum allowed throughput;

- radius, r_{BS},:

$$r_{\,BS\,[\mathrm{km}]}=\frac{\sum_{i=1}^{3} d_{max\,user_i\,[km]}}{3} \tag{3.7}$$

where:

  - $d_{max\,user\,i}$ is the distance to the BS of the further away user for sector i.

- average instantaneous throughput per user, $\overline{R_{b\,user}}$:

$$\overline{R_{b\,user\,[\mathrm{Mbps}]}}=\frac{\sum_{i=0}^{U_{BS}} R_{b\,user_i\,[\mathrm{Mbps}]}}{N_{u\,BS}} \tag{3.8}$$

where:

  - $N_{u\,BS}$ is the total number of served users.

- satisfaction grade, SG_{BS}:

$$SG_{BS}=\frac{\sum_{i=0}^{U_{BS}} \frac{R_{b\,user_i\,[Mbps]}}{R_{b\,request\,user_i\,[Mbps]}}}{N_{u\,BS}} \tag{3.9}$$

where:

- $R_{b\ request\ user}$ is the user request throughput.

- number of users for one modulation, $U_{(QPSK/16QAM/64QAM)}$:

$$U_{(QPSK/16QAM/64QAM)} = \sum_{i=0}^{U_S} user_{i(\ QPSK/16QAM/64QAM)} \quad (3.10)$$

where:

- $User_{(QPSK/16QAM/64QAM)}$ is an user served by one of the modulation.

- total throughput for one modulation, $R_{b(QPSK/16QAM/64QAM)}$:

$$R_{b\ BS\ (QPSK/16QAM/64QAM)}\ [\text{Mbps}] = \sum_{i=0}^{U_S} R_{b\ user\ i\ (QPSK/16QAM/64QAM)}\ [\text{Mbps}] \quad (3.11)$$

where:

- $user_{(QPSK/16QAM/64QAM)}$ is an user served by one of the modulation.

- total number of RBs, RB_{BS}:

$$RB_{BS} = \sum_{i=0}^{U_S} RB_{user_i} \quad (3.12)$$

- total BS traffic transferred in one hour, T:

$$T_{\ [\text{GB/h}]} = \sum_{j=0}^{N_S} N_{uh_j} \times V_{uj}\ [\text{GB/h}] \quad (3.13)$$

where:

- N_{uhj} is the number of users per hour performing the service j in the BS,
- V_{uj} is volume per user associated to service j in the BS;
- N_S is the number of data services.

- The average data volume per user is calculated as follows:

$$\overline{V_{U\ [\text{MB}]}} = \frac{T_{BS\ [\text{MB}]}}{N_{Uh\ BS}} \quad (3.14)$$

where:

- N_{uhBS} is the number of users served in an hour in the BS;

Additionally, the following parameters are also calculated:

- number of delayed users, taking into account that the sum of served and delayed users corresponds to the total number of users covered,
- percentage of satisfied and unsatisfied users, considering a satisfied user one being served with the request throughput.

These parameters, except for the radius, are also presented in the services detailed analysis, where all parameters are considered only for the users performing each one of the services. This analysis is then performed for all BSs in the network, and the average of each of the parameters is calculated for the network, taking the number of users of each service into account. The outputs for these results are shown in Annex G.

For the network analysis, the most relevant parameters for the instantaneous analysis are:

- the average ratio of served users, $\overline{S_{U\ NT}}$:

$$\overline{S_{U\ NT}} = \frac{\sum_{i=0}^{BS_{active}} U_S}{N_{u\ NT}} \quad (3.15)$$

where:

- BS_{active} is the number of BSs actives;

- $N_{u\ NT}$ is the total number of users in the network.

- average network satisfaction grade, $\overline{SG_{NT}}$:

$$\overline{SG_{NT}} = \frac{\sum_{i=0}^{BS_{active}} SG_{BS\ i}}{BS_{active}} \quad (3.16)$$

- average network radius, $\overline{r_{NT}}$:

$$\overline{r_{NT}}_{[km]} = \frac{\sum_{i=0}^{BS_{active}} r_{BS\ i\ [km]}}{BS_{active}} \quad (3.17)$$

- average network throughput, $\overline{R_{b\ NT}}$:

$$\overline{R_{b\ NT}}_{[Mbps]} = \frac{\sum_{i=0}^{BS_{active}} R_{b\ BS\ i\ [Mbps]}}{BS_{active}} \quad (3.18)$$

- average network number RBs, $\overline{RB_{NT}}$:

$$\overline{RB_{NT}} = \frac{\sum_{i=0}^{BS_{active}} RB_{BS\ i}}{BS_{active}} \quad (3.19)$$

- average network number of users for one modulation, $\overline{U_{(QPSK/16QAM/64QAM)\ NT}}$:

$$\overline{U_{(QPSK/16QAM/64QAM)\ NT}} = \frac{\sum_{i=0}^{BS_{active}} U_{(QPSK/16QAM/64QAM)\ i}}{BS_{active}} \quad (3.20)$$

- average network throughput for one modulation, $\overline{R_{b\ BS\ (QPSK/16QAM/64QAM)\ NT}}$:

$$\overline{R_{b\ BS\ (QPSK/16QAM/64QAM)\ NT\ [Mbps]}} = \frac{\sum_{i=0}^{BS_{active}} R_{b\ user\ i\ (QPSK/16QAM/64QAM)\ [Mbps]}}{BS_{active}} \quad (3.21)$$

After the instantaneous analysis, the results are extrapolated for the busy hour analysis, also presented at Annex G. The parameters studied in this analysis are:

- total network traffic per hour, T_{NT}:

$$T_{NT\ [GB/h]} = \sum_{i=0}^{BS_{active}} T_{i\ [GB/h]} \quad (3.22)$$

- total number of served users per hour, $N_{U\ h\ NT}$:

$$N_{Uh\ NT} = \sum_{i=0}^{BS_{active}} N_{U\ h\ BS} \quad (3.23)$$

This analysis is detailed in [Lope08] and [Salv08]. The only modification introduced was a new type of service analyses, Voice service.

3.2.3 Input and Output Files

To run the simulator, it is necessary to insert the following files in the UMTS_Simul application:

- “Ant65deg.TAB”, with the BS’s antenna gain for all directions;
- “DADOS_Lisboa.TAB”, with information regarding the city of Lisbon and all of its districts;
- “ZONAS_Lisboa.TAB”, with the area characterisation, as streets, gardens, and others;
- “users.txt”, containing the users in the network, being the output of SIM module;
- “BSs_Lisbon_map.TAB”, with the information of the location of the BSs in the network.

The UMTS_Simul module creates 2 files used by the DL and UL modules to perform the simulations:

- “data.dat”, a list with all users’ coordinates and BSs in the network, as well as the distance between them. For each user, additional information, such as the user scenario and requested service, is also present;

- “definitions.dat”, with the radio parameters considered, minimum and maximum throughputs for each service, QoS service’s priorities, and other simulations settings.

Based on these files, the LTE DL and UL modules execute the network analysis and produce several output files, two of each are used by the UMTS_Simul to present the results in Map Info:

- “stats.out”, which includes all results for the instantaneous analysis, both for the network analysis and the statistics by service;
- “stats_per_hour.out”, containing the results for the busy hour analysis.

3.3 Simulator Assessment and Number of Users

Before running simulations and analysing the simulator results, it is necessary to validate the simulator, obtain the number of simulations that are necessary and number of users to use in the different scenarios.

In what concerns the simulator validation, all steps responsible for carrying out calculations were validated using several tools. The propagation model and link budget applied were confirmed performing several calculations using Matlab and Excel, to enssure that results are correct and according to the theoretical model. Regarding the users’ insertion in the network, some validations were also performed. It must be enssured that each user is only connected to one BS and for this purpose an output file was created containing the user’s information considering the BSs to which the user is connected. Even though the user may be in the coverage area of several BSs, the simulator only considers the nearest BS to the user. The three reduction strategies were analysed through a controlled scenario, i.e., using a simulation with approximately 500 users and 3 BSs, and for which one every variable and calculation step has been carefully monitored, by several simulations, making use of the debug and observation point in the simulator code, concluding that everything is working accordingly to the respective algorithms. This procedure was also done to ensure that the necessary RBs are correctly attributed to each user. After the simulation, all output results were validated, such as, averages, relative mean errors and standard deviations were inspected using (3.24), (3.25) and (3.26), respectively. This procedure was carried out for the BS analysis as well as for the network one.

$$\bar{z}=\frac{\sum_{i=1}^{n} z_i}{N_z} \tag{3.24}$$

where:

- z_i: sample i;
- N_z: number of samples.

$$\bar{e}=\left|\frac{z_r-z_i}{z_r}\right| \tag{3.25}$$

where:

- z_r: reference value.

$$\sigma = \sqrt{\frac{1}{N_z}\sum_{i=1}^{N_z}(z_i - \bar{z})^2} \tag{3.26}$$

Users' geographical positions, in addition to the requested throughputs and fading margin, are random variables; hence, several simulations must be taken to assure result validation. The default number of users considered per simulation is approximately 1600 – this result is justified later on. Considering this value, 30 simulations were performed, with an average simulation duration of 30 minutes.

The parameters considered in this analysis are ratio of served users, average instantaneous throughput per user, average network radius and effective number of users.

The number of simulations is estimated based on the results presented in Figure 3.5 and Figure 3.6. In Figure 3.7, it is possible to examine the ratio of the standard deviation over the average value for each one of the analysed parameters. From Figure 3.7 one can observe that, for each parameter considered, there is almost no variation in the average, and the standard deviation presents smooth variations. One can further notice that all values are below 0.05, meaning that there is a small variation among simulations; hence, increasing the number of simulations would have a minimal impact on results.

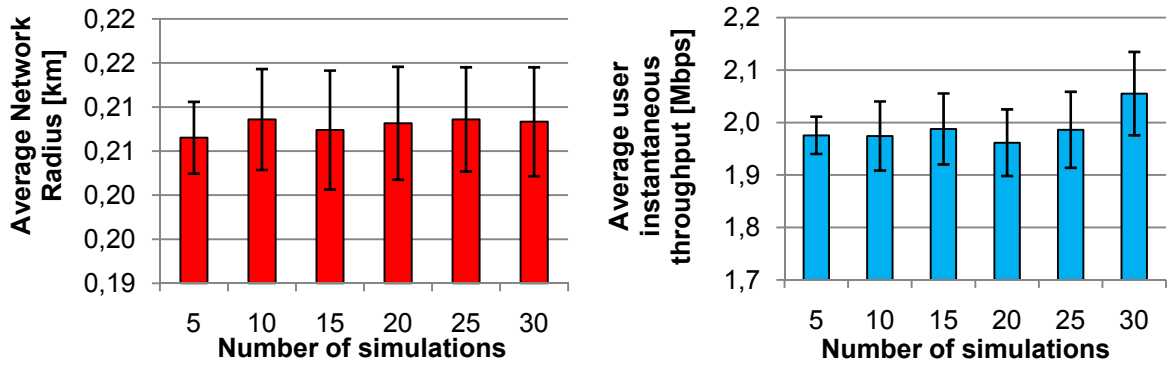

(a) Radius. (b) Throughput.

Figure 3.5. Evolution of the average network radius and average instantaneous throughput per user for 30 simulations.

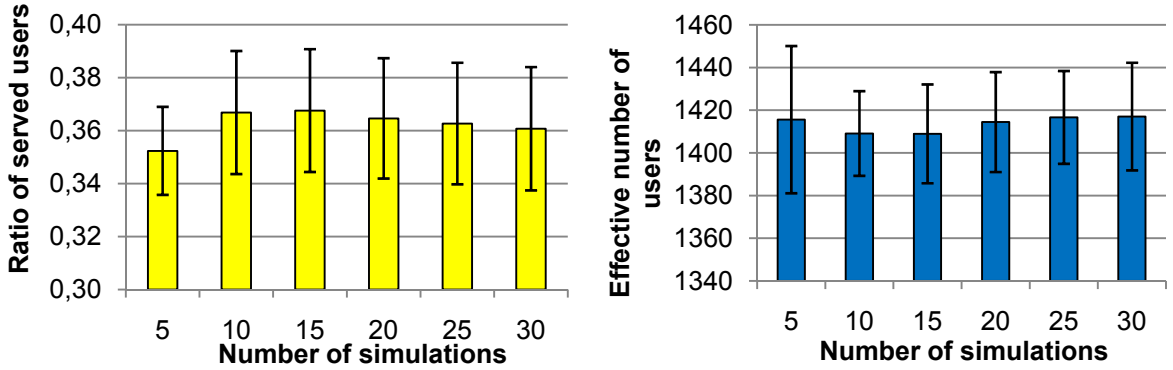

(a) Served Users. (b) Number of Users.

Figure 3.6. Evolution of the ratio of served users and effective number of user for 30 simulations.

Considering the average simulation duration of around 30 minutes, and that when one increases the number of simulations there is no significant decrease of the standard deviation, one has concluded that 10 is the most suitable number of simulations – it allows a good accuracy, and at the same time, it does not require many hours of simulations. These results were obtained for DL simulations. Although DL and UL are different techniques with specific features, the simulator is essentially the same, and

so, the same number of simulations was used for UL. For this analysis, DL was chosen, since it is the link in which services are more demanding and have more coverage area.

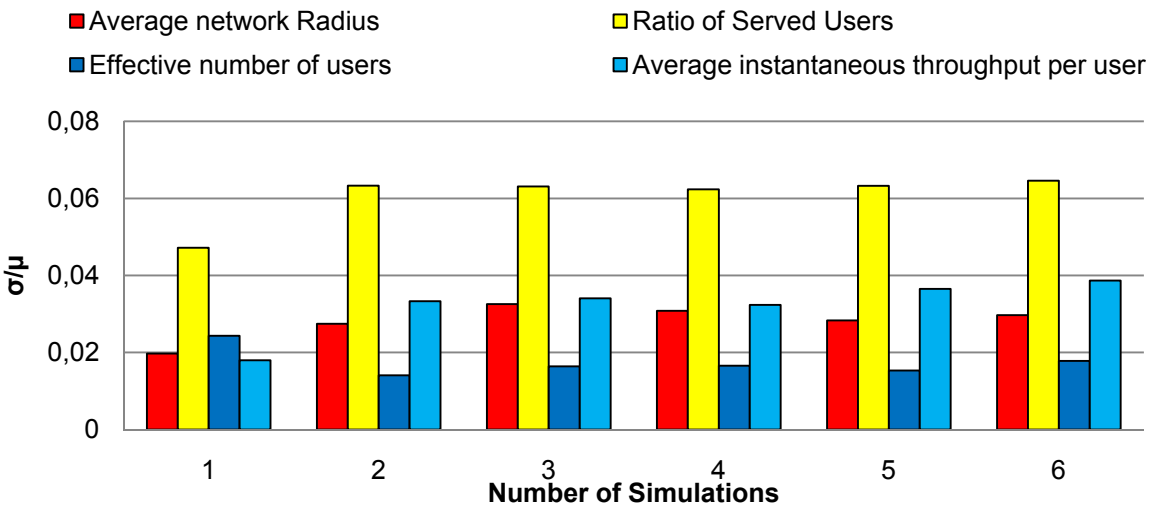

Figure 3.7. Standard deviation over average ratio for 30 simulations.

As expected, with the increases of the number of users, the parameters that evaluate network quality, as the percentage of served users, and the average instantaneous throughput, decrease. The number of covered users increase with the number of users is also expected. By analysing the evolution of the key parameters to evaluate network's performance shown in Table 3.1, the number of users considered for the default scenario throughout this thesis is 1600. It is a choice based on the evolution of all parameters shown on Table 3.1 and taking the coverage area into account, for both DL and UL, and the analysis that was performed.

Table 3.1. Evaluation of the number of users considering several parameters.

Parameters	Approximate number of users							
	800		1200		1600		2000	
	Average	Std. dev.	Average	Std. dev.	Average	Std. dev.	Average	Std. dev.
Average Network Radius [km]	0.18	0.01	0.19	0.01	0.20	0.01	0.22	<0.01
Average Ratio of Served Users	0.54	0.03	0.44	0.02	0.36	0.02	0.32	0.02
Average Effective Number of Users	717	19	1056	16	1409	28	1762	29
Average Instant. Throughput/ user [Mbps]	2.03	0.07	2.01	0.06	1.98	0.07	1.98	0.07

To determine the number of users to use in the default scenario several simulations were performed to analyse the impact of the variation of the number of users on the parameters under analyses, Table 3.1.

For the same reason as the one used for the analysis of the number of simulations, the analysis of the number of users was performed for DL. To perform a fair comparison between DL and UL, the same number of users is used in both links, to ensure that the result's variation is only due to the link. Nevertheless, it is important to emphasise that the services' throughput is limited by the type of system

used. Also it is important to notice that due to the lap of coverage, as shown in Annex H, and the randomness of the users, the percentage of the services in the coverage area is always different and consequently, also, the throughput that is offered to the network.

Chapter 4

Results Analysis

This chapter contains the description of the used scenarios and the analysis of results. First, the simulation scenarios are presented, followed by the presentation of simulation results considering several parameters, such as bandwidth, frequency band, MIMO configuration and type of antenna power fed, alternative profiles, and number of users. A comparison between DL and UL is performed regarding each parameter.

4.1 Scenarios Description

Throughout this thesis, two scenarios are considered, single and multiple users. In the single user scenario there is only one user in the cell the maximum cell radius being calculated for a given throughput, taking that all the resources are dedicated to that user. For the multiple users scenario, users are uniformly distributed along the coverage area performing different services with different associated throughputs.

For both scenarios four types of environments were considered. The pedestrian environment stands for a user at the street level with low attenuation margins; the vehicular one stands for users performing services moving at high speed, where a large value for the slow fading, M_{SF}, and lower value for the fast fading, M_{FF}, margins are considered; the indoor environment characterises users performing services inside buildings. There are two kinds of indoor environment, the low and high losses ones, where the latter is used for users in deep indoor locations with higher penetration attenuation, L_{int}. The percentages taken for the environments into account are in Table 4.1. Indoor environments represent the largest part of the overall percentage as it is, at present, the most common environment for users performing data services. Table 4.1 also shows the attenuation margins associated to each type of environment.

Table 4.1. Slow and fast fading, penetration margin and percentage values (based on [Lope08]).

	Environment			
	Pedestrian	**Vehicular**	**Indoor Low Loss**	**Indoor High Loss**
Percentage [%] (Multiple user)	10	10	50	30
M_{SF} (Single User) [dB]	4.5	7.5	7.0	7.0
M_{SF} (Multiple User) [dB]	Log-Normal Distribution			
	σ=4	σ=7	σ=4	σ=4
M_{FF} (Single User) [dB]	1	0.3	1	1
M_{FF} (Multiple User) [dB]	Rayleigh Distribution			
	σ=4	σ=3	σ=4	σ=4
L_{int} (900 MHz Band) [dB]	0	3.65	3.65	6.3
L_{int} [dB]		11	11	21

The percentages that are considered, in DL and UL, to obtain the application throughput from the physical one are listed at Table 4.2 . The overhead pilot assisted channel estimation is approximately 6% for single transmission. For dual antenna transmission the overhead, is approximately doubled to 11% [MNKF07].

The parameters used for link budget estimation for both scenarios, and the default values considered, are listed in Table 4.3. For the single user scenario, the interference margin and the reduction strategy are not considered. The BS antenna gain is 17 dBi, with a horizontal 65^{o} half power beam width

[CoLa06]. In the single user scenario, the maximum BS antenna gain used. For the 900 MHz band, it was necessary, for the bandwidths of 10 MHz and 15 MHz, to make use of the extension bandwidth, i.e., [880;890] MHz in UL and [925;935] MHz in DL. For the 10 MHz bandwidth, this solution enables to cut the 900 MHz band in three different slices, and the 15 MHz in two.

Table 4.2. System BW efficiency for LTE DL and UL (based on [MNKF07]).

	DL	UL
BW efficiency	0.9	
Cyclic Prefix	0.93	
Pilot Overhead	0.94	----
Dedicated & Common Control Channels	0.715	0.9

Table 4.3. Default values used in DL and UL of LTE link budget (based on [HoTo07]).

Parameter	DL	UL
BS DL Transmission Power [dBm]	40	-----
MT UL Transmission Power [dBm]	-----	24
Frequency (Single User) [MHz]	2110	1920
Frequency (Multiple Users) [MHz]	2145	1955
Modulation (Single User)	16 QAM	
MIMO Configuration	2×2	
Bandwidth [MHz]	10	
MT Antenna Gain [dBi]	0	
Maximum BS Antenna Gain [dBi]	17	
User Losses [dB]	1	
Cable losses between emitter and antenna [dB]	3	
Noise Figure [dB]	7	3
Diversity Gain [dB]	2	-----
Interference Margin [dB]	3	2
Masthead Amplifier Gain [dB]	-----	3
Antennas Feeding Power	Dedicated	
Reduction Strategy	QoS Class Reduction	
Environment (Single User)	Pedestrian	
Reference Service 1 [Mbps]	7.7	5
Reference Service 2 [Mbps]	4	1.4

The maximum and minimum throughput values for the services considered in the default multiple users scenario in UL and DL, as well as the QoS priority list, are presented in Table 4.4. Since LTE is an improvement of UMTS, the throughputs presented, with exception for Voice, were increased regarding the services throughput used as a reference in [Lope08] and [Salv08], since the market trend is the increase of throughputs. The LTE, DL and UL, traffic models characteristics' detailed by

service are presented in Table 4.5.

Table 4.4. Maximum and minimum throughput for the default scenario.

	Maximum Throughput [Mbps]		Minimum Throughput [Mbps]		QoS
Service	**DL**	**UL**	**DL**	**UL**	
Voice	0.064	0.064	0.032	0.032	1
Web	7.2	3.6	1.024	1.024	2
P2P	3.6	3.6	1.024	0.384	7
Streaming	3.6	0.512	1.024	0.512	3
Chat	0.384	0.384	0.064	0.064	6
E-mail	3.6	3.6	1.024	1.024	4
FTP	21.5	3.6	1.024	1.024	5

Table 4.5. LTE DL and UL traffic models (based on [Lope08] and [Salv08]).

Service		**DL**	**UL**
Voice	Average call duration [s]	120	
	Average number of call per user	0.825	
Web	Average page size [OPTW06] [kB]	300	20
	Average reading time [Seba07] [s]	40	
	Average number of pages per session	10	
FTP	Average file size [SBER03] [MB]	10	2
	Average number of files per session	1	
P2P	Average file size [MB]	12.5	
	Average session initiation time [s]	30	
Chat	Average MSN message size [CSEE06] [bytes]	50	
	Average number of received messages during one session	25	
E-mail	Average file size [Seba07] [kB]	100	
	Average number of e-mails per session [Seba07]	1	
Streaming	Average video duration [VNUN07] [s]	150	
	Average video size [MB]	9.6	0.02
	Average number of videos per session [COMS07]	3	3

4.2 Single User Radius Model Analysis

In this section, the analysis for the DL an UL single user results is presented.

4.2.1 DL Evaluation

For all the cell radius results presented in this subsection, the single user model described in Section

3.1 was used, namely using (3.2). The cell radii presented in this section were all calculated for the maximum throughput that is possible to obtain in the different scenarios, i.e., the maximum distance in which is possible to obtain the maximum throughput in a 2×2 MIMO configuration. Figure 4.1 presents the DL cell radii as a function of the bandwidth in a pedestrian environment for the three modulation and the other network parameters as in Table 4.3.

It is possible to observe that while the bandwidth increases, the radius decreases, due to the fact that with the increase of the bandwidth the total noise power, given by (A.8), increases and consequently the SNR, (A.13), decreases, leading to lower radius, as it can be observed through the (3.2). In a single user scenario, all RBs are allocated to the user to obtain the maximum throughput, so with the increasing of the bandwidth the available RBs also increase, Table B.2, together with the maximum throughput. The 1.4 MHz bandwidth allows an average increase of 24, 33, 40, 48, 54% compared to the 3, 5, 10, 15 and 20 MHz bandwidths, respectively and an average throughput decrease of 60, 75, 88, 90 and 94%, respectively.

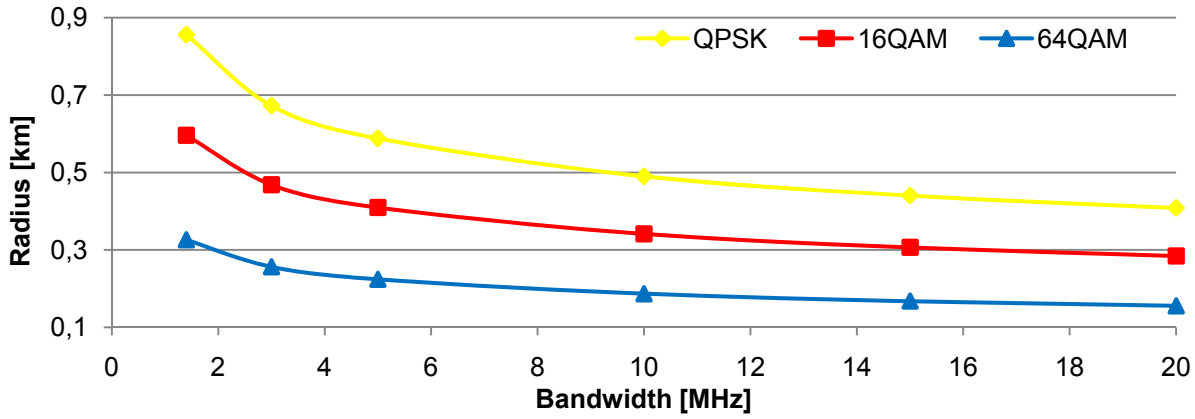

Figure 4.1. DL cell radius for pedestrian environment, considering bandwidth and modulation.

Furthermore, from Figure 4.1 it can be noticed that the modulation in which the radius is higher is QPSK, as expected, since, of the three, it is the most robust one, and at the same time the modulation that allows the lowest throughputs, Table B.5. On the other hand, 64QAM is the modulation that allows higher throughputs, therefore for the maximum throughput it has a smaller radius, since the higher the throughput the higher is the SNR required, as it can be observed through Annex B expressions. For QPSK there is a gain of approximately 162% in the radius, by using it instead of 64QAM, and 40%, instead of 16QAM. Concerning throughputs, with QPSK the maximum throughput possible to achieve is 200% and 550% lower than with 16QAM and 64QAM, respectevely.

In Figure 4.2, one shows the variation of the cell radius as a function of the bandwidth for the four considered environments. As in Figure 4.1, it is possible to observe that the cell radius decreases with the increase of the bandwidth.

Considering the different environments, one can observe that the pedestrian one presents a higher cell radius, compared to the others. The pedestrian environment allows an average increase of 122, 150 and 300% compared to the indoor low loss, vehicular and indoor high loss ones. In Table 4.1, one can observe that the pedestrian environment has lower attenuation margins, which leads to higher cell radius, since the sum of the three margins is considered in the path loss, (A.10) and (A.11). This

explains the similarity of the results for the vehicular and the indoor low loss environments, even though these environments have different characteristics.

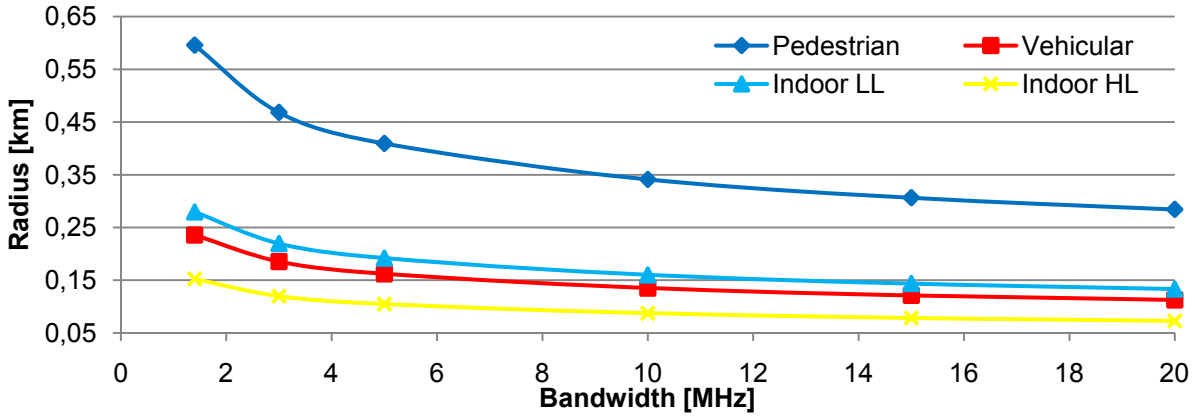

Figure 4.2. DL cell radius for 16 QAM, considering bandwidth and environment.

The frequency band is another parameter that has a high impact in the cell radius. Figure 4.3 shows the cell radius variation, considering a pedestrian environment and 16 QAM.

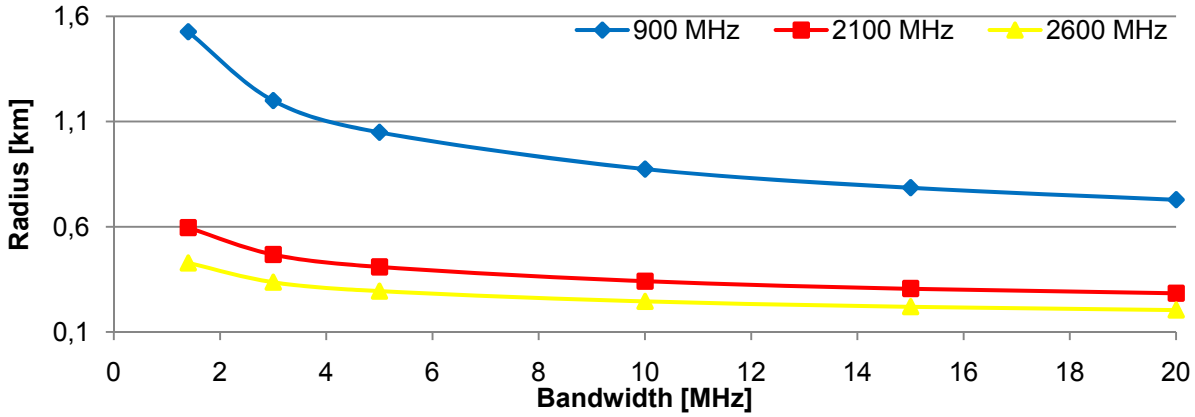

Figure 4.3. LTE DL cell radius for 16 QAM and pedestrian environment, considering bandwidth and frequency band.

Since the propagation model, COST 231 Walfisch-Ikegami, is a function of frequency among others, by increasing the frequency band of the system, the cell radius decreases, as it can be observed in Figure 4.3. Since the 900 MHz band is the lowest one, it has the highest cell radius, with a gain of 150% and 170% over the 2100 MHz and 2600 MHz bands, respectively. As the penetration margins changes with frequency, as Table 4.1 shows, for the other environments, where the penetration margin must be taken into account, the difference between the 900 MHz band radius and the other two bands is higher than in pedestrian environment.

In Annex I, one shows the tables with the main results regarding the single user analysis. Although 4×4 MIMO is implemented in the simulator, an analysis of the results is not done since in a maximum throughput analysis, the increasing of the MIMO configuration will lead to radius equal as the 2×2 MIMO ones but with the higher throughputs. If an analysis to 14.4 Mbps of throughput was done, will show that the radius to 4×4 MIMO is higher than 2×2 MIMO one.

Looking into all the results presented in this analysis, that the radius for high throughputs are very low. For instance, for 64QAM, where the highest throughputs are achieved, just in the 3MHz bandwidth is

possible to have maximum throughput higher than 14.4 Mbps, the radius, for pedestrian environment, is 0.26 km. If an indoor low losses environment was considered, a high probability one in a urban scenario, the radius decrease to 0.12 km, which is very low, mainly in low traffic areas where is very important to have large cells since there is no capacity problems. One of the factors for the radius decreasing is the bandwidth increasing, which also increases the BS capacity, but the decreasing of the radius is lower than the capacity increasing. So there is a compromise between the capacity, bandwidth, and the coverage, cell radius. The two indoor environments considered, which are the ones with more percentage in a urban scenario, considering 16QAM, have radius lower than 0.15 km when throughputs higher than 14.4 Mbps must be achieved, so in low traffic areas, where the BS density is lower, in order to guarantee this throughputs the number of BS it must be increased in this area, since QPSK have higher radius but does not allow 14.4 Mbps. If a pedestrian environment is considered the radius increases significantly, but the percentage of users in a pedestrian environment in an urban scenario is much lower than in indoor one. When 900 MHz frequency band is analysed it becomes clearly the frequency influence in the radius, since is the variation analysed that has the highest impact in the radius, increasing it in such way that the coverage problems that are in the 2100 MHz band will be very few. On the other hand, the 2600 MHz band increases the coverage problems since there is a decrease in the radius, not as significant as the increase in the 900 MHz band.

4.2.2 UL Evaluation

As in DL, for all the cell radius results presented in this subsection, the single user model described in Section 3.1 was used and the cell radii presented were all calculated for the maximum throughput, Table B.6. Also with this UL analysis, a comparison with LTE DL results is performed.

Figure 4.4 presents the UL cell radii as a function of the bandwidth in a pedestrian environment considering the three modulations. As it can be noticed, cell radius, with increasing the bandwidth, presents the same behaviour as in DL, but the radius values are lower, mainly due to the MT power limitations. In UL, the transmission power is lower, which increased the path loss, and consequently decreases the radius. The UL radius cell values are, on average, 65% lower, when compared with the DL ones. Regarding the modulation variation, the behaviour is the same as in DL, where the QPSK, due to its robustness, is the modulation that has the higher radius, but the maximum throughputs achieved are the lowest among the three modulations. There is an average gain of approximately 150% in the radius, by using QPSK instead of 64QAM, and 60%, instead of 16QAM. Concerning throughputs, with QPSK the maximum throughput possible is 336% and 636% lower than with 16QAM and 64QAM.

From Figure 4.5, it can be noticed that, like in DL, the pedestrian environment is the one that allows a higher cell radius, while the indoor high losses is the one with the shortest range for the same reason that is pointed out in DL. The pedestrian environment has a radius 130, 200 and 320% higher, on average, compared with indoor low loss, vehicular and indoor high loss respectively.

The frequency band has the same impact in both UL and DL, since the propagation model is the same in DL and UL, so, an analysis of the frequency band impact on UL is not performed, being the results

presented in Annex I. Annex I, also shows the tables with the main results regarding the single user analysis for UL.

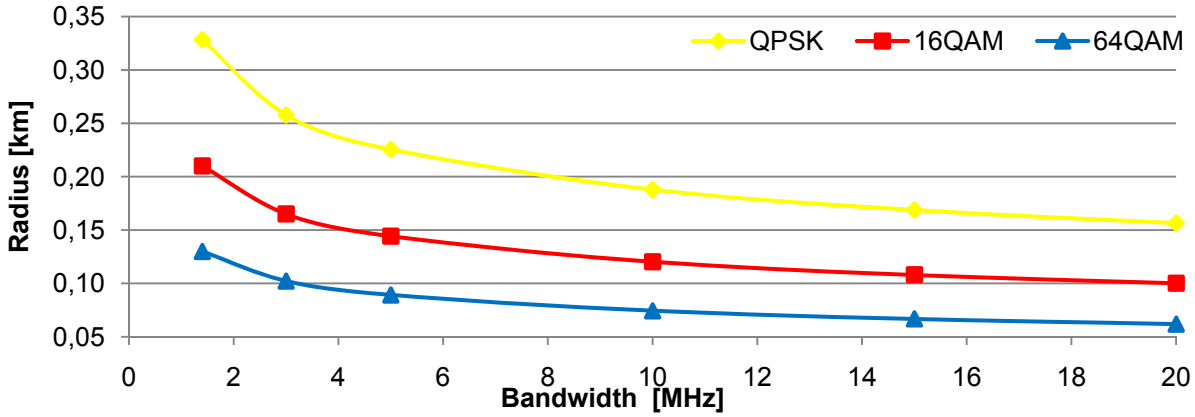

Figure 4.4. UL cell radius for pedestrian environment, considering bandwidth and modulation.

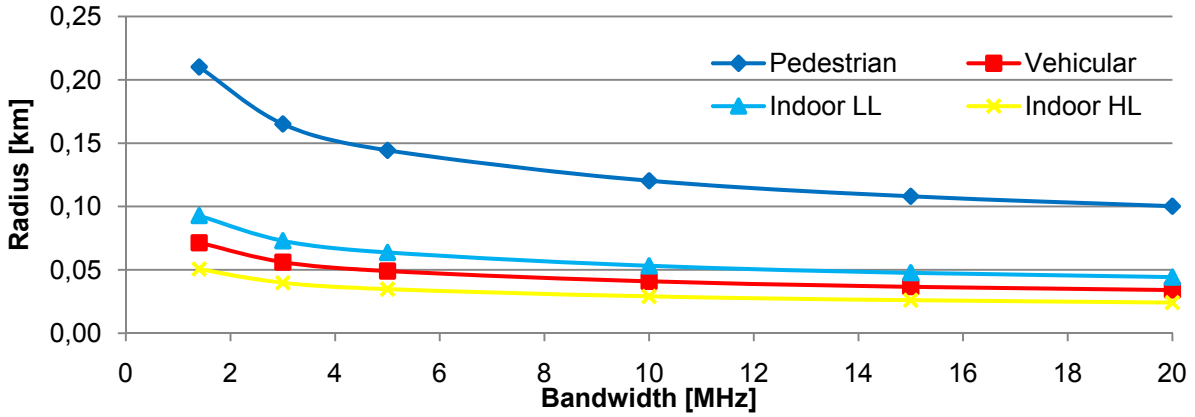

Figure 4.5. UL cell radius for 16 QAM, considering bandwidth and environment.

Considering all the results obtained in this analysis, on that stands out is the lower radius values than in DL, and since the two links are deployed together, UL is the link that will limited the system in coverage issues. For indoor scenarios the radius are lowers than 0.1 km for the maximum throughput in all the bandwidths, and considering the 5.8 Mbps, when is possible to achieve, the radius are also lower than 0.1 km for indoor and vehicular scenarios being the difference between these two radius higher as the bandwidth increases. With these radius values the number of BS has to be increased, not only, in low traffic areas, as concluded also in DL analysis, but probably also in high traffic areas. A lower frequency band can resolve the coverage issue in high traffic areas, and also decrease the number of BS that must has to be introduced in the network, in order to guarantee a 5.8 Mbps in low traffic areas. With the use of a more robust modulation, QPSK, the radius values increase but throughput decreases, just being possible to guarantee the 5.8 Mbps with the 15 MHz bandwidth or higher.

4.3 DL Analysis in a Multiple Users Scenario

In this section, DL results in a multiple users scenario are analysed. First, the results of the default scenario in Section 4.1 are examined. Secondly, simulation results considering system parameter variation, as well as different scenarios, are studied.

4.3.1 Default Scenario

All the results presented in this section were obtained using the multiple users simulator, introduced in Section 3.2, with the objective of giving a more specific insight of a LTE network impact on capacity and coverage. All the results presented take only the coverage users into account.

Considering all served users in all simulations, Figure 4.6 presents the instantaneous user throughput as a function of the SNR and user modulation, in order to observe the AMC with further detail.

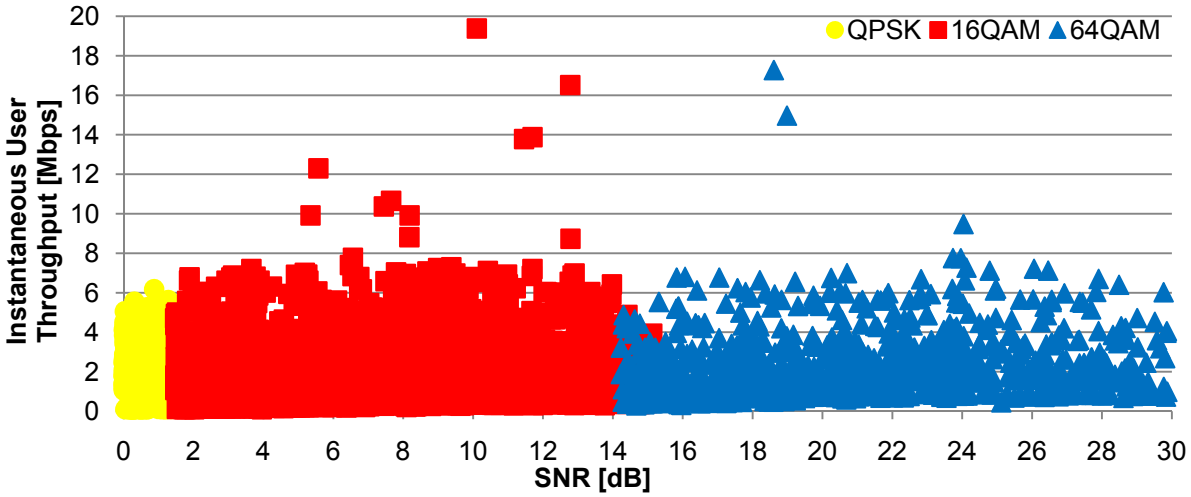

Figure 4.6. DL instantaneous user throughput for all users variation with SNR and distinguishing the modulation of each user.

For lower SNR values, users are served with QPSK, which is a more robust modulation and consequently the RB throughput values are lower than with 16QAM and 64QAM, which are modulations with lower robustness. The same happens for 16QAM and 64QAM, for middle values of SNR, where 16QAM has a better performance. For the higher values of SNR a robust modulation it is not necessary, so 64QAM has a better throughput performance than QPSK and 16QAM, since it is the one that has more symbols per bit. It is important to notice that despite QPSK having fewer symbols per bit than 16QAM, the instantaneous throughputs of the users are similar, since there is not any restriction for the number of RBs per user, besides the capacity of the BS where the user is connected. If the capacity of the BS is exceeded, the number of RBs decreases according to the reduction strategy chosen. So, by instance, the only difference between QPSK and 16QAM users that are served with the same throughput is with the number of RBs that each user needs, where QPSK users need more RBs. In order to observe the transition between modulations, Figure 4.7 has a zoom of Figure 4.6 in the transitions zones. It can be observed that, as expected, the transitions are not

abrupt due to the two channels taken into account, the vehicular and the pedestrian one. These two channels have different expressions for the throughput as a function of the SNR, and consequently the transition happens in different values of SNR.

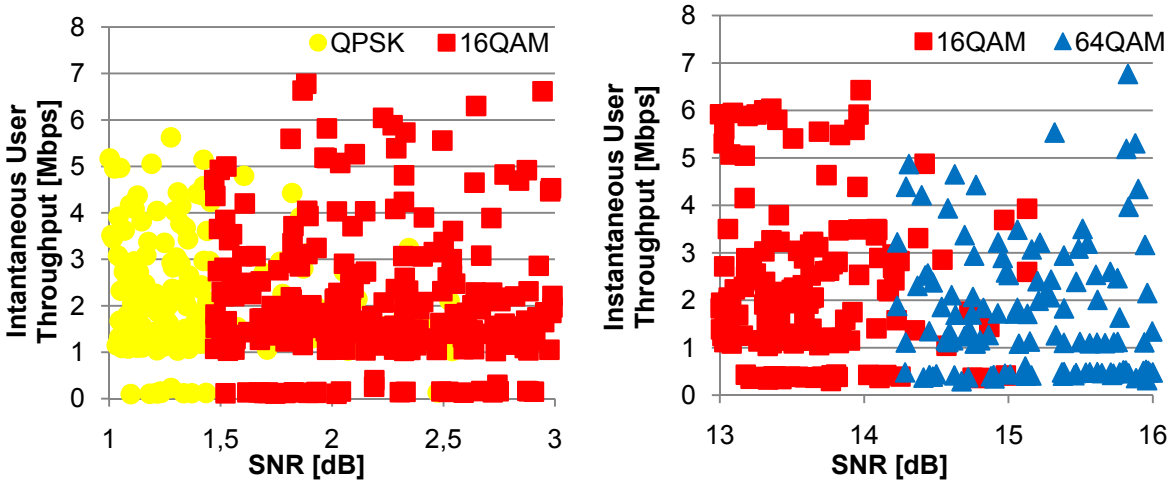

(a) SNR between 1 and 3 dB. (b) SNR between 13 and 16 dB.

Figure 4.7. Figure 4.6 in detail for some SNR values.

To better understand the distribution of users by the three modulations, and throughput contribution of each one for the network, Figure 4.8 shows the average number of users by modulation and the average network throughput. As expected, 16QAM has the highest number of users per BS, since this modulation has a higher density of users and large range of SNR values, which will leads to the modulation with the highest network throughput. QPSK has a low number of users, due to the high references throughputs, which defines the BS coverage and consequently reduces the number of users with a low SNR, since low SNRs are more related with large distances. Concerning the average network throughput, from Figure 4.8 it can be noticed that, as expected, QPSK is the modulation that has less number of users, hence it has the lower average network throughput. 16QAM has more 50% and 30% of users than QPSK and 64QAM, as well as, a 60% and 30% higher average network throughput, comparing with QPSK and 64QAM.

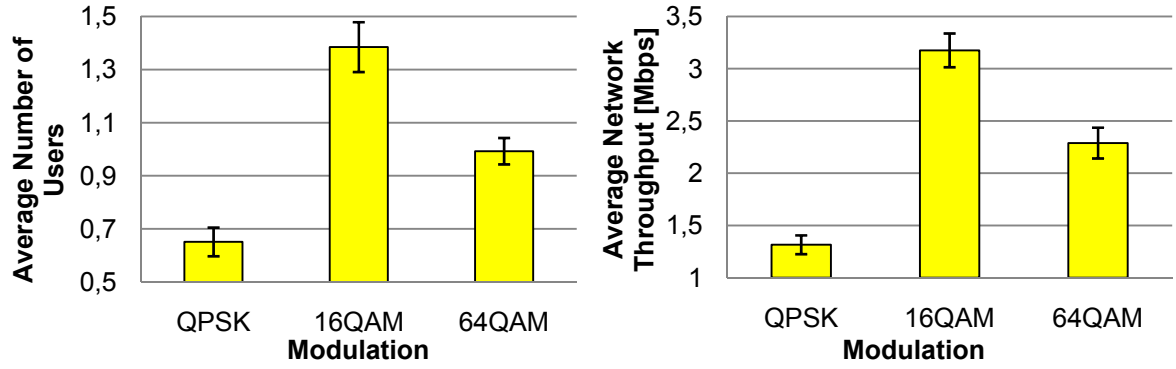

(a) Average Number of Users. (b) Average Network Throughput.

Figure 4.8. DL average number of users and throughput by modulation, for the default scenario.

An analysis per services is done in Figure 4.9, where the average network throughput and average satisfaction grade are presented for each service. Concerning the average network throughput, the services that have highest maximum throughputs are the ones that have highest average network

throughputs. The exception happens for Voice and Chat services, since, Chat has an average throughput lower than Voice, and users performing Voice are never reduced, if possible, contrary to what happens for data services. Moreover, note that the high standard deviation values in Email and FTP services are explained by the fact that these services have a low percentage of users, approximately 1%, having a low statistical relevance.

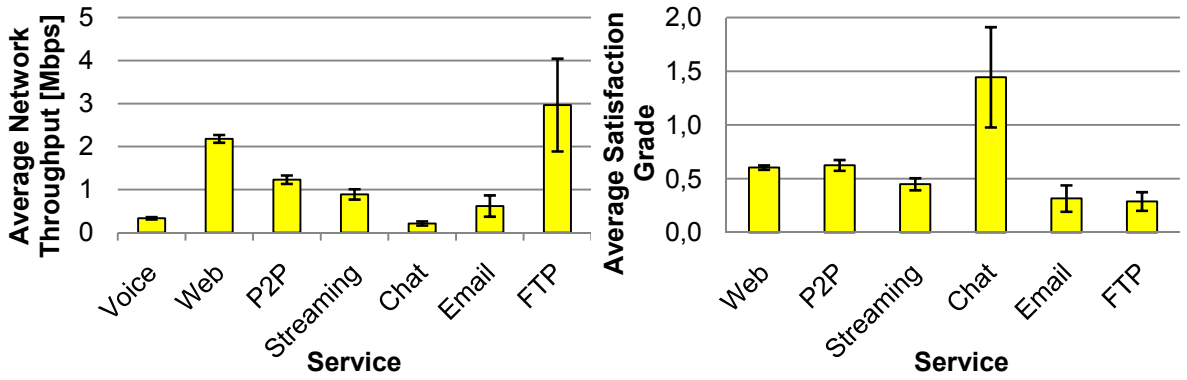

(a) Average Network Throughput. (b) Average Satisfaction Grade.

Figure 4.9. DL Throughput and Satisfaction Grade by services, for the default scenario.

In the average satisfaction grade analysis, it was decided not to analyse Voice since these users are only reduced when there is no data traffic in the BS, and have a higher satisfaction grade. In the satisfaction grades concerning data traffic, it can be noticed that Chat has the highest value, above 1. This fact can be explained by the RB throughput and the lower requested throughput of this service, since one RB can only be used by one user and if the requested throughput of the user is below the capacity of the RB, it is given to the user a higher throughput than the one requested, so the satisfaction grade is above 1. The same happens with Voice, but as the Voice requested throughput is lower than on Chat, the satisfaction grade it is higher, with an average of approximately 9, i.e., the served throughput is 9 times higher than the requested throughput. With this high satisfaction grade value it can be concluded that, mainly, Voice waste network resources, since it is given to Voice users a throughput 9 times higher than the one needed for the service. So Voice users does not profit with the improvements brought by LTE due to the low demanding of the service.

In order to analyse one of the improvements brought by LTE, more precisely by OFDMA, an RBs analysis is fundamental, Figure 4.10. As expected, the RBs behaviour is equal to the average network throughput, since these analyses are very similar. It is interesting to point out that Voice and Chat have an average number of RBs lower than the others due to the lower requested throughputs, as explained previously.

In Figure 4.11, one represents the percentages of offered and served traffic. It is possible to observe that there is a difference in the referred percentages as the network cannot serve all users. Figure 4.11 (b) shows the percentage of the 7 considered services, according to the final number of users effectively served by the network, while in Figure 4.11 (a) one shows the offered service percentages. The most significant difference is for Voice that has the highest QoS priority and is never reduced. On the other hand, P2P percentage of served users decreases, given the lowest QoS priority. Although Email and FTP have the same offered traffic percentage, due to the low requested throughput of Email

compared to FTP, Email users have more probability to be delayed from FTP ones, so the probability of the served Email traffic is lower than FTP one.

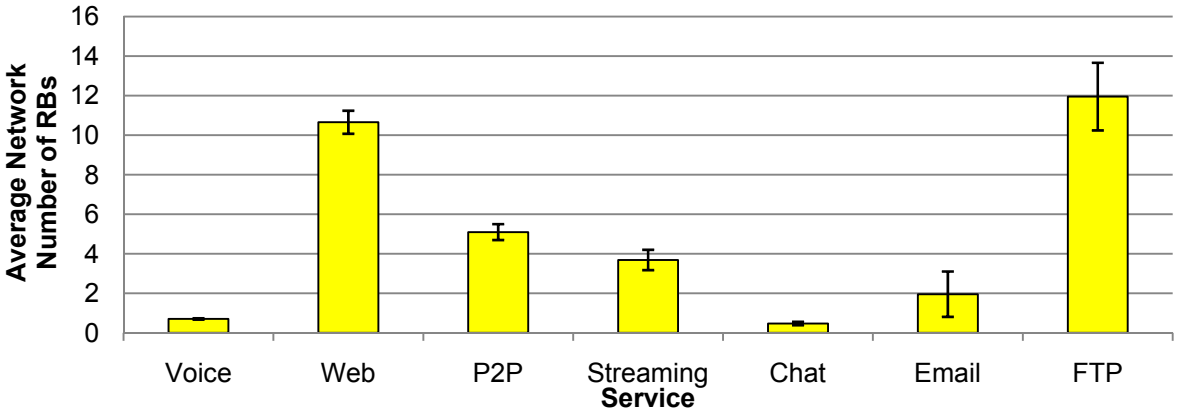

Figure 4.10. DL average number of RBs detailed for services for the default scenario.

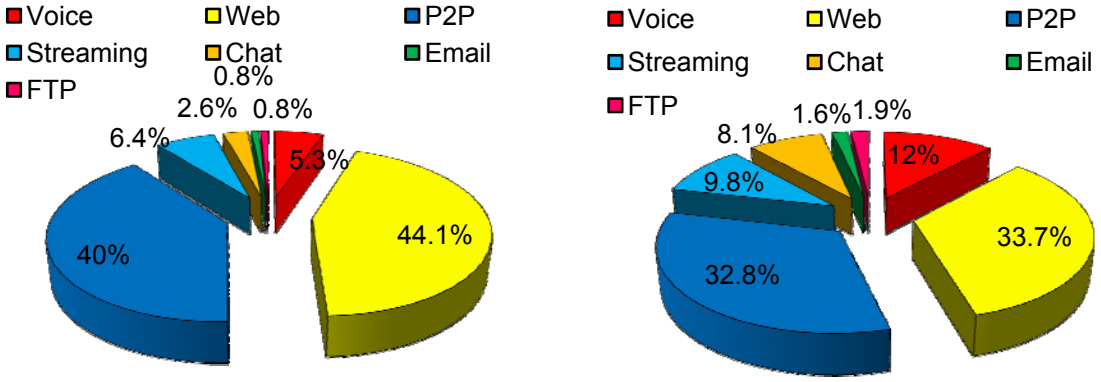

(a) Average Offered Traffic. (b) Average Served Traffic.

Figure 4.11. DL percentage of traffic.

Concerning the overall parameters, an average network throughput of 6.78 Mbps, a satisfaction grade of 1.8 and an average number of RB of 29.2 is obtained. In the analysis for the busy hour, the average network traffic of 119 GB/h is obtained. Regarding the number of users per hour, 49000 users can be served. The uncovered area for this scenario is 20.7% and has in average 191 uncovered users against an average of 1465 covered users, of which 37% are served. The average network radius is 0.21 km.

4.3.2 Bandwidth

In this subsection, the effect of using different bandwidths is presented. The analysis for the 1.4 MHz bandwidth was not done, since maximum throughput possible in this bandwidth is lower than the reference one.

With the increase of the bandwidth, the number of RBs also increases (the number of RB for each bandwidth is show in Table B.2), and, consequently the capacity of the network increases.

From Figure 4.12 (a) it is possible to observe the increase of the average number of RBs used with the increase of bandwidth, as expected. As the capacity of the network increases, more users can be

served, Figure 4.12 (b). Although the theoretical decrease of RBs for the 3 and 5 MHz are 70% and 50% compared to 10 MHz (the default scenario), the decrease observed is 60% and 38%, which can be explained by the fact that some BSs, out of the high traffic area, do not have enough users for the BS maximum capacity to be achieved, meaning that just some BSs benefit with the increase of the RBs. For 15 and 20 MHz bandwidths the theoretical increases of RBs in the network compared with the default bandwidth are 50% and 100% and the observed increase in Figure 4.12 (a) is 24% and 37%, respectively. The reason is the same that for the 3 and 5MHz bandwidths: the BSs in high traffic areas benefit with the capacity increase since the others do not have traffic enough to use all the BS capacity. Also from Figure 4.12 (a), is observed that the slope is decreasing with the bandwidth increasing, i.e., the network will profit less and less with the increasing of the RBs. This can be explained by the BSs outside the high traffic area that does not have enough users to benefit from all the increasing of RBs by the bandwidth. So in the 15, but mainly in the 20 MHz bandwidth, it can be occur some waste of capacity by the BSs in the low traffic areas.

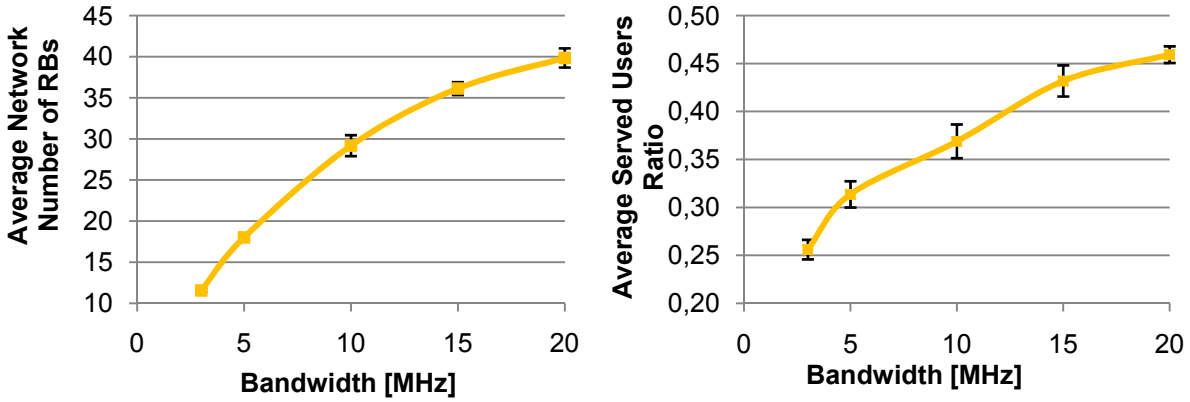

(a) Average Number of RBs. (b) Average Served Users Ratio.

Figure 4.12. DL Number of RBs and Served Users Ratio for the bandwidths of 3, 5, 10, 15 and 20 MHz.

The served users have a decrease of 30% and 15% for the 3 and 5 MHz bandwidths, compared with the default bandwidth, and 15 and 20 MHz have an increase of 17% and 24%, as expected since there is an increase of capacity with the bandwidth.

The average satisfaction grade is presented in Figure 4.3 (a), where it increases with bandwidth, as expected, since if the network has more capacity users do not have to be reduced, or do not have to be reduced as much, and their satisfaction grade increases. The use of 3 and 5 MHz instead 10 MHz leads to a decrease of 19% and 9%, respectively, of the satisfaction grade and the use of 15 and 20 MHz leads to an increase of 13% and 40%. From 15 to 20 MHz the increasing is more stressed, since for this bandwidth, 20 MHz, there are more network resources and similar number of users to be served, once the radius is practically constant, Figure J.2, so the users are less reduced.

The average network throughput has a decrease of 45.5% and 30% compared to the 10 MHz bandwidth for 3 and 5 MHz and an increase of 22% and 39% for 15 and 20 MHz, respectively. As expected the behaviour is equal form the average number of RBs once they are interconnect, as explained in Section 3.2.

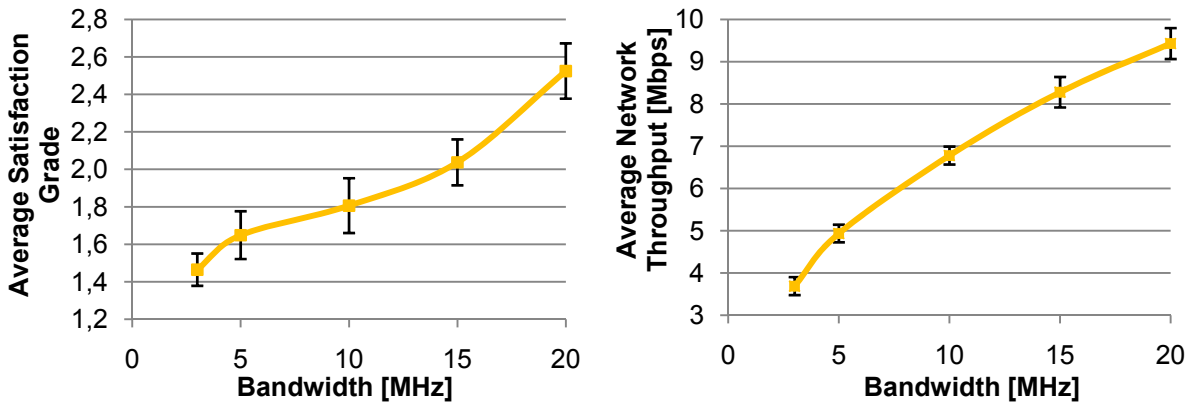

(a) Average Satisfaction Grade. (b) Average Network Throughput.

Figure 4.13. DL Satisfaction Grade and Network Throughput for the bandwidths of 3, 5, 10, 15 and 20 MHz.

The use of 15 and 20 MHz allows an increase of 14% and 33% for the total network traffic and 27.3% and 56.4% for the total number of users served per hour compared to the default case, while the use of 3 and 10 MHz reduces the network traffic by 52% and 31% and the number of users served per hour by 43% and 11%, respectively, Figure J.1. From Figure J.2 it is observed that the radius does not have a high variation with the bandwidth, with values 7% and 5% lower in 3 and 5 MHz compared to 10 MHz and 3% and 4% higher for 15 and 20 MHz.

4.3.3 Frequency Band

As seen in the results for the single user model in Subsection 4.2.1, the frequency band has a major influence in path loss. In this subsection, the frequency band influence regarding several parameters is evaluated. The reduction of the frequency band to the 900 MHz band leads to an increase of the average network radius. This increase is due, as explained in Subsection 4.2.1, to the propagation model, COST 231 Walfisch-Ikegami, which depends on frequency. There is also the fact that in the 900 MHz band the penetration margins are lower, as shown in Table 4.1, so indoor users and vehicular ones, which correspond to 90% of the total, have lower penetration margins, besides the gain in the propagation model. From Figure 4.14 (b), one can observe that in the 900 MHz band the radius has an increase of 50% over 2100 MHz ones. When the frequency band rises to 2600 MHz the average network radius decreases as expected, but in this case just due to the propagation model, since the penetration margins are equal for the two frequency bands, 2600 and 2100 MHz. In this case the network radius has a decrease of 17%.

As expected the served users ratio, Figure 4.14 (a), for 900 MHz, rises up since it is possible to serve users with higher order modulation, i.e., 64QAM, once the SNR of the users increases with the lower frequency and penetration margins. It is possible to serve more users with 64QAM, Figure J.3, so less RB are necessary for each user, and consequently more users can be served. By this fact that served users decrease in 2600 MHz compared to 2100 MHz (a decrease of 7% against the increase of 62.5% in 900 MHz). As the capacity of the system rises, it is possible to serve more users with higher modulation order, increasing the users satisfaction grade by 40%, as shown in Figure 4.15 (b), for 900

MHz compared to 2100 MHz. There is also an increase of 17% in 2600 MHz satisfaction grade, contrary to what was expected, since, as the uncovered area rises, the number of users is lower than in the 2100 MHz, and consequently the users have a greater satisfaction grade, since the radius for the two bands are very similar, contrary to what happens in 900 MHz.

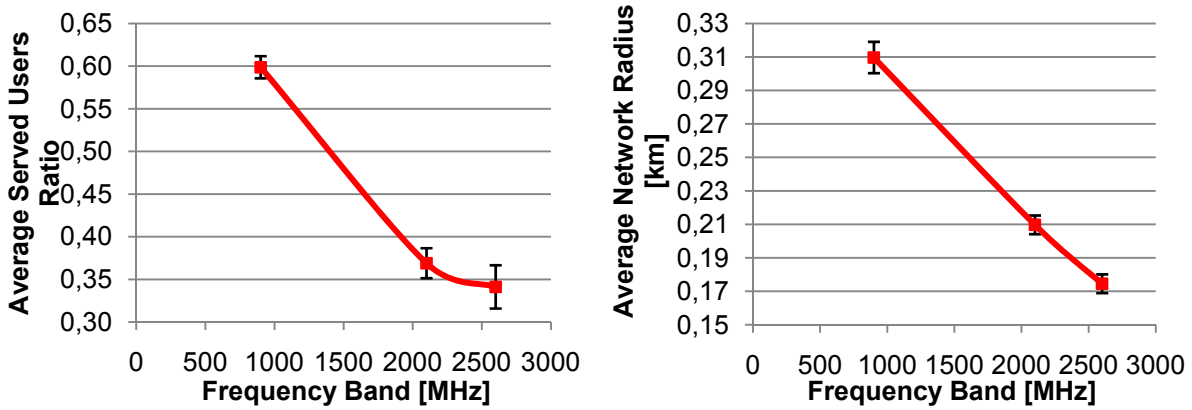

(a) Average Served Users Ratio. (b) Average Network Radius.

Figure 4.14. DL Served Users Ratio and Network Radius for the frequency bands of 900, 2100 and 2600 MHz.

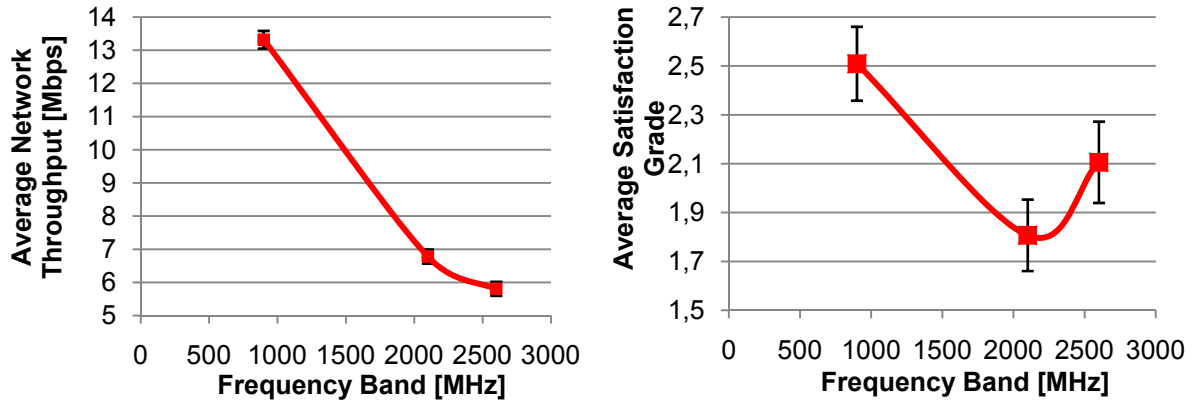

(a) Average Network Throughput. (b) Average Satisfaction Grade.

Figure 4.15. DL Network Throughput and Satisfaction Grade for the frequency bands of 900, 2100 and 2600 MHz.

Concerning the average network throughput, the 900 MHz, is the one that serves more users with higher satisfaction grade, so it has 97% higher than the average network throughput in 2100 MHz, and compared to the 2600 MHz network throughput decreases 14%.

Table 4.6 has detailed coverage parameters for the three frequency bands: the uncovered area increases with the frequency band and consequently increases the number of uncovered users and decreases the covered ones. With the 900 MHz it is possible to cover the entire city without recurring to any additional BSs, contrary to what happen in the 2100 MHz and 2600 MHz, where, mainly in the Zone 2, Annex H, there are gaps of coverage.

The total network traffic and the total number of users served per hour are presented in Figure J.4, where it is possible to observe, as expected with the previous results analysed, an increase of 80% and 107% in the total number of users per hour and total network traffic, respectively, for 900 MHz

compared to the default frequency band and a decrease of 6% and 30%, respectively, for 2600 MHz. Concerning the average number of RBs, Figure J.5, has an increase of 8% for 900 MHz and a decrease of 9.5% for 2600 MHz is observed, compared to the default frequency band, 2100 MHz. Although the 97% higher average network throughput in the 900 MHz relatively to the 2100 MHz band the RBs increase is not so evident, since more users are served with 64QAM, which gives to the RBs more capacity. Regarding the modulation analysis for each frequency band, Figure J.3, as expected, the 900 MHz has the highest number of users and throughput for the 64QAM

Table 4.6. DL Uncovered Area, Uncovered and Covered Users for 900, 2100 and 2600 MHz.

	900 MHz	**2100 MHz**	**2600 MHz**
Uncovered Area [%]	<0.01	20.7	43.6
Uncovered Users	0	191	507
Covered Users	1656	1465	1149

4.3.4 MIMO configuration and Antenna Power Fed

In this subsection, the MIMO configuration is varied regarding the default scenario, and the effect of using split or dedicated antenna power fed is presented. From the default scenario, 2×2 MIMO and dedicated antenna power fed (2_Ded), the MIMO configuration was varied to 4×4 MIMO (4_Ded) and, separately, the antenna power feeding to split (2_Split). Changing the MIMO configuration, the number of antennas in the MT and BS rises to the double, from 2 to 4, and changing the antenna power feeding to split decreases to half the power of each BS antenna, since the analysis is in DL, meaning that the same power that feds the antenna in a SISO configuration will fed the antennas in a MIMO configuration.

As expected, it is possible to observe, from Figure 4.16, that 4×4 MIMO is the configuration that has the best performance. With this configuration it is possible to serve 16% more users than with the default scenario, and has an average radius 16% higher. This is well explained by the need of lower SNRs that 4×4 MIMO need, compared to 2×2, to achieve the same throughput. On the other hand, when the power antenna feeding is changed to split, higher SNRs are needed to achieved the same throughput than in a dedicated one, since the power of each antenna is reduced to half. In this case the served users decrease 2%, and the average network radius 11%.

For the average network throughput and satisfaction grade, Figure 4.17, the behaviour is the same than before by the same reasons. The 4×4 MIMO has an increase, from the default scenario, of 120% and 45% in the satisfaction grade parameter and in the average network throughput, respectively. Concerning the power antenna feeding, the split configuration has a decrease of 10% in both network throughput and satisfaction grade.

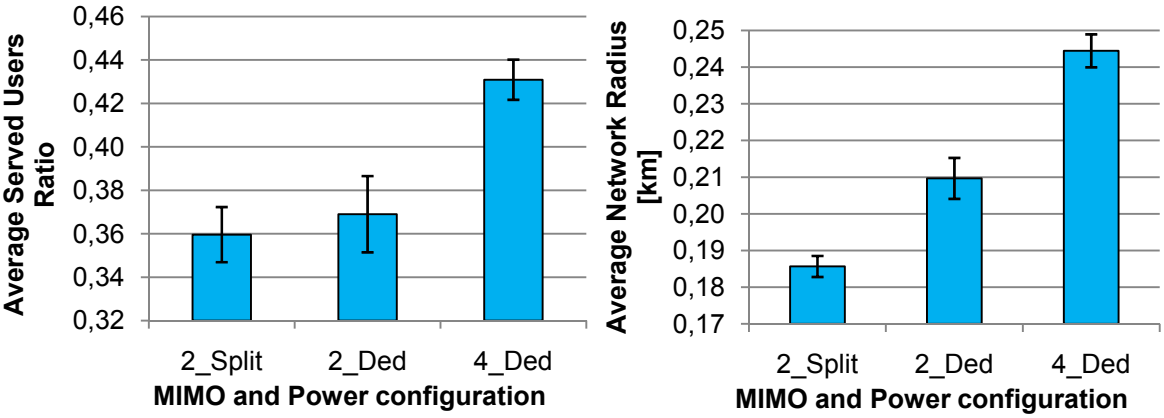

(a) Average Served Users Ratio. (b) Average Network Radius.

Figure 4.16. DL Served Users Ratio and Network Radius for different MIMO configurations and antenna power feeding.

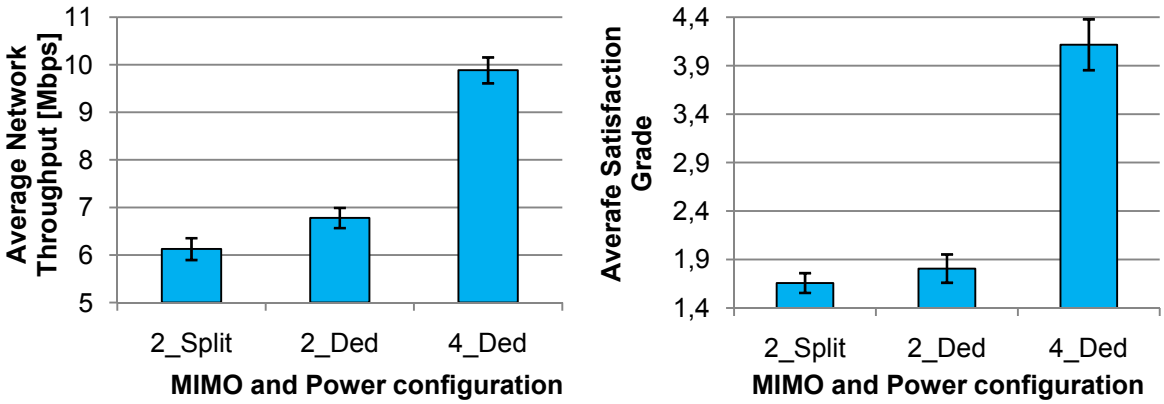

(a) Average Network Throughput. (b) Average Satisfaction Grade.

Figure 4.17. DL Network Throughput Ratio and Satisfaction Grade for different MIMO configurations and antenna power feeding.

Table 4.7 details, for each analysis, the uncovered area, uncovered and covered users. As expected by the latest results the 4×4 MIMO has the highest coverage area since needs lower SNRs values to achieve the same throughput than in the other two analysed configurations. The split power antenna fed is the configuration that has the lowest uncovered area, once there is a division of the transmission power by the antenna which leads to an increasing of the path loss and consequently the decreasing of the radius and covered area. The use of 4×4 MIMO it is also a solution to obtain a high coverage in an urban scenario in the DL, since 3% can be negligible.

Table 4.7. DL Uncovered Area, Uncovered and Covered Users for MIMO configurations and antenna power fed variation.

	2×2 Split	**2×2 Dedicated**	**4×4 Dedicated**
Uncovered Area [%]	33.2	20.7	3.4
Uncovered Users	357	191	19
Covered Users	1299	1465	1639

Concerning the average number of RBs, as predicted by the increase of the RBs capacity with 4×4 MIMO, the average number of RBs, Figure J.7, decreases 30% and further decreases 7% with a split power feeding. The total traffic network decreases 13% for the split configuration and increases 55% for the 4×4 MIMO, with a respectively, decrease of 25% and increase of 89% for the total number of users, Figure J.6.

4.3.5 Alternative Profiles

In this subsection two other profiles, Alternative 1 (A1) and Alternative 2 (A2), described in Table D.1, with different services penetration percentages, are analysed. The results are compared with the ones from the default scenario. In the profiles, the influence of Voice, in A1, and Web, in A2, service being raised, is analysed.

From Figure 4.18 (b), where the served traffic is presented, it is possible to observe that for A1 there is an increase in the Voice traffic of 60%, and A2 increases 22%. Concerning the other services, they all have a slightly decrease for the benefit of the services that increased. This decrease of the services is neater for A2 due to the higher throughput of the Web, which leads to more reduction users than for A1. Concerning to served users ratio, Figure 4.18 (a), A1 is the one with a higher ratio, 14% more than the default, since Voice is the service with the lower throughput which will enable more users to be served, while A2 has a slightly increase of 2%, since Web is an more demanding service than Voice.

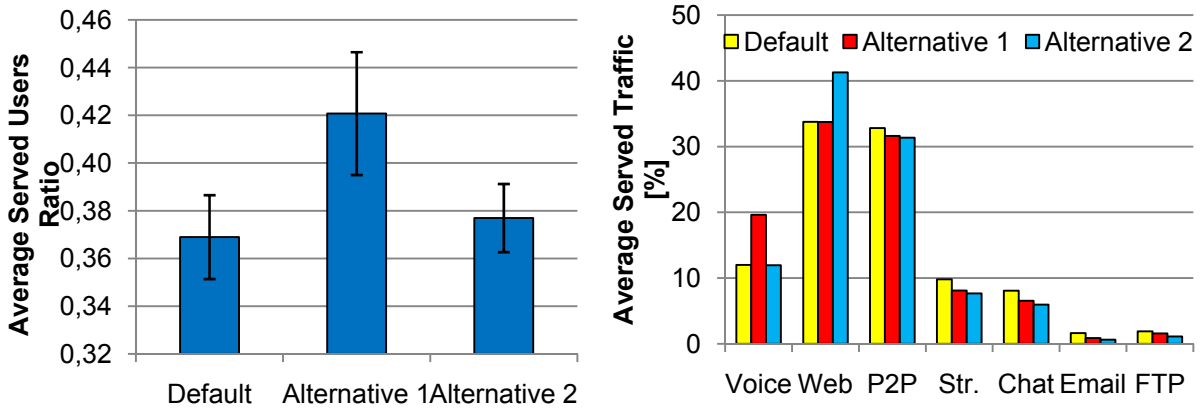

(a) Average Served Users Ratio. (b) Average Served Traffic Percentage.

Figure 4.18. DL Served Users Ratio and Served Traffic for alternative profiles.

In a total network traffic analysis, Figure 4.19 (b), A1 profile has a decrease of 10% and A2 of 8%, due to the fact the more demanding services have higher percentages in the default scenario. Concerning the total number of users, a decrease of 16% and 32% for A1 and A2, respectively, is noticed, since a Web session has a longer time duration, so it has fewer users compared with the other service, Figure 4.19 (a), exception made to Voice. The Voice service has fewer users than Web, once each user has an average of 0.825 calls per hour, still A1 has more users because the averaged served traffic for the other services is higher.

The others parameters evaluated, network radius, number of RBs and network throughput, Figure J.8 and Figure J.9, do not have an expressive variation, with exception of the average satisfaction grade,

Figure J.8 (b), which has an increase of 14% and 8% for A1 and A2, respectively. The increasing is higher for A1 since that is the profile where there is a increasing of the voice users, which have the highest satisfaction grade, as shown in the default scenario analysis.

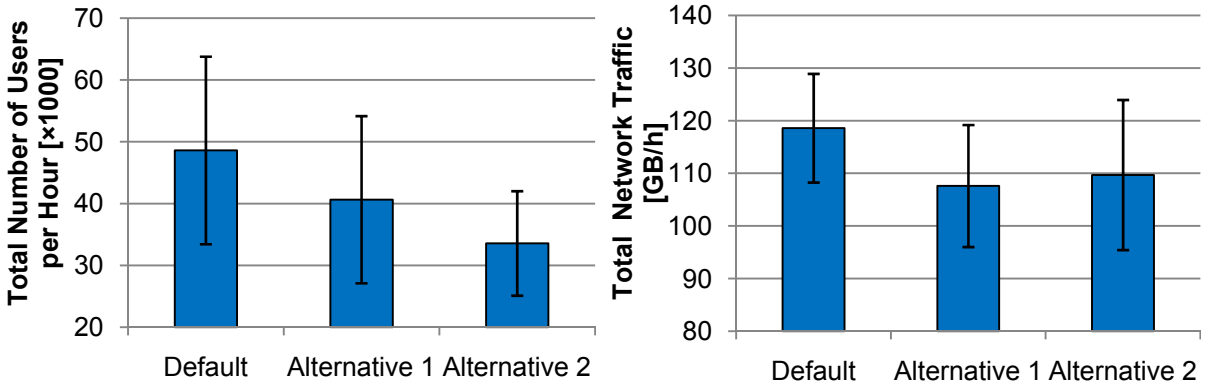

(a) Total Number of Users per Hour. (b) Total Network Traffic.

Figure 4.19. DL Total Users and Total Network Traffic for alternative profiles.

4.3.6 Number of Users

In this analysis, the number of users offering traffic to the network is increased. Increasing the number of users, Figure 4.20 (a), the average network throughput increases around 1.2 Mbps, 15%, as the system has not yet reaches its full capacity and some extra users can still be served. However, this increase is mainly due to the higher number of users that are served in those BSs that are located outside of the areas with higher traffic, which are already overloaded. As a need to serve this increase of traffic, the average number of RBs increases 20%, Figure J.10 (b). By consequence, also, the total network traffic increases 20%, Figure 4.20 (b), compared to the default scenario and more 36% of users can be served per hour, Figure J.11.

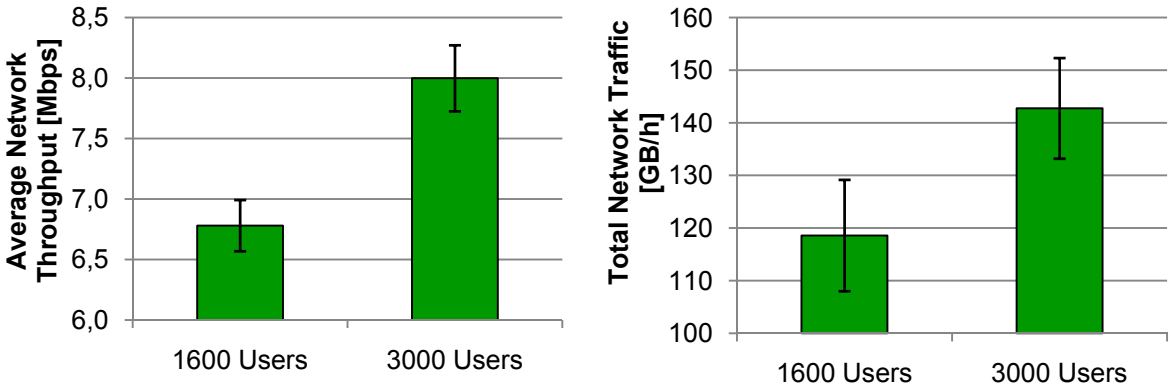

(a) Average Network Throughput. (b) Total Network Traffic.

Figure 4.20. DL Network Throughput and Total Network Traffic for 1600 and 3000 users.

As more users are served, each BS is more loaded, which leads to a decrease of the satisfaction grade of 25%, Figure 4.21 (a), since the same capacity is now distributed a higher number of users. Although the average served users decreases 25%, Figure 4.21 (b), the total number of users

performing services in this scenario is still higher than the effective number of served users in the default one.

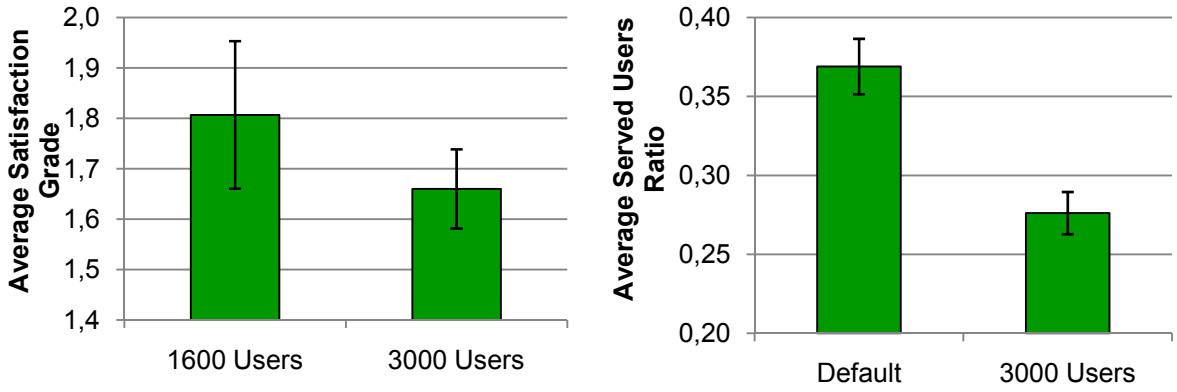

(a) Average Satisfaction Grade. (b) Average Served Users Ratio.

Figure 4.21. DL Satisfaction Grade and Served Users Ratio for 1600 and 3000 users.

The average network radius increases 9.5% as more users are spread over the coverage area, Figure J.10 (a), since the probability of the user being farther away from the BS increases. With the increase of the average network throughput when increasing the number of users, it is expected that the number of RBs increases 13%, Figure J.10 (b). Once the number of users is increased, the total number of users per hour also increases, 37%, Figure J.11.

4.4 UL Analysis in a Multiple Users Scenario

In this section UL results are analysed. First, the results of the default scenario, introduced in Section 4.1, are examined. Afterwards, simulation results considering system and MIMO parameters variation, as well as cell type, are studied. Moreover, a comparison between DL and UL is performed within each subsection.

4.4.1 Default Scenario

Like in DL, the results presented in this section were obtained using the multiple users simulator, introduced in Section 3.2.

Figure 4.22 considers all served users in all simulations performed for the default scenario, presenting the instantaneous user throughput as a function of SNR detailing the modulation of each user, with a zoom of this figure in Figure 4.23, for SNR between 0 and 1. For the same reasons presented in DL, users with lower SNRs are served with QPSK, users with middle values of SNR are served with 16QAM, and higher SNR values users are served with 64QAM. The SNR values where the transition of modulations happens are different from the ones in DL, with lower values of SNR. In UL the QPSK to 16QAM transition occurs in SNR between 0.3 and 0.7 dB, Figure 4.23, and the 16QAM and 64QAM

in SRN values between 13 and 15 dB. For the same reason than in DL, in UL the transition is not abrupt, once two channels are considered, the pedestrian one for the pedestrian and indoor environments and the vehicular one for the vehicular environment. These two channels have different expression to map the SNR onto the throughput, as shown in Annex B, which will leads to different transition values. UL served users throughputs are lower than in DL, since it has lower distances in which the maximum throughput is achieved, which is related to MT power limitations. Due to the use of RBs, the throughput of each user depends, mainly of the number of RBs, so QPSK, 16QAM and 64QAM users can achieved the same maximum throughputs being the difference on the number of RBs, where the QPSK are the users need more RBs and 64QAM the users that need less allocated ones to achieved the same throughput. Comparing with Figure 4.6, one observes that the density of the served users is much lower in UL, since it is the one that has more coverage issues.

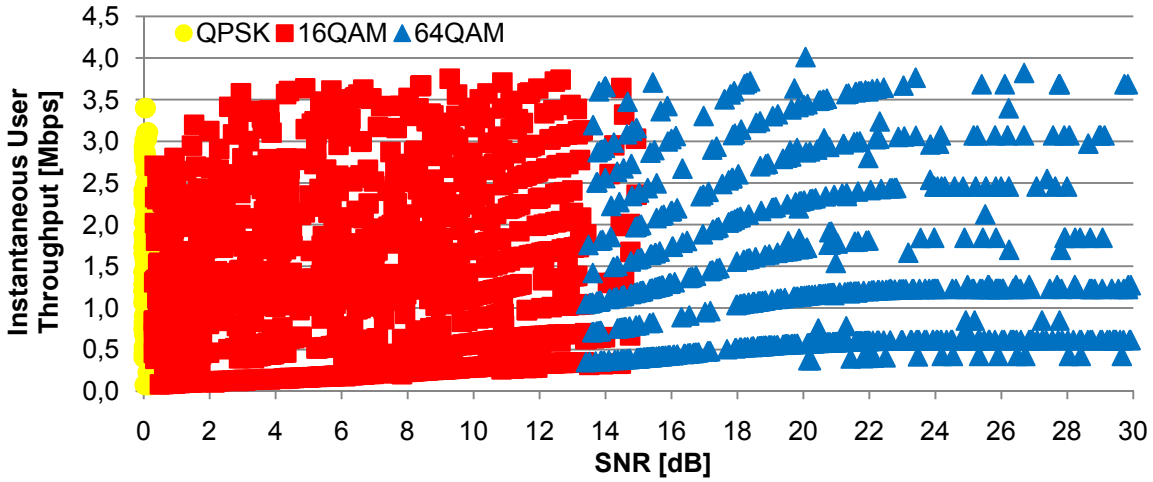

Figure 4.22. UL instantaneous user throughput for all users' variation with SNR and distinguishing the modulation of each user.

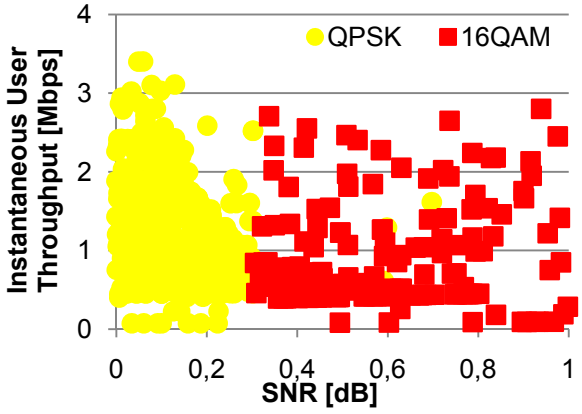

Figure 4.23. Figure 4.22 in detail for SNR values between 0 and 1.

With lower values, the distributions of the average number of users and network throughputs for each modulation, Figure 4.24, are the same that in DL. 16QAM, which is the modulation with more user density in Figure 4.22, serves more 92% and 42% users than QPSK and 64QAM, respectively, and concerning network throughput, 16QAM is higher 70% than QPSK and 35% and 64QAM.

The analysis by service was done also for UL. In UL, services have different requested throughputs

from the DL ones, taking the asymmetric of some services into account. Therefore, some services are more demanding in UL than in DL in a comparison between services, i.e., the service that has the highest throughput in DL does not necessarily corresponding in UL to the service with highest throughput. Taking this into account it is not expected that UL and DL services have the same behaviour in this analysis, Figure 4.25. E-mail and FTP are the services with lower percentage penetration; therefore they are the ones with a higher standard deviation. Associated to the low coverage of UL and the randomness of the users position and services, it gives results with a lower statistic relevance. For this reason, only the remaining services are considered for this analysis.

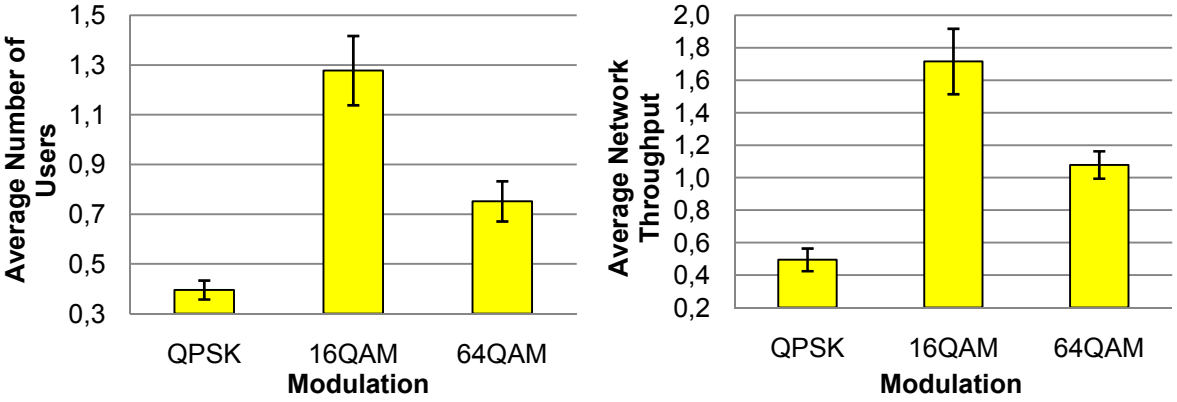

(a) Average Number of Users. (b) Average Network Throughput.

Figure 4.24. UL Number of Users and Throughput detailed for modulation, for the default scenario.

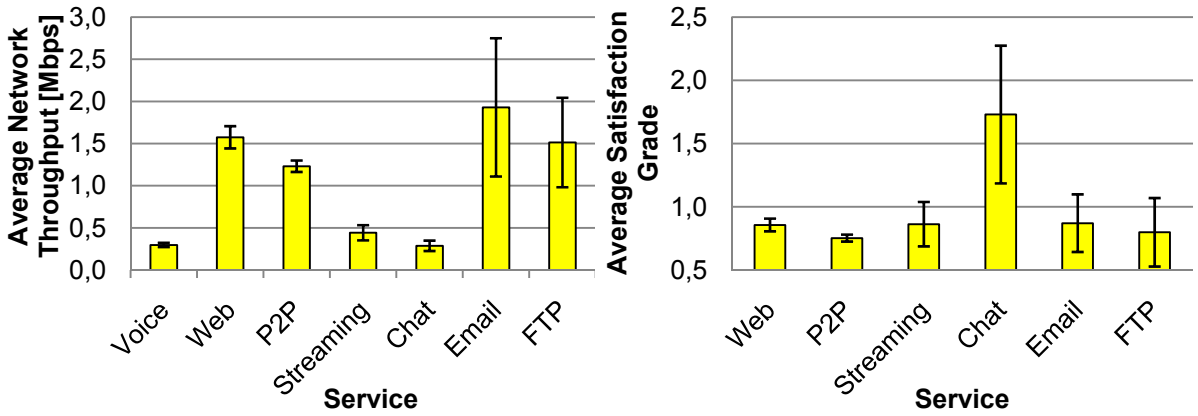

(a) Average Network Throughput. (b) Average Satisfaction Grade.

Figure 4.25. UL Throughput and Satisfaction Grade detailed for services, for the default scenario.

Web is the service that has a higher average network throughput, since it is the one that has a highest requested throughput and a high priority in QoS. Although P2P is the lower in the QoS priority, it has the same requested throughput Web, and taking this into account, as well as the other services throughputs, it explains the decrease of 18% between Web and P2P. Due to the minimum throughput, Streaming has a higher average network throughput than Voice and Chat, and, as in DL, besides Chat having a higher requested throughput, the Voice has a higher average network throughput.

Concerning the satisfaction grade Voice is not analysed in Figure 4.25 for the same reason as in DL, and the average satisfaction grade is 7.6. This value comes to give emphasis to the waste of network resources that voice in LTE causes. Concerning the remaining services, Chat is the one that has the

highest satisfaction grade, since one RB is the minimum served throughput and its capacity is always higher than the Chat request throughput. Therefore, the Chat standard deviation is explained by the RB modulation, QPSK, 16QAM or 64QAM depending on the user SNR, as explained before.

In Figure 4.26, the average number of RBs is examined. The average number of RBs and the average network throughput has similar distributions, since the two are related and the increase of each user's RB results in a proportional increase of the user throughput, as explained in Section 3.2.

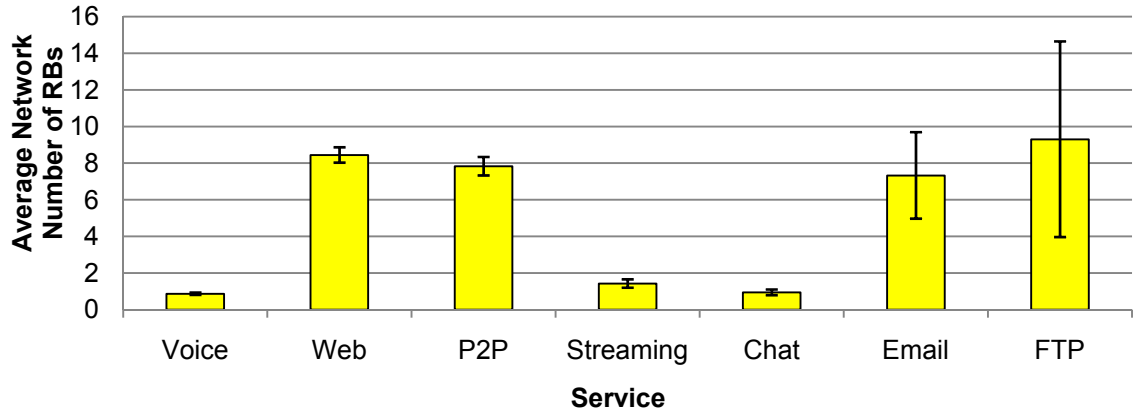

Figure 4.26. UL average number of RBs detailed for services for the default scenario.

In Figure 4.27, one represents the offered and served traffics. As expected, the offered traffic is different from the default characterisation due to the low coverage of UL not all users being served. The reason for the increase and decrease of some services percentages is the same that in DL.

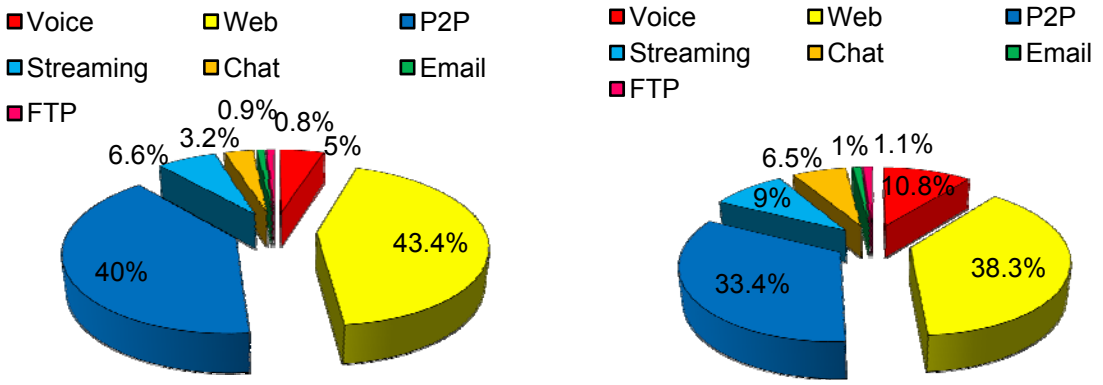

(a) Average Offered Traffic. (b) Average Served Traffic.

Figure 4.27. UL percentage of traffic.

Concerning the overall parameters, an average network throughput of 3.3 Mbps, half from the one in DL as expected due to the system limitation in the UL, a satisfaction grade of 1.9, higher than in DL once with the coverage problems the system does not have enough user for the BSs reach the maximum capacity as it can be observed also through the average number of RB, that is 18.3 with a maximum of 50 RBs per BS. In the analysis for the busy hour, the average network traffic is 55 GB/h. Regarding the number of users per hour, 26000 users can be served. The uncovered area for this scenario is 72.3%, much higher than in DL, and has on average 1008 uncovered users against an average of 648 covered users, of which 46% are served. The average network radius is 0.11 km.

4.4.2 Bandwidth

Similar to DL, a bandwidth variation analysis was performed for UL, also without analysing the 1.4 MHz bandwidth, which does not allow the reference throughput since the maximum throughput reached in this bandwidth is 3.6 Mbps for the reference scenario (Table B.6).

In Figure 4.28, it is possible to observe the average network number of RB, for the five analysed bandwidths and also the average served users ratio.

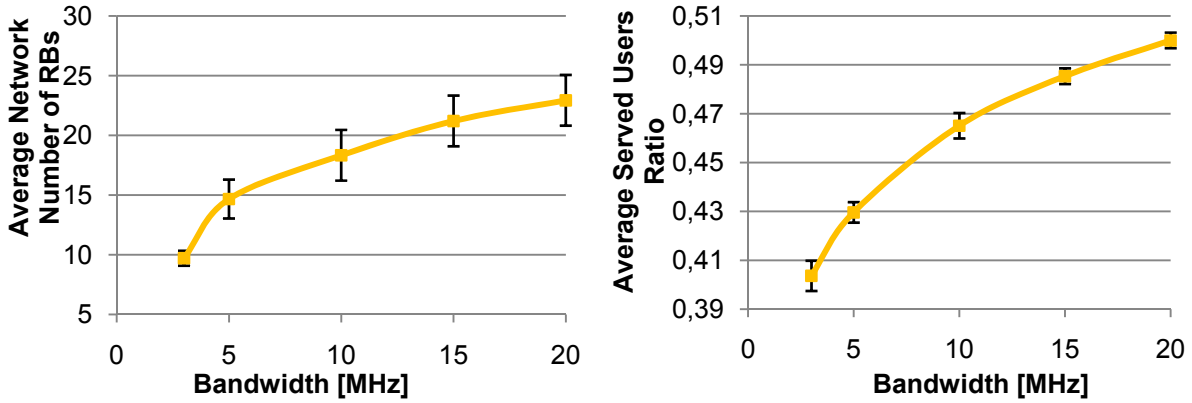

(a) Average Network Number of RBs. (b) Average Served Users Ratio.

Figure 4.28. UL Number of RBs and Served Users Ratio for the bandwidths of 3, 5, 10, 15 and 20 MHz.

These two parameters have similar behaviour with the bandwidth than in DL, but in DL the network has more profit with the RBs once the increasing of the RBs with the bandwidth is higher. Comparing the average number of RBs with the ones of the default scenario, the 3 and 5 MHz bandwidths have a decrease of 50% and 20%, respectively, and 15 and 20 MHz have an increase of 17% and 28%. The slope for increasing to 15 and 20 MHz bandwidths is lower than the 3 and 5 MHz decreasing slope, since the number of BSs that profit from the increase of RBs, due to the coverage, decrease, i.e., the BSs that are outside the areas with high traffic due to the reduced coverage do not have enough users to profit from the increase of RBs. The same behaviour is noticed on the average served users' ratio, comparing with the 10 MHz bandwidth, being observed a decrease of 13 % and 7% for 3 and 5 MHz, respectively, and an increase of 6% and 9% for 15 and 20 MHz. These differences between the decreasing and increasing slopes are explained in the same way as in the RBs analysis. A more complete comparison with DL, shows that for the average served users ratio the values are higher for UL, but it is important to point out that the coverage area is 50% lower in UL, so there are less users to be served and consequently the need of RBs decreases.

With the increase of bandwidth, and therefore the number of RB available to serve users, the average satisfaction grade, Figure 4.29 (a), increases since users are less reduced and, consequently, it leads to an increase of the average network throughput, Figure 4.29 (b). The average network throughput, as expected has a similar behaviour that the average network of RBs, by the same reason as in DL. The 3 and 5 MHz bandwidths have a decrease of, respectively, 10.5% and 5.3% for the satisfaction grade and 32% and 15% for the network throughput, relative to the default scenario. In the same way,

the 15 and 20 MHz increased in 10.5% and 21% the satisfaction grade and 12% and 18% the average network throughput. The satisfaction grade is higher than in DL since there are fewer users to be served.

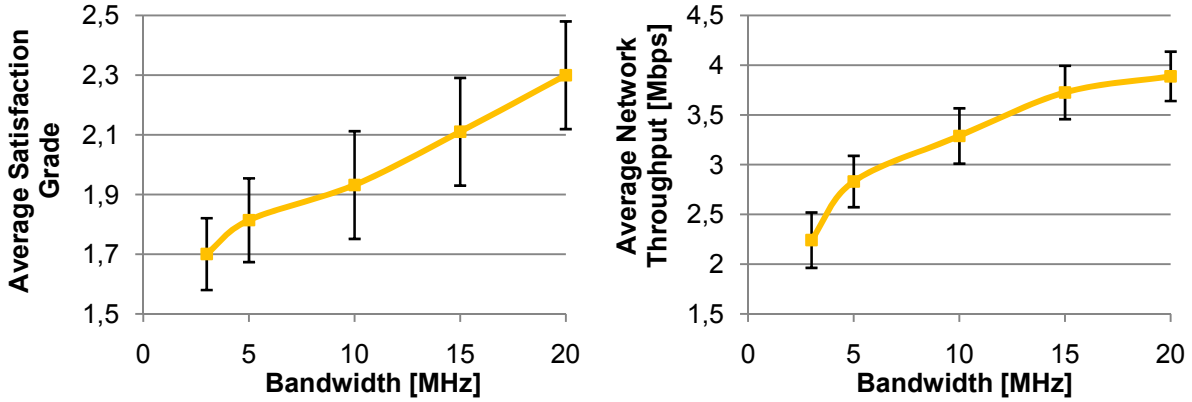

(a) Average Satisfaction Grade. (b) Average Network Throughput.

Figure 4.29. UL Satisfaction Grade and Network Throughput for the 3, 5, 10, 15 and 20 MHz bandwidths.

Concerning the busy hour statistics, the total traffic network decreases 28% and 16% for 3 and 5MHz bandwidths, respectively, and has an increase of 13% and 16% with the 15 and 20 MHz bandwidths, comparing with 10 MHz. The total number of users in the 3 and 5MHz bandwidths is 36% and 26% lower than in 10 MHz and 11% and 32% higher for the 15 and 20 MHz bandwidths, respectively.

The average network radius does not have significant variations, which means that it can be considered constant for the different bandwidths.

4.4.3 Frequency Band

In the path loss, the frequency band has the same impact on UL as on DL, since the propagation model and the penetration margins are the same. The main difference between DL and UL is the rise of the coverage area for the 900 MHz frequency band, which for DL is 20%, i.e., an average more 191 users (12%), and for UL is 57% , i.e., an average of more 879 users (135%) comparing with the 2100 MHz band. Also the impact of the decrease in the coverage area, and consequently the number of covered users, due to the increase of the frequency band to 2600 MHz is different. For UL, these numbers on the three frequency bands are shown in Table 4.8, and for DL on Table 4.6.

Table 4.8. UL Uncovered Area, Uncovered and Covered Users for 900, 2100 and 2600 MHz.

	900 MHz	2100 MHz	2600 MHz
Uncovered Area [%]	15.3	72.3	86.5
Uncovered Users	129	1008	1334
Covered Users	1527	648	322

In the 900 MHz frequency band, as said before, the uncovered area decreases, therefore, there is an increase of approximately of 125% of the average network radius comparing with the 2100 MHz band, Figure 4.30 (b), much higher than in DL. The radius decreases 32% for the 2600 MHz frequency band, also higher than the decrease in DL. As expected the number of served users increases for 900 MHz, as explained in DL, and confirmed by Figure K.3, but in the 2600 MHz band the served users ratio increases, contrary to DL. This difference is explained by the lower average covered users in 2600 MHz and 2100 MHz, where 2600 MHz has 50% less than 2100 MHz, which are the only users that are taken into account for this ratio calculation. So, if instead of this ratio, the average number of served users had been analysed it would have been noticed that the number of served users decreases, as expected, compared to 2600 MHz, which means approximately 265 served users in the 2100 MHz band against 154 served users in the 2600 MHz. The average served users ratio increases 40% and 2.5% for 900 and 2600 MHz, respectively.

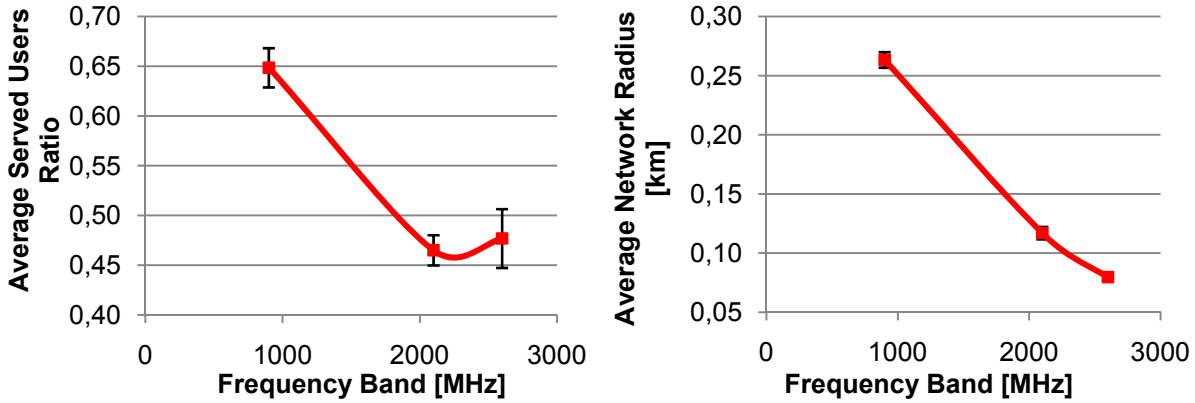

(a) Average Served Users Ratio. (b) Average Network Radius.

Figure 4.30. UL Served Users Ratio and Network Radius for the frequency bands of 900, 2100 and 2600 MHz.

From Figure 4.31, it is possible to analyse the average network throughput and the average satisfaction grade for the different bandwidths. The average network throughput, Figure 4.31 (a), as in DL, has higher throughput values for the lower frequency bands, as explained in DL and supported by Figure K.3. With the high increasing of the network radius and covered area in the 900 MHz, there are users to take profit from the network capacity, being justified by the high increasing of the average network number of RBs. The 900 MHz frequency band has an average network throughput 138% higher than the 2100 MHz and 2600 MHz has 21% less. As expected for 2600 MHz the average network throughput decreases since in this frequency band the covered problems are higher than in 2100 MHz. Regarding the average satisfaction grade, the results have a different behaviour from the DL ones, since the 900 MHz frequency band serves 230% more users compared with 2100 MHz, and the satisfaction grade decreases only 3%. This decrease is insignificant regarding the users increase. In the 2600 MHz band, the satisfaction grade increases 30%.

From these results, it can be seen that the 900 MHz frequency band, resolve the major problem in UL, capacity, since 15% of uncovered area is easily overcame with the introduction in the network of a few BSs. Also the DL results, shows the coverage improvements with 900 MHz. The 2600 MHz frequency

band is undesirable, since the uncovered area in UL is extremely high.

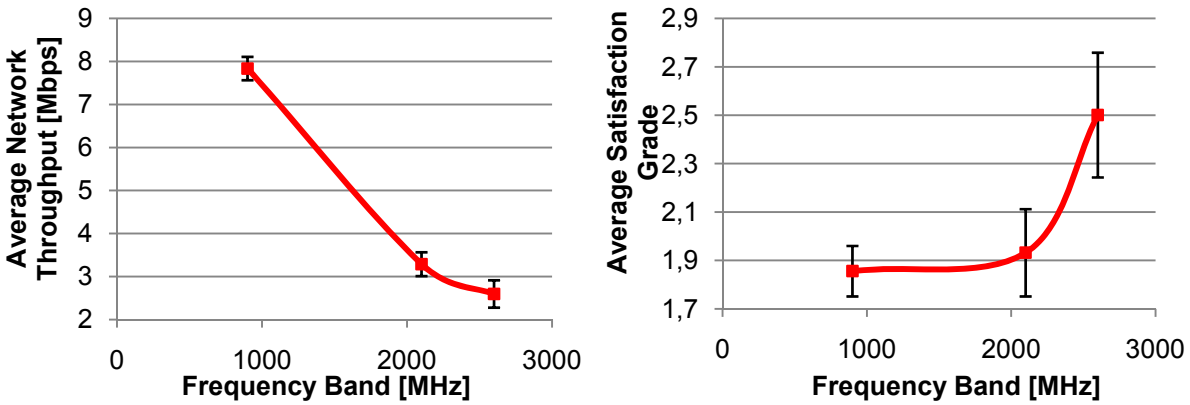

(a) Average Network Throughput. (b) Average Satisfaction Grade.

Figure 4.31. UL Network Throughput Ratio and Satisfaction Grade for the frequency bands of 900, 2100 and 2600 MHz.

The average number of RBs, Figure K.5, at the BSs level is 63% higher and 21% lower, for 900 MHz and 2100 MHz, respectively, than in the default one, as in the average network throughput. Although the increase is higher in 900 MHz for the average network throughput, this is due to the possibility of higher order modulation that can be used in this band, as it is shown in Figure K.3. Regarding the total traffic network in a busy hour and the total number of users, Figure K.4, there is an increase of, respectively, 272% and 207%, observed for the 900 MHz band and a decrease of 50% and 63% for the 2100 MHz one.

4.4.4 MIMO configuration and Antenna Power Fed

The use of 4×4 MIMO and split antenna power in UL is analysed in this subsection. It is important to notice that in UL the use of split antenna power fed in UL represents a capacity increase to SISO with no battery assumption increase, since the antennas in MIMO are fed with the same power that in a SISO configuration, as desired.

With a lower power transmission the uncovered area increases 7.9%, Table 4.9, and also the average network radius decreases 15%, Figure 4.32 (b). The 4×4 MIMO decreases the uncovered area by 10.6%, like in DL and, as a result, there is an increase on the average network radius of 19%.

Table 4.9. UL Uncovered Area, Uncovered and Covered Users for different MIMO configurations and antenna power feeding.

	2×2 Split	2×2 Dedicated	4×4 Dedicated
Uncovered Area [%]	80.2	72.3	61.7
Uncovered Users	1174	1008	791
Covered Users	482	648	865

It is important to notice that if in DL 4×4 MIMO could be a solution to overcome the coverage problems, in UL with 61.7% of uncovered area still, which is very high, and being the number of BSs needed to cover this area is very high, leaves to be a solution, once this two links are deployed together.

Concerning the served users ratio, Figure 4.32 (a), contrary to DL, increases when a split power fed is used and decreases with the use of 4×4 MIMO. These results, are explained by the fewer covered users in UL, and, therefore, the total number of users is analysed. The 2_Split configuration serves an average of 231 users, 2_Ded 298 users and the 4_Ded 380 users. So this decrease is, in reality, an increase of the total served users' number, as expected.

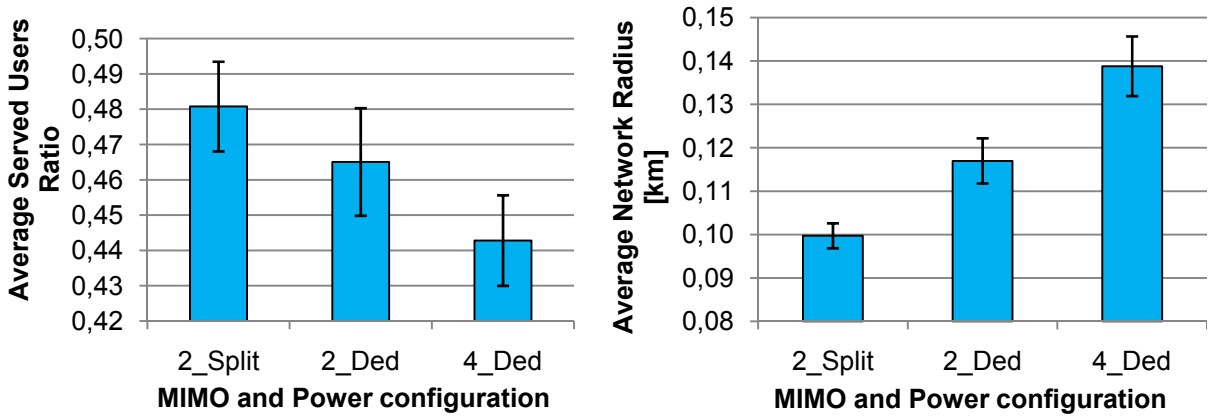

(a) Average Served Users Ratio. (b) Average Network Radius.

Figure 4.32. UL Served Users Ratio and Network Radius for different MIMO configurations and antenna power feeding.

The average network throughput, Figure 4.33 (a), and the average satisfaction grade, Figure 4.33 (b), have a variation similar to DL but with lower values and variation, being the increase of capacity due to 4×4 MIMO less notice. For the average network throughput, the split power fed has the lowest value, with a decrease from the dedicated one of 8% and using 4×4 MIMO gives an average network throughput increase of 30% compared with a 2×2 MIMO. The average satisfaction grade is 5% lower for the split configuration, and 4×4 MIMO has a satisfaction grade 26% higher, as expected, with the increasing of capacity that 4×4 MIMO allows to the system.

Regarding the total number of users per hour and the total network traffic, Figure K.4, there is an increase of 46% and 50% respectively, for 4×4 MIMO, taking as reference the 2×2 MIMO with a dedicated antenna feeding, and the split antenna feeding decreases, respectively, by 40% and 23% these two evaluation network parameters. The average number of RBs decreases 12% with split configuration, since less users are served, and also has a lower average network throughput, and a decrease of 13% with 4×4 MIMO, since the RBs capacity increase with the use of 4×4 MIMO and the number of covered users are very low. The BSs with the number of RBs allowed for this bandwidth and with a 2×2 MIMO have enough capacity to serve all the users and does not profit of all the network resources. So, due to the low increase of the coverage in UL, the trade-off by the increment of capacity through the use of 4×4 MIMO is not as high as in DL.

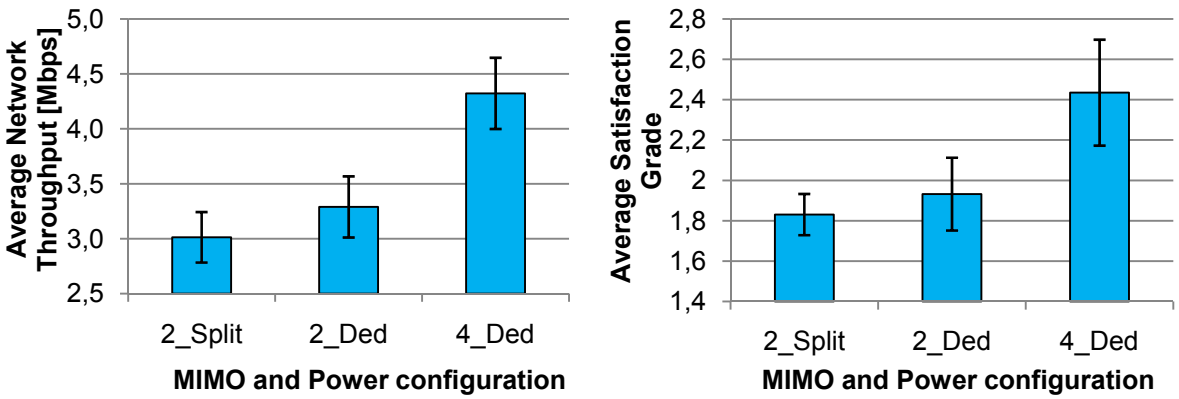

(a) Average Network Throughput. (b) Average Satisfaction Grade.

Figure 4.33. UL Network Throughput and Satisfaction Grade for different MIMO configurations and antenna power feeding.

4.4.5 Alternative Profiles

The high uncovered area percentage affects this analysis, since the randomness of the users' position and services from the input files combined with a low coverage area does not allow that the services penetration percentages of the alternatives profiles to be maintained, as it can be observed in Figure 4.34 (a). So this analysis is not compared to the DL one. Taking the average served traffic percentage into account, and analysing the average served users ratio, Figure 4.34 (b), it is observed that the A1 profile has an increase of 5%, since there are more Voice users (service with the lowest throughput) that will allow more users to be served, and it is constant for the A2 profile, compared with the default scenario. From Figure 4.35, the total number of users per hour can be analysed jointly with the total traffic network. The number of users decreases for both profiles, 5% for A1 and 12% for A2, due to the increase of P2P penetration, since this service is highly demanding being characterised by a large file size, and due to the low throughput tolerated, a long session duration. The decrease is higher for A2, since the Web service penetration is higher than the one in A1, and Web users also have a long session time. The total network traffic also decreases for both profiles, 38% for A1 and 23% for A2. Since Voice is the service with the lowest throughput and A1 is the profile that has a higher penetration of Voice, it is the one that has a lower network traffic.

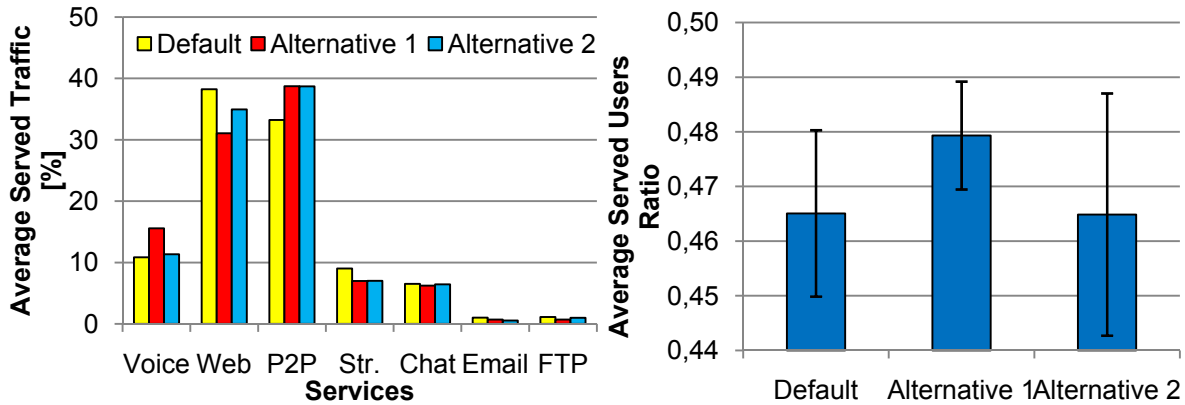

(a) Average Served Traffic Percentage. (b) Average Served Users Ratio.

Figure 4.34. UL Served Traffic and Served Users Ratio for alternative profiles.

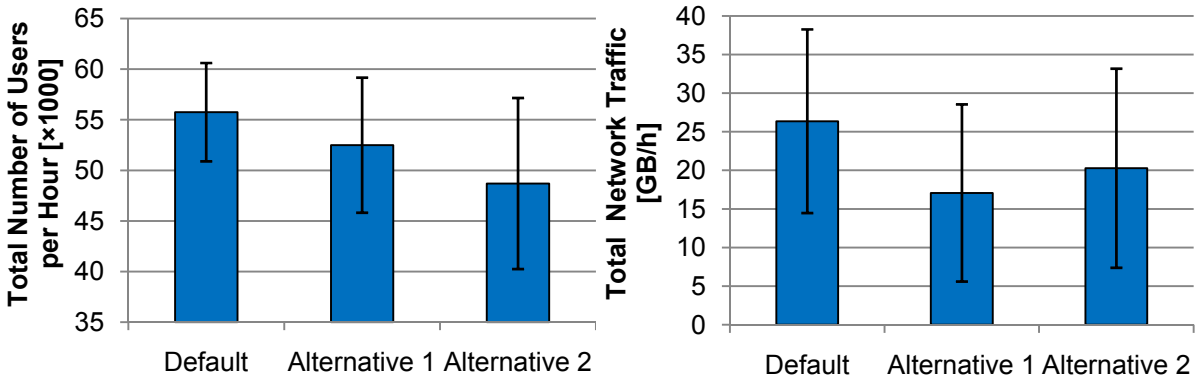

(a) Total Number of Users per Hour. (b) Total Network Traffic.

Figure 4.35. UL Total Users and Total Network Traffic for alternative profiles.

The average network radius, Figure K.8 (a), is practically the same for the three profiles, and the satisfaction grade, Figure K.8 (b), increases for both profiles, 19% for A1 and 16% for A2. Once more, Voice users have an important role, since Voice, as explained, has the highest satisfaction grades, highlighting the others services satisfaction grades. In Figure K.9, the number of RBs and the average satisfaction grade is presented. As expected, A1 has a decrease in both parameters of 44% in the number of RB and 9% on the average throughput, and A2 decreases 41% and 3% in the same parameters.

4.4.6 Number of Users

As a consequence of the RBs increasing, around 16%, Figure K.10, the average network throughput, Figure 4.36 (a), increases 1.3 Mbps, 40%, when one increases the number of users offering traffic to the network, as the system can serve more users at the cost of a reduction of 11% of the satisfaction grade, Figure 4.37 (a). The same phenomenon described for DL is also valid in this case. The average network radius increases around 3% as more users are in the BS coverage area, Figure K.10 (a). The average ratio of served users, Figure 4.37 (b), decreases 4%, but, as in DL, the total number of served users is still higher than the ones in the default scenario. The network traffic, Figure 4.36 (b), increases 35% as more users are served instantaneously. The number of users per BS increases 60%, Figure K.11.

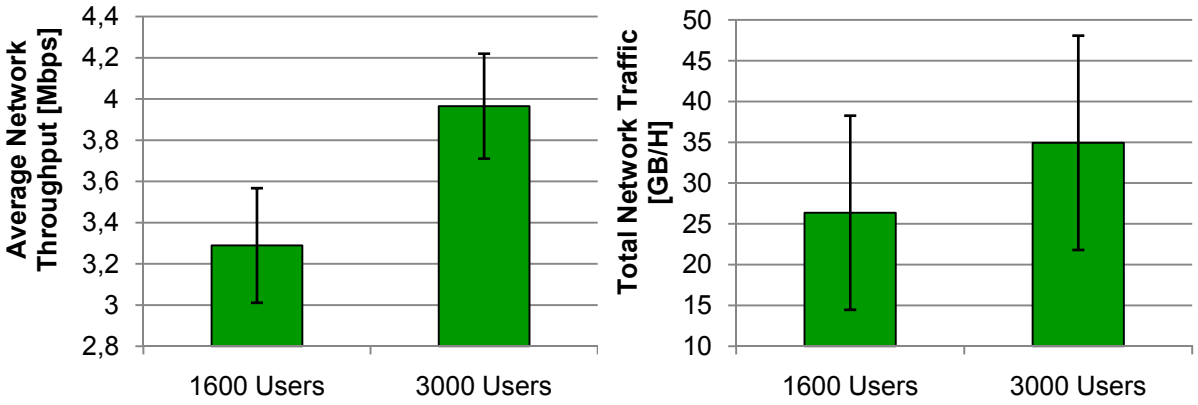

(a) Average Network Throughput. (b) Total Network Traffic.

Figure 4.36. UL Network Throughput and Total Network Traffic for default scenario and 3000 users' scenario.

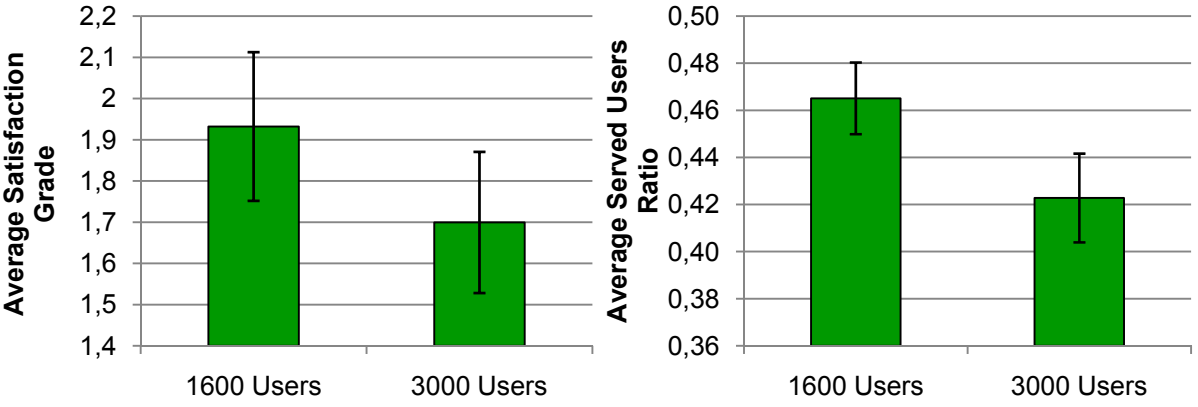

(a) Average Satisfaction Grade. (b) Average Served Users Ratio.

Figure 4.37. UL network parameters (Satisfaction Grade and Served Users Ratio) for default scenario and 3000 users' scenario.

Chapter 5

Conclusions

This chapter point out the main conclusions of this thesis, as well as some suggestion for future work

The main objective of this thesis was to analyse LTE performance in terms of capacity and coverage. To accomplish this goal, a great amount of information was gathered, in order to develop and implement two models: the single and the multiple users. These models were developed based on literature results and on some previously developed models. The COST 231 Walfish Ikegami model was used to calculate the cell radius or the distance to the BS, according with the model, based on this path loss. Since LTE networks are developed to be standalone ones, lower releases of UMTS are not considered in the two developed models. The RMG model, developed by [KuCo07], was applied to predict the improvements in capacity of using MIMO over SISO.

With the main objective of calculating the maximum cell radius for LTE in both DL and UL in a single user scenario, according to the user's requested throughput, the single user model was developed and implemented in C++. This approach was taken in order to have a first approach regarding cellular planning. Concerning different system parameters, as frequency, bandwidth, MIMO configuration, modulation, indoor penetration margin, and both fast and slow fading, among others, the model enables one to calculate the radius for the users requested throughput through its mapping onto SNR.

The aim of the multiple users scenario is to assess the performance in a real network, simulating a multiple users scenario in a snapshot approach, and analysing individually DL and UL. One of the main differences between the two scenarios is that, for the multiple users scenarios the resources available in each BS are shared among all users and the need to account the users' interference emerges through the introduction of the interference margin. Also for a more realistic approach, statistical distributions for the fading margins are considered and AMC was also implemented. With the distance of the user to the BS, the SNR is mapped onto the RB throughput, being possible to calculate the number of RBs that the user needs in order to achieve the requested throughput. After, considering all served users a BS capacity analysis is done in order to verify if the BS users with the given throughput exceed the capacity. When the capacity is exceeded, one of the reduction strategies is applied, where the Voice users are only reduced when there are no RBs allocated for data users in the BS until the maximum capacity is achieved. With all served users taken into account, a network analysis is then performed to evaluate its performance, regarding several parameters, such as MIMO configuration, bandwidth, reduction strategy, frequency, and power feeding antennas among others.

Regarding the default single user scenario, considering a 10 MHz bandwidth, LTE has, for the maximum throughput allowed, a radius of 0.34 km in DL and 0.12 km for UL. For indoor environments, the most common in urban scenarios, the radius decrease to 0.16 in the low losses and to 0.09 km in the high losses one. If lower bandwidths were chosen, the radius increases, but it is important to notice that with the decrease of the bandwidth there is an implicit decrease of the maximum throughput and the 14.4 Mbps cannot be assure. The increase of the bandwidth has the opposite effect. So there is a compromise between the capacity, bandwidth, and the coverage, cell radius. For QPSK and 64QAM, in a 10 MHZ bandwidth the radius is 0.49 and 0.19 km, for DL, respectively, and 0.19 and 0.07 km in the UL; in this case the maximum throughput behaviour varies opposite to the robustness of the modulation. Fixing the requested throughput, the radius increases with the decrease of the bandwidth and also by increasing the robustness of the modulation. The use of 900 MHz

frequency band instead of the 2100 MHz one, leads to a radius increase of 150%, which decrease the coverage problems, and the use of 2600 MHz to a radius reduction around 20%, for both DL and UL.

In the multiple users simulator, for the DL default scenario, an average network radius of 0.21 km is obtained. The average network throughput is 6.78 Mbps, and has an average of 29.2 RBs used in the network by each BS, in a maximum of 50 RBs per BS. The average satisfaction grade ratio is 1.8, due to the higher Voice satisfaction grade and the reduction policy for Voice users. Voice and Chat users have both an average satisfaction grade higher than others, and both are above one, so the use of these undemanding services is a waste of network capacity since one RB just can be allocated for one user. Of the three AMC modulations, the one that serves more users is 16QAM with a higher contribution for the average network throughput, followed by 64 QAM and QPSK. The comparison between the offered and served traffic shows that there is a reduction of the Web and P2P users, which is compensated by the increase of the other services, pointing out Voice that rises from 5.3% to 12%. Due to the QoS differentiation in the reduction strategies, besides Voice, Web is the one with higher priority and the second one with maximum requested throughput, and also with a highest average network throughput, only exceeded by the FTP service that has a maximum requested throughput three times higher than Web, but, due to its low QoS, it is even more reduced, with an average network throughput 0.9 Mbps more than Web.

When considering the UL multiple users default scenario, an average network radius of 0.11 km is obtained. The average network throughput is 3.3 Mbps with an average satisfaction grade ratio of 1.9, higher than in DL due to the lower number of covered users, but also with Voice and Chat users with satisfaction grade above 1. The average number of RBs is 18.3, this lower number being, also, the result of the lower coverage. The modulations transition due to AMC happen in lower SNR values than in DL, but the behaviour is equal. Both offered and service traffics are similar to the DL ones. The data service with highest QoS priority, Web, has an average network throughput of 1.5 Mbps and the highest average satisfaction grade, regarding that E-mail and FTP are not analysed due to its lower statistic relevance. In a coverage analyses, there is 27.7% of coverage area from the total one, less 49.4% than in DL, and around 60% of uncovered users, less 50% than in DL.

The variation of the bandwidth leads to an increase of the average network throughput, due to a higher capacity, by 13% and 40% for an increase from 10 to 15 and 20 MHz bandwidths, respectively, and a reduction of almost 19% and 9% when 3 and 5 MHz bandwidths are used, in DL. For these 5 bandwidths, the average number of RBs decreases 60% and 38% for the 3 and 5 MHz bandwidths and increases 24% and 37% for 15 and 20 MHz taking 10 MHz as reference. These variations are lower than the real variation of the network resources with the bandwidth. The increase of the resources enables one to serve more users, the decreasing of the resources being the opposite effect. It is necessary to taking the compromise between the served users ratio and the satisfaction grade of the users into account, when choosing a bandwidth. For UL the variation of the bandwidth has the same impact in the network than in DL but with lower profits of the RBs increasing since the uncovered area is very high.

Being the path loss so correlated with the frequency, the use of different frequency bands is also

studied. Taking the 2100 MHz frequency band as a reference, the 900 and 2600 MHz ones studied. The cell radius has an increase around 50% for 900 MHz in DL and 125% in UL. Regarding the 2600 MHz band, the radius decreases 17% in DL and 32% in UL. For DL, the coverage area increases 20.7% and decreases 22.9%, respectively, with the decrease and increase of the frequency band. The coverage area has a similar behaviour in UL. The total number of served users rises by decreasing the frequency band, and decreases with the increasing of the frequency band, although in UL the served user's ratio for the 2600 MHz bandwidth is higher than the one in 900 MHz band. In DL, there is an increase of 83% in the number of served users for the 900 MHz band and a decrease of 27% for 2600 MHz. Also for DL, the average network throughput increases 97% at the 900 MHz band compared to 2100 MHz and for 2600 MHz a decrease of 14% is observed. The UL variations due to the frequency band are higher than in DL.

The study of a different MIMO antenna configuration, 4×4, and the use of different antenna power fed solutions was also made. From the default scenario, with 2×2 MIMO and dedicated antenna power fed, one analyses the split power fed and a dedicated power fed the MIMO configuration of 4×4. Regarding that these changes in the network changes the network coverage, a coverage analysis is performed. The highest covered area is obtained in the 4×4 MIMO, with an increase of 17.3% in DL, compared with the reference. The split power fed decreases the covered area in 12.5% in DL. The average network radius decreases 11% for split power fed and increases 16% for 4×4 MIMO in DL. Concerning to the total number of served users, it increases with the 4×4 MIMO and decreases with split power, for DL and UL, despite the fact of the average served users having an opposite behaviour in UL, due to low coverage. 4×4 MIMO increases 120% the average satisfaction grade and the split fed power decreases 10%, in DL. The average network throughput raises 45% in DL with the 4×4 MIMO and decreases with a split power fed in 10% in DL. In UL the network trade-off due to the MIMO configuration and antenna power fed is lower than in DL.

Two alternative profiles were created to study the influence of the variation of the services' penetration percentages, one with higher Voice penetration percentage (A1) and the other with higher Web penetration percentage (A2). The Voice lower throughput and the reduction strategies taken for Voice can be studied through the A1 profile. As a result of the increase of the service with the lowest throughput the average of served users' increases as their satisfaction grade, 14% for both, since there are more Voice users, which have a very high satisfaction grade. The A2 profile with the Web service increase has a major variation in a busy hour analysis, since the Web service has high throughput and also has a service with a high session time, so users decrease 32% and the total traffic 8%. For UL these profiles were not possible to obtain due to the lower coverage of UL.

To evaluate LTE behaviour in load situations, for both DL and UL, one increased the number of users offering traffic to the network. The average network throughput increases 20% and 40% for DL and UL, respectively. The increase of the average network throughput is noticed at the users' level, where there is a reduction of the average satisfaction grade, since the same resources are shared among a larger number of users. Regarding the average network radius there is an increase of 9.5% and 3% for DL and UL, respectively.

The results for the multiple and the single user models show that DL has a larger cell radius than UL. This means that the latter is the one that limits coverage, since DL and UL are deployed together. To increase coverage, a lower frequency band is desirable, since it is the factor with more impact on the radius, but also has an impact in the network capacity since it is possible to serve more users with higher order modulation, in the AMC. Focusing on the new technologies brought by LTE, 4×4 MIMO increases the capacity of the network, which leads to an increase of the average network throughput and served users. Having MIMO with split power feeding reduces the cell radius and the number of served users. The major advantage of increasing the bandwidth is in the high traffic areas where the offered traffic exceeds the BS capacity.

For future work, it is suggested that in a multiple users scenario, an analysis of different bandwidths in the BSs is done, for achieving a better use of the network resources. At the RRM level, it could be interesting to optimise user's connection to the BS, based not only on the users' distance but also in the BS available resources. A reduction strategy based on both the QoS priority and on the users requested resources could also be relevant in future research. Since LTE uses OFDMA, which has a major impact in the decreasing of the interference, intra- and inter-cell ones, a deeper study on this subject is desirable. Also a comparison with WiMAX, which is a technology that uses the same multiple access that LTE, OFDMA, it is interesting to study. Since LTE makes an extensive use of advanced multi-antenna transmission technologies', including beam forming for improved coverage and capacity and spatial multiplexing for higher data rates, an LTE analyses with these technologies is of interest.

Annex A - Link Budget

The link budget used throughout this thesis is based on the Release 99 one, described in detail in [CoLa06] and [Sant04], adapted to LTE.

The path loss, L_p, can be calculated by :

$$L_{P_{[dB]}} = Pt_{[dBm]} + G_{t_{[dBi]}} - Pr_{[dBm]} + G_{r_{[dBi]}} = EIRP_{[dBm]} - Pr_{[dBm]} + G_{r_{[dBi]}} \quad (A.1)$$

where:

- Pt is the transmitting power at antenna port;
- G_t is the transmitting antenna gain;
- P_r is the available receiving power at antenna port;
- G_r is the receiving antenna gain.

If diversity is used, G_r: is replaced by

$$G_{rdiv_{[dB]}} = G_{r_{[dBi]}} + G_{div_{[dB]}} \quad (A.2)$$

where:

- G_{div} is the diversity gain.

The Equivalent Isotropic Radiated Power (EIRP) can be calculated for DL by (A.3), and for UL by (A.4).

$$EIRP_{[dBm]} = P_{Tx_{[dBm]}} - L_{C_{[dB]}} + G_{t_{[dBi]}} - P_{sig_{[dBm]}} \quad (A.3)$$

$$EIRP_{[dBm]} = P_{Tx_{[dBm]}} - L_{U_{[dB]}} + G_{t_{[dBi]}} - G_{MHA_{[dB]}} - P_{sig_{[dBm]}} \quad (A.4)$$

where:

- P_{Tx} is the total BS transmission power;
- L_c is the cable losses between transmitter and antenna;
- L_u is the body losses;
- G_{MHA} is the masthead amplifier gain.

The received power can be calculated by (A.5) for DL and (A.6) for UL:

$$P_{Rx_{[dBm]}} = P_{r_{[dBm]}} - L_{U_{[dB]}} \quad (A.5)$$

$$P_{Rx_{[dBm]}} = P_{r_{[dBm]}} - L_{C_{[dB]}} \quad (A.6)$$

where:

- P_{Rx} is the received power at receiver input.

The LTE receiver sensitivity can be approximated by :

$$P_{Rx_{min\,[dBm]}} = N_{[dBm]} + \rho_{[dB]} \quad (A.7)$$

where:

- ρ is the SNR;
- N is the total noise power given by:

$$N_{[dBm]}=-174+10\log(\Delta f_{[Hz]})+F_{[dB]}+M_{I_{[dB]}} \quad (A.8)$$

where:

- Δf is the bandwidths of the RB allocated for the user,
- F is the receiver's noise figure;
- M_I is the interference margin.

To calculate the number of served users is necessary to take the interference into account to evaluate the throughput due to the user distance. The interference margin is calculated based on the total number of users of the BS coverage area. It is most likely that the BS with the higher number of users in its coverage area is the BS with more served users. For the BS with the higher number of users connected to it is assigns the maximum interference margin value, and for the other BSs, the interference margin for LTE at a given BS is estimated by:

$$M_{I_{j\,[dB]}}=\frac{N_{u_j}}{N_{U_{max}}^{BS}}\cdot\beta_{[dB]} \quad (A.9)$$

where:

- β is the maximum interference value considered;
- N_{u_j} is the number of users in the BS j;
- $N_{U_{max}}^{BS}$ the number of users of the most populated BS.

Some margins must be taken into account, to adjust additional losses caused by radio propagation and others:

$$M_{[dB]}=M_{SF_{[dB]}}+M_{FF_{[dB]}}+L_{int_{[dB]}} \quad (A.10)$$

where:

- M_{SF} is the slow fading margin;
- M_{FF} is the fast fading margin;
- L_{int} is the indoor penetration losses;

The total path loss can then be calculated by,

$$L_{P\,total_{[dB]}}=L_{P_{[dB]}}-M_{[dB]} \quad (A.11)$$

The total path loss is used as input in the COST 231 Walfisch-Ikegami propagation model, described in [DaCo99], to calculate the cell radius, R, for the single user model. In Section 3.1, this calculus is briefly shown. For some LTE frequencies, f, the values used ([2110, 2170] MHz, [2500, 2570] MHz and [2620, 2690] MHz) exceed the frequency validation values and some of the calculated cell radius are below the distance validation values, namely for high data rates. Nevertheless, the model was used, since it is adjusted to urban non-line of site propagation.

The COST 231 Walfisch-Ikegami propagation model is valid for [DaCo99]:

- $f \in [800, 2000]$ MHz ;
- $R \in [0.02, 5]$ km ;
- BS height between 4 and 50 m;

- MT height between 1 and 3 m.

In Table A.1 the values for the propagation model's parameters are listed. For the parameter that represents the frequency losses dependence due to diffraction by a set of knife-edges, k_f, only the urban centre case was considered.

Table A.1. Values used in the COST 231 Walfisch-Ikegami propagation model (based on [CoLa06]).

Parameter name	Value
Street Width [m]	24
Building Separation [m]	48
BS height [m]	26
Building height [m]	24
MT height [m]	1.8
Orientation angle [º]	90

3GPP outlined three channels for LTE, based on low, medium and high delay spreads, specifically Extended Pedestrian A (EPA), Extended Vehicular A (EVA) and Extended Typical Urban (ETU). There are also three Doppler frequencies outlined representing low, medium and high Doppler environments. [3GPP07b] The values for the Doppler frequency and delay spread for each channel are shown in Table A.2.

Table A.2. Overview of channel models (adapted from [3GPP07c] and [3GPP07b]).

Channel Model	Doppler Frequency [Hz]	Delay Spread [ns]
EPA 5Hz	5	43
EVA 5Hz	5	357
EVA 70Hz	70	357
ETU 70Hz	70	991
ETU 300Hz	300	991

In the scope of this thesis only the EPA 5Hz and ETU 70Hz are considered.

Regarding the situation where it is necessary to calculate the throughput due to the distance between the user and the BS, the first step is to determine the path loss associated to the user distance, described in [CoLa06] and [Sant04]. After the path loss calculation, the receiver sensitivity is determined, resulting:

$$P_{Rx_{[dBm]}} = EIRP_{[dBm]} - L_{p_{[dB]}} + G_{r_{[dB]}} - L_{u_{[dB]}} \quad (A.12)$$

Rearranging (A.7), the SNR associated to a certain user distance is calculated by:

$$\rho_{[dB]} = P_{Rx_{min\,[dBm]}} - N_{[dBm]} \quad (A.13)$$

Annex B – Expressions for Models

Using results from [3GPP07] and [3GPP07a], for the UL and DL, respectively, polynomial interpolation was used to calculate the values of SNR as a function of the throughput, R_b, using Matlab and Excel, assuring a relative error below 5%, as it is exemplified in Figure B.1. These expressions are step-wise due to the fact that all polynomial expressions given by Matlab and Excel presented relative errors higher than 5%. For the channels that are not available in those simulations, in UL or DL, was made an extrapolation to get an approximation. In order to obtain a approximation for DL of the EPA 5Hz channel model, since that in DL is just available simulation for EVA 5Hz and ETU 70Hz channel models, an extrapolation was done, with UL simulations for 10 MHz and for each modulation of EVA 5Hz graphics to achieve a relationship with the EPA 5Hz. The results and the corresponding mean relative error, $\overline{\varepsilon_r}$, are presented at Table B.1.

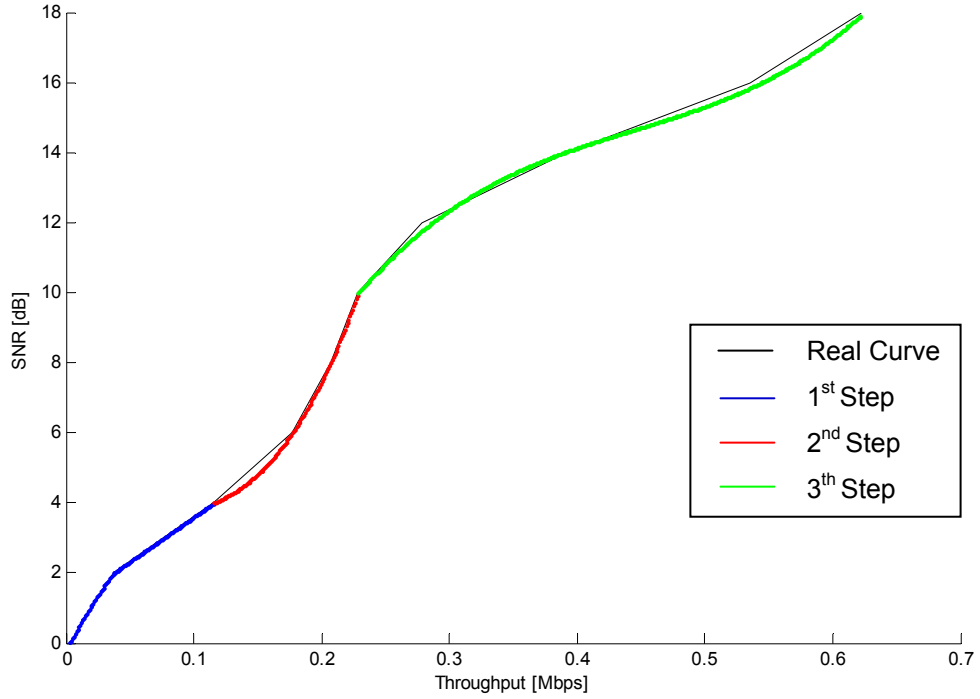

Figure B.1. Interpolation for DL, bandwidth of 10MHz, SIMO, 64QAM rate ¾ and EPA 5Hz in DL.

An extrapolation was made to obtain at UL an approximation for the channel model ETU 70Hz and the modulation 64 QAM. This extrapolation is presented together with the interpolation of the simulations and has a mean relative error of 24.4%. It is important to enhance that almost interpolations and extrapolations have a mean relative error below 5%.

Some simulations were just available for full RB, so an approximation was done in order to have the results for a single RB. The size of a RB is the same for all bandwidths; therefore, the number of RB changes with the bandwidth. The number of RB per bandwidths is presented at Table B.2.

Table B.1. Extrapolation EVA 5Hz - EPA 5Hz.

Modulation	$\frac{\text{EPA 5Hz}}{\text{EVA 5Hz}}$	$\overline{\varepsilon_r}$ [%]
QPSK	1.027	5.3
16 QAM	1.061	4.6
64 QAM	1.04	15.2

Table B.2. Number of RB per bandwidths.

Bandwidths [MHz]	1.4	3	5	10	15	20
Number of RB	6	15	25	50	75	100

The results of all interpolations and extrapolation, in DL and UL, are presented on what follows.

For DL, the interpolations are for simulations, SIMO configurations and normal CP. For QPSK with a coding rate of 1/3 the SNR as a function of throughput is given by:

- EPA 5Hz

$$\rho_{[dB]}=\begin{cases}139.1968058\cdot R_{b\,[Mbps]}-12.9993\ ,\ 0.079019806<R_{b\,[Mbps]}<0.093387952\\ 733.4013\cdot R_{b\,[Mbps]}-68.49085\ ,\ 0.093387952<R_{b\,[Mbps]}<0.096114972\end{cases} \quad (B.1)$$

- ETU 70Hz

$$\rho_{[dB]}=\begin{cases}80.48807972\cdot R_{b\,[Mbps]}-5.95475,\ 0.0491346<R_{b\,[Mbps]}<0.073983\\ 133.7077\cdot R_{b\,[Mbps]}-9.8921\ ,\ 0.073983<R_{b\,[Mbps]}<0.088941\\ \left(1.1798\cdot R_{b\,[Mbps]}-0.10293\right)\cdot 10^{3}\ ,\ 0.088941<R_{b\,[Mbps]}<0.0906362\end{cases} \quad (B.2)$$

For 16 QAM with a coding rate of 1/2 the SNR in function of throughput is given by:

- EPA 5Hz

$$\rho_{[dB]}=\begin{cases}41.37141679\cdot R_{b\,[Mbps]}-4.138024,\ 0.051678764<R_{b\,[Mbps]}<0.100021319\\ \left(1.5568\cdot R_{b\,[Mbps]}^{3}-0.9155\cdot R_{b\,[Mbps]}^{2}+0.2088\cdot R_{b\,[Mbps]}-0.0133\right)\cdot 10^{3},\\ 0.100021319<R_{b\,[Mbps]}<0.286368144\end{cases} \quad (B.3)$$

- ETU 70Hz

$$\rho_{[dB]}=\begin{cases}36.99712399\cdot R_{b\,[Mbps]}-2.034694,\ 0.000937744<R_{b\,[Mbps]}<0.054996\\ \left(\begin{array}{c}2.1664\cdot R_{b\,[Mbps]}^{4}-1.3996\cdot R_{b\,[Mbps]}^{3}+\\ +0.3082\cdot R_{b\,[Mbps]}^{2}-0.0221\cdot R_{b\,[Mbps]}+0.0005\end{array}\right)\cdot 10^{4},\ 0.054996<R_{b\,[Mbps]}<0.27349\end{cases} \quad (B.4)$$

For 64 QAM with a coding rate of 3/4 the SNR in function of throughput is given by:

- EPA 5Hz

$$\rho_{[dB]}=\begin{cases}-291.0892\cdot R_{b\,[Mbps]}^2+70.0593\cdot R_{b\,[Mbps]}-0.21\ ,\ 0.003036072<R_{b\,[Mbps]}<0.037337248\\ 25.4196\cdot R_{b\,[Mbps]}+1.0509\ ,\ 0.037337248<R_{b\,[Mbps]}<0.116016576\\ 966.0917\cdot R_{b\,[Mbps]}^3-108.0894\cdot R_{b\,[Mbps]}^2+1.3053\cdot R_{b\,[Mbps]}+3.7948\ ,\\ 0.116016576<R_{b\,[Mbps]}<0.2287376\\ 225.0551\cdot R_{b\,[Mbps]}^3-299.6906\cdot R_{b\,[Mbps]}^2+144.2672\cdot R_{b\,[Mbps]}-10.03,\\ 0.2287376<R_{b\,[Mbps]}<0.62271664\end{cases} \quad (B.5)$$

- ETU 70Hz

$$\rho_{[dB]}=\begin{cases}58.3431\cdot R_{b\,[Mbps]}+2\ ,\ 0<R_{b\,[Mbps]}<0.03428\\ 16.7175\cdot R_{b\,[Mbps]}+3.4269\ ,\ 0.03428<\mathrm{R}_{b\,[Mbps]}<0.1539152\\ \left(1.2031\cdot R_{b\,[Mbps]}^2-0.3610\cdot \mathrm{R}_{b\,[Mbps]}++0.03305\right)\cdot 10^3,\ 0.1539152<R_{b\,[Mbps]}<0.221184\\ \left(\begin{array}{c}2.0618\cdot R_{b\,[Mbps]}^4-3.2095\cdot R_{b\,[Mbps]}^3+\\ +1.7699\cdot R_{b\,[Mbps]}^2-0.3847\cdot R_{b\,[Mbps]}+0.0403\end{array}\right)\cdot 10^3,\ 0.221184<R_{b\,[Mbps]}<0.587772\\ 88.6997\cdot R_{b\,[Mbps]}-32.1352\ ,\ 0.587772<R_{b\,[Mbps]}<0.61032\end{cases} \quad (B.6)$$

For the UL, the interpolations are for simulations with MIMO configurations 2×2 and 4×4 and normal CP. For QPSK with a coding rate of 1/3 and MIMO configuration of 2×2 the SNR in function of throughput is given by:

- EPA 5Hz

$$\rho_{[dB]}=\begin{cases}\left(1.1274\cdot R_{b\,[Mbps]}^2-0.2015\cdot R_{b\,[Mbps]}+0.009001\right)\cdot 10^5,\ 0.08792454<R_{b\,[Mbps]}<0.09550812\\ \left(5.4466\cdot R_{b\,[Mbps]}-0.5162\right)\cdot 10^3,\ 0.09550812<R_{b\,[Mbps]}<0.09587532\\ \left(1.6041\cdot R_{b\,[Mbps]}-0.1532\right)\cdot 10^4\ ,\ 0.09587532<R_{b\,[Mbps]}<0.096\end{cases} \quad (B.7)$$

- ETU 70Hz

$$\rho_{[dB]}=\begin{cases}134.8574927\cdot R_{b\,[Mbps]}-9.012743359\ ,\ 0.06683161<R_{b\,[Mbps]}<0.08166208\\ 231.8423935\cdot R_{b\,[Mbps]}-16.93273209\ ,\ 0.08166208<R_{b\,[Mbps]}<0.09028863\\ 459.5736076\cdot R_{b\,[Mbps]}-37.49427141\ ,\ 0.09028863<R_{b\,[Mbps]}<0.09464049\\ 1644.425808\cdot R_{b\,[Mbps]}-149.6292642\ ,\ 0.09464049<R_{b\,[Mbps]}<\ 0.09585672\end{cases} \quad (B.8)$$

For 16 QAM with a coding rate of 3/4 and MIMO configuration of 2×2 the SNR in function of throughput is given by:

- EPA 5Hz

$$\rho_{[dB]}=\begin{cases}-675.6188\cdot R_{b\,[Mbps]}^3+364.4272\cdot R_{b\,[Mbps]}^2-17.8417\cdot R_{b\,[Mbps]}-0.5122\ ,\\ 0.07884248<R_{b\,[Mbps]}<0.2725038\\ \left(1.6370\cdot R_{b\,[Mbps]}^3-1.5249\cdot R_{b\,[Mbps]}^2+0.5011\cdot R_{b\,[Mbps]}-0.0484\right)\cdot 10^3,\\ 0.2725038<R_{b\,[Mbps]}<0.4162308\end{cases} \quad (B.9)$$

- ETU 70Hz

$$\rho_{[dB]}=\begin{cases}-887.0042\cdot R_{b\,[Mbps]}^3+600.5976\cdot R_{b\,[Mbps]}^2-79.2833\cdot R_{b\,[Mbps]}+4.4602\ ,\\ 0.11705298<R_{b\,[Mbps]}<0.3362749\\ 702.3316\cdot R_{b\,[Mbps]}^2-462.6239\cdot R_{b\,[Mbps]}+88.172\ ,\\ 0.3362749<R_{b\,[Mbps]}<0.4207883\end{cases} \quad (B.10)$$

For 64 QAM with a coding rate of 5/6 and MIMO configuration of 2×2 the throughput in function of SNR is given by:

- EPA 5Hz

$$\rho_{[dB]}=\begin{cases}-644.1481\cdot R_{b\,[Mbps]}^4+581.2997\cdot R_{b\,[Mbps]}^3-137.502\cdot R_{b\,[Mbps]}^2+33.3898\cdot R_{b\,[Mbps]}+1.1911, \\ \qquad 0.11640088<R_{b\,[Mbps]}<0.5095352 \\ 104.2152\cdot R_{b\,[Mbps]}^2-95.7213\cdot R_{b\,[Mbps]}+37.727\ ,\ 0.5095352<R_{b\,[Mbps]}<0.7034354\end{cases} \quad (B.11)$$

- ETU 70Hz

$$\rho_{[dB]}=\begin{cases}218.1556\cdot R_{b\,[Mbps]}^3-20.3603\cdot R_{b\,[Mbps]}^2+21.9913\cdot R_{b\,[Mbps]}+1.1564\ ,\ 0.1245<R_{b\,[Mbps]}<0.27163 \\ 873.1686\cdot R_{b\,[Mbps]}^2-387.3231\cdot R_{b\,[Mbps]}+50.7834,\ 0.27163<R_{b\,[Mbps]}<0.30584 \\ -327.5755\cdot R_{b\,[Mbps]}^3+168.9751\cdot R_{b\,[Mbps]}-28.3087,0.30584<R_{b\,[Mbps]}<0.3828 \\ 30.8949\cdot R_{b\,[Mbps]}^2+20.2801\cdot R_{b\,[Mbps]}+5.7096\ ,\ 0.3828<R_{b\,[Mbps]}<0.46866 \\ 78.2614\cdot R_{b\,[Mbps]}-14.6782\ ,\ 0.46866<R_{b\,[Mbps]}<0.4942\end{cases} \quad (B.12)$$

For QPSK with a coding rate of 1/3 and MIMO configuration of 4×4 the SNR in function of throughput is given by:

- EPA 5Hz

$$\rho_{[dB]}=46360.68614\cdot R_{b\,[Mbps]}-4448.625869\ ,\ 0.09595686<R_{b\,[Mbps]}<0.096 \quad (B.13)$$

- ETU 70Hz

$$\rho_{[dB]}=\begin{cases}570.9897\cdot R_{b\,[Mbps]}-52.4763\ ,\ 0.09190412<R_{b\,[Mbps]}<0.09540681 \\ \left(3.3716\cdot R_{b\,[Mbps]}-0.3197\right)\cdot 10^3\ ,\ 0.09540681<R_{b\,[Mbps]}<0.096\end{cases} \quad (B.14)$$

For 16 QAM with a coding rate of 3/4 and MIMO configuration of 4×4 the SNR in function of throughput is given by:

- EPA 5Hz

$$\rho_{[dB]}=\begin{cases}-331.6065\cdot R_{b\,[Mbps]}^2+203.4191\cdot R_{b\,[Mbps]}-26.6376\ ,\ 0.18947086<R_{b\,[Mbps]}<0.2656774 \\ 8.2876\cdot R_{b\,[Mbps]}^2+20.9817\cdot R_{b\,[Mbps]}-2.1593\ ,\ 0.2656774<R_{b\,[Mbps]}<0.4158826\end{cases} \quad (B.15)$$

- ETU 70Hz

$$\rho_{[dB]}=\begin{cases}425.6356\cdot R_{b\,[Mbps]}^2-108.5150\cdot R_{b\,[Mbps]}+6.7234\ ,\ 0.1487703<R_{b\,[Mbps]}<0.2267275 \\ 849.2806\cdot R_{b\,[Mbps]}^3-538.8943\cdot R_{b\,[Mbps]}^2+257.31\cdot R_{b\,[Mbps]}-28.8814\ , \\ \qquad 0.2267275<R_{b\,[Mbps]}<0.4094698 \\ 106.0468\cdot R_{b\,[Mbps]}-33.4230\ ,\ 0.4094698<R_{b\,[Mbps]}<0.4283294\end{cases} \quad (B.16)$$

For 64 QAM with a coding rate of 5/6 and MIMO configuration of 4×4 the SNR in function of throughput is given by:

- EPA 5Hz

$$\rho_{[dB]}=\begin{cases}13.0921\cdot R_{b\,[Mbps]}^2+15.2877\cdot R_{b\,[Mbps]}-1.5438\ ,\ 0.093498<R_{b\,[Mbps]}<0.290408 \\ 39.9829\cdot R_{b\,[Mbps]}-7.6114,\ 0.290408<R_{b\,[Mbps]}<0.3404294 \\ 100.7861\cdot R_{b\,[Mbps]}-28.3106,\ 0.3404294<R_{b\,[Mbps]}<0.3602734 \\ 47.1514\cdot R_{b\,[Mbps]}-8.9874,\ 0.3602734<R_{b\,[Mbps]}<0.40269 \\ 23.0273\cdot R_{b\,[Mbps]}^2-6.8221\cdot R_{b\,[Mbps]}+9.0837\ ,\ 0.40269<R_{b\,[Mbps]}<0.7089816\end{cases} \quad (B.17)$$

- ETU 70Hz

$$\rho_{[dB]}=\begin{cases} 68.4795\cdot R_{b\,[Mbps]}^2+7.7103\cdot R_{b\,[Mbps]}-1.2429\ ,\ 0.089015107<R_{b\,[Mbps]}<0.274404959 \\ 96.9622\cdot R_{b\,[Mbps]}-20.5777\ ,\ 0.274404959<R_{b\,[Mbps]}<0.294730413 \\ 357.6813\cdot R_{b\,[Mbps]}-97.4196\ ,\ 0.294730413<R_{b\,[Mbps]}<0.300321983 \\ 73.5699\cdot R_{b\,[Mbps]}-12.0946,\ 0.300321983<R_{b\,[Mbps]}<0.327507025 \\ 740.8213\cdot R_{b\,[Mbps]}^3-950.9916\cdot R_{b\,[Mbps]}^2+424.8991\cdot R_{b\,[Mbps]}-51.1773\ , \\ \quad 0.327507025<R_{b\,[Mbps]}<0.54809562 \\ 71.3183\cdot R_{b\,[Mbps]}-21.0892\ ,\ 0.54809562<R_{b\,[Mbps]}<0.576138926 \end{cases} \quad \text{(B.18)}$$

To ensure the approximation validity the mean relative error value was calculated, Table B.3. The values are within an acceptable interval, hence, the approximation was used to obtain the SNR as a function of the intended throughput.

Table B.3. Mean relative error for the SNR in function of throughput interpolation curves.

Modulation		Mean Relative Error [%]	Mean Relative Error [%]
QPSK	DL	5.3	0.1
	UL 2×2	0.4	0
	UL 4×4	0	0.1
16QAM	DL	2.6	1.1
	UL 2×2	1.2	0.8
	UL 4×4	0	0
64QAM	DL	15.2	0.7
	UL 2×2	0.6	24.4
	UL 4×4	0.6	24.4

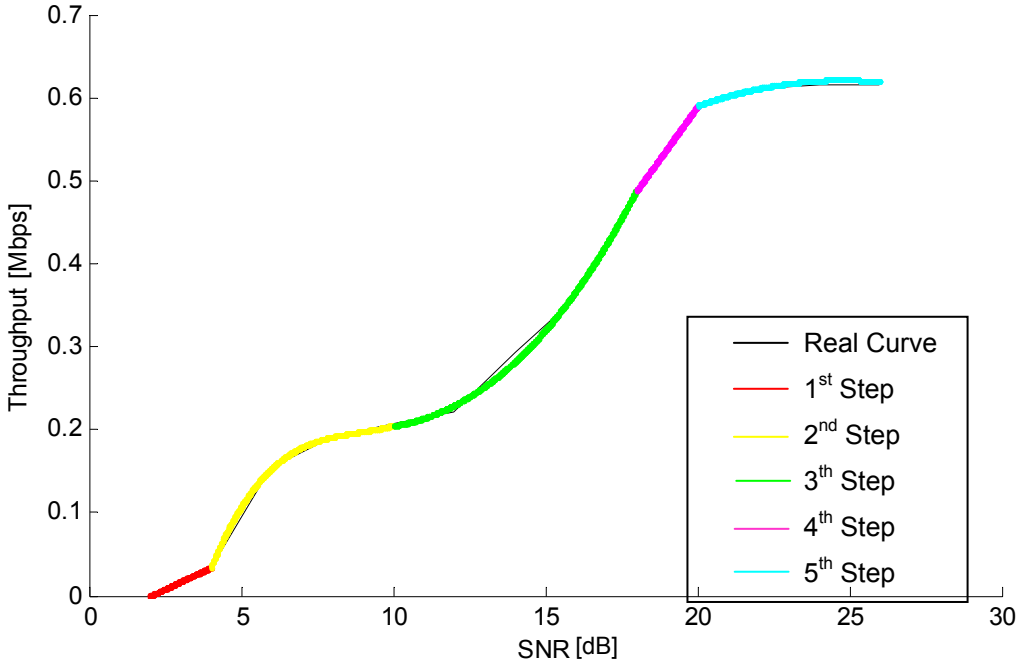

Figure B.2. Interpolation for 64QAM rate 3/4 and ETU 70Hz in DL.

For the DL, interpolations are for simulations for 10MHz of bandwidth, SIMO configurations and normal CP. For QPSK with a coding rate of 1/3 the throughput in function of SNR is given by:

- EPA 5Hz

$$R_{b\,[\text{bps}]}=\begin{cases}\left(0.0190\cdot\rho_{[\text{dB}]}^{3}-0.1455\cdot\rho_{[\text{dB}]}^{2}+0.3516\cdot\rho_{[\text{dB}]}+9.3388\right)\cdot10^{4}, & -2<\rho_{[\text{dB}]}<2\\ \left(0.0063\cdot\rho_{[\text{dB}]}+9.6009\right)\cdot10^{4}, & 2<\rho_{[\text{dB}]}<4\end{cases} \tag{B.19}$$

- ETU 70Hz

$$R_{b\,[\text{bps}]}=\begin{cases}\left(1.2424\cdot\rho_{[\text{dB}]}+7.3983\right)\cdot10^{4}, & -2<\rho_{[\text{dB}]}<0\\ \left(7.4795\cdot\rho_{[\text{dB}]}+73.983\right)\cdot10^{3}, & 0<\rho_{[\text{dB}]}<2\\ \left(0.0848\cdot\rho_{[\text{dB}]}+8.7246\right)\cdot10^{4}, & 2<\rho_{[\text{dB}]}<4\\ 90632, & 4<\rho_{[\text{dB}]}<6\end{cases} \tag{B.20}$$

For 16 QAM with a coding rate of 1/2 the throughput in function of SNR is given by:

- EPA 5Hz

$$R_{b\,[\text{bps}]}=\begin{cases}\left(-0.000945\cdot\rho_{[\text{dB}]}^{4}+0.0103\cdot\rho_{[\text{dB}]}^{3}-0.0141\cdot\rho_{[\text{dB}]}^{2}+0.1696\cdot\rho_{[\text{dB}]}+1.0083\right)\cdot10^{5}, & -2<\rho_{[\text{dB}]}<6\\ \left(0.0048\cdot\rho_{[\text{dB}]}^{3}-0.1503\cdot\rho_{[\text{dB}]}^{2}+1.5644\cdot\rho_{[\text{dB}]}-2.4858\right)\cdot10^{5}, & 6<\rho_{[\text{dB}]}<12\\ 293820, & 12<\rho_{[\text{dB}]}<14\end{cases} \tag{B.21}$$

- ETU 70Hz

$$R_{b\,[\text{bps}]}=\begin{cases}\left(2.7029\cdot\rho_{[\text{dB}]}+5.4996\right)\cdot10^{4}, & -2<\rho_{[\text{dB}]}<0\\ \left(0.0479\cdot\rho_{[\text{dB}]}^{3}-0.4804\cdot\rho_{[\text{dB}]}^{2}+3.1387\cdot\rho_{[\text{dB}]}+5.4719\right)\cdot10^{4}, & 0<\rho_{[\text{dB}]}<8\\ 14893\cdot\rho_{[\text{dB}]}-124463, & 8<\rho_{[\text{dB}]}<10\\ \left(0.0116\cdot\rho_{[\text{dB}]}+2.6190\right)\cdot10^{5}, & 10<\rho_{[\text{dB}]}<12\\ 275820, & 12<\rho_{[\text{dB}]}<14\end{cases} \tag{B.22}$$

For 64 QAM with a coding rate of 3/4 the throughput in function of SNR is given by:

- EPA 5Hz

$$R_{b\,[\text{bps}]}=\begin{cases}\left(-0.1292\cdot\rho_{[\text{dB}]}^{3}+1.3299\cdot\rho_{[\text{dB}]}^{2}-0.4279\cdot\rho_{[\text{dB}]}+0.3036\right)\cdot10^{4}, & 0<\rho_{[\text{dB}]}<6\\ \left(-0.1018\cdot\rho_{[\text{dB}]}^{2}+2.92\cdot\rho_{[\text{dB}]}+3.8494\right)\cdot10^{4}, & 6<\rho_{[\text{dB}]}<10\\ \left(0.0585\cdot\rho_{[\text{dB}]}^{2}-1.0032\cdot\rho_{[\text{dB}]}+6.4581\right)\cdot10^{5}, & 10<\rho_{[\text{dB}]}<16\\ \left(0.4354\cdot\rho_{[\text{dB}]}-1.6098\right)\cdot10^{5}, & 16<\rho_{[\text{dB}]}<18\\ \left(-0.0241\cdot\rho_{[\text{dB}]}^{2}+1.0214\cdot\rho_{[\text{dB}]}-4.33555\right)\cdot10^{5}, & 18<\rho_{[\text{dB}]}<22\\ 647085, & 22<\rho_{[\text{dB}]}<26\end{cases} \tag{B.23}$$

- ETU 70Hz

$$R_{b\,[\mathrm{bps}]}=\begin{cases} 17140\cdot\rho_{[\mathrm{dB}]}+34280\ ,\ 2<\rho_{[\mathrm{dB}]}<4 \\ \left(0.006\cdot\rho_{[\mathrm{dB}]}^{3}-0.159\cdot\rho_{[\mathrm{dB}]}^{2}+1.4327\cdot\rho_{[\mathrm{dB}]}-3.3994\right)\cdot 2\cdot 10^{5},\ 4<\rho_{[\mathrm{dB}]}<10 \\ \left(0.001\cdot\rho_{[\mathrm{dB}]}^{3}-0.00139\cdot\rho_{[\mathrm{dB}]}^{2}-0.2088\cdot\rho_{[\mathrm{dB}]}+3.2774\right)\cdot 10^{5}\ ,\ 10<\rho_{[\mathrm{dB}]}<18 \\ \left(50.916\cdot\rho_{[\mathrm{dB}]}-427.91\right)\cdot 10^{3}\ ,\ 18<\rho_{[\mathrm{dB}]}<20 \\ \left(-0.0068\cdot\rho_{[\mathrm{dB}]}^{2}+0.3366\cdot\rho_{[\mathrm{dB}]}-1.0573\right)\cdot 2\cdot 10^{5}\ ,\ 20<\rho_{[dB]}<26 \end{cases} \quad (B.24)$$

For the UL, the interpolations are for simulations for 10MHz, MIMO configurations 2×2 and 4×4 and normal CP. For QPSK with a coding rate of 1/3 and MIMO configuration of 2×2 the throughput in function of SNR is given by:

- EPA 5Hz

$$R_{b\,[\mathrm{bps}]}=\left(0.0021\cdot\rho_{[\mathrm{dB}]}^{3}-0.0364\cdot\rho_{[\mathrm{dB}]}^{2}+0.2089\cdot\rho_{[\mathrm{dB}]}+4.3976\right)\cdot 2\cdot 10^{4}\ ,\ 0<\rho_{[\mathrm{dB}]}<8 \quad (B.25)$$

- ETU 70Hz

$$R_{b\,[\mathrm{bps}]}=\begin{cases} \left(-0.0567\cdot\rho_{[\mathrm{dB}]}^{2}+0.8052\cdot\rho_{[\mathrm{dB}]}+6.7150\right)\cdot 10^{4},\ 0<\rho_{[\mathrm{dB}]}<6 \\ 403.36\cdot\rho_{[\mathrm{dB}]}+92629.84\ ,\ 6<\rho_{[\mathrm{dB}]}<8 \end{cases} \quad (B.26)$$

For 16 QAM with a coding rate of 3/4and MIMO configuration of 2×2 the throughput in function of SNR is given by:

- EPA 5Hz

$$R_{b\,[\mathrm{bps}]}=\begin{cases} \left(-0.0017\cdot\rho_{[\mathrm{dB}]}^{4}+0.0425\cdot\rho_{[\mathrm{dB}]}^{3}-0.317\cdot\rho_{[\mathrm{dB}]}^{2}+1.905\cdot\rho_{[\mathrm{dB}]}+3.9032\right)\cdot 2\cdot 10^{4},\ 0<\rho_{[\mathrm{dB}]}<12 \\ \left(-0.0801\cdot\rho_{[\mathrm{dB}]}^{2}+2.7554\cdot\rho_{[\mathrm{dB}]}-2.1906\right)\cdot 2\cdot 10^{4},\ 12<\rho_{[\mathrm{dB}]}<18 \end{cases} \quad (B.27)$$

- ETU 70Hz

$$R_{b\,[\mathrm{bps}]}=\begin{cases} \left(-0.001415\cdot\rho_{[\mathrm{dB}]}^{4}+0.0515\cdot\rho_{[\mathrm{dB}]}^{3}-0.6331\cdot\rho_{[\mathrm{dB}]}^{2}+5.0866\cdot\rho_{[\mathrm{dB}]}+3.7749\right)\cdot 10^{4},\ 2<\rho_{[\mathrm{dB}]}<14 \\ \left(-0.0189\cdot\rho_{[\mathrm{dB}]}^{2}+0.7093\cdot\rho_{[\mathrm{dB}]}-2.4465\right)\cdot 10^{5},\ 14<\rho_{[\mathrm{dB}]}<18 \end{cases} \quad (B.28)$$

For 64 QAM with a coding rate of 5/6 and MIMO configuration of 2×2 the throughput in function of SNR is given by:

- EPA 5Hz

$$R_{b\,[\mathrm{bps}]}=\begin{cases} \left(-0.000245\cdot\rho_{[\mathrm{dB}]}^{4}+0.0208\cdot\rho_{[\mathrm{dB}]}^{3}-0.4757\cdot\rho_{[\mathrm{dB}]}^{2}+5.481\cdot\rho_{[\mathrm{dB}]}-9.8308\right)\cdot 2\cdot 10^{4},\ 4<\rho_{[\mathrm{dB}]}<18 \\ \left(-0.0149\cdot\rho_{[\mathrm{dB}]}^{2}+0.7174\cdot\rho_{[\mathrm{dB}]}-5.0529\right)\cdot 2\cdot 10^{5},\ 18<\rho_{[\mathrm{dB}]}<24 \end{cases} \quad (B.29)$$

- ETU 70Hz

$$R_{b\,[\mathrm{bps}]}=\begin{cases} \left(0.0011719\cdot\rho_{[\mathrm{dB}]}^{4}-0.035372\cdot\rho_{[\mathrm{dB}]}^{3}+0.204\cdot\rho_{[\mathrm{dB}]}^{2}+3.1745\cdot\rho_{[\mathrm{dB}]}-1.554\right)\cdot 10^{4}\ ,\ 4<\rho_{[\mathrm{dB}]}<18 \\ \left(-0.01165\cdot\rho_{[\mathrm{dB}]}^{2}+0.6762\cdot\rho_{[\mathrm{dB}]}-4.566\right)\cdot 10^{5},\ 18<\rho_{[\mathrm{dB}]}<24 \end{cases} \quad (B.30)$$

For QPSK with a coding rate of 1/3 and MIMO configuration of 4×4 the throughput in function of SNR is given by:

- EPA 5Hz

$$R_{b\,[\mathrm{bps}]}=\begin{cases}\left(0.0011\cdot\rho_{[\mathrm{dB}]}+4.7978\right)\cdot 2\cdot 10^{4}, & 0<\rho_{[\mathrm{dB}]}<2\\ 4800000\ , & 2<\rho_{[\mathrm{dB}]}<6\end{cases} \tag{B.31}$$

- ETU 70Hz

$$R_{b\,[\mathrm{bps}]}=\begin{cases}\left(0.1751\cdot\rho_{[\mathrm{dB}]}+9.1904\right)\cdot 10^{4}, & 0<\rho_{[\mathrm{dB}]}<2\\ \left(0.0297\cdot\rho_{[\mathrm{dB}]}+9.1904\right)\cdot 10^{4}, & 2<\rho_{[\mathrm{dB}]}<4\\ 96000\ , & 4<\rho_{[\mathrm{dB}]}<6\end{cases} \tag{B.32}$$

For 16 QAM with a coding rate of 3/4and MIMO configuration of 4×4 the throughput in function of SNR is given by:

- EPA 5Hz

$$R_{b\,[\mathrm{bps}]}=\begin{cases}\left(-0.0045\cdot\rho_{[\mathrm{dB}]}^{4}+0.062\cdot\rho_{[\mathrm{dB}]}^{3}-0.1263\cdot\rho_{[\mathrm{dB}]}^{2}+0.7612\cdot\rho_{[\mathrm{dB}]}+9.4781\right)\cdot 2\cdot 10^{4}, & 0<\rho_{[\mathrm{dB}]}<8\\ \left(-0.0078\cdot\rho_{[\mathrm{dB}]}^{2}+0.1979\cdot\rho_{[\mathrm{dB}]}+3.0807\right)\cdot 10^{5}, & 8<\rho_{[\mathrm{dB}]}<14\\ 432000\ , & 14<\rho_{[\mathrm{dB}]}<18\end{cases} \tag{B.33}$$

- ETU 70Hz

$$R_{b\,[\mathrm{bps}]}=\begin{cases}\left(-0.000703\cdot\rho_{[\mathrm{dB}]}^{4}+0.01481\cdot\rho_{[\mathrm{dB}]}^{3}-0.0874\cdot\rho_{[\mathrm{dB}]}^{2}+0.3562\cdot\rho_{[\mathrm{dB}]}+1.4951\right)\cdot 10^{5}, & 0<\rho_{[\mathrm{dB}]}<10\\ \left(0.0126\cdot\rho_{[\mathrm{dB}]}^{3}-0.5935\cdot\rho_{[\mathrm{dB}]}^{2}+9.2854\cdot\rho_{[\mathrm{dB}]}-5.1927\right)\cdot 10^{4}\ , & 10<\rho_{[\mathrm{dB}]}<16\\ 430473\ , & 16<\rho_{[\mathrm{dB}]}<18\end{cases} \tag{B.34}$$

For 64 QAM with a coding rate of 5/6 and MIMO configuration of 4×4 the throughput in function of SNR is given by:

- EPA 5Hz

$$R_{b\,[\mathrm{bps}]}=\begin{cases}\left(\begin{array}{c}-0.0005\cdot\rho_{[\mathrm{dB}]}^{5}+0.017975\cdot\rho_{[\mathrm{dB}]}^{4}-0.2035\cdot\rho_{[\mathrm{dB}]}^{3}+\\ +0.7046\cdot\rho_{[\mathrm{dB}]}^{2}+1.8927\cdot\rho_{[\mathrm{dB}]}+4.6679\end{array}\right)\cdot 2\cdot 10^{4}\ , & 0<\rho_{[\mathrm{dB}]}<14\\ \left(-0.0064\cdot\rho_{[\mathrm{dB}]}^{2}+0.2227\cdot\rho_{[\mathrm{dB}]}-1.2142\right)\cdot 10^{6}, & 14<\rho_{[\mathrm{dB}]}<18\\ 720800\ , & 18<\rho_{[\mathrm{dB}]}<24\end{cases} \tag{B.35}$$

- ETU 70Hz

$$R_{b\,[\mathrm{bps}]}=\begin{cases}\left(0.000285\cdot\rho_{[\mathrm{dB}]}^{4}-0.005537\cdot\rho_{[\mathrm{dB}]}^{3}+0.01017\cdot\rho_{[\mathrm{dB}]}^{2}+0.38058\cdot\rho_{[\mathrm{dB}]}+0.9\ \right)\cdot 10^{5}, & 0<\rho_{[\mathrm{dB}]}<14\\ \left(0.000269\cdot\rho_{[\mathrm{dB}]}^{3}-0.0182\cdot\rho_{[\mathrm{dB}]}^{2}+0.4118\cdot\rho_{[\mathrm{dB}]}-2.5431\right)\cdot 10^{6}, & 14<\rho_{[\mathrm{dB}]}<24\end{cases} \tag{B.36}$$

Table B.4. Mean relative error for the throughput in function of SNR interpolation curves.

Modulation		Mean Relative Error [%] EPA 5Hz	Mean Relative Error [%] ETU 70Hz
QPSK	DL	5.3	0
	UL 2×2	0.1	0.4
	UL 4×4	0	0
16QAM	DL	4.6	0.5
	UL 2×2	0.9	0.7
	UL 4×4	0.2	0.7
64QAM	DL	15.2	1
	UL 2×2	0.8	24.4
	UL 4×4	0.5	24.4

At Table B.5 and Table B.6 the maximum values for the interpolation according the modulation, channel, MIMO configuration and bandwidth for DL and UL, respectively.

Table B.5. Maximum values for each DL interpolation.

Maximum Throughput [Mbps]								
Modulation	Channel	MIMO	Bandwidth [MHz]					
			1.4	3	5	10	15	20
QPSK	EPA	2x2	0.99	2.47	4.12	8.24	12.36	16.48
		4x4	1.98	4.94	8.24	16.48	24.72	32.95
	ETU	2x2	0.93	2.33	3.88	7.77	11.65	15.54
		4x4	1.86	4.66	7.77	15.54	23.31	31.08
16QAM	EPA	2x2	2.95	7.36	12.27	24.55	36.82	49.09
		4x4	5.89	14.73	24.55	49.09	73.64	98.18
	ETU	2x2	2.81	7.03	11.72	23.44	35.16	46.88
		4x4	5.63	14.07	23.44	46.88	70.33	93.77
64QAM	EPA	2x2	6.41	16.01	26.69	53.38	80.06	106.75
		4x4	12.81	32.03	53.38	106.75	160.13	213.50
	ETU	2x2	6.28	15.69	26.16	52.31	78.47	104.63
		4x4	12.56	31.39	52.31	104.63	156.94	209.25

Table B.6. Maximum values for each UL interpolation.

Maximum Throughput [Mbps]								
Modulation	**Channel**	**MIMO**	**Bandwidth [MHz]**					
			1.4	**3**	**5**	**10**	**15**	**20**
QPSK	EPA	2x2	0.49	1.23	2.06	4.11	6.17	8.23
		4x4	0.49	1.23	2.06	4.11	6.17	8.23
	ETU	2x2	0.49	1.23	2.05	4.11	6.16	8.22
		4x4	0.49	1.23	2.06	4.11	6.17	8.23
16QAM	EPA	2x2	2.14	5.35	8.92	17.84	26.76	35.68
		4x4	2.14	5.35	8.91	17.82	26.74	35.65
	ETU	2x2	2.16	5.41	9.02	18.03	27.05	36.07
		4x4	2.20	5.51	9.18	18.36	27.54	36.71
64QAM	EPA	2x2	3.62	9.04	15.07	30.15	45.22	60.29
		4x4	3.65	9.12	15.19	30.38	45.58	60.77
	ETU	2x2	2.54	6.35	10.59	21.18	31.77	42.36
		4x4	2.96	7.41	12.35	24.69	37.04	49.38

Annex C – Relative MIMO Gain Model

In order to predict the improvement in capacity of using MIMO over SISO based on simulation results, the RMG Model, [KuCo07], was chosen. The description of this model is next presented based on [KuCo07] and [Bati08]. The model of the capacity gains of MIMO described in [KuCo07] is based on simulation results from a MIMO radio channel simulator that takes into account the Geometrically Based Single Bounce (GBSB) channel model.

The RMG is defined as the ratio between the MIMO and SISO capacities of a radio link (2.10), with the RMG model being a statistical model developed to approximate the distribution of the RMG, based on simulation results. In order to maintain a low-complexity of the model, the distribution of the RMG is modelled with an inverse Sigmoid function (also known as logistic function or *S*-shape function), which is completely modelled by its mean and variance. The general sigmoid function is given by:

$$\delta(x,\mu,s) = \frac{1}{1+e^{-\frac{x-\mu}{s}}} \tag{C.1}$$

where:

- μ, is the mean value of the distribution;
- *s,* is the determines the slope which is related to σ^2 by:

$$\sigma^2 = \frac{\pi^2}{3}s^2 \tag{C.2}$$

- σ^2 is the variance;

Both the mean value and the variance depend on the number of Tx and Rx antennas, while the mean value also depends on the distance between Tx and Rx. Focusing on obtaining a model that gives a realistic statistical RMG as a result, the inverse of the distribution is required:

$$g(u,\mu_{RMG},\sigma_{RMG}) = \mu_{RMG}(d,N_T,N_R) - \frac{\sqrt{3\sigma^2_{RMG}(d,N_T,N_R)}}{\pi}\ln\frac{1-u}{u} \tag{C.3}$$

where:

- *u,* is the random value with a Uniform distribution, i.e., $u = U[0,1]$;
- *d*, is the distance between BS and MT;
- $\sigma^2_{RMG}(d,N_T,N_R)$, is the variance depending on the cell type, N_T and N_R;
- $\mu_{RMG}(d,N_T,N_R)$, is the average RMG depending on the cell type, N_T and N_R.

In Table C.1, the simulation parameters of the default RMG model are presented. The values for the variance needed for this thesis are presented in Table C.2, and the mean results of the RMG model are presented in Table C.3 and Table C.4. Other values for others MIMO configurations are in [KuCo07]. In Figure C.1, one can see the modelled values of the RMG plotted for various antenna configurations and its variation with distance.

Table C.1 Simulation parameters (extracted from [KuCo07]).

Carrier frequency [GHz]	2		
Bandwidth [MHz]	5		
Time resolution (receiver filter) [ns]	200		
Antenna spacing	λ		
Noise floor	-150		
SNR [dB]	10		
Cluster density [10^{-4} m^2]	**pico**	**Micro**	**macro**
	8.9	2.2	2.2
Avg. number of scatterers per cluster	10		
N_T	[2 - 16]		
N_R	[2 - 16]		
Number of runs	100		
Distance [m]	**pico**	**Micro**	**macro**
	[10 – 60]	[100 – 600]	[1200 – 2400]

Table C.2 Variance for different number of Tx and Rx antennas (adapted from [KuCo07]).

$\sigma^2_{RMG}(10^{-3})$		**[10 – 60] m**		**[100 – 600] m**		**[1200 – 2400] m**	
N_R		**2**	**4**	**2**	**4**	**2**	**4**
N_T	**2**	18.5	10.4	24.0	15.9	1.9	1.8
	4	11.8	45.4	15.9	71.4	0.8	1.1

Table C.3. μ_{RMG} for systems with $N_{T/R} = 2$ for different distances (adapted from [KuCo07]).

$N_{R/T}$	μ_{RMG}
2	1.54

Table C.4. μ_{RMG} for systems with $N_{T/R} > 2$ for different distances (adapted from [KuCo07]).

$N_T \times N_R$	**Range [m]**	μ_{RMG}
4 × 4	10-31	$50.32d_{[km]} + 1.77$
	31-57	3.36
4 × 4	57-686	$-2.00d_{[km]} + 3.47$
4 × 4	686-2400	2.10

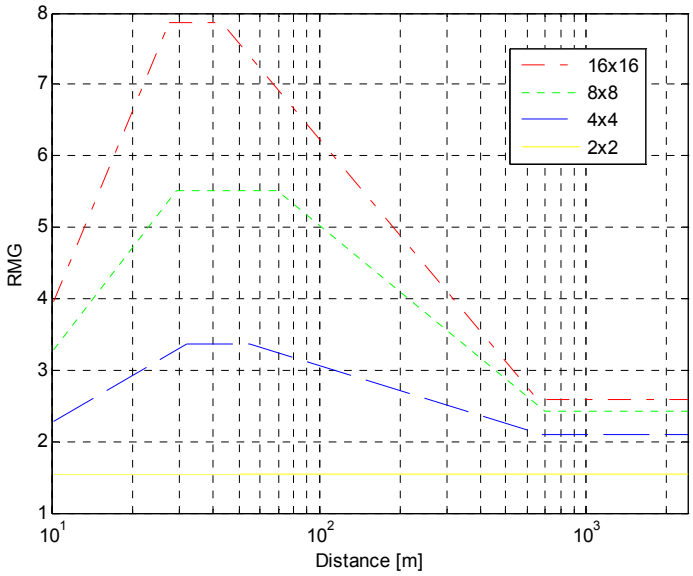

Figure C.1. Distribution of the RMG for multiple antenna configurations (extracted from [Bati08]).

Annex D – Services' Characterisation

The user's generator program is based on parameters provided by the MOMENTUM project, [MOME04]. The previously existing profiles were adapted to the new services, Table D.1, having a relation between the service traffic distribution files used in this thesis and the ones from MOMEMTUM, with similar service percentages. All the other input parameters were left unchanged, being the ones used in [CoLa06]. In Table D.2, the services' penetration percentages and QoS priority list for the scenarios studied are presented.

Table D.1. Traffic distribution files correspondence.

MOMENTUM traffic distribution file	New traffic distribution file	Service name
Streaming3.rst	Voice.rst	Voice
Speech3.rst	Web.rst	Web
	P2P.rst	P2P
E-mail3.rst	Streaming.rst	Streaming
File_down3.rst	Chat.rst	Chat
MMS3.rst	Email.srt	Email
	FTP.rst	FTP

Table D.2. Default and alternative scenarios characterisation.

Services	Penetration Percentage [%]	Penetration Percentage [%]		QoS priority
	Default	Alternative 1	Alternative 2	
Voice	5	10	5	1
Web	44.1	41.8	46.8	2
P2P	40.1	38	38	7
Streaming	5.9	5.6	5.6	3
Chat	2.9	2.8	2.8	6
Email	1	0.9	0.9	4
FTP	1	0.9	0.9	5

Annex E – LTE Reduction Strategies

In this annex, the flow charts regarding the LTE reduction strategies are presented. The three reduction algorithms are: “Throughput reduction”, Figure E.1, “QoS class reduction”, Figure E.2, and “QoS one by one reduction”, Figure E.3.

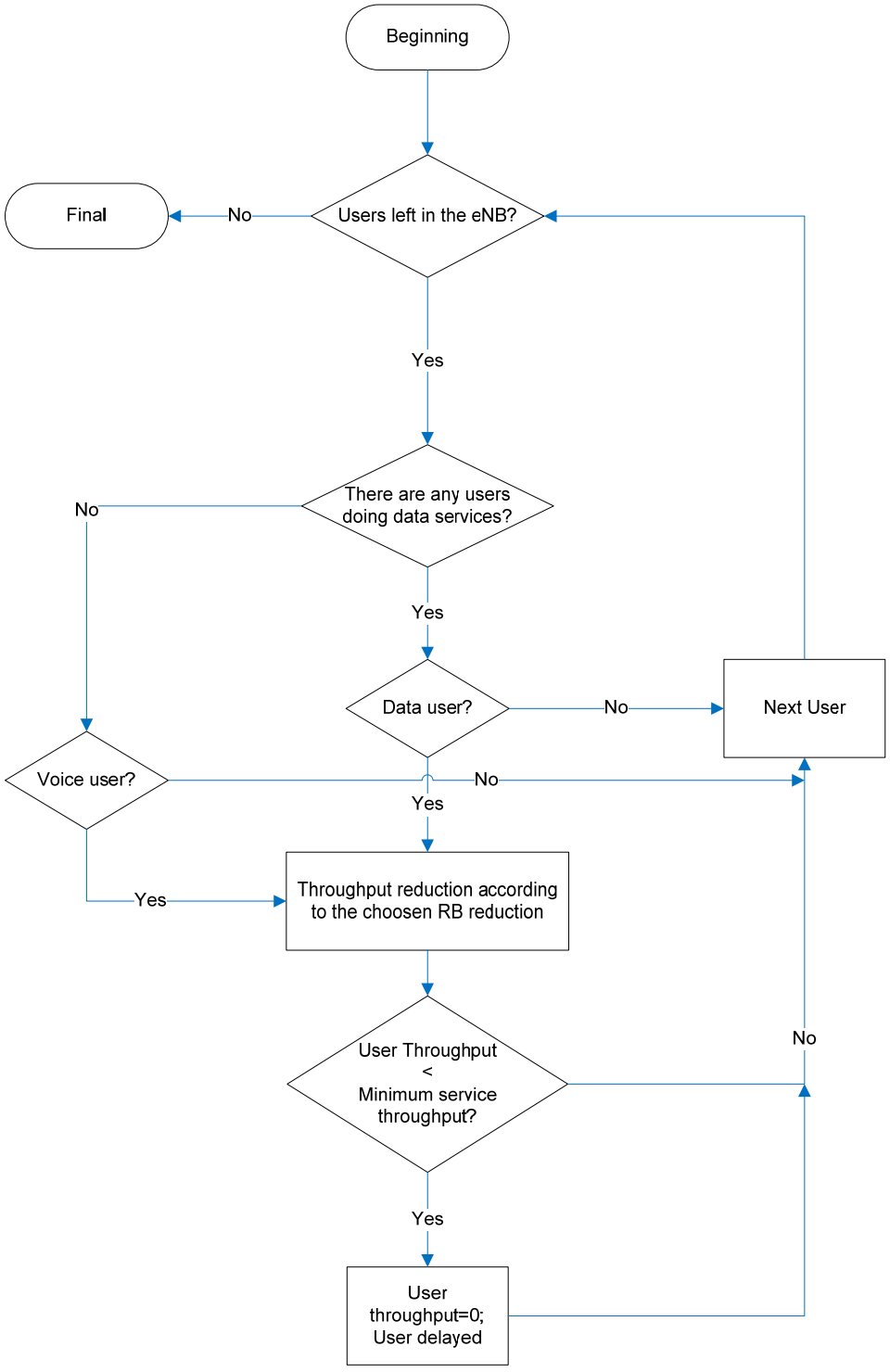

Figure E.1. LTE algorithm for the “Reduction throughput” strategy.

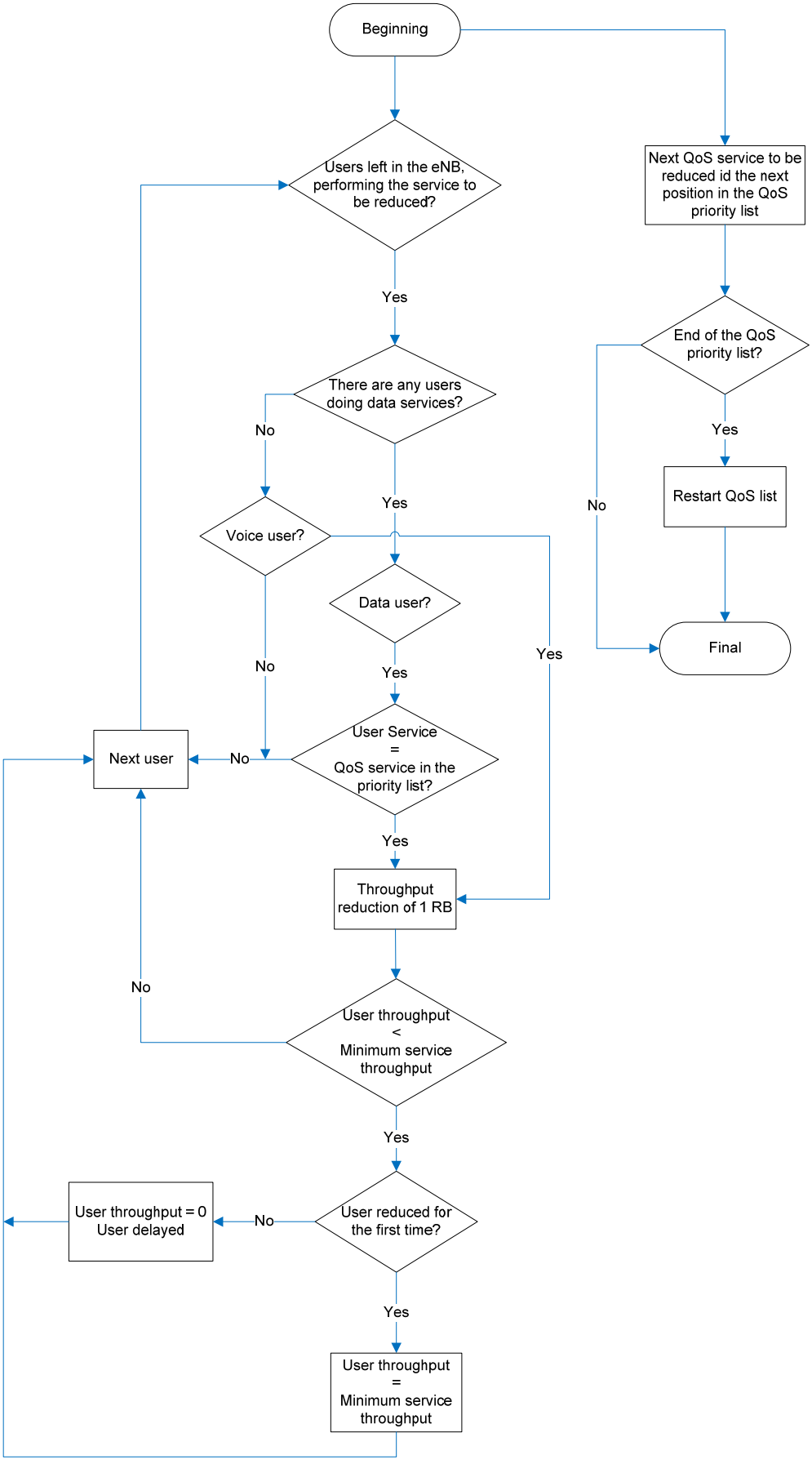

Figure E.2. LTE algorithm for the “QoS class reduction” strategy.

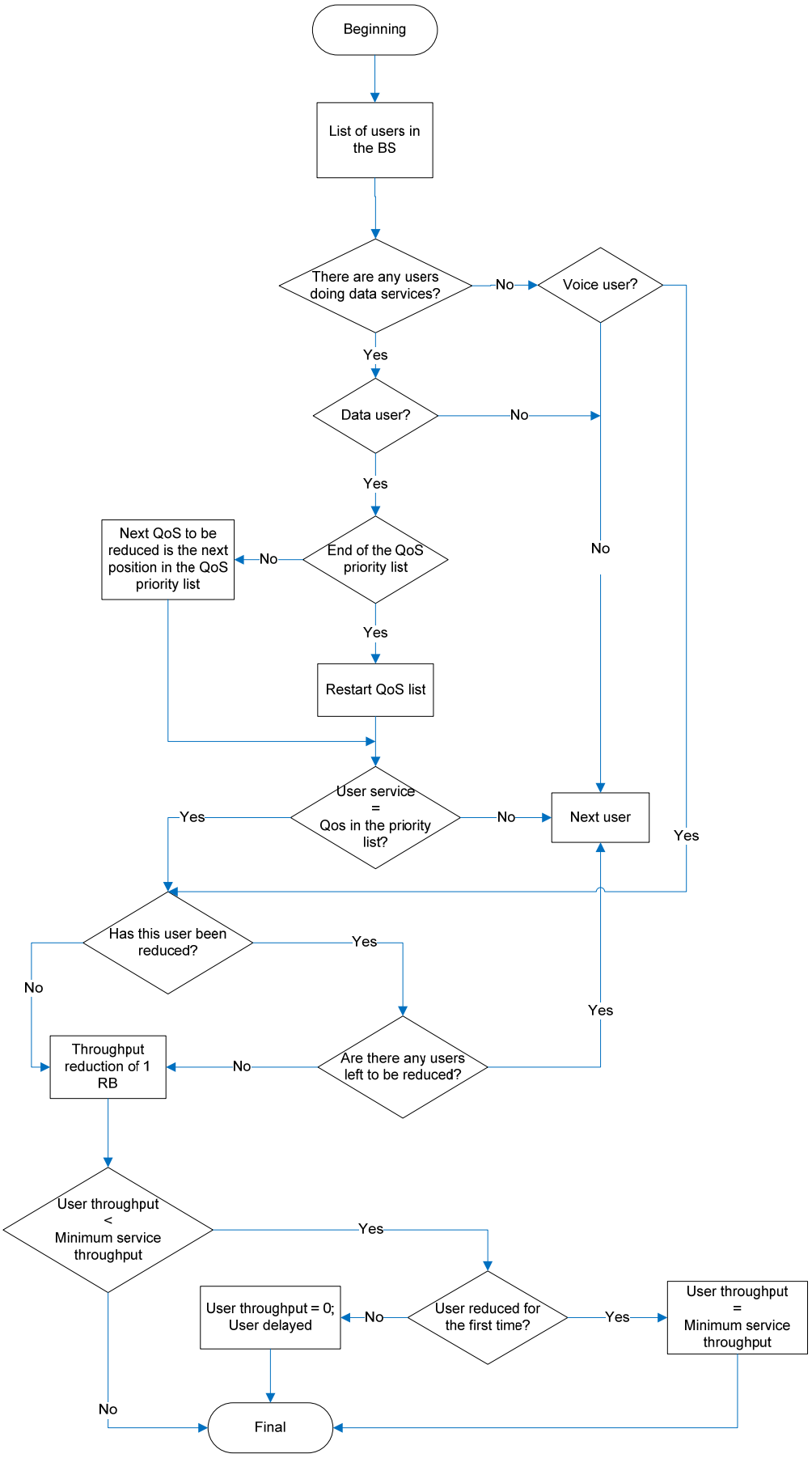

Figure E.3. LTE algorithm for the “QoS one by one reduction” strategy.

Annex F – Single User Model Interface

In this annex, the single user and single service model interface is presented for LTE-DL.

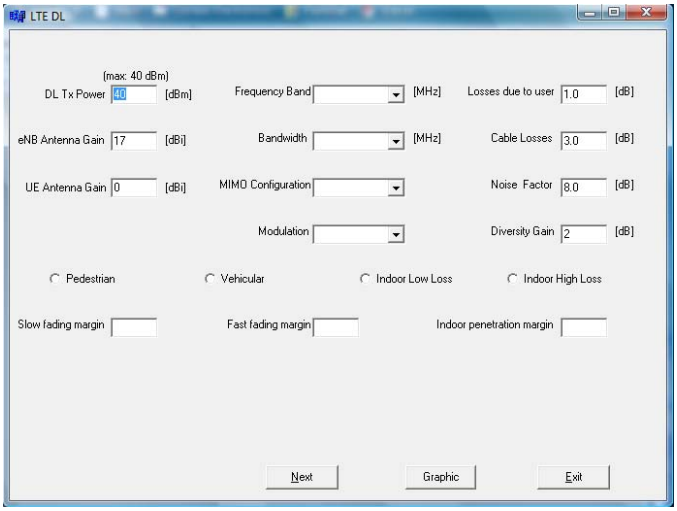

Figure F.1. DL single service user model interface.

After choosing the several parameters, Figure F.1, it is necessary to press the Graphic button to have a graphic of the radius as a function of the possible throughput, Figure F.2, or the Next button in order to have the radius for a specific throughput, Figure F.3. In the last option, it is possible do go back to change the parameter if desired, or to put the throughput desired and press on the Run button and obtain the result, Figure F.4. If is not possible to obtaining the desired throughput with the configuration chosen a error message is shown with the valid range of the possible throughput. After obtain the result it is possible to run a new simulation pressing the button New Simulation, returning to the interface of Figure F.1. In all interfaces it is possible to exit of this program pressing in the Exit button.

For UL, the single user model interface is equal with some differences in the input parameters.

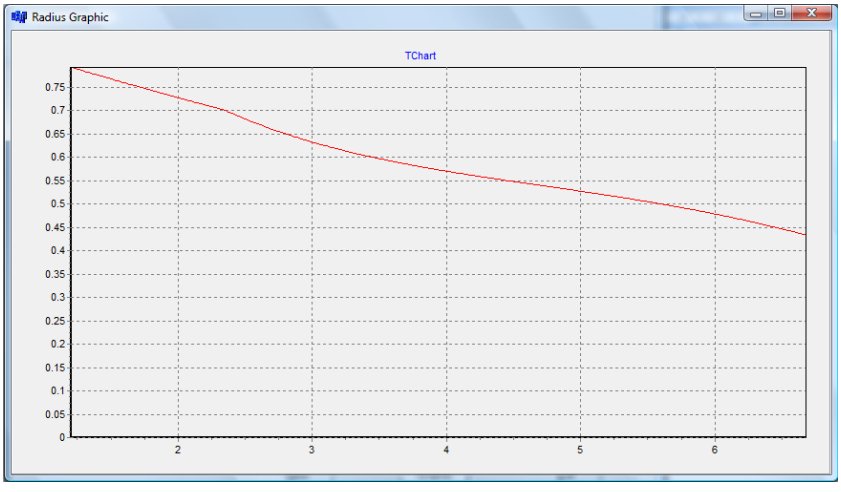

Figure F.2. DL single service user model interface for graphic option.

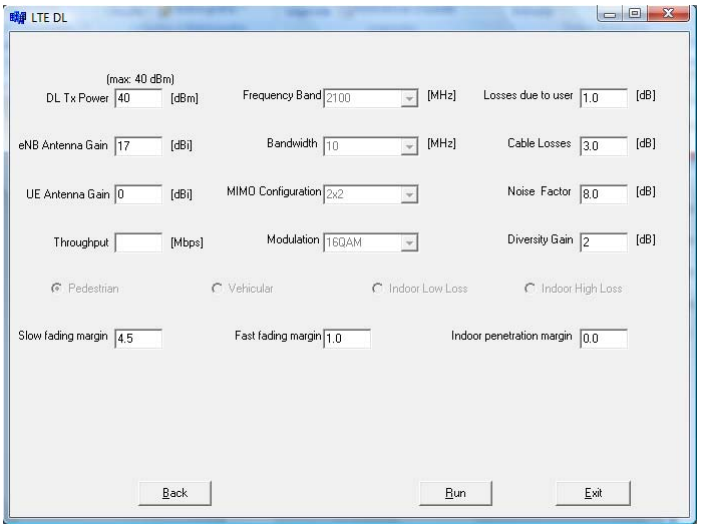

Figure F.3. DL single service user model interface to obtain the radius for a given throughput.

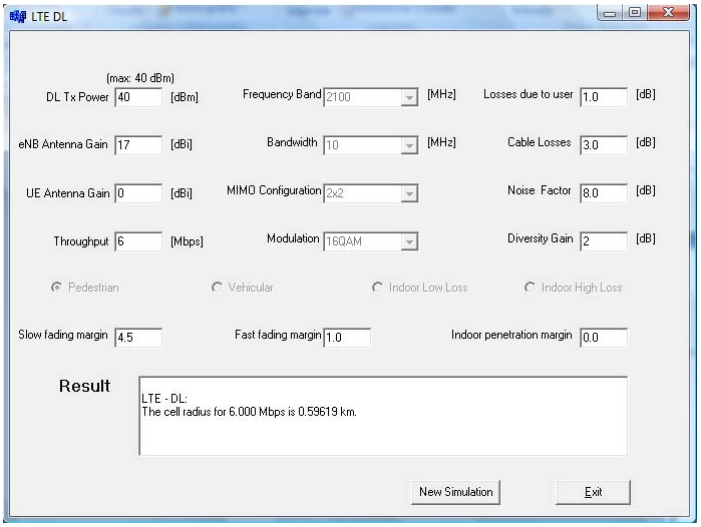

Figure F.4. DL single service user model interface with results of the radius for a given throughput.

Annex G – User's Manual

In this annex, one presents the simulator's user manual. To start the application, it is necessary to introduce 3 input files:

- "Ant65deg.TAB", with the BS antenna gain for all directions;
- "DADOS_Lisboa.TAB", with information regarding the city of Lisbon and all its districts;
- "ZONAS_Lisboa.TAB", with the area characterisation, like streets, gardens along with others, Figure G.1.

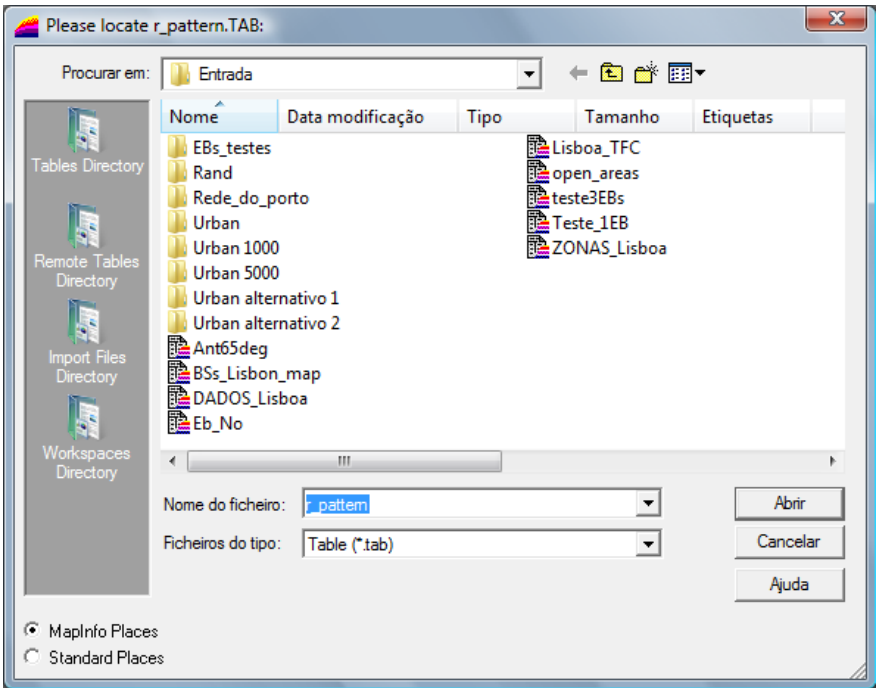

Figure G.1. Window for the introduction of ZONAS_Lisboa.TAB file.

After the introduction of the geographical information, a new options bar is displayed in MapInfo, where it is possible to choose between LTE-DL and LTE-UL, Figure G.2, and define the simulation's characteristics.

Among the several options that are available for DL and UL, the windows for the propagation model and services' colours are common for both systems, Figure G.3 and Figure G.4, respectively, since the propagation model parameters are the same and the service's colour are only a graphical information.

With DL and UL Settings and windows, Figure G.5, it is possible to modify the different radio parameters of both systems, along with the reference scenario, reference services and reduction strategy. The default values are presented in Section 4.1. After choosing the parameters, the User Profile window is enabled, Figure G.6, and it is possible to change the maximum and minimum desired throughputs for each service, in both DL and UL User Profile windows. The values for the minimum throughput are the ones presented in Figure G.6 and Table 4.4, not being possible to define a

minimum service throughput lower than the ones presented. The maximum throughputs are defined by the maximum throughput that is possible to obtain due to bandwidth, MIMO configuration and modulation.

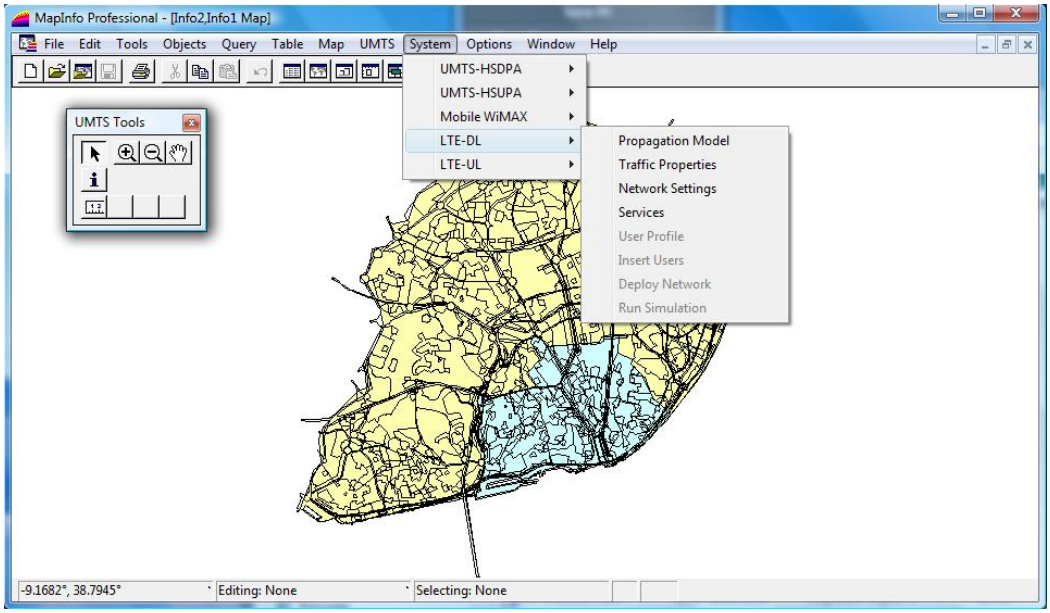

Figure G.2. View of the simulator and menu bar with the several options for each one of the systems.

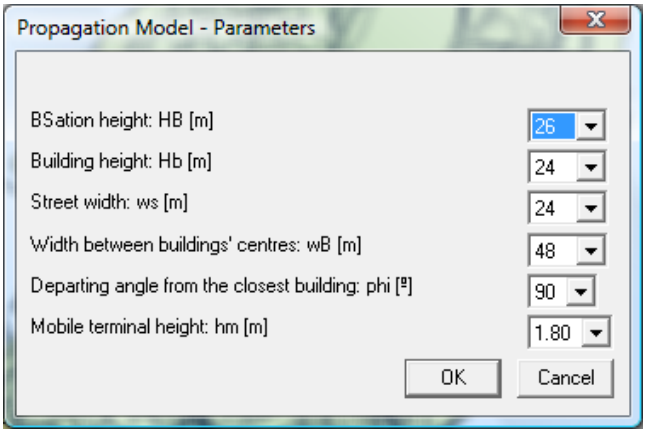

Figure G.3. Propagation model parameters

Figure G.4. Services' colour assignment.

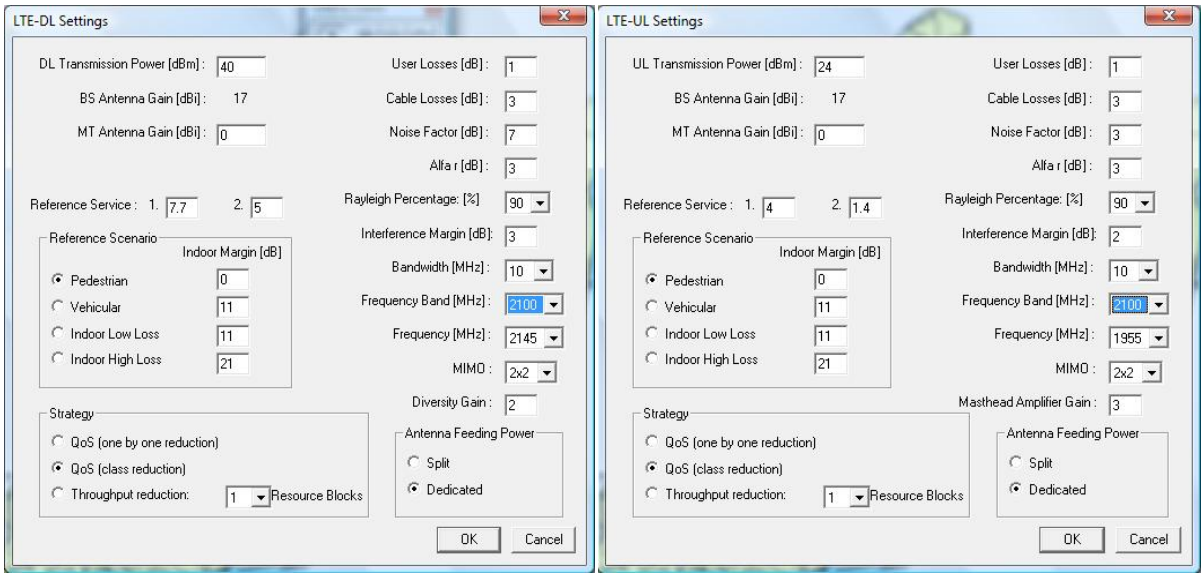

(a) DL (b) UL

Figure G.5. DL and UL simulations' parameters.

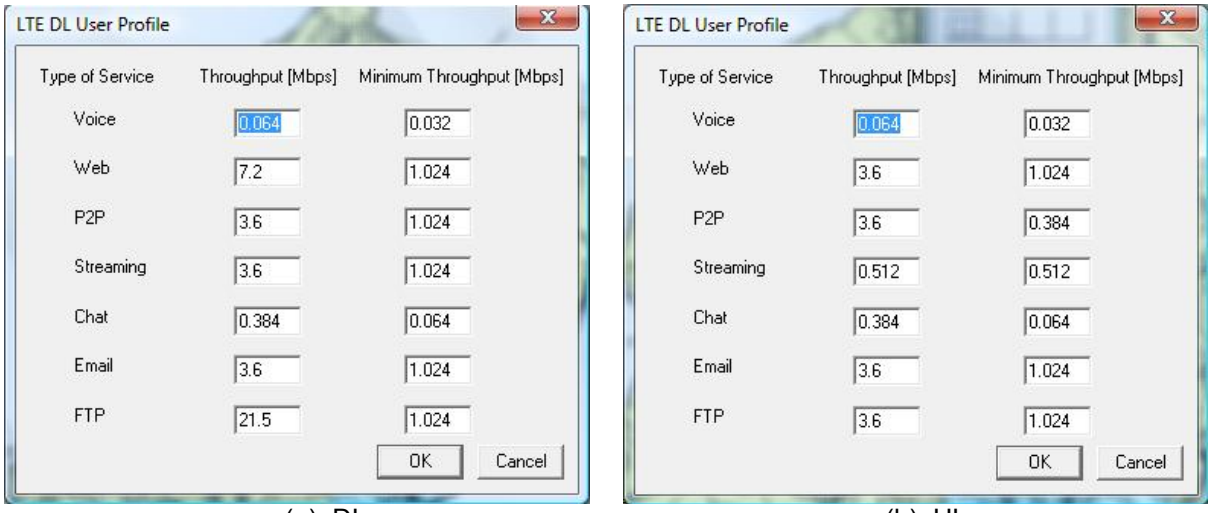

(a) DL (b) UL

Figure G.6. DL and UL maximum and minimum service throughput.

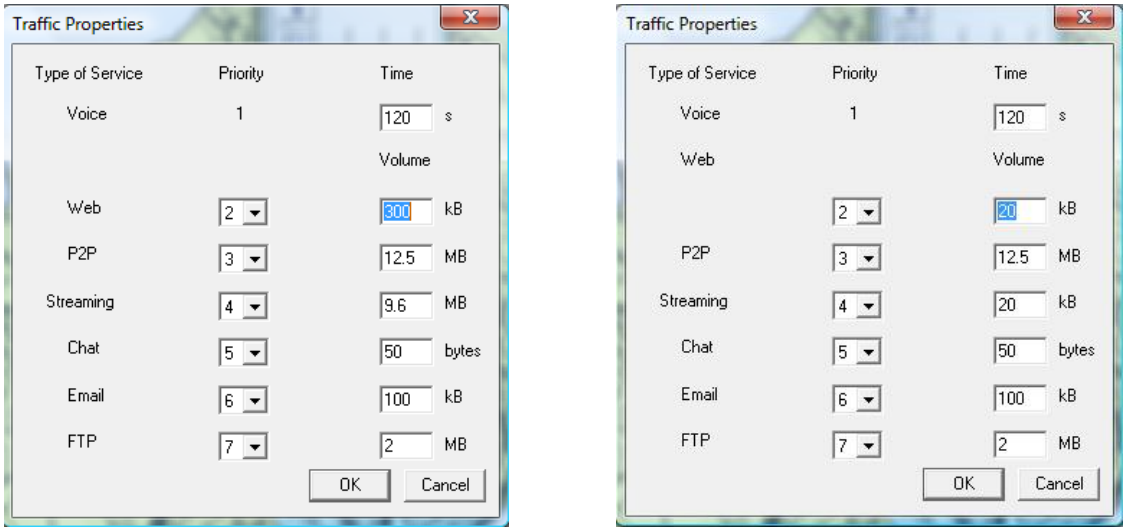

(a) DL (b) UL

Figure G.7. DL and UL traffic properties window.

After pressing the “OK” button, it is displayed in the “Message” window the results regarding the cell radius for the two reference services and the different services considered in Figure G.6. The window in Figure G.8 presents DL results. From now on, only DL windows are presented, since the procedures are identical for both links.

Later, in the network setting window, the functionality “Insert Users” is activated, to introduce users in the network, by choosing one of the user files from the SIM application, Figure G.8. In Table G.1, one presents the relation between the number of users effectively considered and the ones that are necessary to consider as input parameter in the SIM program, as there are some users that are placed outside of the network area, not being considered in the analysis. Afterwards, the menu “Deploy Network” becomes active, requesting a file containing the BSs’ location, so that these can be placed in the city area, Figure G.9.

Table G.1. Evaluation of the number of users considered taking several parameters into account.

SIM input number of users	Effective number of users
1000	800
1500	1200
2000	1600
2500	2000

After showing Figure G.9, the menu “Run Simulation” is switched on, and when executed, the simulation takes place with the various simulations’ results being displayed by pressing the “OK” button. In Figure G.10, Figure G.11 and Figure G.12 the results for 228 BSs and around 1000 users are presented.

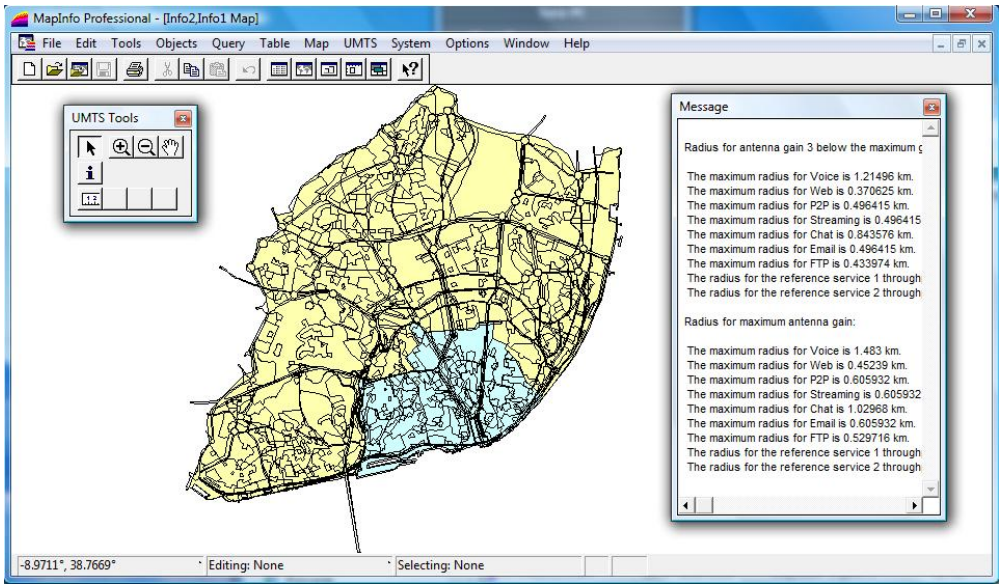

Figure G.8. Visual aspect of the application after running the DL settings window.

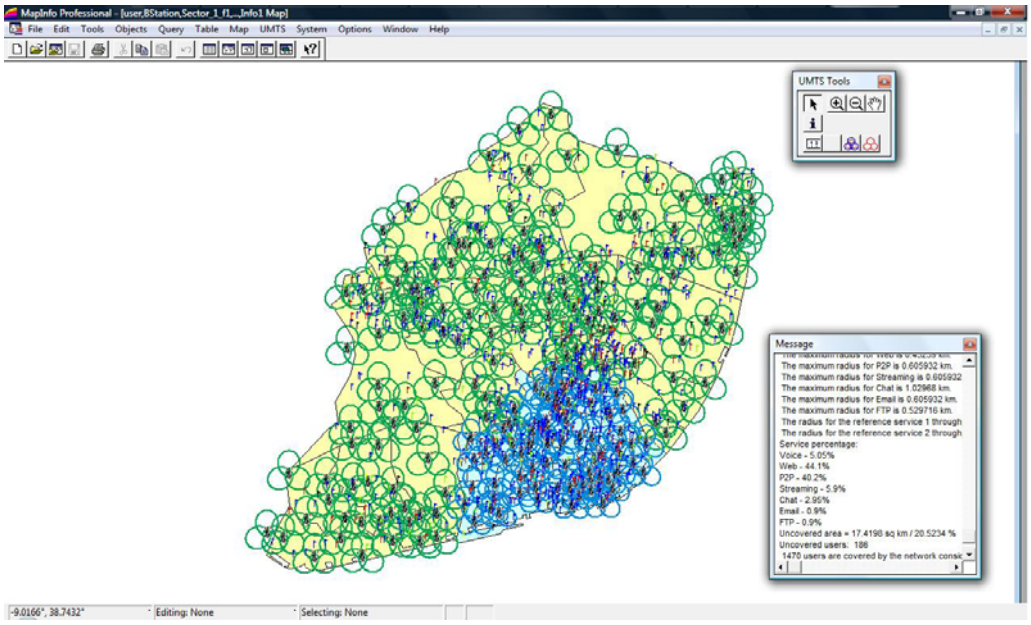

Figure G.9. Result of the “Network Deployment” with 228 tri-sectored BSs’ coverage area.

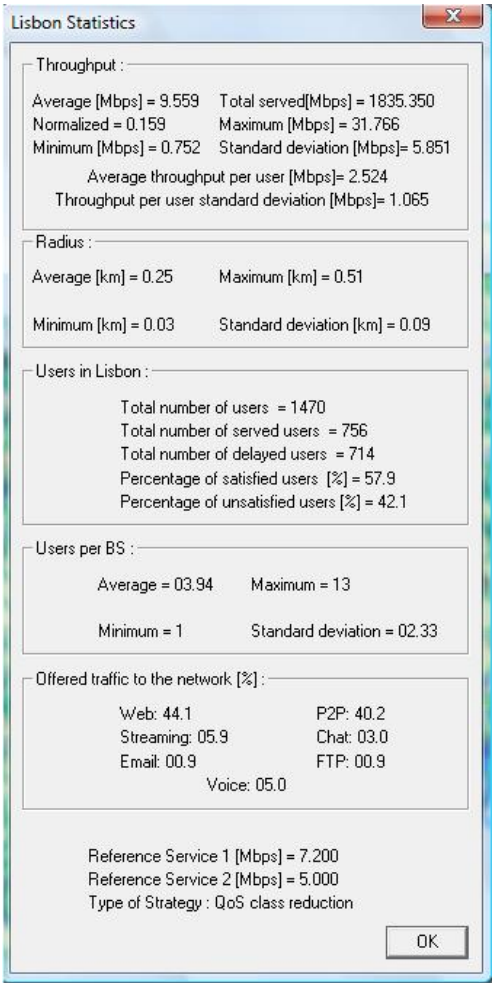

Figure G.10. DL instantaneous results for the city of Lisbon.

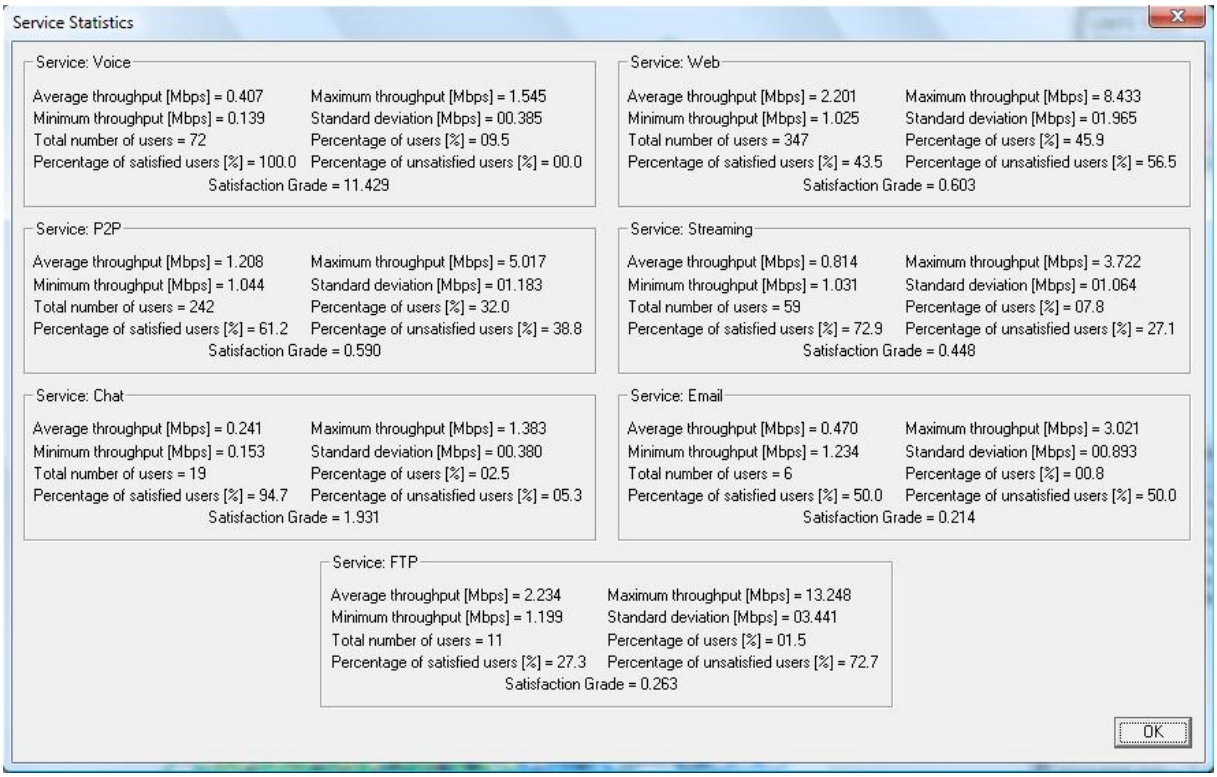

Figure G.11. DL instantaneous results detailed by service for the city of Lisbon.

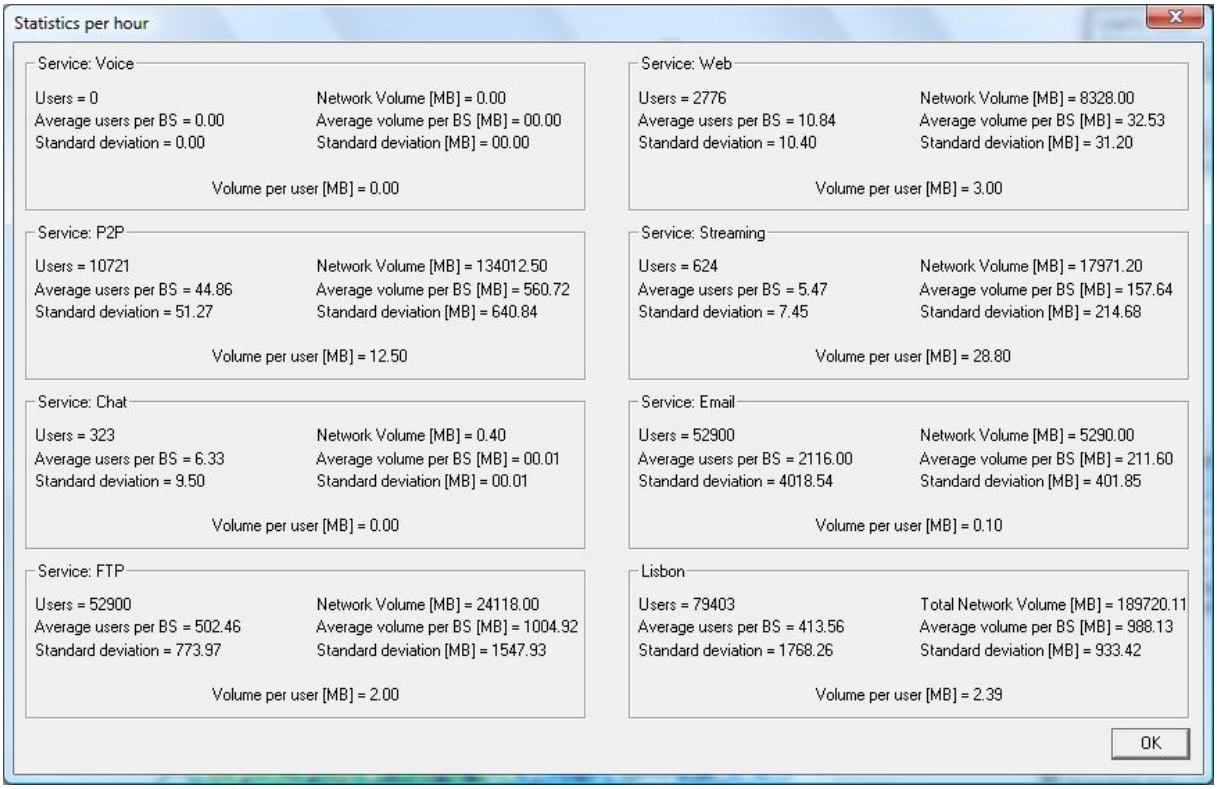

Figure G.12. DL extrapolation results for the hour analysis.

Annex H – One Reference Service Vs. Two Reference Services

In this annex one shows the impact in terms of coverage on considering two reference services instead one.

The reference service for the radius calculation was set at 7.7 Mbps, in DL, since this value is the lowest maximum for QPSK in the 10 MHz bandwidth. For UL, for the choice of the reference service the same criterion was considered as in DL, being set to 4 Mbps. Figure H.1 represents the coverage area, for DL and UL, with a reference service of 7.7 Mbps and 4 Mbps, respectively. As it can be seen, the uncovered area, mainly for UL, is high, 82.3% and 35% for UL and DL respectively and in approximately in 1600 user, 350 users, for DL, and 1174 users for UL, are in uncovered areas, i.e., 25% and 71% of uncovered users for the same users input file. These simulations were made for the default scenario, Table 4.1.

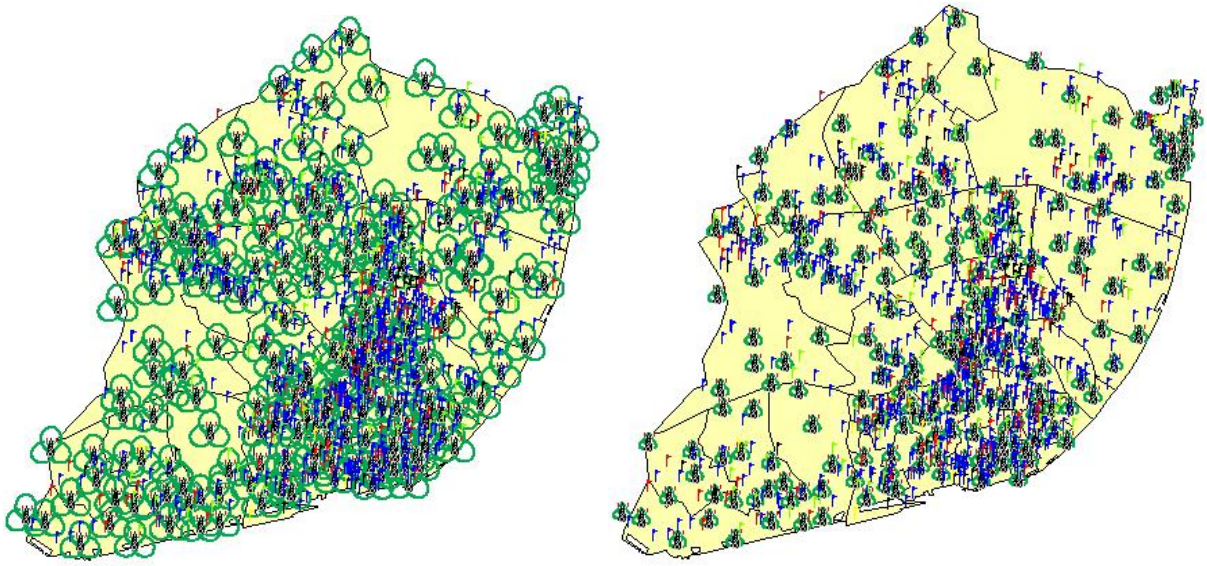

(a) DL (Reference Service – 7.7 Mbps) (b) UL (Reference Service – 4 Mbps)

Figure H.1. Results for 228 tri-sectored BSs' coverage area for one reference service.

In order to improve the coverage area and users, the Lisbon city was divided in two zones according the density of BSs, Figure H.2. Zone 1 has a high density of BSs, so for this zone it is considered a higher reference service comparing to Zone 2, with a lowest BSs density, therefore two reference services are considered. For Zone 1 a reference service 1 of 7.7 Mbps was defined and for Zone 2 of 5 Mbps, as default values, however it is possible to change these values, according to the limitation of the system, in the DL Settings Values' window, Figure G.5. In UL for Zone 1 was set as a default value 4 Mbps and in Zone 2 1.4 Mbps. Like in DL, it is possible to change these two values at UL Settings Values' window, Figure G.5.

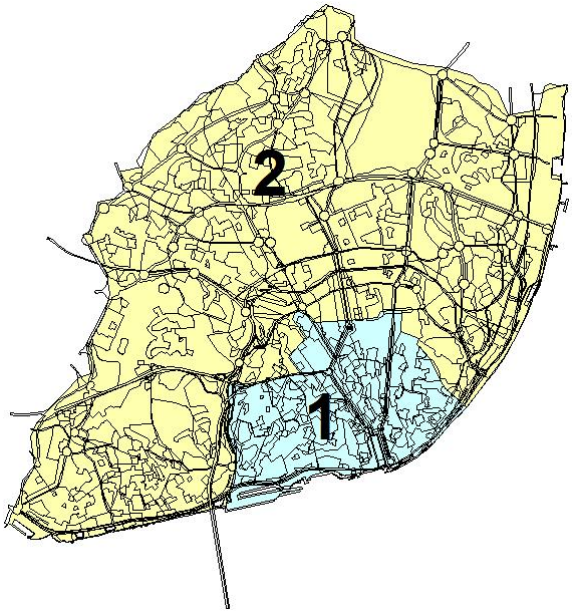

Figure H.2. Division of Lisbon in 2 zones.

For the default values, 7.7 Mbps and 4Mbps for reference service 1 and 5 Mbps and 1.4 Mbps for reference service 2, for DL and UL respectively; the results are presented at Figure H.3. The uncovered area decreases to 20.7 % in DL and to 72.3% in UL and there are more 150 users covered in DL and 220 in UL, i.e., the coverage area raised 10% approximately, in both DL and UL, and there are 10% more covered user.

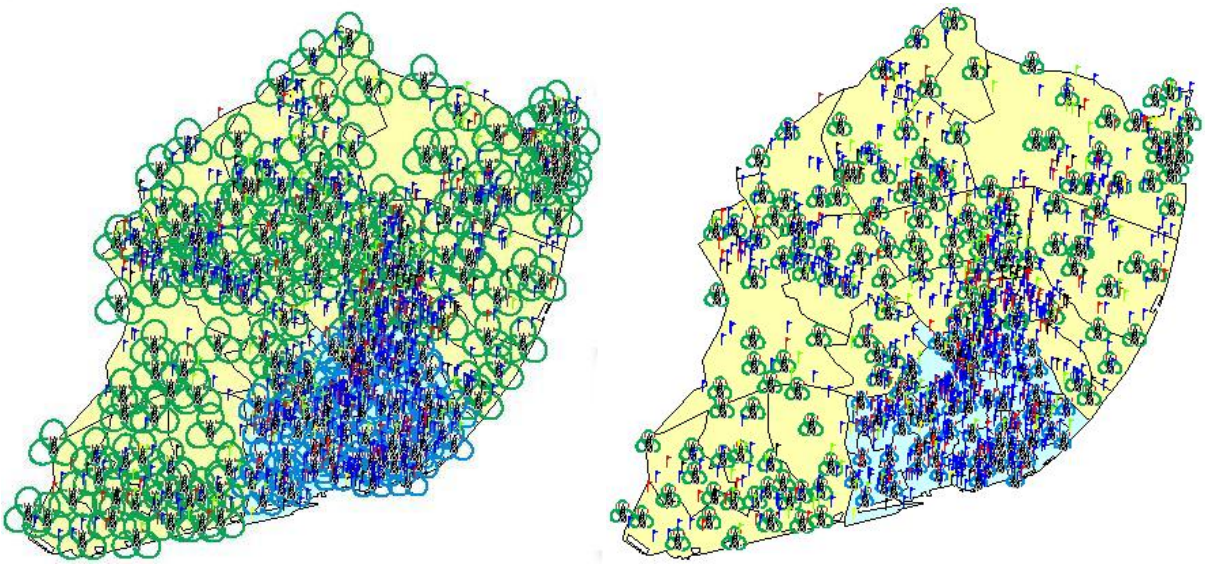

(a) DL

Reference Service 1 – 7.7 Mbps

Reference Service 2 – 5 Mbps

(b) UL

Reference Service 1 – 4 Mbps

Reference Service 2 – 1.4 Mbps

Figure H.3. Results for 228 tri-sectored BSs' coverage area for two reference services.

Annex I – Single User Results

In this annex, the DL, Table I.1, Table I.2 and Table I.3, and UL, Table I.4, Table I.5 and Table I.6, single cell radius results for the model presented in Section 3.1 are detailed. The values for the minimum throughput, when possible are 14.4 Mbps in DL and 5.8 Mbps for UL. For the scenarios that were not possible to have the established minimum throughput, only the maximum throughput radii were taken. Table B.5 and Table B.6 have the maximum throughputs for each scenario considered.

Table I.1. DL single user radii for 900 MHz frequency band.

				RADIUS [km]					
				Bandwidth [MHz]					
Modulation	Environment	MIMO	Throughput	1.4	3	5	10	15	20
QPSK	Pedestrian	2×2	Min.						1.28
			Max.	2.19	1.72	1.51	1.26	1.13	1.05
		4×4	Min.				1.53	1.44	1.33
			Max.	2.19	1.72	1.51	1.26	1.13	1.05
	Vehicular	2×2	Min.						0.76
			Max.	1.36	1.07	0.93	0.78	0.70	0.65
		4×4	Min.				0.91	0.97	0.93
			Max.	1.36	1.07	0.93	0.78	0.70	0.65
	Indoor Low	2×2	Min.						0.94
			Max.	1.61	1.27	1.11	0.92	0.83	0.77
		4×4	Min.				1.13	1.06	0.98
			Max.	1.61	1.27	1.11	0.92	0.83	0.77
	Indoor High	2×2	Min.						0.80
			Max.	1.37	1.07	0.94	0.78	0.70	0.65
		4×4	Min.				0.96	0.90	0.83
			Max.	1.37	1.07	0.94	0.78	0.70	0.65
16QAM	Pedestrian	2×2	Min.				1.16	1.21	1.23
			Max.	1.53	1.20	1.05	0.87	0.79	0.73
		4×4	Min.		1.23	1.39	1.48	1.42	1.33
			Max.	1.53	1.20	1.05	0.87	0.79	0.73
	Vehicular	2×2	Min.				0.70	0.76	0.78
			Max.	0.95	0.74	0.65	0.54	0.49	0.45
		4×4	Min.			0.84	0.93	0.89	0.85
			Max.	0.95	0.84	0.65	0.54	0.49	0.45
	Indoor Low	2×2	Min.				0.85	0.89	0.90
			Max.	1.12	0.88	0.77	0.64	0.58	0.53
		4×4	Min.		0.90	1.02	1.08	1.04	0.98
			Max.	1.12	0.88	0.77	0.64	0.58	0.53
	Indoor High	2×2	Min.				0.72	0.76	0.77
			Max.	0.95	0.75	0.65	0.54	0.49	0.45
		4×4	Min.		0.77	0.87	0.92	0.89	0.83
			Max.	0.95	0.75	0.65	0.54	0.49	0.45
64QAM	Pedestrian	2×2	Min.		0.72	0.77	1.01	1.01	0.97
			Max.	0.83	0.66	0.57	0.48	0.43	0.40
		4×4	Min.		0.95	1.22	1.17	1.10	1.04
			Max.	0.83	0.66	0.57	0.48	0.43	0.40
	Vehicular	2×2	Min.		0.43	0.47	0.67	0.65	0.62
			Max.	0.46	0.36	0.31	0.26	0.23	0.22
		4×4	Min.		0.60	0.81	0.74	0.68	0.64
			Max.	0.46	0.36	0.31	0.26	0.23	0.22
	Indoor Low	2×2	Min.		0.53	0.56	0.74	0.74	0.71
			Max.	0.61	0.48	0.42	0.35	0.32	0.29
		4×4	Min.		0.70	0.89	0.86	0.80	0.76

Table I.1 (Cont.). DL single user radii for 900 MHz frequency band.

				RADIUS [km]					
				Bandwidth [MHz]]					
Modulation	Environment	MIMO	Throughput	1.4	3	5	10	15	20
64QAM	Indoor Low	4×4	Max.	0.61	0.48	0.42	0.35	0.32	0.29
	Indoor High	2×2	Min.		0.45	0.48	0.63	0.63	0.61
			Max.	0.52	0.41	0.36	0.30	0.27	0.25
		4×4	Min.		0.59	0.76	0.73	0.68	0.65
			Max.	0.52	0.41	0.36	0.30	0.27	0.25

Table I.2. DL single user radii for 2100 MHz frequency band.

				RADIUS [km]					
				Bandwidth [MHz]					
Modulation	Environment	MIMO	Throughput	1.4	3	5	10	15	20
QPSK	Pedestrian	2×2	Min.						0.50
			Max.	0.86	0.67	0.59	0.49	0.44	0.41
		4×4	Min.				0.60	0.56	0.52
			Max.	0.86	0.67	0.59	0.49	0.44	0.41
	Vehicular	2×2	Min.						0.19
			Max.	0.34	0.27	0.23	0.19	0.17	0.16
		4×4	Min.				0.23	0.24	0.23
			Max.	0.34	0.27	0.23	0.19	0.17	0.16
	Indoor Low	2×2	Min.						0.23
			Max.	0.40	0.32	0.28	0.23	0.21	0.19
		4×4	Min.				0.28	0.26	0.24
			Max.	0.40	0.32	0.28	0.23	0.21	0.19
	Indoor High	2×2	Min.						0.13
			Max.	0.22	0.17	0.15	0.13	0.11	0.10
		4×4	Min.				0.15	0.14	0.13
			Max.	0.22	0.17	0.15	0.13	0.11	0.10
16QAM	Pedestrian	2×2	Min.				0.45	0.47	0.48
			Max.	0.60	0.47	0.41	0.34	0.31	0.28
		4×4	Min.		0.48	0.54	0.58	0.55	0.52
			Max.	0.60	0.47	0.41	0.34	0.31	0.28
	Vehicular	2×2	Min.				0.17	0.19	0.19
			Max.	0.24	0.19	0.16	0.13	0.12	0.11
		4×4	Min.			0.21	0.23	0.22	0.21
			Max.	0.24	0.21	0.16	0.13	0.12	0.11
	Indoor Low	2×2	Min.				0.21	0.22	0.22
			Max.	0.28	0.22	0.19	0.16	0.14	0.13
		4×4	Min.		0.23	0.25	0.27	0.26	0.24
			Max.	0.28	0.22	0.19	0.16	0.14	0.13
	Indoor High	2×2	Min.				0.12	0.12	0.12
			Max.	0.15	0.12	0.10	0.09	0.08	0.07
		4×4	Min.		0.12	0.14	0.15	0.14	0.13
			Max.	0.15	0.12	0.10	0.09	0.08	0.07
64QAM	Pedestrian	2×2	Min.		0.28	0.30	0.40	0.39	0.38
			Max.	0.33	0.26	0.22	0.19	0.17	0.16
		4×4	Min.		0.37	0.47	0.46	0.43	0.41
			Max.	0.33	0.26	0.22	0.19	0.17	0.16
	Vehicular	2×2	Min.		0.11	0.12	0.17	0.16	0.15
			Max.	0.11	0.09	0.08	0.07	0.06	0.05
		4×4	Min.		0.15	0.20	0.18	0.17	0.16
			Max.	0.11	0.09	0.08	0.07	0.06	0.05
	Indoor Low	2×2	Min.		0.13	0.14	0.19	0.18	0.18
			Max.	0.15	0.12	0.10	0.09	0.08	0.07
		4×4	Min.		0.17	0.22	0.21	0.20	0.19
			Max.	0.15	0.12	0.10	0.09	0.08	0.07
	Indoor High	2×2	Min.		0.07	0.08	0.10	0.10	0.10

Table I.2 (Cont.). DL single user radii for 2100 MHz frequency band.

				RADIUS [km]					
				Bandwidth [MHz]					
Modulation	Environment	MIMO	Throughput	1.4	3	5	10	15	20
64QAM	Indoor High	2×2	Max.	0.08	0.07	0.06	0.05	0.04	0.04
		4×4	Min.		0.09	0.12	0.12	0.11	0.10
			Max.	0.08	0.07	0.06	0.05	0.04	0.04

Table I.3. DL single user radii for 2600 MHz frequency band.

				RADIUS [km]					
				Bandwidth [MHz]					
Modulation	Environment	MIMO	Throughput	1.4	3	5	10	15	20
QPSK	Pedestrian	2×2	Min.						0.36
			Max.	0.62	0.48	0.42	0.35	0.32	0.29
		4×4	Min.				0.43	0.40	0.37
			Max.	0.62	0.48	0.42	0.35	0.32	0.29
	Vehicular	2×2	Min.						0.14
			Max.	0.24	0.19	0.17	0.14	0.13	0.12
		4×4	Min.				0.16	0.17	0.17
			Max.	0.24	0.19	0.17	0.14	0.13	0.12
	Indoor Low	2×2	Min.						0.17
			Max.	0.29	0.23	0.20	0.17	0.15	0.14
		4×4	Min.				0.20	0.19	0.18
			Max.	0.29	0.23	0.20	0.17	0.15	0.14
	Indoor High	2×2	Min.						0.09
			Max.	0.16	0.12	0.11	0.09	0.08	0.08
		4×4	Min.				0.11	0.10	0.10
			Max.	0.16	0.12	0.11	0.09	0.08	0.08
16QAM	Pedestrian	2×2	Min.				0.32	0.34	0.34
			Max.	0.43	0.34	0.29	0.25	0.22	0.20
		4×4	Min.		0.34	0.39	0.41	0.40	0.37
			Max.	0.43	0.34	0.29	0.25	0.22	0.20
	Vehicular	2×2	Min.				0.13	0.14	0.14
			Max.	0.17	0.13	0.12	0.10	0.09	0.08
		4×4	Min.	0.00	0.00	0.15	0.17	0.16	0.15
			Max.	0.17	0.15	0.12	0.10	0.09	0.08
	Indoor Low	2×2	Min.				0.15	0.16	0.16
			Max.	0.20	0.16	0.14	0.11	0.10	0.10
		4×4	Min.		0.16	0.18	0.19	0.19	0.18
			Max.	0.20	0.16	0.14	0.11	0.10	0.10
	Indoor High	2×2	Min.				0.08	0.09	0.09
			Max.	0.11	0.09	0.08	0.06	0.06	0.05
		4×4	Min.		0.09	0.10	0.11	0.10	0.10
			Max.	0.11	0.09	0.08	0.06	0.06	0.05
64QAM	Pedestrian	2×2	Min.		0.20	0.22	0.28	0.28	0.27
			Max.	0.23	0.18	0.16	0.13	0.12	0.11
		4×4	Min.		0.27	0.34	0.33	0.31	0.29
			Max.	0.23	0.18	0.16	0.13	0.12	0.11
	Vehicular	2×2	Min.		0.08	0.08	0.12	0.12	0.11
			Max.	0.08	0.06	0.06	0.05	0.04	0.04
		4×4	Min.		0.11	0.14	0.13	0.12	0.12
			Max.	0.08	0.06	0.06	0.05	0.04	0.04
	Indoor Low	2×2	Min.		0.10	0.10	0.13	0.13	0.13
			Max.	0.11	0.09	0.08	0.06	0.06	0.05
		4×4	Min.		0.13	0.16	0.15	0.14	0.14
			Max.	0.11	0.09	0.08	0.06	0.06	0.05
	Indoor High	2×2	Min.		0.05	0.06	0.07	0.07	0.07
			Max.	0.06	0.05	0.04	0.03	0.03	0.03
		4×4	Min.		0.07	0.09	0.08	0.08	0.07
			Max.	0.06	0.05	0.04	0.03	0.03	0.03

Table I.4. UL single user radii for 900 MHz frequency band.

				RADIUS [km]					
				Bandwidth [MHz]					
Modulation	Environment	MIMO	Throughput	1.4	3	5	10	15	20
QPSK	Pedestrian	2×2	Min.					0.60	0.55
			Max.	0.77	0.61	0.53	0.44	0.40	0.37
		4×4	Min.					0.60	0.55
			Max.	1.03	0.81	0.71	0.59	0.53	0.49
	Vehicular	2×2	Min.					0.31	0.37
			Max.	0.48	0.37	0.33	0.27	0.24	0.23
		4×4	Min.					0.40	0.37
			Max.	0.68	0.48	0.42	0.35	0.31	0.29
	Indoor Low	2×2	Min.					0.41	0.38
			Max.	0.53	0.42	0.36	0.30	0.27	0.25
		4×4	Min.					0.41	0.38
			Max.	0.71	0.55	0.48	0.40	0.36	0.34
	Indoor High	2×2	Min.					0.35	0.32
			Max.	0.45	0.36	0.31	0.26	0.23	0.22
		4×4	Min.					0.35	0.32
			Max.	0.60	0.47	0.41	0.34	0.31	0.29
16QAM	Pedestrian	2×2	Min.			0.49	0.59	0.58	0.54
			Max.	0.50	0.39	0.34	0.28	0.25	0.24
		4×4	Min.			0.62	0.66	0.60	0.55
			Max.	0.71	0.56	0.49	0.41	0.37	0.34
	Vehicular	2×2	Min.			0.30	0.38	0.40	0.33
			Max.	0.26	0.21	0.18	0.15	0.13	0.12
		4×4	Min.			0.37	0.44	0.40	0.37
			Max.	0.37	0.29	0.26	0.21	0.13	0.18
	Indoor Low	2×2	Min.			0.34	0.40	0.40	0.37
			Max.	0.34	0.27	0.23	0.19	0.17	0.16
		4×4	Min.			0.43	0.46	0.41	0.38
			Max.	0.49	0.39	0.34	0.28	0.25	0.23
	Indoor High	2×2	Min.			0.29	0.34	0.34	0.31
			Max.	0.29	0.23	0.20	0.17	0.15	0.14
		4×4	Min.			0.36	0.39	0.35	0.32
			Max.	0.42	0.33	0.29	0.24	0.22	0.20
64QAM	Pedestrian	2×2	Min.		0.37	0.48	0.51	0.47	0.43
			Max.	0.31	0.24	0.21	0.18	0.16	0.15
		4×4	Min.		0.48	0.64	0.63	0.47	0.55
			Max.	0.44	0.35	0.31	0.25	0.23	0.21
	Vehicular	2×2	Min.		0.17	0.29	0.34	0.31	0.29
			Max.	0.18	0.14	0.12	0.10	0.09	0.09
		4×4	Min.		0.24	0.37	0.41	0.40	0.37
			Max.	0.23	0.18	0.16	0.13	0.12	0.11
	Indoor Low	2×2	Min.		0.25	0.33	0.35	0.32	0.30
			Max.	0.21	0.17	0.14	0.12	0.11	0.10
		4×4	Min.		0.33	0.44	0.43	0.32	0.38
			Max.	0.31	0.24	0.21	0.17	0.16	0.15
	Indoor High	2×2	Min.		0.22	0.28	0.30	0.27	0.25
			Max.	0.18	0.14	0.12	0.10	0.09	0.09
		4×4	Min.		0.28	0.38	0.37	0.27	0.32
			Max.	0.26	0.20	0.18	0.15	0.13	0.12

Table I.5. UL single user radii for 2100 MHz frequency band.

				RADIUS [km]					
				Bandwidth [MHz]					
Modulation	Environment	MIMO	Throughput	1.4	3	5	10	15	20
QPSK	Pedestrian	2×2	Min.					0.26	0.23
			Max.	0.33	0.26	0.23	0.19	0.17	0.16
		4×4	Min.					0.18	0.16
			Max.	0.30	0.24	0.21	0.17	0.16	0.14
	Vehicular	2×2	Min.					0.09	0.10
			Max.	0.13	0.10	0.09	0.07	0.07	0.06
		4×4	Min.					0.10	0.09
			Max.	0.17	0.12	0.10	0.09	0.08	0.07
	Indoor Low	2×2	Min.					0.11	0.10
			Max.	0.14	0.11	0.10	0.08	0.07	0.07
		4×4	Min.					0.08	0.07
			Max.	0.13	0.11	0.09	0.08	0.07	0.06
	Indoor High	2×2	Min.					0.06	0.06
			Max.	0.08	0.06	0.05	0.05	0.04	0.04
		4×4	Min.					0.04	0.04
			Max.	0.07	0.06	0.05	0.04	0.04	0.03
16QAM	Pedestrian	2×2	Min.			0.21	0.25	0.25	0.23
			Max.	0.21	0.17	0.14	0.12	0.11	0.10
		4×4	Min.			0.18	0.20	0.18	0.16
			Max.	0.30	0.17	0.14	0.12	0.11	0.10
	Vehicular	2×2	Min.			0.08	0.10	0.11	0.09
			Max.	0.07	0.06	0.05	0.04	0.04	0.03
		4×4	Min.			0.09	0.11	0.10	0.09
			Max.	0.17	0.07	0.06	0.05	0.03	0.04
	Indoor Low	2×2	Min.			0.09	0.11	0.11	0.10
			Max.	0.09	0.07	0.06	0.05	0.05	0.04
		4×4	Min.			0.08	0.09	0.08	0.07
			Max.	0.13	0.07	0.06	0.05	0.05	0.04
	Indoor High	2×2	Min.			0.05	0.06	0.06	0.05
			Max.	0.05	0.04	0.03	0.03	0.03	0.02
		4×4	Min.			0.04	0.05	0.04	0.04
			Max.	0.07	0.04	0.03	0.03	0.03	0.02
64QAM	Pedestrian	2×2	Min.		0.16	0.21	0.22	0.20	0.18
			Max.	0.13	0.10	0.09	0.07	0.07	0.06
		4×4	Min.		0.14	0.19	0.19	0.14	0.16
			Max.	0.19	0.10	0.09	0.07	0.07	0.06
	Vehicular	2×2	Min.		0.05	0.08	0.09	0.08	0.08
			Max.	0.05	0.04	0.03	0.03	0.03	0.02
		4×4	Min.		0.06	0.09	0.10	0.10	0.09
			Max.	0.17	0.04	0.04	0.03	0.03	0.03
	Indoor Low	2×2	Min.		0.07	0.09	0.10	0.09	0.08
			Max.	0.06	0.05	0.04	0.03	0.03	0.03
		4×4	Min.		0.06	0.08	0.08	0.06	0.07
			Max.	0.13	0.05	0.04	0.03	0.03	0.03
	Indoor High	2×2	Min.		0.04	0.05	0.05	0.05	0.04
			Max.	0.03	0.02	0.02	0.02	0.02	0.01
		4×4	Min.		0.03	0.05	0.04	0.03	0.04
			Max.	0.07	0.02	0.02	0.02	0.02	0.02

Table I.6. UL single user radii for 2600 MHz frequency band.

				RADIUS [km]					
				Bandwidth [MHz]					
Modulation	Environment	MIMO	Throughput	1.4	3	5	10	15	20
QPSK	Pedestrian	2×2	Min.					0.17	0.16
			Max.	0.22	0.18	0.15	0.13	0.11	0.11
		4×4	Min.					0.12	0.11
			Max.	0.21	0.16	0.14	0.12	0.11	0.10
	Vehicular	2×2	Min.					0.06	0.07
			Max.	0.09	0.07	0.06	0.05	0.05	0.04
		4×4	Min.					0.07	0.06
			Max.	0.12	0.08	0.07	0.06	0.05	0.05
	Indoor Low	2×2	Min.					0.08	0.07
			Max.	0.10	0.08	0.07	0.06	0.05	0.05
		4×4	Min.					0.05	0.05
			Max.	0.09	0.07	0.06	0.05	0.05	0.04
	Indoor High	2×2	Min.					0.04	0.04
			Max.	0.05	0.04	0.04	0.03	0.03	0.03
		4×4	Min.					0.03	0.03
			Max.	0.05	0.04	0.03	0.03	0.03	0.02
16QAM	Pedestrian	2×2	Min.			0.14	0.17	0.17	0.15
			Max.	0.22	0.11	0.10	0.08	0.07	0.07
		4×4	Min.			0.12	0.13	0.12	0.11
			Max.	0.21	0.11	0.10	0.08	0.07	0.07
	Vehicular	2×2	Min.			0.06	0.07	0.07	0.06
			Max.	0.09	0.04	0.03	0.03	0.02	0.02
		4×4	Min.			0.06	0.07	0.07	0.06
			Max.	0.12	0.05	0.04	0.04	0.02	0.03
	Indoor Low	2×2	Min.			0.06	0.07	0.07	0.07
			Max.	0.10	0.05	0.04	0.04	0.03	0.03
		4×4	Min.			0.05	0.06	0.05	0.05
			Max.	0.09	0.05	0.04	0.04	0.03	0.03
	Indoor High	2×2	Min.			0.03	0.04	0.04	0.04
			Max.	0.05	0.03	0.02	0.02	0.02	0.02
		4×4	Min.			0.03	0.03	0.03	0.03
			Max.	0.05	0.03	0.02	0.02	0.02	0.02
64QAM	Pedestrian	2×2	Min.		0.11	0.14	0.15	0.13	0.13
			Max.	0.08	0.07	0.06	0.05	0.05	0.04
		4×4	Min.		0.10	0.13	0.13	0.09	0.11
			Max.	0.08	0.07	0.06	0.05	0.05	0.04
	Vehicular	2×2	Min.		0.03	0.05	0.06	0.06	0.05
			Max.	0.13	0.03	0.02	0.02	0.02	0.02
		4×4	Min.		0.04	0.06	0.07	0.07	0.06
			Max.	0.12	0.03	0.03	0.02	0.02	0.02
	Indoor Low	2×2	Min.		0.05	0.06	0.06	0.06	0.06
			Max.	0.10	0.03	0.03	0.02	0.02	0.02
		4×4	Min.		0.04	0.06	0.06	0.04	0.05
			Max.	0.09	0.03	0.03	0.02	0.02	0.02
	Indoor High	2×2	Min.		0.03	0.03	0.04	0.03	0.03
			Max.	0.05	0.02	0.01	0.01	0.01	0.01
		4×4	Min.		0.02	0.03	0.03	0.02	0.03
			Max.	0.05	0.02	0.01	0.01	0.01	0.01

Annex J – DL Additional Results

In this annex, supplementary results regarding the DL analysis for the multiple scenario are presented. Concerning the bandwidth analysis the total number of users per hour and total network traffic are presented in Figure J.1 and the average network radius in Figure J.2.

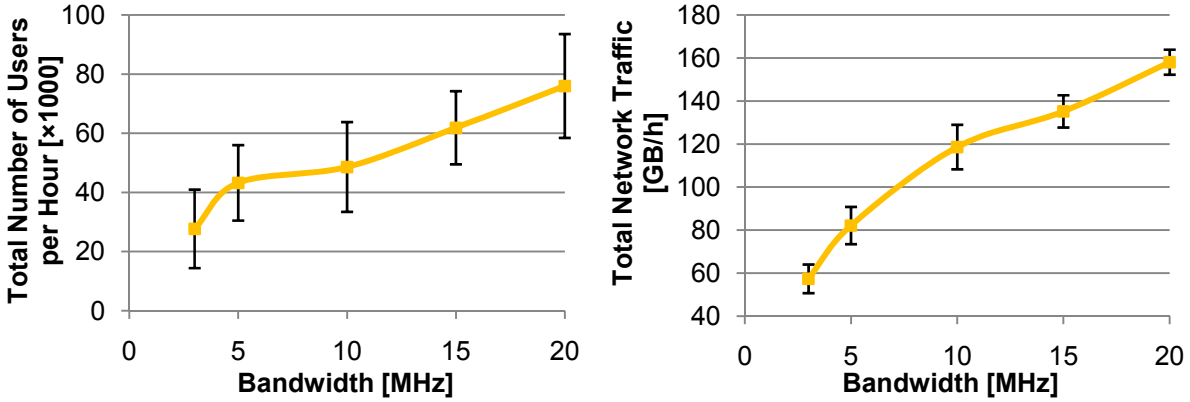

(a) Total Number of Users per Hour. (b) Total Network Traffic.

Figure J.1. DL Number of Users and Total Network Traffic for the bandwidths of 3, 5, 10, 15 and 20 MHz.

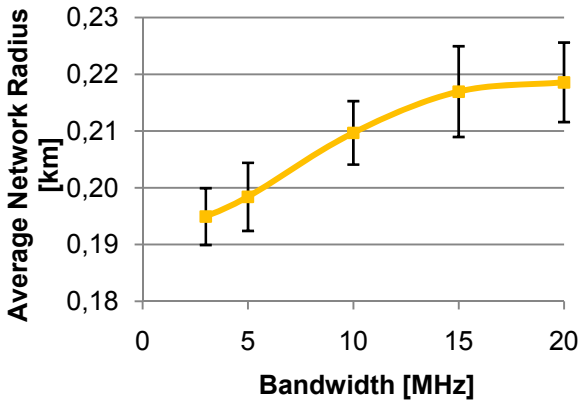

Figure J.2. DL Average Network Radius for the bandwidths of 3, 5, 10, 15 and 20 MHz.

For the frequency band variation, the average number of users and average network throughput for each modulation for the three frequency bands are presented in Figure J.3, the total number of users per hour and total network traffic are presented in Figure J.4 and the average number of RB is in Figure J.5.

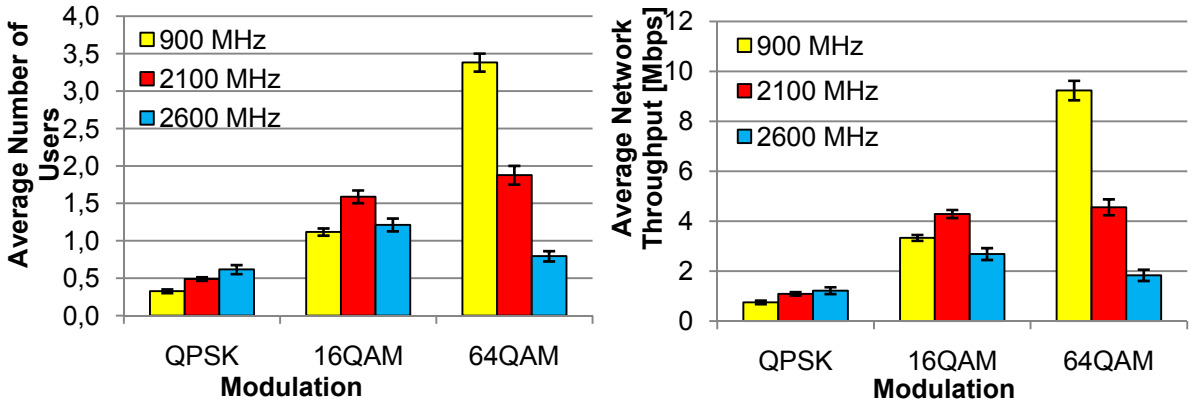

(a) Average Number of Users. (b) Average Network Throughput.

Figure J.3. DL Numbers of Users and Average Throughput as function of the modulation for the frequency bands of 900, 2100 and 2600 MHz.

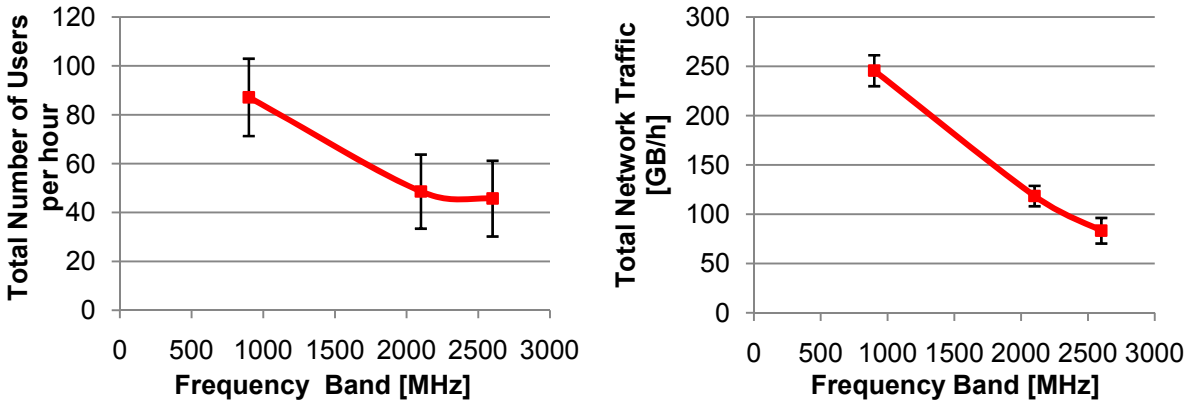

(a) Total Number of Users per Hour. (b) Total Network Traffic.

Figure J.4. DL Total Users and Total Network Traffic for the frequency bands of 900, 2100 and 2600 MHz.

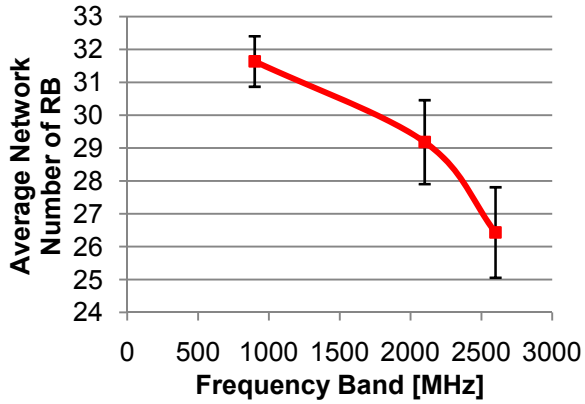

Figure J.5. DL Average Number of RB for the frequency bands of 900, 2100 and 2600 MHz.

The total number of users per hour and total network traffic for the 4×4 MIMO variation and split power fed variation are presented in Figure J.6 and the average number of RBs in Figure J.7.

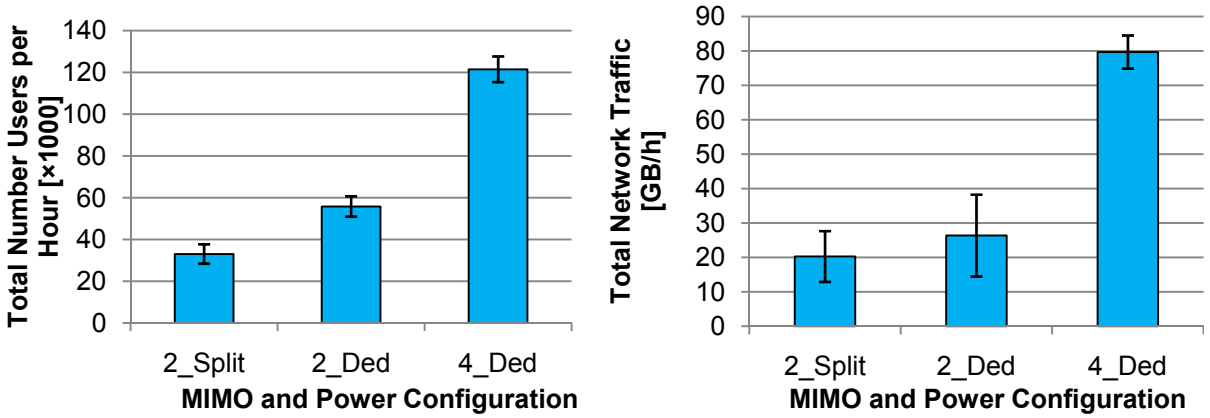

(a) Total Number of Users per Hour. (b) Total Network Traffic.

Figure J.6. DL Total Users and Total Network Traffic for different MIMO and antenna power feeding configurations.

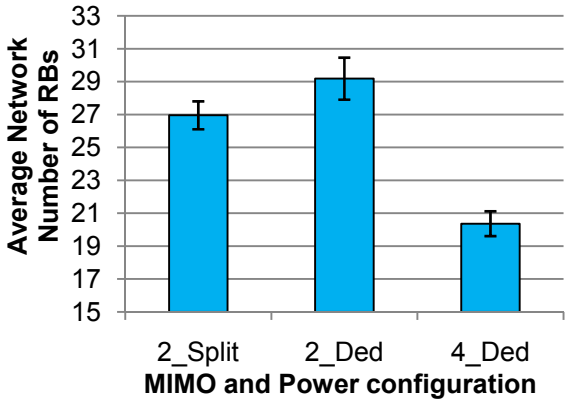

Figure J.7. DL Average Number of RB for different MIMO and antenna power feeding configurations.

Regarding the alternative profiles studied the results for the average network radius and average satisfaction grade are presented in Figure J.8 , the average number of RBs and the average network throughput in Figure J.9.

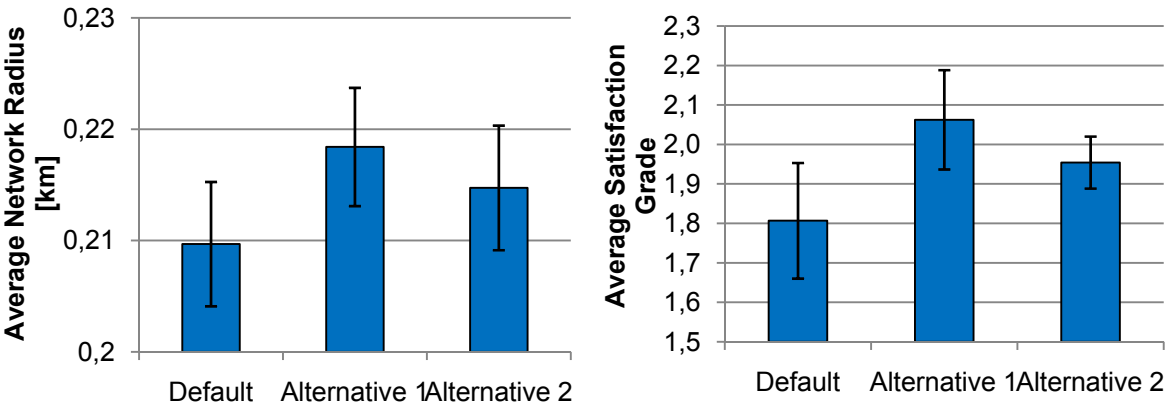

(a) Average Network Radius. (b) Average Satisfaction Grade.

Figure J.8. DL Network Radius and Satisfaction Grade for different profiles.

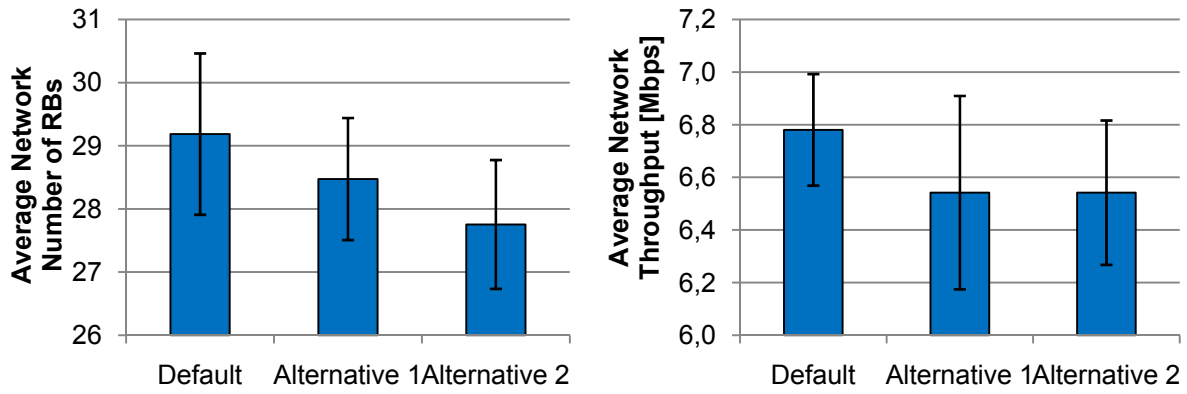

(a) Average Number of RBs. (b) Average Network Throughput.

Figure J.9. DL Number of RBs and Network Throughput for different profiles.

Concerning the variation where the number of users was increased to 3000, in Figure J.10 one presents the average network radius and the average number of RBs and in Figure J.11 the total number of users per hour.

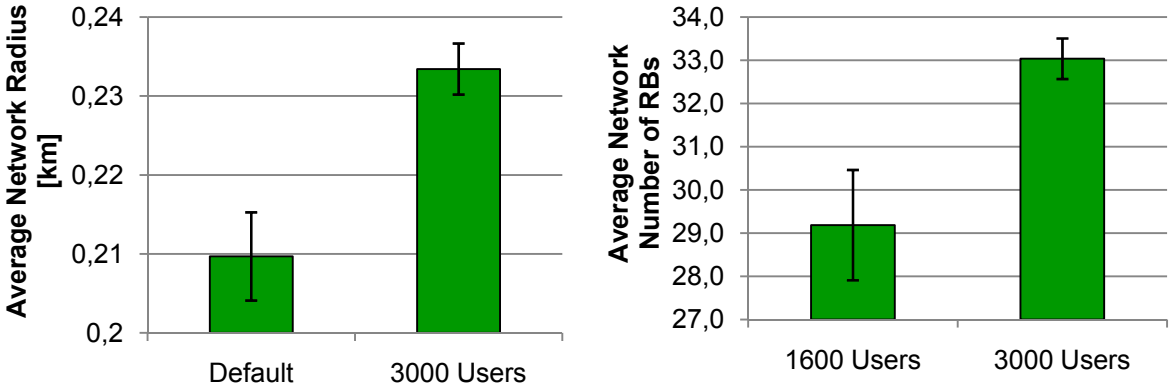

(a) Average Network Radius. (b) Average Number of RBs.

Figure J.10. DL Network Radius and Number of RBs for 1600 and 3000 users' scenario.

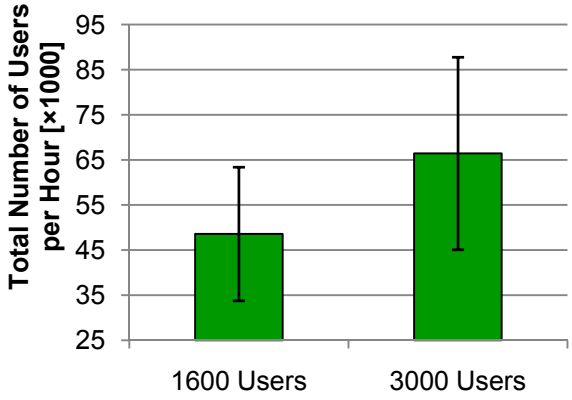

Figure J.11. DL Number of users for 1600 and 3000 Users' scenario.

Annex K – UL Additional Results

In this annex, supplementary results regarding the UL analysis for the multiple scenario are presented. Concerning the bandwidth analysis the total number of users per hour and total network traffic are presented in Figure K.1 and the average network radius in Figure K.2.

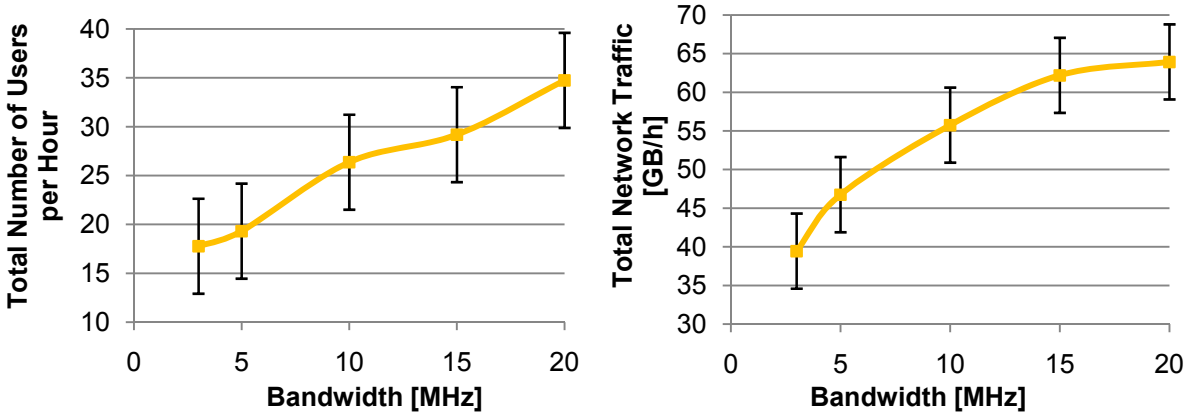

(a) Total Number of Users per Hour. (b) Total Network Traffic.

Figure K.1. UL Number of Users and Total Network Traffic for the bandwidths of 3, 5, 10, 15 and 20 MHz.

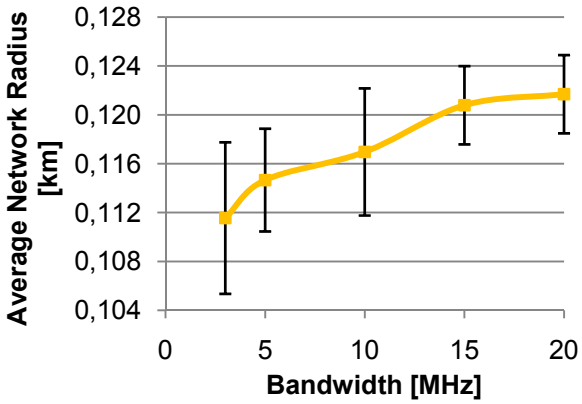

Figure K.2. UL Average Network Radius for the bandwidths of 3, 5, 10, 15 and 20 MHz.

For the frequency band variation, the average number of users and average network throughput for each modulation for the three frequency bands are presented in Figure K.3, the total number of users per hour and total network traffic are presented in Figure K.4 and the average number of RB is in Figure K.5.

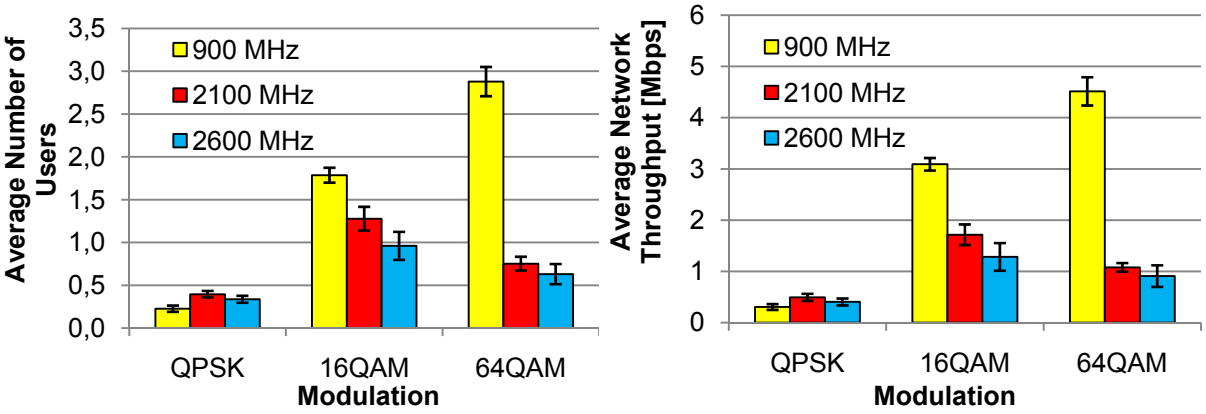

(a) Average Number of Users. (b) Average Network Throughput.

Figure K.3. UL Numbers of Users and Average Throughput as a function of the modulation for the frequency bands of 900, 2100 and 2600 MHz.

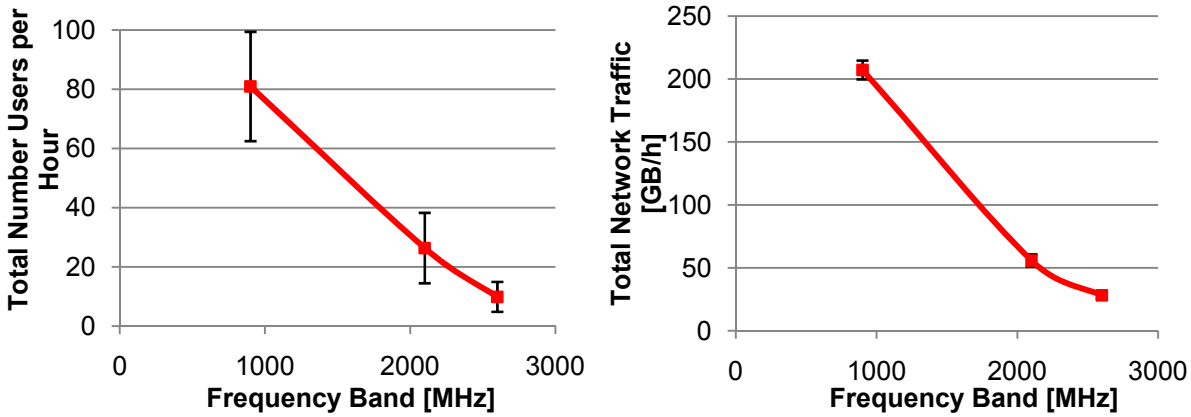

(a) Total Number of Users per Hour. (b) Total Network Traffic.

Figure K.4. UL Total Users and Total Network Traffic for the frequency bands of 900, 2100 and 2600 MHz.

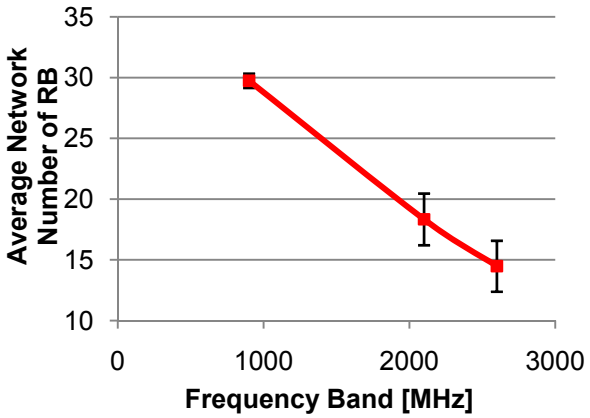

Figure K.5. UL Average Number of RB for the frequency bands of 900, 2100 and 2600 MHz.

The total number of users per hour and total network traffic for the 4×4 MIMO variation and split power fed variation are presented in Figure K.6 and the average number of RBs in Figure K.7.

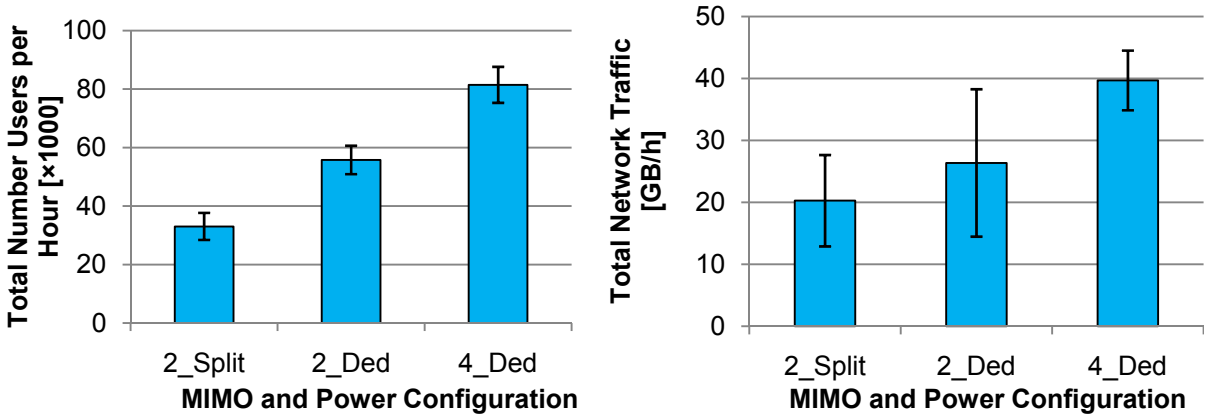

(a) Total Number of Users per Hour. (b) Total Network Traffic.

Figure K.6. UL Total Users and Total Network Traffic for different MIMO and antenna power feeding configurations.

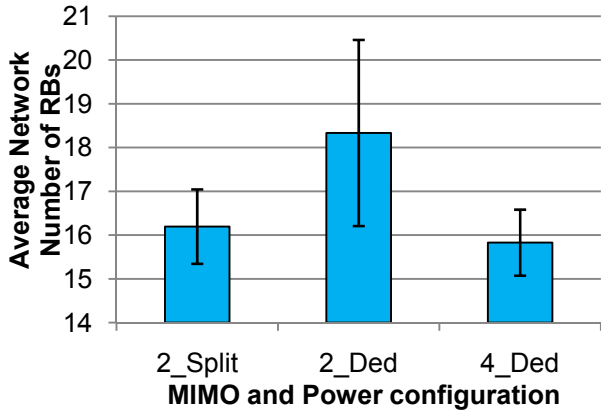

Figure K.7. UL Average Number of RB for different MIMO and antenna power feeding configurations.

Regarding the alternative profiles studied the average network radius and average satisfaction grade results are presented in Figure K.8, and, the average number of RBs and the average network throughput in Figure K.9.

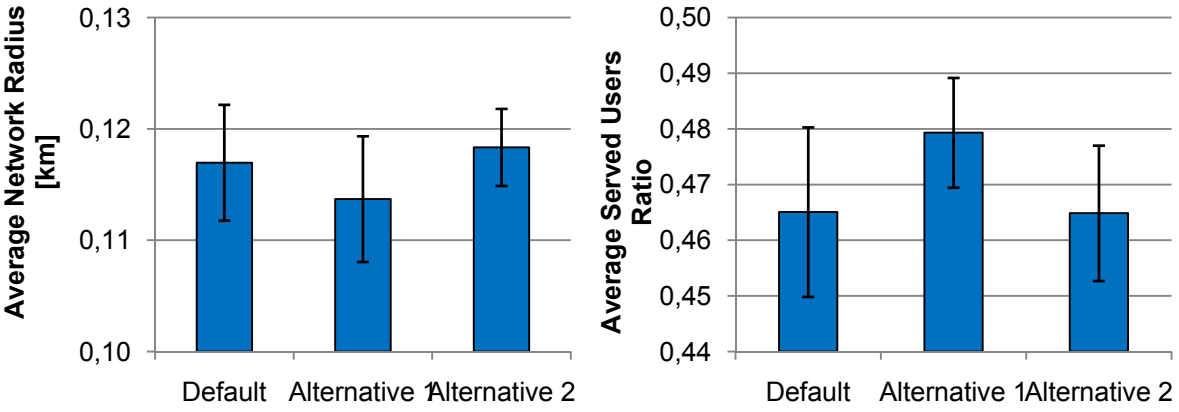

(a) Average Network Radius. (b) Average Satisfaction Grade.

Figure K.8. UL Network Radius and Satisfaction Grade for different profiles.

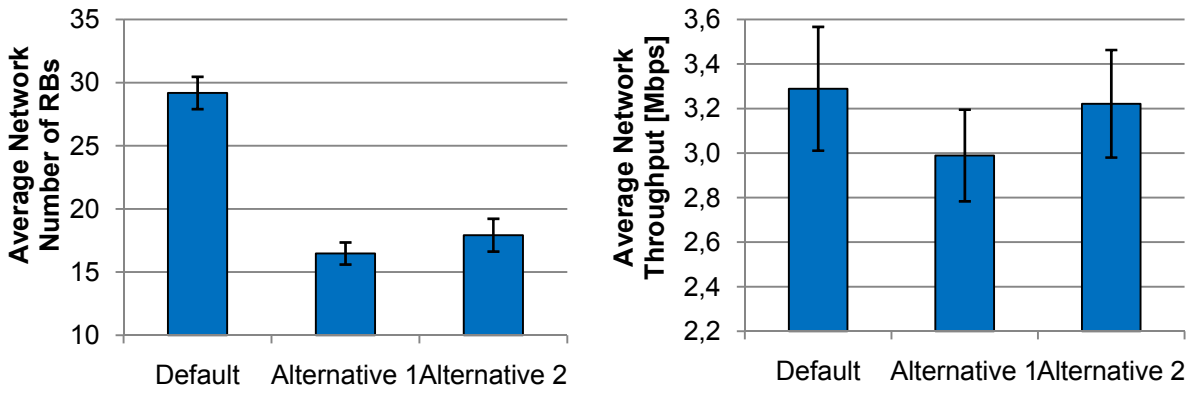

(a) Average Number of RBs. (b) Average Network Throughput.

Figure K.9. UL Number of RBs and Network Throughput for different profiles.

Concerning the variation where the number of users was increased to 3000, in Figure K.10 one presents the average network radius and the average number of RBs and in Figure K.11 the total number of users per hour.

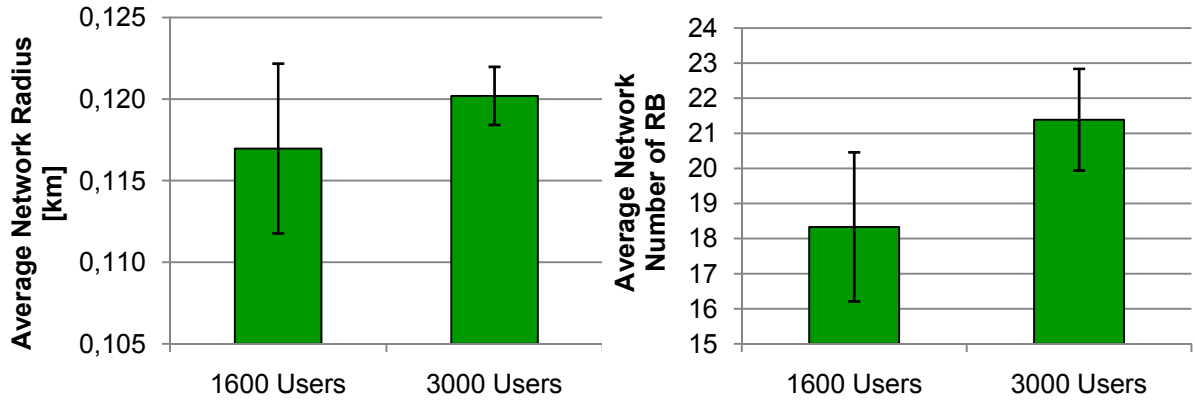

(a) Average Network Radius. (b) Average Number of RBs.

Figure K.10. UL Network Radius and Number of RBs for 1600 and 3000 users' scenario.

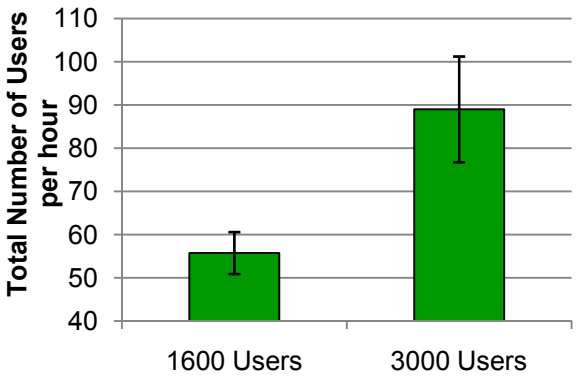

Figure K.11. UL Number of users for 1600 and 3000 Users' scenario.

References

[3GPP01] 3GPP, Technical Specification Group Services and System Aspects, *Service aspects; Services and Service Capabilities (Release 99)*, Report TS 22.105, V3.10.0, Oct. 2001 (http://www.3gpp.org/).

[3GPP02] 3GPP, Technical Specification Group Services and System Aspects, *Quality of Service (QoS) concept and architecture (Release 99)*, Report TS 23.107, V3.9.0, Sep. 2002 (http://www.3gpp.org/).

[3GPP07] 3GPP, Technical Specification Group - Radio Access Network Working, *PUSCH Simulation Results*, Report R4-071730, Shangai, China, Oct. 2007 http://www.3gpp.org/.

[3GPP07a] 3GPP, Technical Specification Group - Radio Access Network Working, *Collection of PDSCH results*, Report R4-072182, Jeju, Korea, Nov. 2007 http://www.3gpp.org/.

[3GPP07b] 3GPP, Technical Specification Group - Radio Access Network Working, *Proposal for LTE channel Models*, Report R4-070572, Kobe, Japan, May 2007 http://www.3gpp.org/.

[3GPP07c] 3GPP, Technical Specification Group - Radio Access Network Working, *PUSCH Simulation Assumptions*, Report R4-072210, Shangai, China, Oct. 2007 http://www.3gpp.org/.

[3GPP08] 3GPP, Technical Specification Evolved UTRA Aspects, *Overall description (Release 8)*, Report TS 36.300, V8.3.0, Jan. 2008 (http://www.3gpp.org/).

[Agil07] White Paper, *Agilent Technologies Solutions for 3GPP LTE - Technical Overview*, Agilent, Sep. 2007.

[Bati08] Batista,T., *Capacity Increase in UMTS/HSPA+ Through the Use of MIMO Systems*, M.Sc. Thesis, Instituto Superior Técnico, Lisbon, Portugal, Jul. 2008.

[BoTa07] White Paper, Bourse,Didier, Tafazolli,Rahim, *Beyond 3G/4G Radio Access Technologies (RATs)and Standards Roadmaps,* eMobility Technology Platform, Version 1.0, Dez. 07.

[Card06] Cardeiro,J., *Optimisation of Base Station Location in UMTS-FDD for Realistic Traffic Distribution*, M.Sc. Thesis, Instituto Superior Técnico, Lisbon, Portugal, Mar. 2006.

[CoLa06] Costa,P. and Ladeira,D., *Planning of UMTS Cellular Networks for Data Services Based on HSDPA* (in Portuguese), Graduation Thesis, IST-UTL, Lisbon, Portugal, 2006.

[COMS07] http://www.comscore.com/press/release.asp?press=1678, Oct. 2007.

[Corr08] Correia,L.M., *Mobile Communication Systems – Course Notes*, IST-UTL, Lisbon, Portugal, Mar. 2008.

[CSEE06] www.cse.ohio-state.edu/~lguo/presentation/imslides.ppt, Oct. 2007.

[DaCo99] Damasso,E. and Correia,L.M., *Digital Mobile Radio Towards Future Generation,* COST231 Final Report, 1999 (http:/www.lx.it.pt/cost231/).

[DPSB07] Dahlman,E., Parkvall,S., Sköld,J. and Beming,P., *3G Evolution: HSPA and LTE for Mobile Broadband*, Academic Press, Oxford, UK, 2007.

[Dziu04] Dziunikowski,W., *Multiple-Input Multiple-Output (MIMO) Antenna Systems*, in Chandran, S. (ed.), *Adaptive Antenna Arrays*, Springer, Berlin, Germany, 2004.

[ECGF05] El Zein,G., Cosquer,R., Guillet,J., Farhat,H., Sagnard,F., "Characterisation and Modeling of the MIMO Propagation Channel: An Overview", in *European Conference Wireless Technology*, *O*ct. 2005.

[EFKM06] Ekström,H., Furuskär,A., Karlsson, J., Meyer,M., Parkvall,S., Torsner,J. and Wahlqvist, M., "Technical Solutions for the 3G Long-Term Evolution", *IEEE Communications Magazine*, Volume 44, No. 3, March 2006, pp. 38-45.

[EMQG08] Eastwood,L., Migaldi,S., Qiaobing Xie, Gupta,V., "Mobility using IEEE 802.21 in a heterogeneous IEEE 802.16/802.11-based, IMT-advanced (4g) network", *IEEE Wireless Communications*, Volume 15, No. 2, April 2008, pp.26-34.

[EsPe06] Esteves,H. and Pereira,M., *Impact of intra- and inter-cell interference on UMTS-FDD* (in Portuguese), Graduation Thesis, Instituto Superior Técnico, Lisbon, Portugal, June 2006.

[FoGa98] Foschini,G.J. and Gans,M.J., "On Limits of Wireless Communications in a Fading Environment when Using Multiple Antennas", *Wireless Personal Communication*, Vol. 6, No. 3, Autumn 1998, pp. 311-335.

[Gold05] Goldsmith,A., *Wireless Communications*, Cambridge University Press, UK, 2005.

[HoTo04] Holma,H. and Toskala,A., *WCDMA for UMTS* (3rd Edition), John Wiley & Sons, Chichester, UK, 2004.

[HoTo06] Holma,H. and Toskala,A., *HSDPA/HSUPA for UMTS* (1st Edition), John Wiley & Sons, Chichester, UK, 2006.

[HoTo07] Holma,H. and Toskala,A., *WCDMA for UMTS – HSPA Evolution and LTE* (4rd Edition), John Wiley & Sons, Chichester, UK, 2007.

[Huaw07] White Paper, *LTE/SAE Techonology & Product Roadmap*, Huawey Techonologies, Sep. 2007.

[Koko05] Kokoszkiewicz,H., *MIMO Geometrically Based Channel Model*, M.Sc. Thesis, IST-UTL, Lisbon, Portugal, 2005.

[KuCo07] Kuipers,M., Correia, L.M., "Modelling the Relative MIMO Gain", in *Proc. of PIMRC'08 - IEEE Personal, Indoor and Mobile Radio Communications*, Cannes, France, Sep. 2008.

[Lope08] Lopes,J., *Performance of UMTS/HSDPA/HSUPA at the Cellular Level,* M.Sc. Thesis, IST-UTL, Lisbon, Portugal, 2008.

[Maćk07] Maćkowiak,M., *Geometrically Based Multibounce MIMO Channel Models*, M.Sc. Thesis, IST-UTL, Lisbon, Portugal, 2007.

[Marq08] Marques,A., *Modelling of building height interference dependence in UMTS,* M.Sc. Thesis, IST-UTL, Lisbon, Portugal, Sep. 2008.

[MNKF07] Mogensen,P., Wei Na, Kovacs,I.Z., Frederiksen,F., Pokhariyal,A., Pedersen,K.I., Kolding,T., Hugl,K., Kuusela,M., "LTE Capacity Compared to the Shannon Bound", in *Proc. of VTC'07 – 65th IEEE Vehicular Technology Conference,* Dublin, Ireland, Apr. 2007.

[Molis04] Molisch,A.F., *Wireless Communications*, John Wiley & Sons, Chichester, UK, 2005.

[MOME04] IST-MOMENTUM – Models and Simulation for Network Planning and Control of UMTS (http://momentum.zib.de/).

[Nuay07] Nuaymi,L., *WiMAX – Technology for Broadband Wireless Access*, John Wiley and Sons, Chichester, UK, 2007.

[Pede05] Pedersen,K.I., "Quality Based HSDPA Access Algorithms", in *Proc. of VTC'05 – 62nd IEEE Vehicular Technology Conference*, Dallas, Texas, USA, Sep. 2005.

[PeTM04] Pedersen,K., Toskala,A., Mogensen,P., "Mobility Management and Capacity Analysis for High Speed Downlink Packet Access in WCDMA", in *Proc. of VTC'04 – 60th IEEE Vehicular Technology Conference*, Los Angeles, California, USA, Sep. 2004.

[Preg08] Preguiça,R., *Comparison between UMTS/HSPA+ and WiMax/IEEE 802.16e in Mobility Scenarios*, M.Sc. Thesis, Instituto Superior Técnico, Lisbon, Portugal, Sep. 2008.

[Proa01] Proakis,J.,G., *Digital Communications*, MacGraw Hill, New York, USA, 2001.

[OPTW06] http://www.optimisationweek.com/reviews/average-Web-page/, Oct. 2007.

[RYSA07] White Paper, *EDGE, HSPA and LTE – The Mobile Bradband Advantage*, RYSAVY Research, Sep. 2007.

[Sant04] Santo,L., *UMTS Performance in Multi-Service Non-Uniform Traffic Networks,* M.Sc. Thesis, IST-UTL, Lisbon, Portugal, 2004.

[SeCa04] Sebastião,D. and Cardeiro,J., *Modelation and Traffic Dimensioning in the UMTS Radio Interface* (in Portuguese), Graduation Thesis, Instituto Superior Técnico, Lisbon, Portugal, Oct. 2004.

[Salv08] Salvado,L., *UMTS/HSDPA comparison with WiMAX/IEEE 802.16e in mobility scenarios*, M.Sc. Thesis, Instituto Superior Técnico, Lisbon, Portugal, Fev. 2008.

[SBER03] http://www2.sims.berkeley.edu/research/projects/how-much-info-2003/internet.htm#ftp, Oct. 2007.

[ScLü05] Schulze,H., Lüders,C., *Theory and Applications of OFDM and CDMA - Wideband Wireless Communications*, John Wiley & Sons, Chichester, UK, 2005.

[Seba07] Sebastião,D., *Algorithms for Quality of Service in a WiFi Network*, M.Sc. Thesis, Instituto Superior Técnico, Lisbon, Portugal, Dec. 2007.

[VNUN07] http://www.vnunet.com/vnunet/news/2194446/three-quarters-surfers-stream, Oct. 2007.

[XaVe02] Xavier,D. and Venes,J., *Caracterisation of the signal penetration in building for GSM* (in Portuguese), Graduation Thesis, Instituto Superior Técnico, Lisbon, Portugal, June 2006.

[WIMA08] http://www.wimaxforum.org/home/, June 2008.

[WiMF06b] “Mobile WiMAX – Part II: A Comparative Analysis”, WiMAX Forum, May 2006.